

# Durham E-Theses

---

## *Thin aligned organic polymer films for liquid crystal devices*

Kathryn Ellen Foster

### How to cite:

---

Foster, Kathryn Ellen (1997) Thin aligned organic polymer films for liquid crystal devices. Doctoral thesis, Durham University.

### Use policy

---

The full-text may be used and/or reproduced, and given to third parties in any format or medium, without prior permission or charge, for personal research or study, educational, or not-for-profit purposes provided that:

- a full bibliographic reference is made to the original source
- a <https://etheses.durham.ac.uk/id/eprint/4895/> is made to the metadata record in Durham E-Theses
- the full-text is not changed in any way

The full-text must not be sold in any format or medium without the formal permission of the copyright holders.

Please consult the [full Durham E-Theses policy](#) for further details.

Thin Aligned Organic Polymer Films  
for Liquid Crystal Devices

Kathryn Ellen Foster

The copyright of this thesis rests with the author. No quotation from it should be published without the written consent of the author and information derived from it should be acknowledged.

A thesis submitted for the degree of  
Doctor of Philosophy at the Chemistry Department of the University of Durham

August 1997



20 MAY 1998

## **Abstract**

### **Thin Aligned Organic Polymer Films for Liquid Crystal Devices**

This project was designed to investigate the possibility of producing alignment layers for liquid crystal devices by cross-linking thin films containing anisotropic polymer bound chromophores via irradiation with polarised ultra-violet light. Photocross-linkable polymers find use in microelectronics, liquid crystal displays, printing and UV curable lacquers and inks; so there is an increasing incentive for the development of new varieties of photopolymers in general.

The synthesis and characterisation of two new photopolymers that are suitable as potential alignment layers for liquid crystal devices are reported in this thesis. The first polymer contains the anthracene chromophore attached via a spacer unit to a methacrylate backbone and the second used a similarly attached aryl azide group. Copolymers of the new monomers with methyl methacrylate were investigated to establish reactivity ratios in order to understand composition drift during polymerisation.

## **Memorandum**

The work reported in this thesis was carried out at the Interdisciplinary Research Centre in Polymer Science and Technology at Durham University between August 1994 and July 1997. This work has not been submitted for any other degree and is the original work of the author except where acknowledged by reference.

## **Statement of Copyright**

The Copyright of this thesis rests with the author. No quotation from it should be published without her prior written consent and information derived from it should be acknowledged.

## **Financial Support**

The Defence Research Agency (Malvern) is gratefully acknowledged for providing a grant for the work described herein.

## Acknowledgments

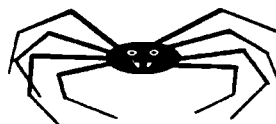
Firstly, I would like to thank Prof. Jim Feast for giving me this opportunity and encouragement throughout my years in the IRC. Also thanks to Helen Varley and Prof. Randal Richards for comprising the other half of this project and giving me various advice along the way. A big thankyou to Dr. Andrew Grainger, Dr. Lois Hobson and Dr. Lesley Hamilton for being tremendous help in the lab, also the rest of the IRC mob, especially synth. lab 2. Thanks to Dr. Ian Sage and Dr. Guy Bryan-Brown of the DRA Malvern.

Dr. Alan Kenwright and Julia Say for NMR guidance, Gordon Forrest for GPC and TGA analysis, Ray Hart and Gordon Haswell for mending all my breakages in the lab.

My biggest thankyou is to my family, especially my parents who have been an enormous source of encouragement and support (emotionally and financially). This is for you, Mum and Dad.

Expect the Unexpected

**Kate**



## Contents

	page
Abstract	ii
Memorandum, Statement of Copyright and Financial Support	iii
Acknowledgments	iv
Contents	v
<b>CHAPTER 1: General Introduction and Background</b>	
1.1 Liquid crystals	1
1.2 Liquid crystal cells	4
1.3 Alignment of liquid crystal	7
1.3.1 Mechanical alignment methods	7
1.3.2 Photosensitive polymers	10
1.4 Poly(vinyl cinnamate)	12
1.4.1 Synthesis of poly(vinyl cinnamate)	13
1.4.2 Use of poly(vinyl cinnamate) as a potential alignment layer	15
1.5 New photopolymers for liquid crystal alignment	18
References for Chapter One	20
<b>CHAPTER 2: Synthesis and Characterisation of an Anthracenyl Homopolymer</b>	
2.1 Introduction	22
2.2 Experimental	32
2.2.1 Purification of Starting Materials	32
2.2.2 Synthesis of Anthracene Homopolymer	35
2.3 Results and Discussion	42

2.4	Film forming and Cross-linking	54
2.5	Conclusions	57
	References for Chapter Two	59
<b>CHAPTER 3: Synthesis and Characterisation of an Azide Homopolymer</b>		
3.1	Introduction	60
3.2	Experimental	
	3.2.1 Purification of Starting Materials	68
	3.2.2 Synthesis of Azido Homopolymer	68
3.3	Results and Discussion	72
3.4	Film forming and Cross-linking	90
3.5	Conclusions	91
	References for Chapter Three	93
<b>CHAPTER 4: Synthesis and Investigation of Copolymers of the Anthracene and Azide Monomers with Methyl Methacrylate</b>		
4.1	Introduction	95
4.2	Experimental	
	4.2.1 Purification of Starting Materials	99
	4.2.2 Copolymer Synthesis	99
4.3	Results and Discussion	
	4.3.1 Results of Synthesis	104
	4.3.2 Reactivity Ratios	116
	4.3.3 Composition Drift of the Anthracene/MMA System	128
4.4	Conclusions	133
	References for Chapter Four	135

## **CHAPTER 5:Future work for the Synthesis of Alignment Layers for Liquid**

### **Crystal Devices**

5.1	Photochemistry of Azide Polymer	136
5.2	Future Work	142
	References for Chapter Five	149

### **APPENDICES**

	Appendix One - Instrumentation	152
	Appendix Two - Analytical data for chapter two	153
	Appendix Three - Analytical data for chapter three	168
	Appendix Four - Analytical data for chapter four	184
	Appendix Five - Lectures and Conferences attended	194
	<b>BIBLIOGRAPHY</b>	197

# Chapter One

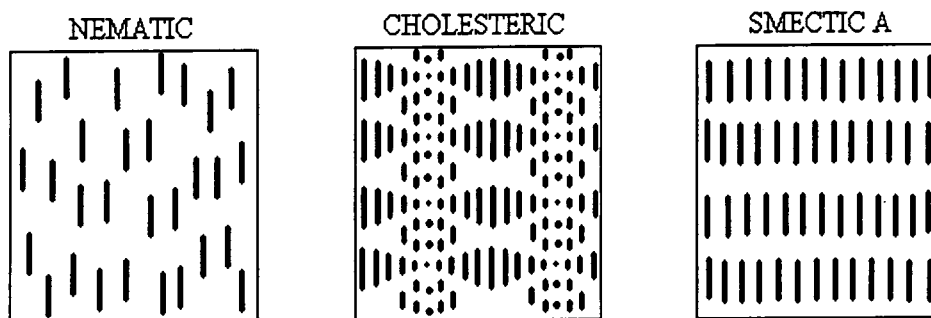
## General Introduction and Background

### 1.1 Liquid Crystals

Liquid crystals are defined as, “A state of matter that is intermediate between the solid crystalline and the ordinary (isotropic) liquid phases.”<sup>1</sup> This definition is appropriate because liquid crystals (also known as mesophases) display properties exhibited by both solids and liquids, for example, liquid crystals flow like liquids but can also show some of the anisotropic properties found in solids, such as birefringence and shear behaviour, due to a certain amount of ordering. There are many organic compounds that are known to form liquid crystal phases.

There are three basic types of liquid crystal known as smectic, nematic and cholesteric<sup>2</sup>, these are represented schematically below.

Figure 1.1 Types of Liquid Crystal



Nematic liquid crystals are the type mainly used in liquid crystal display cells of interest for the work reported in this thesis so cholesteric and smectic liquid crystals will be dealt with only very briefly. Nematic liquid crystals possess long range orientational order in the direction of their long molecular

axes which are aligned parallel to a preferred direction known as the director.

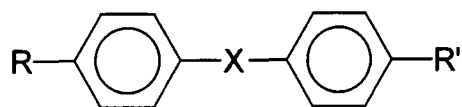
The molecules can rotate freely about their long axes and apart from the ordering in the direction of the director, they are distributed at random as in a liquid.

Nematic liquid crystal molecules exhibit anisotropy, are uniaxial with an electrical dipole in the direction of the long axis and are strongly birefringent.

The molecules have a tendency to align themselves due to the anisotropy caused by the shape and polarity of the molecules. Without any external alignment methods, electrical or magnetic fields and mechanical effects, the liquid crystal alignment is limited to microscopic domains. In a large volume of nematic liquid crystal the direction of the director in the microdomains is not the same but alters throughout the volume due to convection, flow and other forces.

Nematic liquid crystal behaviour is found in elongated molecules consisting of six membered rings linked through their 1, 4-positions either directly or through a small sub-unit. Some conjugated aromatic systems are shown below by way of illustration.

Figure 1.2 Basic Structure of Aromatic Nematic Liquid Crystals<sup>3</sup>

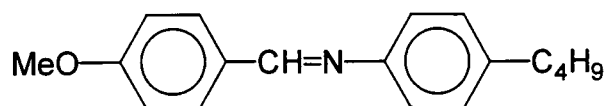


where X is a linking group, e.g. -N=N-

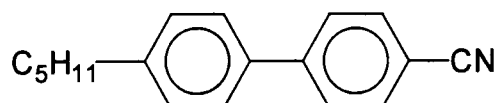
R and R' are short chain alkyls or polar substituent groups

Figure 1.3 Examples of compounds that exhibit a nematic phase

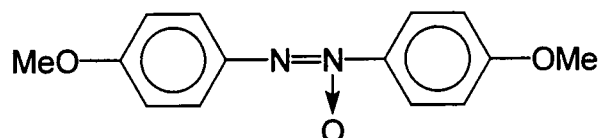
MBBA 4-Methoxybenzylidene-4'-butylaniline



PCB 4-Pentyl-4'-cyanobiphenyl

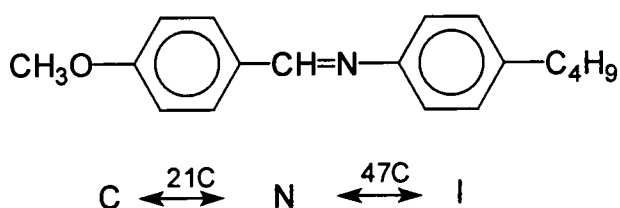


PAA para-Azoxyanisole



Nematic liquid crystals are thermotropic so pass through mesophases in response to temperature changes, for example,

Figure 1.4 Thermal Transitions of 4-Methoxybenzylidene-4'-butylaniline<sup>4</sup>



C, N and I denote the phases; crystalline, nematic and isotropic respectively. The temperatures shown correspond to the phase transitions, thus for this example the crystalline solid transforms to a nematic liquid crystal at 21C and the nematic phase is stable up to 47C when a second transition occurs to give an isotropic melt. These details are important in that they define the working range of a specific liquid crystal material; in practice mixtures of liquid crystals are used for many applications.

Cholesteric liquid crystals are chiral, optically active molecules. The first examples of cholesteric liquid crystals were the cholesteryl esters extracted from cholesterol, hence the name of this liquid crystal phase. The cholesteric liquid crystal molecules are arranged in layers, with each subsequent layer rotated by a given angle from the axes of the molecules in the preceding layer. As a consequence of this the molecules form a helical structure, see Figure 1.1.

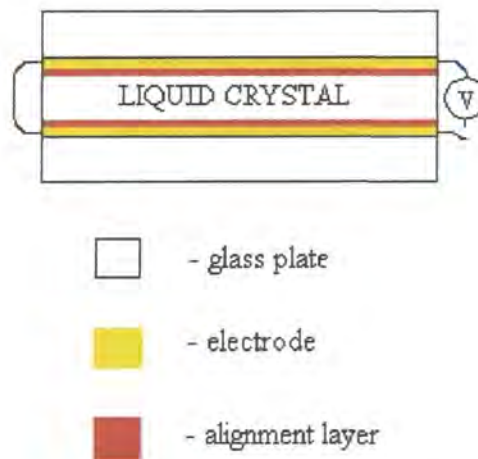
Smectic liquid crystals can be used in liquid crystal cells and exhibit somewhat similar optical properties to nematic liquid crystals. However, the smectic phase has a greater degree of order compared to the nematic phase. The smectic liquid crystal molecules are ordered in layers with the molecular axes in the same direction, see Figure 1.1. This layering gives the smectic liquid crystals a larger amount of 'rigidity' compared to other types of liquid crystal. The molecules are long with the long molecular axes lying parallel to the director. Several different types of smectic liquid crystals exist, denoted A, B, C etc. but all have the same basic characteristics.

## **1.2 Liquid Crystal Cells**

Liquid crystal displays are ubiquitous in modern society, they are to be found in digital watches, instrument displays, laptop computer displays and, probably in the future, flat-screen colour televisions. They have made this enormous impact in technology because they are flat, thin, lightweight and have a low power consumption which means they have considerable technological and economic merit.

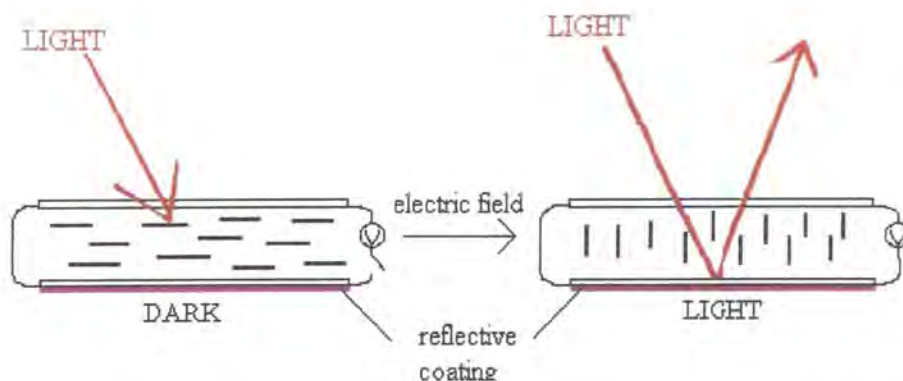
The construction of a typical display cell<sup>5</sup> is shown schematically below.

Figure 1.5 A sandwich-type liquid crystal cell



The glass plates are usually coated with a layer of transparent conducting material, for example, indium tin oxide. To create patterns in the cell the indium tin oxide coating can be etched so only part of the liquid crystal is 'switched' when an electrical field is applied. One of the plates is often coated with a reflective layer, e.g. vapour-deposited aluminium, to reflect incident light through the liquid crystal and back out of the cell.

Figure 1.6 Switching of a Liquid Crystal Cell



An electric field is applied across the cell which induces alignment with the field of the electrical dipole along the long axes of the liquid crystal molecules and

causes them to 'switch' to an upright position. The transmission properties of the liquid crystal are anisotropic, being transparent when vertically aligned and opaque when horizontal so a change in the appearance (dark to light) of the liquid crystal cell can be observed. The liquid crystal cell does not produce any light itself but acts as a kind of shutter, in the case discussed it affects whether the incident light is absorbed or reflected.

The alignment layers, Figure 1.5, are there to help align the liquid crystal uniformly in one direction. Liquid crystals have a natural tendency to align but this alignment does not occur in only one direction, many microdomains are formed. For efficient 'switching' of the liquid crystal cell the liquid crystal must be uniformly aligned, hence the use of the alignment layer.

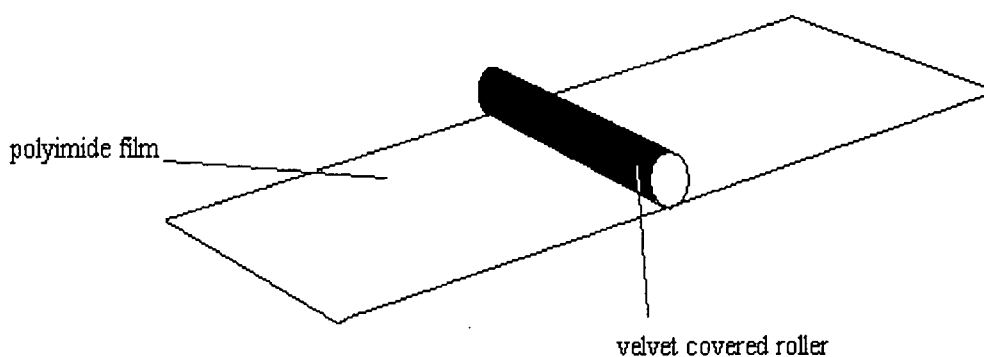
Clean technology is used in manufacturing liquid crystal cells as dirt and impurity can affect their function. The thickness of the glass and liquid crystal layer are important and must not vary by more than a few micrometers otherwise uneven field strength and hence an erratic electro-optical effect results. The work to be described in this thesis was designed to address the science and technology of alignment and this is the topic of the next section.

### 1.3 Alignment of Liquid Crystal

#### 1.3.1 Mechanical Alignment Methods

The usual method of aligning liquid crystals is to use a rubbed film of polyimide<sup>6</sup>. This mechanical method is believed to work by forming small grooves in the polymer film with which the low molecular mass liquid crystal molecules align. This rubbing is accomplished by passing the polyimide film beneath a velvet covered roller. Mechanical rubbing can also be used on glass and the rubbing performed with paper or cloth. This method of alignment is used in the manufacture of liquid crystal cells because it allows mass production, the treatment of large areas of polymeric film, is relatively simple and has a low cost.

Figure 1.7 Aligning of a Polyimide Film by Rubbing

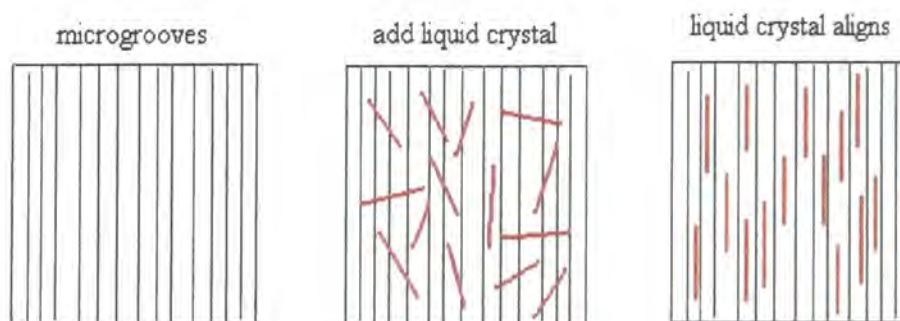


Various parameters can be altered to change the alignment such as the type of rubbing cloth used, rotation speed of the roller, speed that the polymer film passes under the roller and pile depth of the cloth.

There has been much debate as to the exact mechanism by which alignment by a rubbed film occurs. The first theory was that the small liquid crystal molecules fall into the microgrooves in the film and hence align

unidirectionally<sup>7</sup>. However, microscopic examination of rubbed surfaces suggested that the microgrooves were generally too wide and irregular for liquid crystal to align, nevertheless the more regular and narrow the microgrooves are, the better the alignment<sup>7</sup>.

Figure 1.8 Microgrooves Aligning Liquid Crystal Molecules

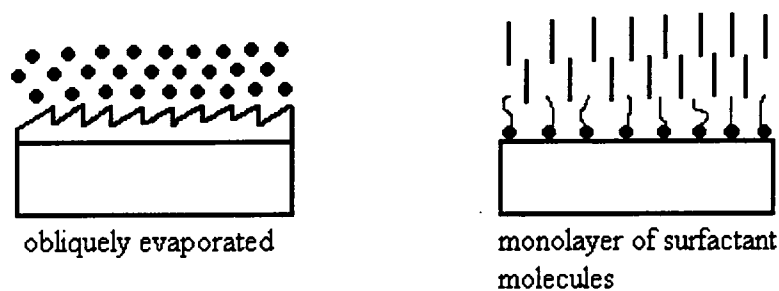


Further investigation into the process revealed that alignment on a rubbed polymer film depends on the type of polymer used rather than the rubbing direction, i.e. when using poly(vinyl alcohol), liquid crystal aligns along the rubbed direction but when using polystyrene the orientation occurs at  $90^{\circ}$  to the direction of rubbing<sup>8</sup>. These results suggest that the liquid crystal may be aligned by a physical chemical, e.g. dipolar or Van der Waals interactions with the polymer films. The rubbing method only produces weak coupling between the liquid crystal and the substrate. Anisotropic Van der Waals forces probably form the main surface to liquid crystal interaction which causes alignment. Hydrogen bonding and dipole interactions between the molecules may also contribute to liquid crystal alignment. It is now generally thought that the formation of microgrooves aligns the polymer chains in the surface of the film which then

cause the alignment of the liquid crystal molecules by weak intermolecular attractions.

Vapourisation of metals or oxides (e.g.  $\text{SiO}_2$ ) on to the surface of the glass of the cell at an oblique angle of incidence is another technique for producing an alignment layer<sup>9</sup>. This technique can also introduce a tilt of the nematic liquid crystals which is beneficial as it causes faster switching of the liquid crystal cell, see Figure 1.9.

Figure 1.9 Aligning Liquid Crystal Layers by Evaporation of a Metal or Oxide or a Monolayer of Surfactant Molecules on the Cell Surface<sup>9</sup>



Another alignment technique shown schematically in Figure 1.9 is to use monolayer Langmuir coatings applied from aqueous solution to a surface. A glass slide is passed through an aqueous solution of surfactant (e.g. hexadecyltrimethylammonium bromide) and emerges coated in a monolayer of the surfactant. How the nematic liquid crystal is aligned depends on the concentration of the surfactant and the rate at which the glass plate is drawn through the solution.

Other alignment techniques include curing a liquid crystal network in the presence of an electric field and stress-induced anisotropic deformation of the polymer backbone caused by compressing or stretching the polymer films.

These mechanical techniques have many disadvantages. Often they are relatively 'dirty' and awkward processes and some are difficult to carry out on a large scale. If a polyimide film is rubbed with a velvet-covered roller, bits of the velvet will stick to the polyimide surface. Liquid crystal cell manufacturing is supposed to be clean technology as dirt impairs the functioning of the cells. Rubbing inevitably creates friction and consequently electrostatic charges form on the polyimide films which affect the efficient switching of the liquid crystal cell. Other disadvantages are that the rubbing is hard to control as the velvet pile is not uniform. The speed of rubbing and velvet quality must be accurately maintained in order to obtain even microgrooves and hence even alignment. Larger scratches can also form in the polymer film from the rubbing technique, leading to significant film scrap.

If an orientation layer could be produced by a remote non-contact technique such as ultra-violet irradiation, it would provide clear technological and manufacturing advantages.

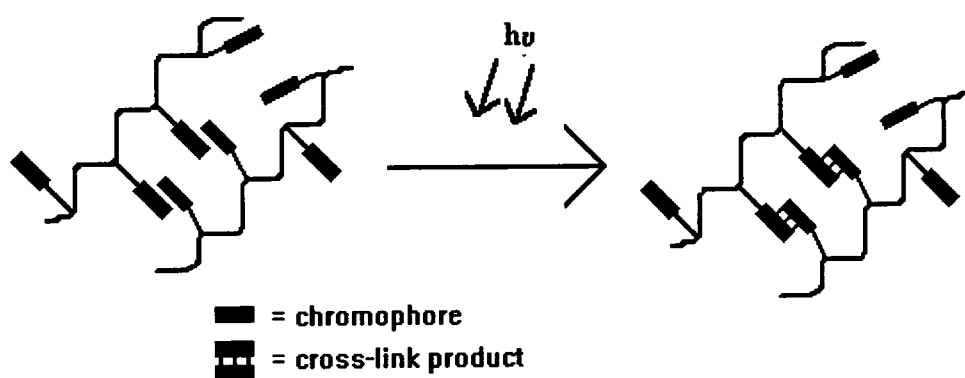
### **1.3.2 Photosensitive Polymers**

Photocross-linking polymers are becoming increasingly useful, they are found in microelectronics, photoresists, printing and ultra-violet curable inks. A variety of photosensitive polymers which can be made insoluble by irradiation with UV or visible light have been attracting much interest because of their many

uses; so there is an increasing incentive for the development of new varieties of photopolymer. The cross-linking chromophore can be located within the polymer main chain or be appended to the main chain by a spacer group.

Photocross-linkable polymers become cross-linked by formation of inter-chain bonds under the influence of light. When cross-links form, a network results and the polymer becomes insoluble. Cinnamate and chalcone groups have been used as side-chain chromophores for this purpose.<sup>10, 17</sup>

Figure 1.10 Cross-linking of Side-chain Chromophores by Polarised UV Light



These photopolymers function by the reactive chromophore in the side-chain dimerising when irradiated with ultra-violet light. If polarised light is used only chromophores which have the appropriate transition dipole lying in the direction of the electric vector of the polarised light will dimerise, forming cross-links between the polymer chains. Therefore with these photo-dimerised units lying in one direction, the cross-linked polymer film will have an anisotropic structure and the potential for use as an alignment layer for liquid crystal devices. This concept, as illustrated in Figure 1.10 above, has been demonstrated for cinnamates and its realisation in a practical application would be a major breakthrough for liquid crystal orientation as this remote technique would be

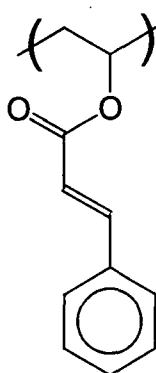
efficient and clean and so would have clear technological and manufacturing advantages over conventional rubbed polymer films. The cross-linking caused by polarised ultra-violet light aligns the photo-dimerised units in a uniform direction which in turn causes the liquid crystal molecules to align unidirectionally.

#### 1.4 Poly(vinyl cinnamate)

Poly(vinyl cinnamate) was the earliest photopolymer studied and has been studied extensively for use as a thin film alignment layer for liquid crystal devices<sup>11</sup>.

The structure of poly(vinyl cinnamate) is shown below. It comprises of a polyvinyl backbone with cinnamoyl side chains which cross-link on irradiation.

Figure 1.11 Poly(vinyl cinnamate)



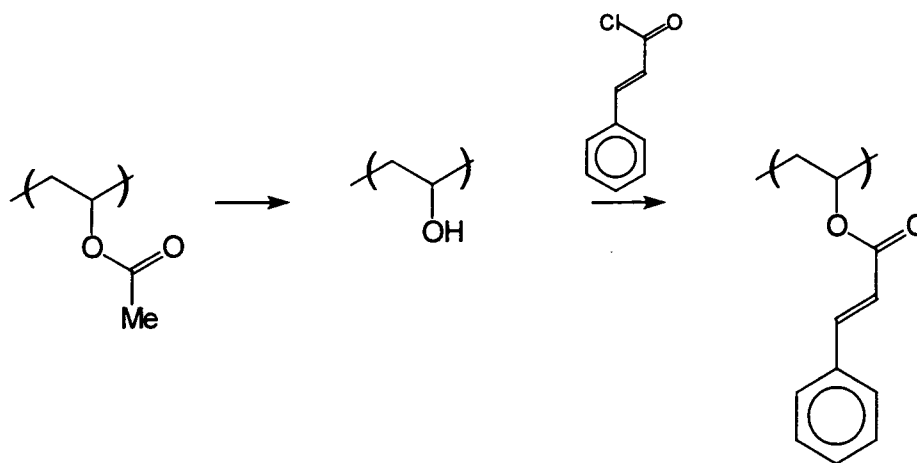
The basic unit necessary to produce cross-linking in polymers based on poly(vinyl cinnamate) is the  $-C=C-CO-$  unit. Depending on where and how this unit is attached to the polymer chain, the response to irradiation and the resultant physical properties can be modified. Poly(vinyl cinnamate) has good thermal

stability, reasonably good tensile strength, photosensitivity and good solubility, all of which are important for practical use of a photocross-linkable polymer. The system has been used commercially as a resist material for printing applications.

#### 1.4.1 Synthesis of Poly(vinyl cinnamate)

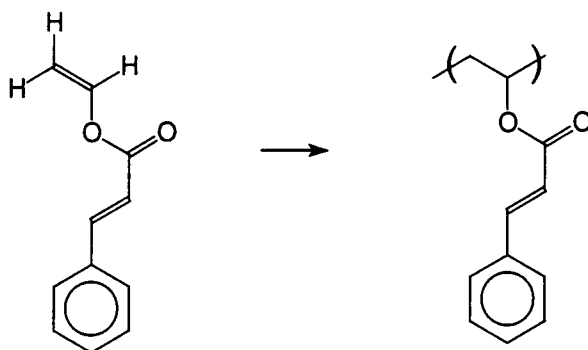
Poly(vinyl cinnamate) can be prepared from poly(vinyl alcohol)<sup>12</sup> which is obtained from poly(vinyl acetate) by hydrolysis. Reaction of poly(vinyl alcohol) with cinnamoyl chloride gives the desired product. Incomplete reaction at any stage can leave acetate or alcohol residues on the polymer chain. This method of synthesis does not yield a product carrying a cinnamoyl group on every available alcohol residue.

Figure 1.12 Synthesis of Poly(vinyl cinnamate)



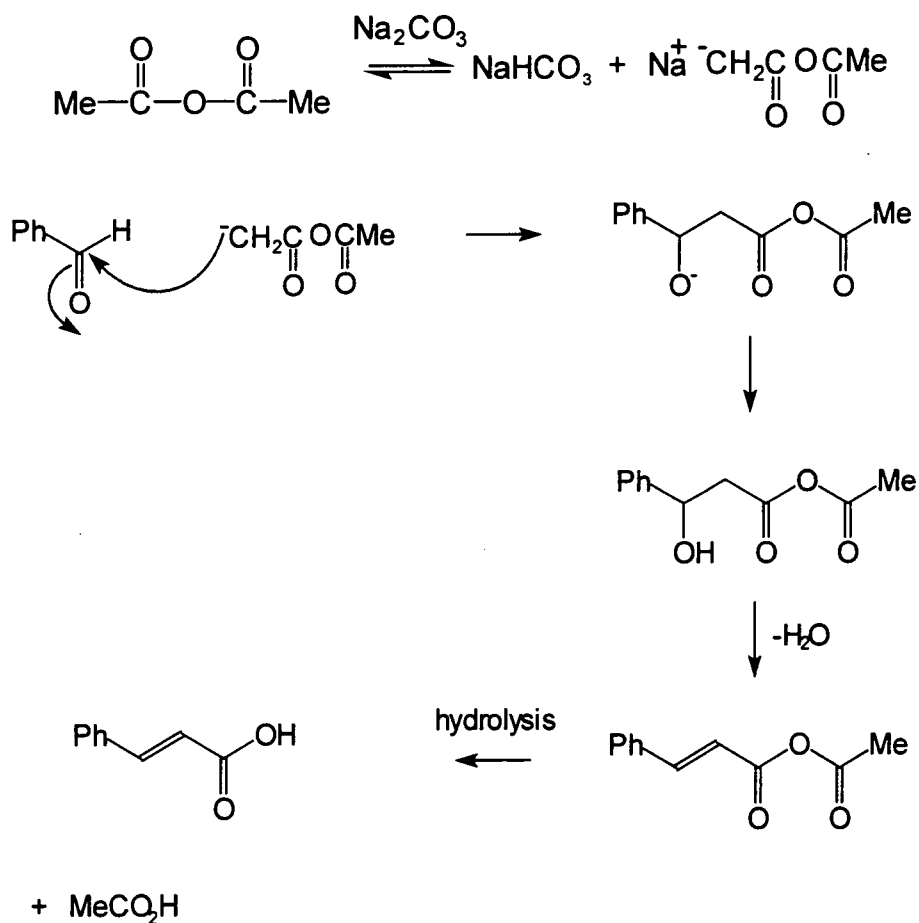
Alternatively poly(vinyl cinnamate) can be produced by polymerising the monomer directly. Cinnamate containing monomers are polymerised cationically as free radical polymerisation leads to a cross-linked and therefore insoluble product.

Figure 1.13 Polymerisation of vinyl cinnamate



The cinnamate group is synthesised using the Perkin reaction<sup>13</sup>. The Perkin reaction involves the condensation of an acid anhydride with an aromatic aldehyde. A carboxylate ion is used as a catalyst.

Figure 1.14 Perkin Reaction forming Cinnamic acid

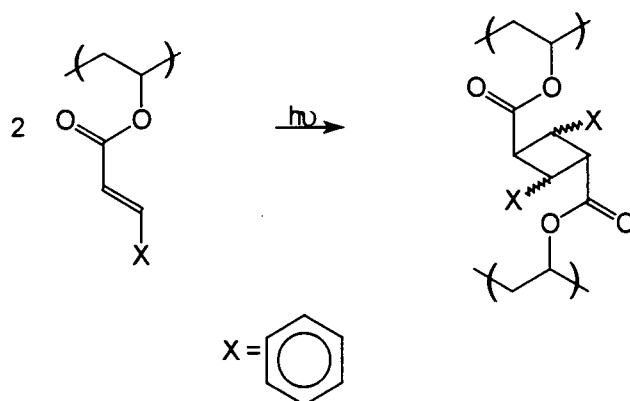


The anhydride reacts with the basic carbonate ion to provide a carbanion. The carbanion attacks the carbonyl group of the aldehyde then, after protonation, the newly formed anhydride undergoes dehydration followed by hydrolysis to form the product, cinnamic acid.

#### **1.4.2 Use of Poly(vinyl cinnamate) as a potential Alignment Layer**

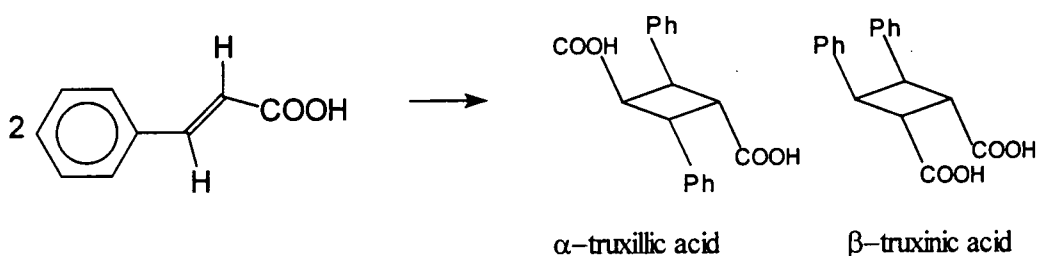
On irradiating polymers containing cinnamic acid, a cross-linked polymer product results. In the simplest picture of the photocross-linking process, irradiation of this polymer results in a cinnamoyl side-chain on a polyvinyl backbone undergoing a 2+2 photocycloaddition with another cinnamoyl group on an adjacent polymer chain so forming a substituted cyclobutane cross-link. While this picture is widely accepted, and is essentially correct, it is incomplete. It has been suggested that part of the cross-linking process occurs via a radical mechanism but this is also uncertain. Attempts to identify the cyclobutane derivatives in irradiated films of poly(vinyl cinnamate) in complete stereochemical detail have proved difficult. Experiments have been carried out on the photoproducts and it has been found that in general, over 65% of poly(vinyl cinnamate) photoproducts are cyclic dimers of one kind or another and the remainder are oligomers which have not yet been fully characterised.<sup>14</sup>

Figure 1.15 Cross-linking of Poly(vinyl cinnamate)



Photodimerisation of cinnamic acid derivatives produces two dimers, the truxillic and truxinic acids. There are further stereoisomers of these dimers which depend on the position of the substituents on the cyclobutane ring.

Figure 1.16 Dimerisation of Cinnamic acid

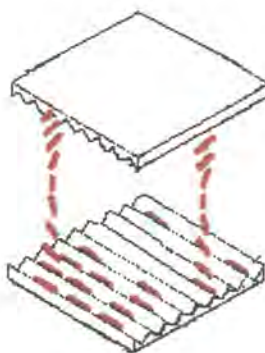


Irradiation of poly(vinyl cinnamate) results in the formation of  $\alpha$ -truxillic acid exclusively, which has been proved by hydrolysis of the photoproduct and chromatographic analysis of the reaction products.<sup>10</sup> This is probably due to steric effects controlling possible chromophore orientations resulting from the steric effect of the polymer chains.

When exposed to irradiation with polarised ultra-violet light (325nm), cross-linking occurs at the chromophores as expected and gives rise to anisotropy in the surface layer which can be used to enhance alignment of a liquid crystal layer, thus films formed from poly(vinyl cinnamate) in this way are effective as alignment layers. The ultra-violet light must be polarised so that only molecules

lying in a certain direction will undergo cross-linking to give the anisotropy and resultant alignment required. It was established that poly(vinyl cinnamate) films have the ability to align liquid crystal layers after irradiation with polarised ultraviolet light<sup>15</sup>. Poly(vinyl cinnamate) films provide planar and  $90^\circ$  twist alignment with only some pre-tilt of the liquid crystal and a strong polar anchoring effect. This means that there is a good physical chemical interaction between the poly(vinyl cinnamate) and the liquid crystal. Planar alignment arises when the alignment layers are parallel and  $90^\circ$  twist alignment occurs when the alignment layers are arranged at  $90^\circ$  to one another, see Figure 1.17. The nematic liquid crystal molecules gradually twist throughout the bulk of the liquid crystal until they match both alignment layers. Pre-tilt of the liquid crystal means the molecules are slightly tilted towards the direction they are going to 'switch' to so faster, improved functioning of the liquid crystal results, see Figure 3.2, chapter 3.

Figure 1.17  $90^\circ$  Twist Aligned Cell



It has now been established that in this system it was not the product of cross-linking which was causing the alignment, as was originally proposed but

the alignment of the residual chromophores that had not cross-linked in the poly(vinyl cinnamate) film surface. Also it has been proposed that radical abstraction of hydrogen from the backbone occurs as well as cyclobutane formation during irradiation.<sup>14</sup> Other disadvantages of poly(vinyl cinnamate) are that there is only a small pre-tilt angle and some degradation of the aligning ability occurs after a few temperature cycles.

### **1.5 New Photopolymers for Liquid Crystal Alignment**

New materials that align liquid crystal are desirable in order to study the cross-linking and alignment processes in more detail so as to establish effective systems for eventual application. The criterion for new materials for liquid crystal alignment was that anisotropy induced by light was the absolute priority. The intention was that this primary aim was to be accomplished with the following points in mind.

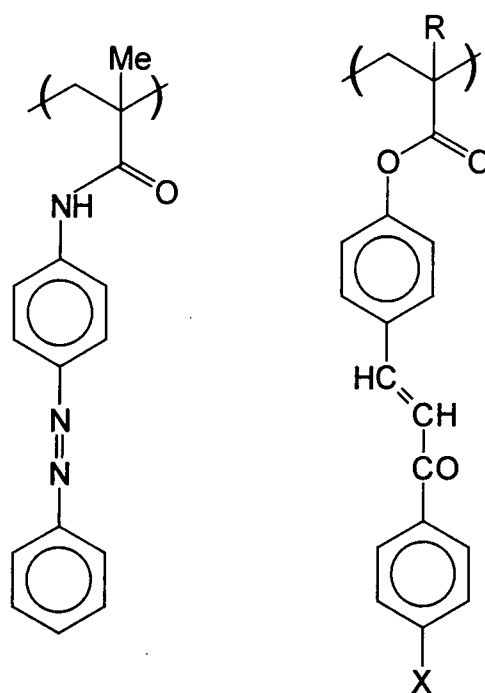
1. Photo-induced positive anisotropy in the polymer is necessary. A material is said to possess positive anisotropy when all the molecules are aligned in the same direction which causes certain physical properties to be different in this direction.
2. The polymer must be insoluble in the liquid crystal after exposure.
3. The polymer must be photo-stable to visible light (400-700nm) after exposure.
4. No ions are to be left in the polymer.

The reasons for the first three requirements are self-evident. The fourth point relates to the intended use of such layers in active matrix displays; if ions were

free in the cells their migration under the influence of the electrical fields could cause problems.

Other photosensitive polymers apart from poly(vinyl cinnamate) have been studied, for example, polymers containing azobenzene or chalcone groups.<sup>16, 17</sup>

Figure 1.18 Examples of other Photosensitive Polymers



In this thesis the synthesis, characterisation and testing of new photosensitive polymers containing anthracene chromophores and azide groups is described.

## References

1. Meier G., Sackman E. and Grabmaier J.G., Applications of Liquid Crystals, Springer Verlag 1975, page 1.
2. Chandrasekhar S., Liquid Crystals, Cambridge University Press, 1977.
3. Meier G., Sackman E. and Grabmaier J.G., Applications of Liquid Crystals, Springer Verlag 1975, page 4.
4. Blinov L.M., Electro-optical and Magneto-optical Properties of Liquid Crystals, John Wiley & Sons Ltd. 1983, page 5.
5. Meier G., Sackman E. and Grabmaier J.G., Applications of Liquid Crystals, Springer Verlag, 1975, chapter 1.
6. van Aerle N.A.J.M., Barmantlo M. and Hollering R.W.J., Effect of rubbing on the molecular orientation within polyimide orienting layers of liquid-crystal displays, J. Appl. Phys. (74), N° 5, 1993, pages 3111-20.
7. Ito T., Nakanishi K., Nishikawa M., Yokoyama Y. and Takeuchi Y., Regularity and Narrowness of the Intervals of the Microgrooves on the Rubbed Polymer Surfaces for Liquid Crystal Alignment, Polymer Journal (27) N° 3, 1995, pages 240-46.
8. Ishihara S., Wakemoto H., Nakazima K. and Matsuo Y., The Effect of Rubbed Polymer Films on the Liquid Crystal Alignment, Liquid Crystals (4) N° 6, 1989, pages 669-75.
9. Blinov L.M., Electro-optical and Magneto-optical Properties of Liquid Crystals, John Wiley & Sons Ltd. 1983, page 103.
10. Williams J.L.R., Photopolymerisation and photocrosslinking of polymers, Fortsch Chem., Fortsch 13, 1969, pages 227-50.

11. Marusii T.Ya. and Reznikov Yu.A., Photosensitive Orientants for Liquid Crystal Alignment, Mol. Mat. (3), 1993, pages 161-68.
12. Minsk L.M., Van Deusen W.P. and Robertson E.M., Photosensitization of Polymeric Cinnamic Acid Esters, US Patent 2610120, 1952.
13. Vogel A., Textbook of Practical Organic Chemistry, 5<sup>th</sup> edition, Longman Scientific and Technical, 1989.
14. Egerton P.L., Pitts E. and Reiser A., Photocycloaddition in Solid Poly(vinyl cinnamate). The Photoreactive Polymer Matrix as an Ensemble of Chromophore Sites, J. Am. Chem. Soc. (14) N° 1, 1981, pages 95-100.
15. Schadt M., Schmitt K., Koznikov V. and Chigrinov V., Surface-induced parallel alignment of liquid crystals by linearly polymerised photopolymers, Jpn. J. Appl. Phys. (31), 1992, pages 2155-64.
16. Kawanishi Y., Tamaki T., Seki T., Sakuragi M., Suzuki Y. and Ichimura K., Multifarious Liquid Crystalline Textures Formed on a Photochromic Azobenzene Polymer Film, Langmuir (7), 1991, pages 1314-15.
17. Rami Reddy A.V., Subramanian K., Krishnasamy V. and Ravichandran J., Synthesis, Characterisation and Properties of Novel Polymers Containing Pendant Photocrosslinkable Chalcone Moiety, Eur. Polym. J. (32), N° 8, 1996, pages 919-26.

## Chapter Two

### Synthesis and Characterisation of an Anthracenyl Homopolymer

#### 2.1 Introduction

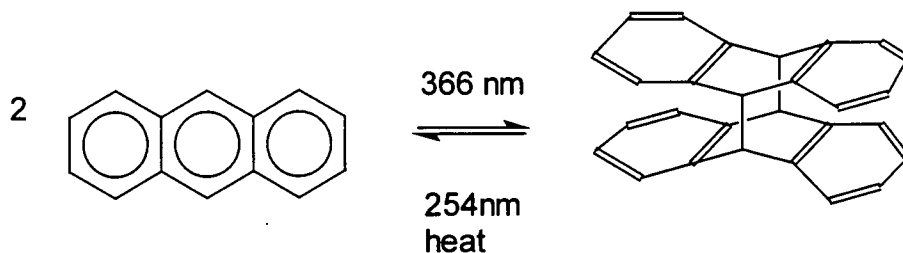
Anthracene was considered to be a suitable chromophore for investigation as the active component of a photo-induced alignment material. This first target was chosen by the sponsors of this work. The photochemistry and photophysics of anthracene has been studied in great detail over many years.<sup>1</sup> The chromophore has several advantages for the purposes of this study for the reasons listed below.

1. The system is well understood.
2. The basic chemistry was expected to be fairly straightforward and the compounds involved stable, the only problem anticipated being the possible addition of dioxygen across the 9, 10-positions (see later).
3. The aspect ratio of the anthracenyl residue and its photodimer make both appropriate as potential alignment groups.
4. The 4+4 photodimerisation of anthracene is wavelength dependent giving, in principle, a write/erase potential, see Figure 2.1. Thus, dimerisation occurs readily at wavelengths  $>365\text{nm}$  and the dimer is cleaved at wavelengths  $<255\text{nm}$ , in practice some photodimerisation occurs at wavelengths  $<255\text{nm}$  as well as cleavage and a competition occurs.

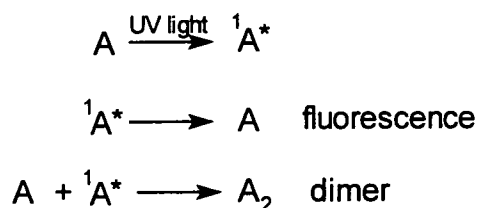
The dimer can be cleaved at high temperature, usually above  $180\text{C}$  but to some extent substituent dependent, this temperature is higher than anticipated

processing or working temperatures so it will not affect the functioning of an anthracenyl polymer as a photo-induced alignment material.

Figure 2.1 The dimerisation and cleavage of anthracene



Anthracene photodimerises by a 4+4 cycloaddition reaction through the 9, 10 positions.<sup>2</sup> In the simplest picture of this process, irradiation with ultra-violet light causes the excitation of an electron to an antibonding orbital associated with the anthracene molecule without changing its spin; that is, an excited singlet is formed. This excited state anthracene can then either release this excitation energy as fluorescence or combine with a ground state anthracene molecule to form a dimer.

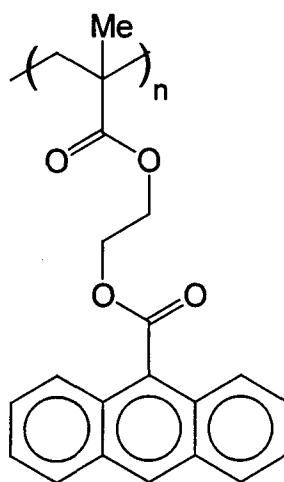


Other processes may occur such as internal conversion, that is a return to the ground state with no emission or intersystem crossing, that is spin inversion to give a triplet (possibly followed by phosphorescence) but these were anticipated to be likely to occur only to a very limited extent in this instance.

The polymer shown in Figure 2.2 was chosen as the first target for synthesis. It was thought that this might prove to be an interesting polymer for assessment as an alignment layer for liquid crystal systems. Selective

photocross-linking of the anthracene chromophores under the influence of polarised ultra-violet light (365nm) was the proposed mechanism for producing anisotropically modified material with an anisotropic surface. As the material will cleave back from the dimer under irradiation with ultra-violet light of <255nm, two approaches to the production of the alignment layer were considered. Namely, anisotropically selective photodimerisation of an isotropic film using polarised light or anisotropic dimer cleavage using polarised light in an isotropically cross-linked film.

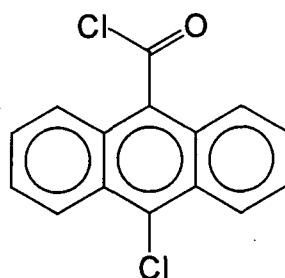
Figure 2.2 Target Anthracenyl Homopolymer (Poly(9'-anthracenoate-2-ethyl methacrylate))



The spacer chain was included so that the anthracene units were allowed sufficient mobility to come into contact with one another and cross-link efficiently. It was hoped that this polymer would perform more effectively than poly(vinyl cinnamate) as an alignment layer, since the physical dimensions, stereoregularity and anisotropy of the photodimers acting as the alignment units were likely to be greater.

To synthesise this polymer the monomer was first made and then polymerised by free radical initiated polymerisation<sup>3</sup>. The first stage was to make 9-anthracenecarboxylic acid chloride from 9-anthracenecarboxylic acid which is commercially available. The method found in the literature<sup>4,5</sup> was followed (carboxylic acid with thionyl chloride heated at 50C) but this proved unsuccessful as a mixture of products was obtained, the main product being not the expected 9-anthracenecarboxylic acid chloride but the analogue carrying an extra chlorine at the 10- position. The product was undesirable for this project since the 10-chlorosubstituent might effect the stability of the photodimer and the attached heavy atom would be expected to modify the photophysics of the system.

Figure 2.3 10-Chloro-9-anthracenecarboxylic acid chloride



This undesired result was reproduced in several attempts at different temperatures, the reaction conditions were clearly too harsh and para chlorination in the 10- position of the anthracene ring occurred, probably via a radical chain process, even at 50C. Chlorination using the Vilsmeier reaction<sup>6</sup> was attempted and this produced the desired product. The Vilsmeier reaction involves the addition of a trace amount of N, N-dimethylformamide (DMF) to the thionyl chloride and carboxylic acid. The reaction can then be performed at room temperature so further aromatic ring chlorination does not occur. The DMF acts

as a catalyst and the mechanistic rationalisation and reaction pathway is outlined below, Figure 2.4.

Figure 2.4 Reaction mechanism of the Vilsmeier chlorodehydroxylation reaction

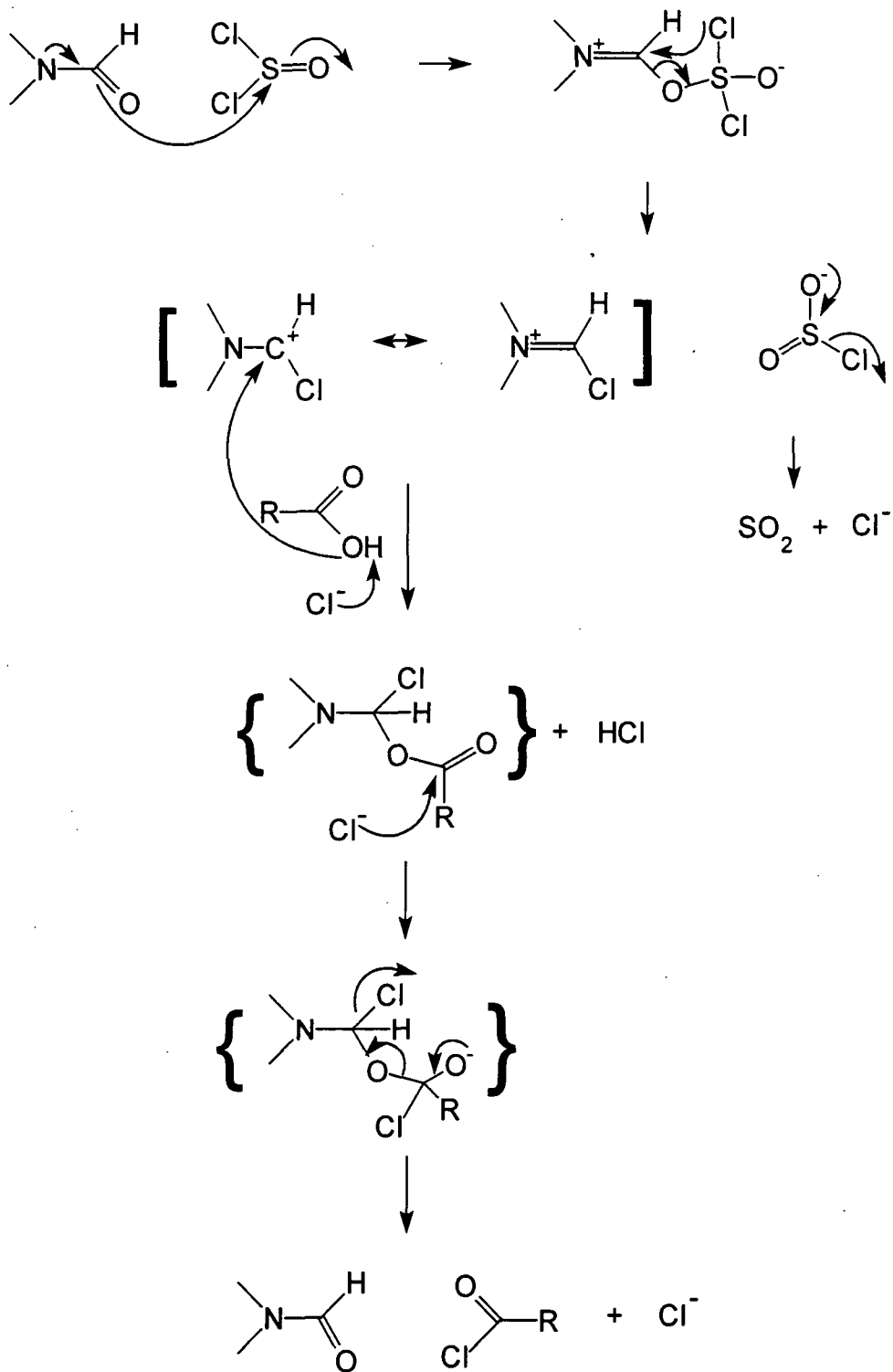
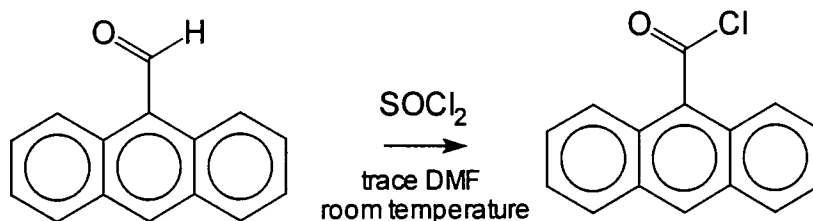
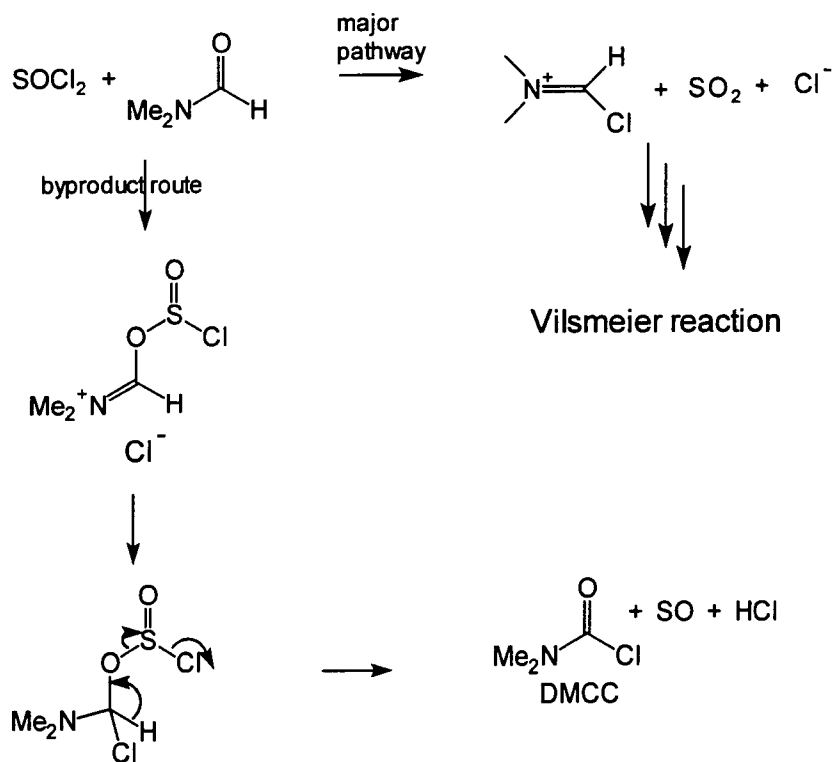


Figure 2.5 Vilsmeier chlorination of anthracenecarboxylic acid



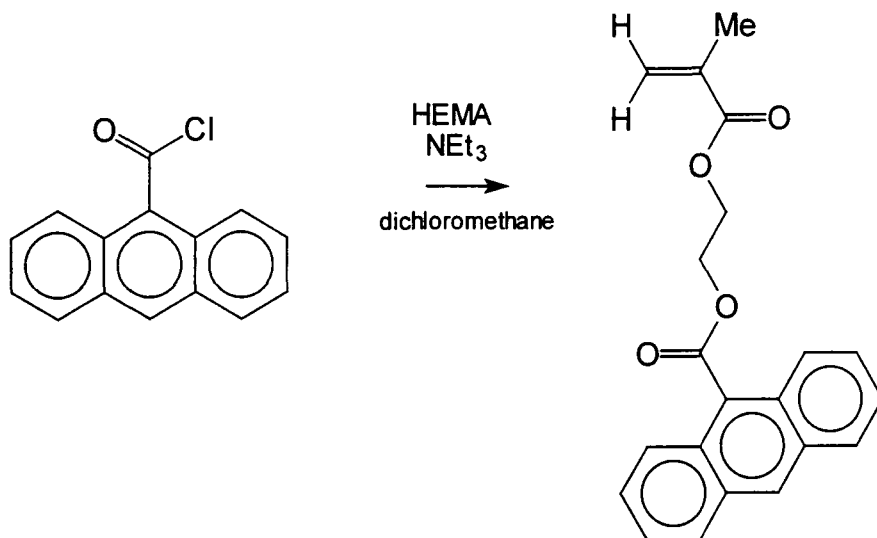
There has been much concern recently over the use of DMF as a catalyst in chlorodehydroxylations<sup>7</sup> such as the Vilsmeier reaction. It was found that dimethylcarbamoyl chloride (DMCC) is formed as a side-product during the reaction, see Figure 2.6. This causes much concern, as DMCC is a known animal carcinogen and potential human carcinogen. Therefore strict safety precautions are required for this reaction.

Figure 2.6 Formation of DMCC as a by-product of the Vilsmeier reaction<sup>7</sup>



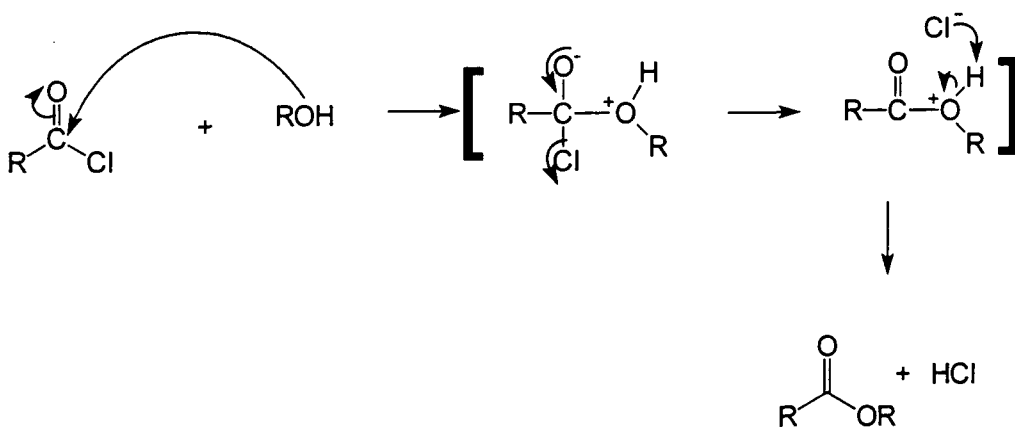
The next stage was to react the 9-anthracenecarboxylic acid chloride with 2-hydroxyethyl methacrylate (HEMA) to form the required monomer.

Figure 2.7 Monomer synthesis



This type of reaction is known as alcoholysis and involves the conversion of an acid halide into an ester<sup>8</sup>.

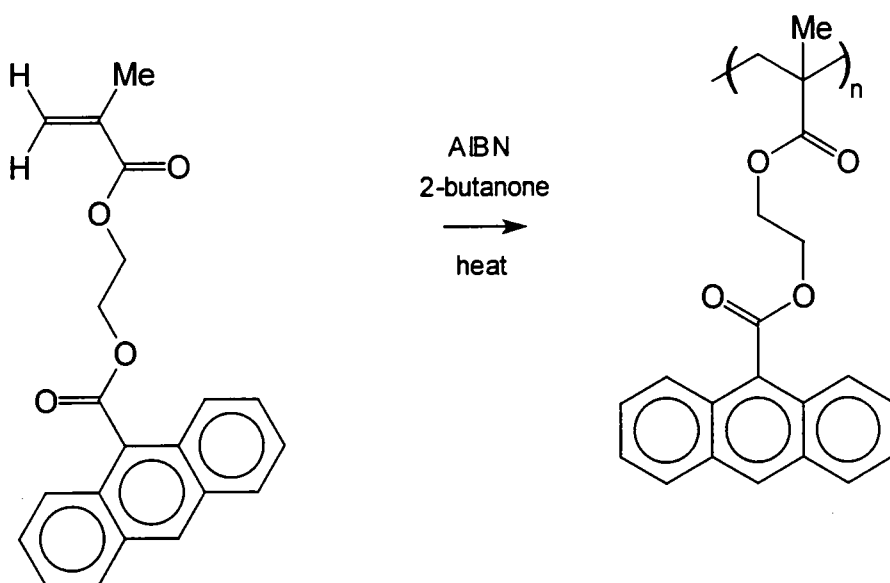
Figure 2.8 Ester formation mechanistic pathway



The reaction was carried out in the presence of triethylamine to react with the HCl formed during the reaction and prevent the formation of by-products from side reactions. If this was not done, the HCl might react with the alcohol to form an alkyl chloride or it might add onto the C=C of the monomer.

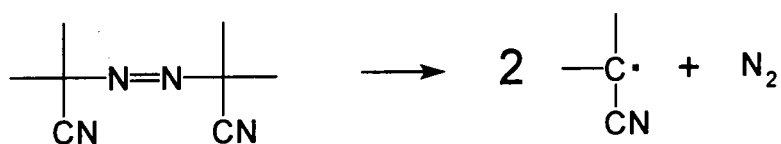
The final reaction in forming the homopolymer was a free radical initiated chain-growth polymerisation<sup>3</sup> using azobisisobutyronitrile (AIBN) as the initiator.

Figure 2.9 Free radical polymerisation



The initiator, azobisisobutyronitrile (AIBN), decomposes on heating to form two radical species that initiate the polymerisation. AIBN can also be used as a photo-initiator but for this reaction the thermal route was chosen as photo-initiation may have caused the anthracene units to cross-link during the polymerisation.

Figure 2.10 AIBN decomposition



There are a minimum of three processes required to describe a free radical polymerisation:-

1. INITIATION



2. PROPAGATION



3. TERMINATION

a) Combination



b) Disproportionation



$R^{\bullet}$  = radical species from initiator

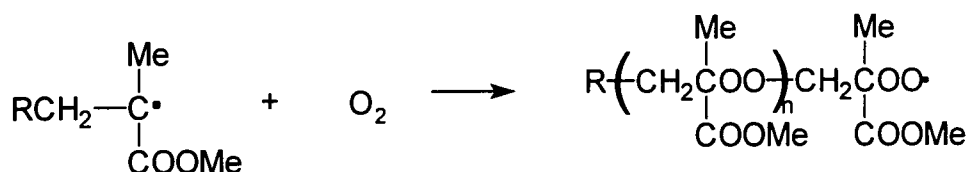
M = monomer

$\bullet$  = single electron of radical species

Termination can also occur by chain transfer of the radical to solvent, initiator or impurities in the reaction mixture. 2-Butanone was the solvent of choice as it has a low chain transfer constant so would not interfere in the polymerisation reaction to a significant extent. Azo initiators, unlike peroxides are not susceptible to chain transfer to initiator, so AIBN was used to initiate the polymerisation. Solution polymerisation was chosen as the preferred polymerisation method as viscosity can be kept low throughout the reaction and the solvent dissipates the heat from the exothermic polymerisation process. This polymerisation was expected to be quite straight forward and conventional. Methacrylates are well established and widely used monomers as a consequence of their structures, they react with electrophilic, free radical and nucleophilic reagents. The electron-withdrawing inductive effect of the ester carbon atom and

the electron-donating resonance effect of the C=O adjacent to the site of the propagating radical account for their ready polymerisability by radical methods. Care has to be taken to eliminate oxygen from the reaction vessel as it inhibits polymerisation and can form an alternating copolymer with the monomer which, being a polyperoxide, is potentially dangerously explosive.<sup>9</sup>

Figure 2.11 Copolymerisation of a methacrylate with oxygen



The presence of dioxygen in methacrylate polymerisations results in a decrease in molecular weight and rate of polymerisation and the formation of a mixture of the copolymer with oxygen and the desired homopolymer.

## 2.2 Experimental

### 2.2.1 Purification of Starting Materials

#### 1. Recrystallisation of Anthracenecarboxylic acid

Anthracenecarboxylic acid was placed in a beaker with a magnetic stirrer bar. Hot ethanol was added with stirring and further heating until all the carboxylic acid had dissolved. The hot solution was filtered quickly through a hot Buchner funnel under vacuum from a water pump then left to cool. Once cool the solution was placed in a refrigerator for two days. The crystals produced were collected by filtration and dried in a vacuum oven at 40C. To confirm the purity of the anthracenecarboxylic acid, thin layer chromatography, melting point,  $^1\text{H}$  NMR,  $^{13}\text{C}$  NMR, IR and mass spectroscopy were used to characterise the acid. Thin layer chromatography showed only one spot indicating only one compound present and the melting point was 219.2-220.1C (literature value 220C from Aldrich catalogue); the spectra were consistent with a pure compound, see appendices.

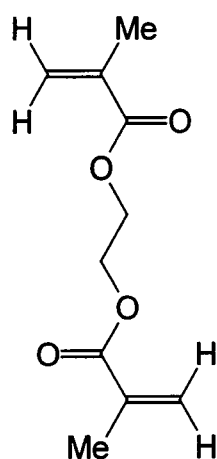
#### 2. Distillation of Thionyl Chloride

Standard distillation equipment was used with the addition of a scrubbing column containing sodium hydroxide solution attached to the top of the condenser to prevent hydrogen chloride and sulphur dioxide gases being released into the atmosphere. The apparatus was purged with nitrogen at the start. The oil bath was at 120C and the distillation head temperature reached 76C during the distillation. Colourless thionyl chloride was collected and securely sealed until required, the material was used within two weeks.

### 3. Distillation of 2-Hydroxyethyl methacrylate

Standard vacuum distillation equipment was used. The 2-hydroxyethyl methacrylate is a monomer that will polymerise when heated so only a low temperature could be applied. The distillation was therefore executed at 35-40C and a pressure of 5mm Hg. Colourless 2-hydroxyethyl methacrylate was collected and stored over activated 4Å molecular sieves in a sealed flask which was wrapped in aluminium foil and kept in the refrigerator (-5C). Distillation is necessary to remove inhibitor (usually hydroquinone or a hindered phenol) from the monomer which is added to prevent polymerisation during storage and also to remove ethylene glycol dimethacrylate which is also present as an impurity in commercial HEMA. Redistilled HEMA is stable for several weeks under these storage conditions.

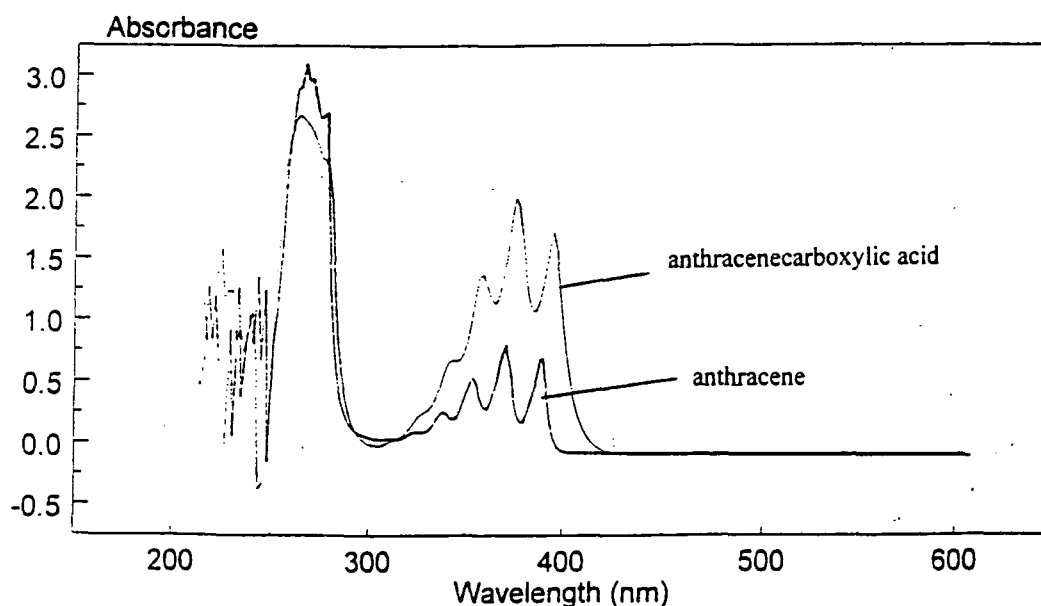
Figure 2.12 Ethylene glycol dimethacrylate



### 4. Decolourisation of Anthracenecarboxylic acid

Anthracenecarboxylic acid is yellow and it would have been better if it were colourless or white for forming films for photo-alignment layers for liquid

crystal cells. Three methods of decolourisation were attempted. The first involved dissolving the anthracenecarboxylic acid in THF then adding decolourising carbon (2% decolourising carbon by weight of the carboxylic acid). This mixture was boiled for 15 minutes then carefully filtered hot through a thick layer of Hyflo filtration aid. The anthracenecarboxylic acid did not decolourise. A second method was tried which involved dissolving the anthracenecarboxylic acid again in THF then filtering it cold through a filter funnel stopped up with cotton wool then filled with decolourising carbon. Finally anthracenecarboxylic acid (4g) was sublimed using temperature gradient sublimation equipment. A heating element heated the carboxylic acid to 200C while it was under vacuum ( $10^{-3}$  mm Hg). The anthracenecarboxylic acid sublimed, solidifying further up the apparatus as small yellow crystals. At this point it was assumed that anthracenecarboxylic acid is intrinsically yellow and cannot be decolourised. UV/vis spectra were run of anthracenecarboxylic acid and anthracene as a comparison. The absorptions were different with anthracenecarboxylic acid having an absorption tailing into the violet/blue region of the visible spectrum which is the reason for the pale yellow colouration.



## 5. Recrystallisation of AIBN

AIBN was dissolved in a minimum amount of methanol at room temperature. The AIBN solution was then placed in a refrigerator for five days. The AIBN crystals that formed were collected by filtration, dried under vacuum at room temperature, stored in a bottle, wrapped in aluminium foil and kept in the refrigerator. Initiator purified and stored in this manner is useful for 2 or 3 months.

### 2.2.2 Synthesis of Anthracene Homopolymer

#### *Synthesis of Anthracenecarboxylic acid chloride*

The acid chloride was synthesised following the scheme outlined in the introduction of this chapter. 9-Anthracenecarboxylic acid(26.08g, 0.117moles) was placed in a single necked round bottom flask, to which a Claisen head was attached leading to a condenser, a liquid air cooled collection flask and a vacuum pump. The Claisen head outlets carried a septum seal and a dropping funnel. The apparatus was purged with nitrogen before starting the experiment. Thionyl chloride(80ml, 1.097moles) was added slowly to the anthracenecarboxylic acid with stirring, after the addition of all the thionyl chloride the mixture was left to stir for 10 minutes. A trace amount (3 or 4 drops) of fresh, dry N, N-dimethylformamide was added through the septum seal using a syringe. The reaction mixture was then left to stir for an hour being continually flushed with nitrogen. The anthracenecarboxylic acid was insoluble in the thionyl chloride but the acid chloride was soluble so when the contents of the flask changed from a

yellow suspension to a pale brown solution the reaction was judged to be complete.

The excess thionyl chloride was removed using low-pressure distillation, 50mm Hg and 40C, residual traces of thionyl chloride were removed by placing the flask of anthracenecarboxylic acid chloride under vacuum overnight ( $10^{-3}$ mm Hg). Step two of the monomer synthesis must be carried out on the next day otherwise the anthracenecarboxylic acid chloride can become partially chlorinated by residual traces of thionyl chloride and this complicates purification. The anthracenecarboxylic acid chloride was obtained in yields of 94-98% and was characterised by melting point 94.4-96.8C (lit. 93.5-94.5C)<sup>3</sup>, <sup>1</sup>H NMR, <sup>13</sup>C NMR, IR and mass spectroscopy, see appendices.

#### *Synthesis of Anthracene Monomer*

The 9-anthracenecarboxylic acid chloride was reacted with 2-hydroxyethyl methacrylate in the presence of triethylamine. Anthracenecarboxylic acid chloride(26.94g, 0.112moles) was placed in a two-neck round bottom flask with a dropping funnel and a condenser attached to the flask. The apparatus was purged with nitrogen during the entire experiment. Dichloromethane(100ml) was added slowly to the flask then left to stir for 20 minutes then triethylamine(8ml, 0.057moles) was slowly added to the stirring dichloromethane solution. 2-Hydroxyethyl methacrylate(15ml, 0.124moles) was dissolved in dichloromethane(30ml) and placed in the dropping funnel. The HEMA solution was added very slowly to the stirring acid chloride solution, ensuring that the reaction temperature did not rise above 20C and left to stir for 2 hours. After the reaction, the dichloromethane solution was washed three times

with an equal volume of distilled water, dried over anhydrous magnesium sulphate then filtered. The dichloromethane was removed by rotary evaporation and the last residual trace of solvent was removed by placing the flask under vacuum overnight. The product was recrystallised by dissolving it in a minimum amount of ethanol at room temperature then placing the solution in a refrigerator at -5C for two days. The crystals were recovered by filtration and were dried under vacuum at room temperature. The monomer had a melting point of 63.7-65.2C.

The experimental conditions recorded above provide a reproducible synthesis, it is important to take care over temperature and rates of addition of reagents; for example, if triethylamine is added too rapidly an exotherm is observed and only triethylamine hydrochloride and starting materials are recovered.

Crystals of the monomer were grown to try to obtain an X-ray crystal structure which might be useful in assigning the alignment of the anthracene functional groups in the photodimer. These crystals were grown by making a concentrated solution of the monomer in ethyl acetate and placing this solution in a 6mm diameter test-tube up to a height of 3cm. An equal volume of hexane was then carefully dripped on top of the ethyl acetate solution, the tube was sealed with a rubber septum and the tube left for four weeks at room temperature in the dark. A few large crystals formed but unfortunately were not good enough for X-ray crystallographic analysis.

### *Synthesis of Anthracene Homopolymer*

The monomer was polymerised using free radical initiated polymerisation. Solution polymerisation was attempted using AIBN as the initiator and 2-butanone as the solvent.

The apparatus consisted of a 250ml flange flask with an overhead electrical stirrer, condenser, thermometer and septum seal attached. There was also an inlet and outlet for nitrogen gas. The apparatus was purged with nitrogen before the experiment and a constant flow of nitrogen was maintained during the experiment. Anthracenyl monomer(15g, 0.045moles) was placed in the flange flask with 2-butanone(80ml) and nitrogen was bubbled through the solution for two hours. The monomer solution was then stirred and heated until the 2-butanone was refluxing (80C). Then AIBN(0.06g, 0.366mmol) dissolved in 2-butanone(10ml) was injected in four aliquots at half hourly intervals into the reaction via the septum seal using a syringe. The reaction mixture was left to stir for four hours then the heat source was removed and the reaction mixture allowed to cool. The reaction mixture was added slowly to stirring hexane to precipitate the polymer. The polymer was dried in a vacuum oven at 40C then characterised by <sup>1</sup>H NMR, <sup>13</sup>C NMR and IR spectroscopy and GPC, see appendices and section 2.3.

The polymers were purified by dissolving the polymeric material in a minimum amount of chloroform then precipitating the polymer by adding the chloroform solution to an excess of cold stirring ethanol. This was repeated three times. The polymer was dried in a vacuum oven at 60C and characterised as before.

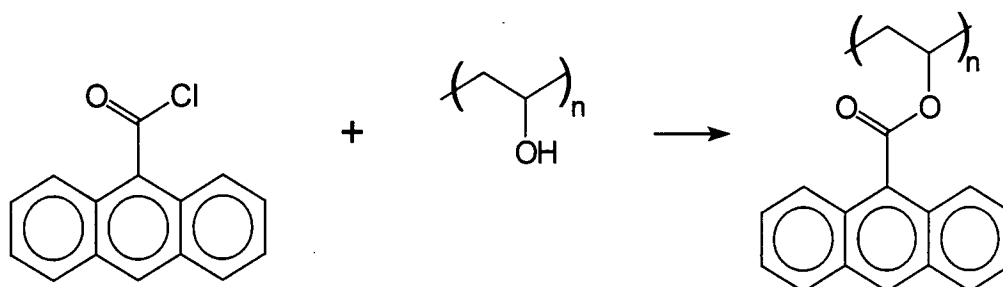
An alternative route for the synthesis of an anthracenyl homopolymer was investigated. This involved the reaction of poly(vinyl alcohol) with 9-anthracenecarboxylic acid chloride. Poly(vinyl alcohol) dissolves in very few solvents, most of which react with acid chlorides. Two methods were attempted.

The anthracenecarboxylic acid chloride had to be rigorously purified for this reaction to make sure that there was no residual thionyl chloride as this would cause undesirable side reactions. Anthracenecarboxylic acid chloride was synthesised as previously and placed overnight under vacuum ( $10^{-3}$  mm Hg). The flask of anthracenecarboxylic acid chloride was let down to nitrogen gas and sealed with a septum seal. A minimum amount of anhydrous toluene was introduced into the flask via injection with a syringe and the mixture was stirred until the acid chloride dissolved. The flask was placed in a refrigerator for three days until crystals formed which were recovered by filtration and used in the next stage.

The reaction was carried out in the same way as the monomer synthesis, the apparatus was the same. Poly(vinyl alcohol) (5g,  $\sim 1 \times 10^{-4}$  moles) was placed in a single-neck round bottom flask with N,N-dimethylformamide (100ml) and heated to 80C with stirring for two hours. The mixture was then cooled to 60C and triethylamine (12ml) was slowly added, then the mixture was left to stir for half an hour. An excess of purified anthracenecarboxylic acid chloride (12g, 0.05moles) was dissolved in 30ml anhydrous DMF and placed in the dropping funnel. This solution was added dropwise to the PVA solution and the reaction mixture left to stir for a further two hours. The DMF was removed by low-pressure distillation (5mm Hg, 50C) then the product was washed with ethanol,

then chloroform to remove any residual impurities. This left a pale brown solid that was not readily soluble. The product was characterised using GPC, melting point, IR,  $^1\text{H}$  NMR,  $^{13}\text{C}$  NMR and mass spectroscopy, see later.

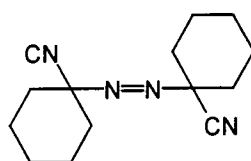
Figure 2.13 Reaction of PVA with anthracenecarboxylic acid chloride



The second method involved dissolving poly(vinyl alcohol) (4.09g,  $\sim 8.2 \times 10^{-5}$  moles) in pyridine (130ml) overnight with refluxing and stirring. A further 90ml pyridine was added to the solution then it was cooled to 50C. Recrystallised anthracenecarboxylic acid chloride (10.02g, 0.042 moles) was dissolved in pyridine (40ml) and added slowly with stirring to the poly(vinyl alcohol) solution. The reaction mixture was left to stir for 4 hours 30 minutes at 50C. The product was washed with chloroform to remove residual impurities, then dried under vacuum overnight ( $10^{-3}$  mm Hg).

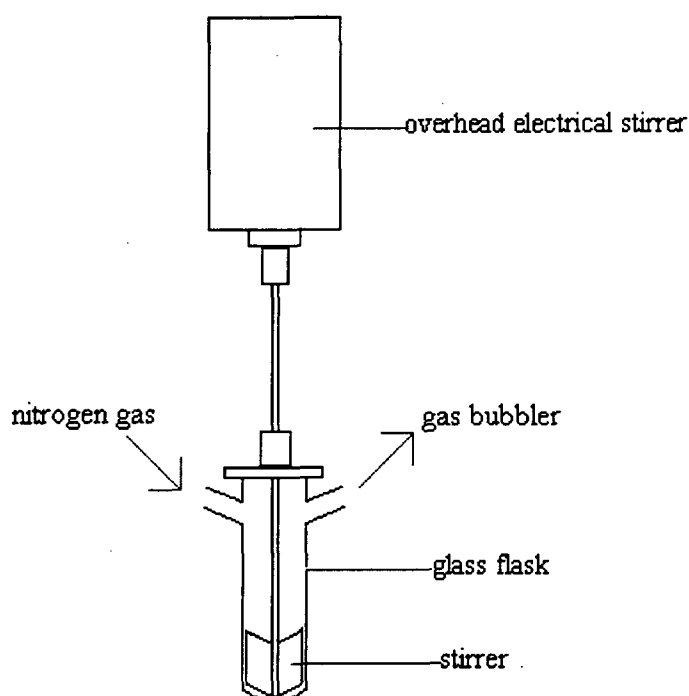
Bulk polymerisation to synthesise the homopolymer was attempted using 1,1'-azobis-(cyclohexanecarbonitrile) as the free radical initiator. This free radical initiator was used as it has a longer half-life at higher temperature than AIBN so was more suitable for this reaction.

Figure 2.14 1,1'-azobis-(cyclohexanecarbonitrile)



For the bulk homopolymerisation, anthracenyl derivatised HEMA (2.04g, 0.0061 moles) was placed in the polymerisation vessel shown below and heated to 68C until all the monomer had melted. A constant stream of nitrogen was maintained throughout the reaction.

Figure 2.15 Bulk polymerisation apparatus



The temperature was raised to 75C and 1,1'-azobis-(cyclohexanecarbonitrile) (0.04g-) was added quickly via an inlet and the reaction mixture was left to stir until it changed from liquid to solid. The reaction was stopped and the product cooled to room temperature, dissolved in chloroform, precipitated in ethanol and dried in a vacuum oven ( $10^{-3}$  mm Hg, 40C).

## 2.3 Results and Discussion

### *9-Anthracenecarboxylic acid chloride*

The anthracene carboxylic acid chloride was difficult to characterise as on contact with the atmosphere it reacted with water and reverted back to anthracenecarboxylic acid. 9-Anthracenecarboxylic acid chloride was produced in good yields as a yellow solid. The melting point observed was 94.4-96.8C, which is slightly higher than the literature value of 93.5-94.5C<sup>5</sup>, the difference and the relatively broad melting range are probably both indications of the difficulty of obtaining this compound absolutely pure.

Figure 2.16 9-Anthracenecarboxylic acid chloride

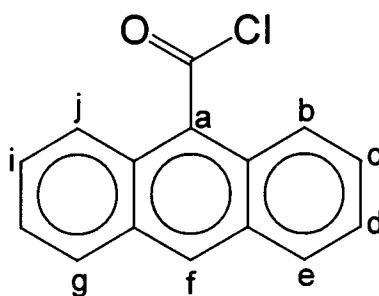


Table 2.1 Yields from acid chloride synthesis

Experiment Code	Mass of Product (g)	% Yield
KEF6	21.21	98
KEF12	26.94	94
KEF15	39.63	94
KEF24	40.12	95
KEF 30	29.72	94

Elemental analysis gave the following results.

Table 2.2 Elemental Analysis of 9-anthracenecarboxylic acid chloride

	C	H	N
experimental	76.86	4.06	0.14
theoretical	74.83	3.77	0

The experimental values fall outside the normal error range for the technique and indicate that either the sample was impure or partially hydrolysed during analysis. The expected molecular ion ( $m/e$  240) with the appropriate  $P+2$  for one chlorine atom was identified by mass spectroscopy and the fragmentation pattern was consistent with that expected for the anthracene acid chloride ( $M-Cl$ , 205;  $M-COCl$ , 177). The  $^1H$  and  $^{13}C$  NMR spectra, see appendices, were consistent with the expected structure, see below, but showed some evidence of impurities. Nevertheless this material was good enough for the next stage of the synthesis and the monomer eventually produced could be satisfactorily purified.

Table 2.3 Assignment of the  $^1H$  NMR spectrum of anthracenecarbonyl chloride

SHIFT/ppm	MULTIPLICITY	INTEGRAL	ASSIGNMENT
7.25	S		chloroform
7.60	MULT (sextet when pure)	4	c, d, h, i
8.08	MULT (DD when pure)	4	b, e, g, j
8.57	S	1	f

In the  $^{13}\text{C}$  NMR spectrum the carbonyl peak (170ppm) and the complicated aromatic region (123-132ppm) can be clearly seen; however, there are more resonances than expected which indicates the presence of an impurity, probably the carboxylic acid.

The IR spectrum (KBr disc) showed a strong absorption for the carbonyl group at  $1679\text{cm}^{-1}$  though there is a peak in the hydroxyl region possibly indicating the presence of anthracenecarboxylic acid, although it may be due (in part) to damp KBr.

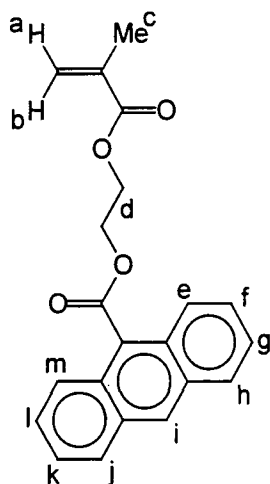
#### *Anthracenyl Monomer*

The anthracenyl monomer was produced in yields of 75-87% by the route described earlier. It had a melting point of 63.7-66.2C and was a pale yellow microcrystalline solid.

Table 2.4 Yields of monomer synthesis

Experiment Code	Mass of Product (g)	% Yield
KEF7	22.04	75
KEF13	32.73	87
KEF25	46.77	84
KEF27	72.83	76

Figure 2.17 9'-Anthracenoate-2-ethyl methacrylate



Elemental analysis gave the values shown below which are well within the error limits of the technique.

Table 2.5 C H N analysis of anthracenyl monomer

	C	H	N
experimental	75.20	5.23	0
theoretical	75.43	5.43	0

Mass spectroscopy showed the expected molecular ion ( $m/e$  334) and the fragmentation pattern was consistent with that expected for the monomer ( $M-C_6H_9O_3$ , 205;  $M-C_7H_9O_4$ , 177;  $M-C_{15}H_9O_2$ , 113;  $C_{17}H_{14}O_3$ , 69). The  $^1H$  NMR spectrum, see appendix two) showed the following signals.

Table 2.6 Assignment of Peaks of  $^1\text{H}$  NMR spectrum of monomer

SHIFT/ppm	MULTIPLICITY	INTEGRAL	ASSIGNMENT
1.58	S		water (contamination of NMR solvent)
1.99	S	3	c
4.61	T	2	d
4.88	T	2	d
5.64	S	1	a
6.23	S	1	b
7.26	S		chloroform
7.51	MULT	4	f, g, k, l
8.02	DD	4	e, h, j, m
8.54	S	1	i

The  $^{13}\text{C}$  NMR spectrum, using KEF13 as an example (see appendix 2), showed the two carbonyls (169 and 167ppm), the methyl group (18ppm), the two  $\text{CH}_2$  groups (62 and 63ppm) and multiple peaks in the range 124-135ppm accounting for aromatic and vinylic carbons. The IR spectrum showed a very complicated fingerprint region but clearly showed the carbonyl ( $1714\text{cm}^{-1}$ ), C-H stretches ( $3048$  and  $2960\text{cm}^{-1}$ ) and a small, broad OH stretch which was probably due to residual ethanol from the recrystallisation process or damp KBr.

### *Anthracenyl Homopolymer*

Solution polymerisation, as described in the Experimental section, gave yields, number average molecular weight and polydispersities as illustrated by the examples recorded in Table 2.7.

Table 2.7 Yields and molecular mass of polymers produced

Experiment Code	Mass of Product (g)	% Yield	$M_n^*$	Polydispersity
KEF20	7.57	50	13200	2.50
KEF23	9.63	55	11800	2.05
KEF46	11.62	57	14000	2.04

\* GPC in chloroform using column set: guard column, PL gel  $5\mu\text{m } 100\text{\AA}$ , PL gel  $5\mu\text{m } 10^3\text{\AA}$ , PL gel  $5\mu\text{m } 10^5\text{\AA}$  and polystyrene calibrants.

The GPC data unambiguously demonstrated that a polymer had been produced. All the polydispersities are around 2 which is the expected molecular weight distribution for a typical well-behaved chain growth polymerisation terminated by disproportionation so it seems reasonable to conclude that the free radical polymerisation is mainly terminated by disproportionation. Yields are not very good and were not improved, in any of twenty experiments, by altering the reaction conditions. This may be a consequence of the bulk of the anthracene unit resulting in steric hindrance and preventing efficient monomer addition. Another possibility may be that anthracene is quenching the free radicals in the polymerisation but the author has no evidence to support either of these hypotheses.

The  $^1\text{H}$  NMR spectrum of the purified homopolymer, see appendix 2, indicated the product was pure. Broadening of the spectrum peaks and the absence of peaks representing the hydrogens of the monomer double bond are consistent with polymer formation. The minor sharp peaks marked S are associated with solvent impurities. The free radical polymerisation of methyl methacrylate displays a tendency towards syndiotacticity. The  $^1\text{H}$  NMR spectrum has been analysed in detail<sup>10</sup> and predominantly syndiotactic and isotactic materials can be readily distinguished on the basis of shift and multiplicity of the hydrogen signals associated with the methyls and methylenes of the backbone. In the case of this substituted methacrylate polymer the broad band at 0.71ppm and the broad band with superimposed sharp line at 1.57ppm are similar, although not identical with the published spectra of predominantly syndiotactic poly(methyl methacrylate).<sup>10</sup>

Figure 2.18 Poly(9'-anthracenoate-2-ethyl methacrylate)

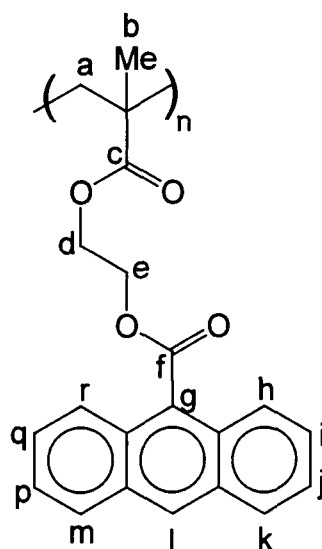


Table 2.8 Assignment of peaks of  $^1\text{H}$  NMR spectrum of homopolymer

SHIFT/ppm	INTEGRAL	ASSIGNMENT
0.71	3	b
1.57	2	a
4.02	2	d
4.35	2	e
7.25	4	i, j, q, p
7.74	4	h, k, r, m
8.16	1	l

The IR spectrum showed a carbonyl peak at  $1725\text{cm}^{-1}$  broadened and shifted to higher frequency when compared to the monomer, C-H stretches at 2940-3065ppm. The non-conjugated ester carbonyl of the polymethacrylate is expected to occur at higher frequency and the broadening is consistent with overlap of the conjugated and non-conjugated carbonyl bond. Stretches for C-O and aromatic C-H and C=C can be found in the complicated fingerprint region. The  $^{13}\text{C}$  NMR spectrum, see appendix 2, was assigned as follows.

Table 2.9 Assignment of peaks of  $^{13}\text{C}$  NMR spectrum of homopolymer

Peak (ppm)	Assignment
18.3	b
30.9	a
62.5	d
63.3	e
77.0	chloroform
124-135	aromatic carbons
167.1	c
169.3	f

These assignments follow in a straight forward manner from literature compilations and the monomer assignment. The spectrum is remarkably clean and simple and raises questions about the tacticity of the polymer. Thus, it is established that even at 75.5 MHz the carbonyl carbon of free radically polymerised MMA can be resolved into eight lines in the region 175 to 179ppm<sup>10</sup> and these lines have been fully assigned to pentad sequences. The  $^{13}\text{C}$  spectra of the anthracenyl polymer was recorded at 100MHz and there were no carbonyl signals in this chemical shift range, indeed only two unresolved lines were detected, that at 169.3ppm is assigned to the anthracenyl carbonyl with the 167.1ppm signal to the methacrylate carbonyl, the implication being that the polymer is highly tactic and presumably, on the basis of the  $^1\text{H}$  NMR analysis, syndiotactic. The other backbone carbon resonances were expanded and that associated with the methyl signal could be resolved into two signals with the

predominant signal constituting 85% of the intensity. The methylene backbone carbon was unresolved. Taken together these NMR data indicate that the polymer is most probably 85% syndiotactic, although the general lack of resolved fine structure in the characterising  $^{13}\text{C}$  resonances probably merits further study. The result, namely 85% syndiotacticity on free radical polymerisation of a methacrylate carrying a bulky substituent is not unreasonable.

The attempted synthesis of an anthracenyl polymer from poly(vinyl alcohol) proved unrewarding, the experimental details have been given earlier. A typical experiment is summarised below.

Table 2.10 Reaction of PVA and anthracenecarboxylic acid chloride in  $\text{NEt}_3$

Experiment Code	Mass of PVA (g)	Volume Triethyl-amine (ml)	Volume DMF (ml)	Mass of Acid Chloride(g)	Mass of Product
KEF31	5	12	190	12	5.03

This reaction did not appear to be successful. The IR spectrum was very similar to that of the poly(vinyl alcohol)(PVA) starting material, with a large OH stretch ( $3440\text{cm}^{-1}$ ) indicating the presence of many OH groups remaining on the polymer backbone. However, there was a small carbonyl stretch at  $1717\text{cm}^{-1}$  indicating the presence of the anthracenoate unit. The  $^1\text{H}$  spectrum in deuterated DMSO, see appendix 2, duplicated that of a poly(vinyl alcohol) spectrum, except for some very small peaks in the aromatic region (8-8.4ppm). Finally the  $^{13}\text{C}$  NMR spectrum showed no anthracene present, as there were no aromatic peaks so the spectrum was of poly(vinyl alcohol). The product resembled the PVA

starting material in consistency and appearance, the only difference being a slight change in colour from white to pale beige. From these results it is evident that the reaction did not work as planned, the presence of a small amount of the anthracenoate units in the product may mean that it is trapped within the polymer and will not wash out properly or there was a very small amount of addition of the anthracenecarboxylic acid chloride to some of the hydroxyl sites on the poly(vinyl alcohol).

Table 2.11 Reaction of PVA and anthracenecarboxylic acid chloride in pyridine

Experiment Code	Mass of PVA (g)	Volume of pyridine (ml)	Mass of Acid Chloride (g)	Mass of Product (g)
KEF37	4.09	260	10.02	4.27

The IR spectrum of the product from this reaction, see appendix 2, was different to that of PVA as there was a very complicated fingerprint region, a good carbonyl peak ( $1790\text{cm}^{-1}$ ) and peaks in the aromatic region ( $1076\text{cm}^{-1}$ ). There was still a large OH stretch but it was not as large as that of the starting material. A  $^{13}\text{C}$  NMR spectrum was not possible as the product was only sparingly soluble so not enough would dissolve in any of the available NMR solvents to give a good carbon spectrum. The  $^1\text{H}$  NMR spectrum in deuterated DMSO duplicated that of the PVA starting material, see appendix 2, apart from small peaks in the aromatic region (7-9ppm) indicating the presence of the anthracene group. The product from this reaction looked different from the PVA starting material. It was pale brown in colour and absorbed solvents on their addition forming a sticky solid which was less soluble than the product from the

earlier attempt (KEF31). From the characterisation results it looked as if the anthracene had added onto the PVA partially but not as well as hoped or perhaps the anthracene was just trapped in the polymer structure. Even if the PVA and acid chloride reactions had worked it would be unlikely that the anthracene side chain would occur as frequently along the polymer chain as in the anthracene monomer polymerisation. This method does not give the amount of control needed to produce an efficient alignment layer. Also a shorter spacer chain would result which may not provide the anthracene units with enough mobility to come into contact with one another and dimerise.

The bulk polymerisation method was much more successful and polymer was readily obtained in 91% yield. However, characterisation of this homopolymer was unsuccessful as it was insoluble so only an IR spectrum could be obtained. The insolubility was probably due to the formation of branches and cross-linking during the polymerisation which is less controlled than the solution route. The IR spectrum resembled the IR spectra of solution made anthracenyl polymers, the carbonyl could be seen at  $1726\text{cm}^{-1}$ , C-O and aromatic stretches at  $1198$  and C-H stretches at  $2925\text{cm}^{-1}$ .

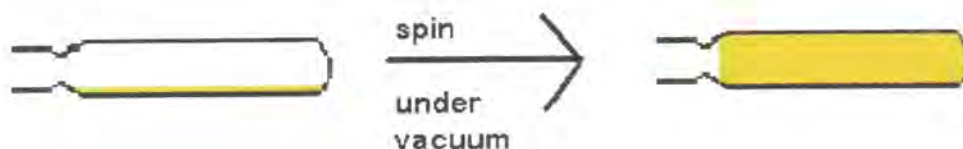
High molecular mass in bulk polymerisations is due to the Trommsdorf effect. As the polymerisation proceeds, there is a marked increase in viscosity which reduces the diffusion rate of the polymer chains. If the diffusion rate decreases, the rate of termination of radicals decreases as the growing chain ends can no longer easily reach one another as they are slow moving and few in number. Therefore the chains add more monomer residues and there is an

increase in molecular mass. The formation of cross-links occurs by a chain transfer mechanism involving hydrogen abstraction from the polymer chain as well as by cross-linking of the chromophores.

#### 2.4 Film Forming and Cross-linking

The film forming ability of the polymer was tested by forming a film in a glass vessel using a rotary evaporator, see figure 2.19 below. A solution of the homopolymer dissolved in chloroform was placed in a glass tube then the tube was spun on a rotary evaporator. A vacuum was applied slowly using a water pump and the chloroform evaporated, leaving a fairly even coating of film on the surface of the glass tube. It was possible to scrape off this film so producing a free standing transparent film which was fairly brittle and cracked when folded.

Figure 2.19 Formation of a film of poly(9'-anthracenoate-2-ethyl methacrylate)

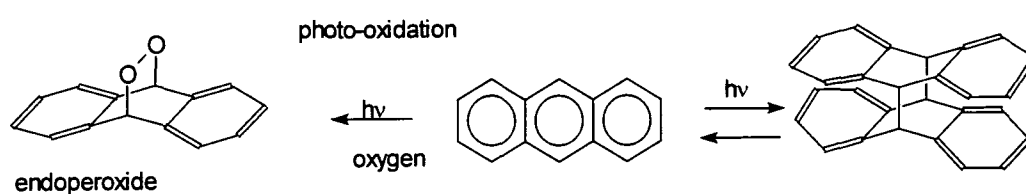


In practical applications the polymer would be spin-coated onto a layer of ITO coated glass from a 2-5% solution of chlorobenzene and dichloromethane with the film layer being approximately 30nm-1 $\mu$ m thick. The fact that this material gives brittle free standing film is not an important factor in this application.

Anthracene was chosen as the chromophore because of its unusual property of cross-linking at one wavelength (>290nm) to give a dimer which is cleaved at a lower wavelength (<254nm). Heat can also cause the latter process

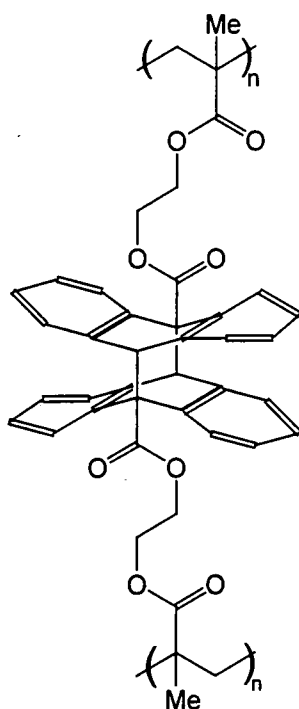
of cleavage but this should not affect the application of the anthracene derivative of poly(hydroxy-2-ethyl methacrylate) as the temperature is sufficiently high so as not to be a problem during production or the functioning of the alignment layer. It must be noted though, that oxygen quenches photodimerisation of anthracene by forming an endoperoxide across the 9, 10 positions (see earlier)<sup>9</sup>.

Figure 2.20 Photo-oxidation and dimerisation of anthracene



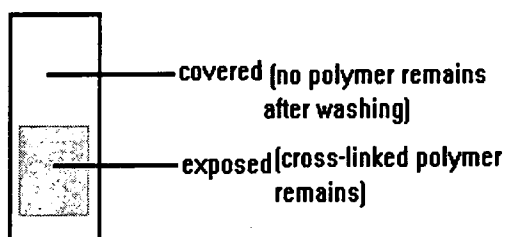
Therefore to produce only the photodimer, oxygen must be eliminated from the film. Tests on cross-linking have been carried out in the laboratories at the DRA Malvern by Dr. Ian Sage and Dr. Guy Bryan-Brown. The concept on which this work was based has been established since the initial findings show that the homopolymer material works as well as poly(vinyl cinnamate) as an alignment layer. The anthracene homopolymer undergoes photochemical modification and exhibits photo-induced birefringence.

Figure 2.21 Cross-linked poly(9'-anthracenoate-2-ethyl methacrylate)



A quartz slide was coated with a thin film of the anthracenyl homopolymer using a Dynapert Precima Ltd. photoresist spinner to spin cast the films. The slide was irradiated by a deuterium lamp (30W,  $\lambda=185-370\text{nm}$ ), with one half covered with black card. After irradiation the slide was washed with chloroform.

Figure 2.22 Quartz slide after exposure to UV light



The polymer film that had been covered by the card washed off the slide but the film that had been irradiated by the deuterium lamp was insoluble. Therefore something had occurred and it was presumed that the film had cross-linked via

the anthracene units. Samples of the homopolymer were given to the DRA and Helen Varley (Ph.D. student working on this project) for further investigation into the process that was occurring. It was found that the film was cross-linking as had been predicted.

## 2.5 Conclusions

The anthracenecarboxylic acid chloride was made in good yields when the Vilsmeier method was used instead of the literature method<sup>6</sup>. The substituted HEMA monomer was produced in good yields. This proved that the chemistry worked and the monomer could be produced. Problems were encountered when producing the polymer as the procedure adopted produced only low yields of product, the highest being 57%. The probable explanation is that either steric hindrance from the anthracene groups or quenching of free radicals by anthracene is occurring during the reaction. It is fairly easy to purify the products and good samples of pure homopolymer have been obtained. Other methods of polymerisation were investigated but these did not work satisfactorily. The direct reaction of 9-anthracenecarboxylic acid chloride with poly(vinyl alcohol) did not work well. The aromatic hydrogens seen in the <sup>1</sup>H NMR spectra have small peak intensities. This was probably due to the fact that only a small amount of anthracenecarboxylic acid chloride added onto the PVA hydroxyl groups or the anthracenecarboxylic acid chloride is trapped in the PVA matrix and has not added to the polymer at all. Bulk polymerisation produced polymer in good yields but the reaction was not well controlled and the product was insoluble so could not be fully characterised or used as an alignment layer. Therefore solution

polymerisation seemed the best method to use to produce poly(9'-anthracenoate-2-ethyl methacrylate) homopolymer.

Poly(9'-anthracenoate-2-ethyl methacrylate) formed films from chlorinated solvents and when exposed to ultra-violet light became insoluble. It was assumed that this implies that cross-linking occurred. Samples of the homopolymer were given to the DRA in Malvern and Helen Varley (Ph.D. student) for further investigation. Results from these tests showed that the anthracene does cross-link when irradiated with polarised ultra-violet light and the cross-linked polymer aligns liquid crystal when incorporated into a cell. This system works at least as well as poly(vinyl cinnamate) as an alignment layer for liquid crystal devices. Work at Malvern suggests that this material works by a different alignment mechanism to that found in poly(vinyl cinnamate). The mechanism is still under investigation.

## References

1. Durr H. and Bouas-Laurent H. ed., Photochromism Molecules and Systems, Elsevier Science Publishers B.V. 1990, pages 562-80.
2. Gilbert A. and Baggott J., Essentials of Molecular Photochemistry, Blackwell Scientific Publishers, 1991.
3. Bevington J.C., Radical Polymerisation, Academic Press Inc., 1961.
4. Salari H., Yeung M., Douglas S. and Morozowich W., Detection of Prostaglandins by High-performance Liquid Chromatography after Conversion to para(9-anthroyloxy)phenacyl esters, Analytical Biochemistry (165), 1987, page 222.
5. Goeckner N.A. and Snyder H.R., The Reaction of Cyanide Ion with Carbonyl Compounds in Dipolar Aprotic Solvents, J. Org. Chem. (38) N° 3, 1973, pages 481-3.
6. Fieser and Fieser, Reagents for Organic Synthesis, John Wiley & Sons Ltd. 1967, pages 286-9.
7. Levin D., Toxicological Concerns, letter to Chemistry and Industry N° 1, January 1997, page 2.
8. McMurry J., Organic Chemistry, 2<sup>nd</sup> edition, Brooks/Cole Publishing Company, 1988.
9. Cowie J.M.G., Polymer: Chemistry and Physics of Modern Materials, 2<sup>nd</sup> edition, Thomson Litho Ltd., 1991.
10. Ibbett R.N., NMR Spectroscopy of Polymers, Blackie Academic and Professional, 1993, pages 28-39.

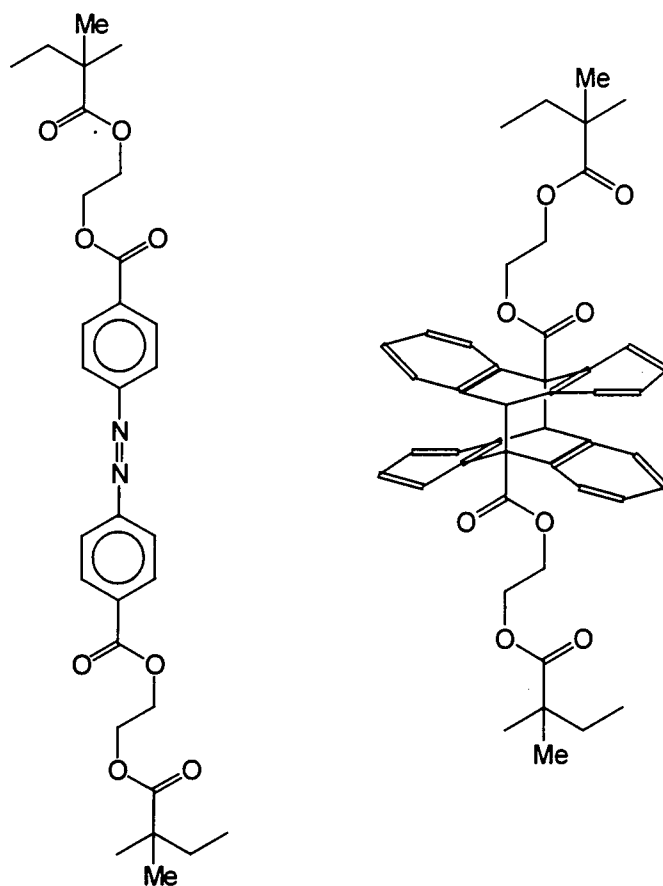
## Chapter Three

### Synthesis and Characterisation of an Azide Homopolymer

#### 3.1 Introduction

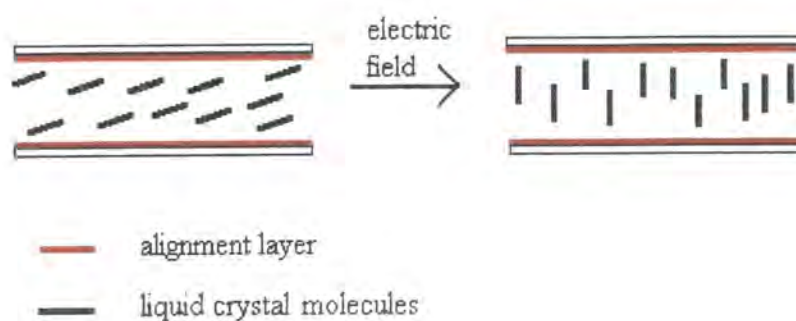
The next homopolymer considered to be a suitable material for liquid crystal alignment was a methacrylate with appended azide groups. It was hoped that this polymer would perform better than the anthracene homopolymer, as it would incorporate some pre-tilt into the alignment layer. Pre-tilt of the liquid crystal occurs when there is an angle between the liquid crystal director and the polymer alignment layer surface.<sup>1</sup> The pre-tilt is caused by electronic interaction and steric repulsion between the liquid crystal molecules and the alignment layer surface. These effects are influenced by molecular surface structures and alignment layer polymer conformation<sup>2</sup> (length and surface density of chains). Figure 3.1 shows a comparison of cross-linked anthracene and azide polymers. When the anthracene polymer is exposed to polarised light the polarisability anisotropy decreases but the opposite effect was predicted for the azide system because of the expected structure. If the polarisability anisotropy increases the cross-linked polymer will align the liquid crystals and related systems have caused a degree of pre-tilt. The exact mechanism for the process occurring is unknown but there is ongoing investigation by other research groups into pre-tilt angles and their causes.

Figure 3.1 A Comparison of the Structures of cross-linked Poly(anthracenoate-2-ethyl methacrylate) with an Azobenzene cross-linked Azido Polymer



The pre-tilt effect allows more efficient 'switching' of the nematic liquid crystal by an electric field. The liquid crystal molecules are already slightly tilted towards the direction they are going to 'switch'. As a consequence, when an electric field is applied the liquid crystal molecules move faster to the upright position, see figure 3.2.

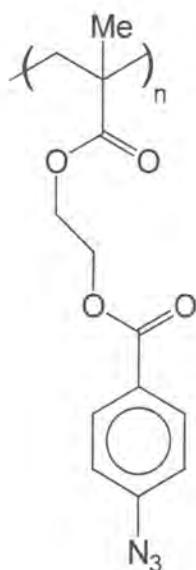
Figure 3.2 Switching of Pre-tilted Liquid Crystal



Cross-linking of this polymer was expected to be accomplished by photochemically promoted nitrogen elimination from the aryl azide followed by dimerisation to form azobenzene links. This would give an enhancement in polarisability anisotropy on dimerisation and the transition moment would be along the principal polarisability axis. The cross-linking reaction is irreversible and the system would be expected to provide a pre-tilted alignment with reasonable stability (see previous page).

The polymer shown below was chosen as the target for synthesis and study.

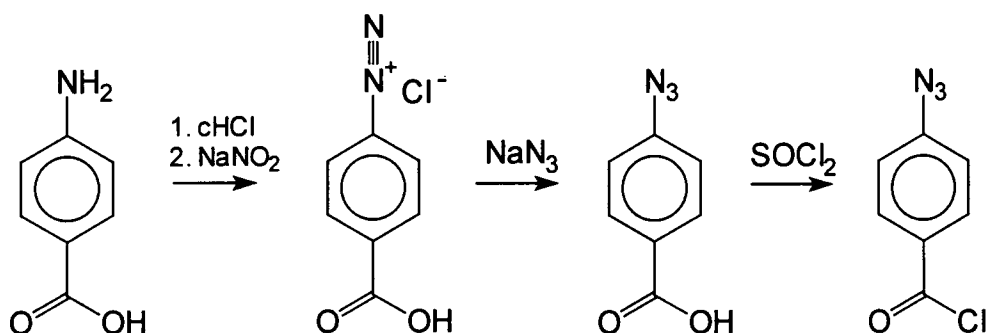
Figure 3.3 Poly(para-azidobenzoate-2-ethyl methacrylate)



An azide group attached to an aromatic ring is appended to a polymer chain. Azide polymers have been found to respond quite effectively to irradiation but have been mainly used previously as cross-linkers for photoresists<sup>3</sup> and not as alignment layers for liquid crystal devices.

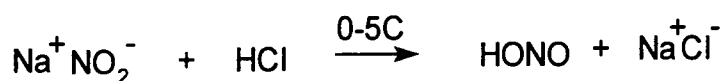
The first step in the synthesis was to convert 4-aminobenzoic acid to 4-azidobenzoic acid chloride. This was accomplished in two stages, the initial stage being the formation of the azide group from the amine then the 4-azidobenzoic acid was chlorinated with thionyl chloride.

Figure 3.4 Formation of 4-Azidobenzoyl chloride



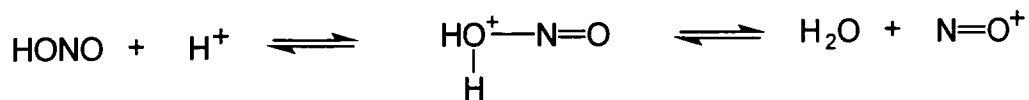
Diazotisations are performed at low temperature (0-5C) because nitrous acid (HONO) decomposes rapidly at room temperature. Nitrous acid is reasonably stable at low temperatures and has to be prepared as required because it cannot easily be stored. The nitrous acid was formed by the reaction of aqueous sodium nitrite with hydrochloric acid.

Figure 3.5 Formation of Nitrous Acid



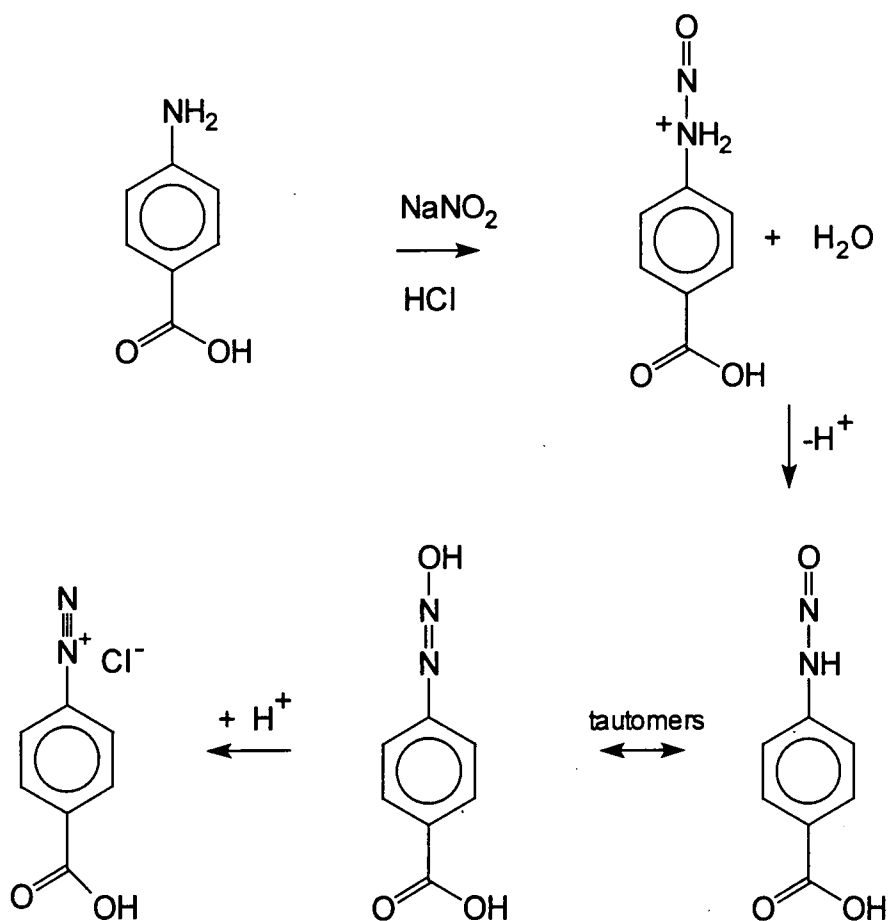
The nitrosonium ion ( $\text{NO}^+$ ) is the reactive species in reactions involving nitrous acid.

Figure 3.6 Formation of the Nitrosonium Ion



Diazo compounds are not generally isolated in their solid form as they tend to be explosive. The first step of diazotisation is the nucleophilic attack of the primary amine on the reactive nitrosonium ion, followed by loss of a proton. Then the oxygen is protonated and water eliminated giving the aromatic diazonium salt.

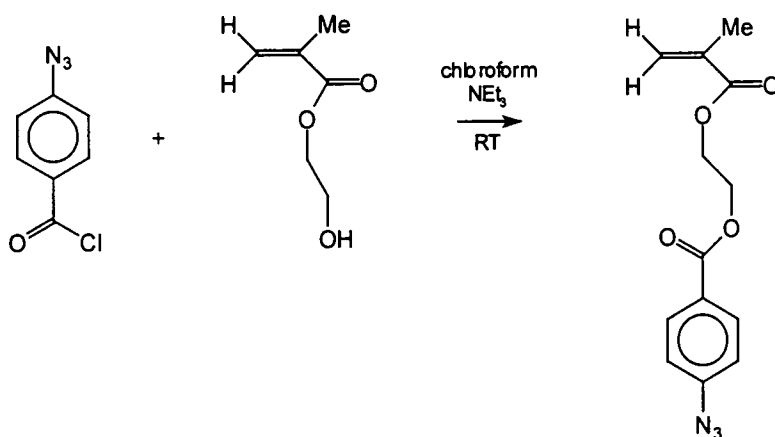
Figure 3.7 Formation of a Diazonium Salt



The diazonium salt is converted to 4-azidobenzoic acid by the addition of aqueous sodium azide. 4-Azidobenzoic acid is then chlorinated using thionyl chloride to produce 4-azidobenzoyl chloride.

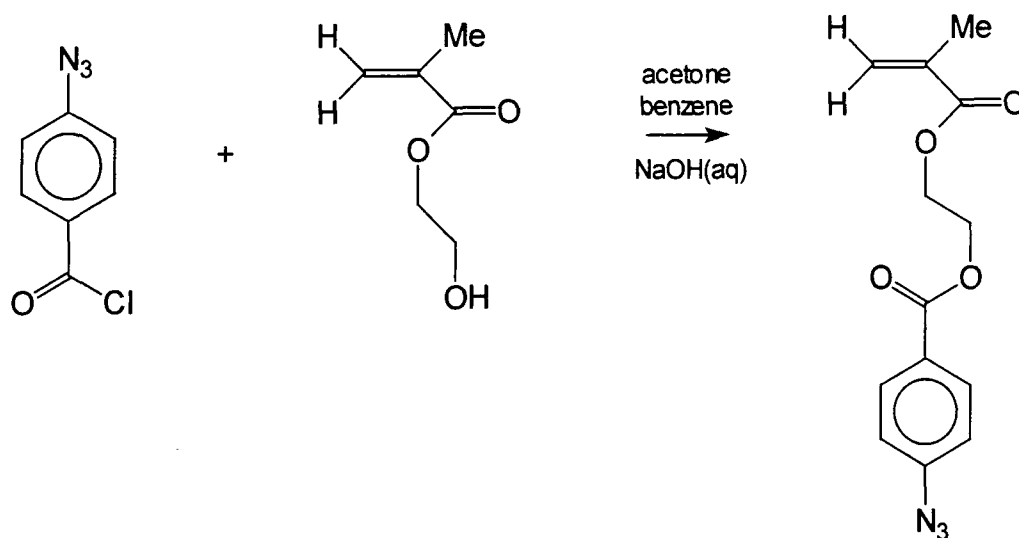
The next stage was the formation of the desired monomer from 2-hydroxyethyl methacrylate (HEMA) and 4-azidobenzoyl chloride. The first method attempted is outlined in the reaction pathway below.

Figure 3.8 Monomer Synthesis 1



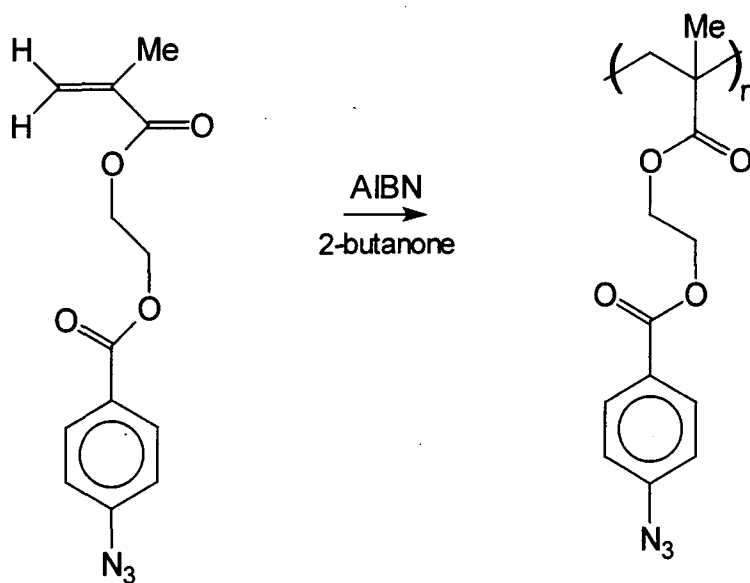
This did not work as expected (see Results and Discussion section) so a different approach was attempted involving the Schotten-Baumen reaction<sup>4</sup>. There is a problem with the Schotten-Baumen reaction as one of the solvents used is water and one of the reactants an acid chloride. Hydrolysis of the acid chloride must be slower than ester formation for this reaction to work successfully. The strong base, sodium hydroxide, prevents side reactions occurring with the hydrogen chloride formed, such as addition to the double bond.

Figure 3.9 Monomer Synthesis 2



The reaction used to polymerise the azide monomer was a free radical initiated polymerisation using 2-butanone as the solvent and AIBN as the initiator. The process of free radical polymerisation was discussed in Chapter 2 (p29).

Figure 3.10 Polymerisation of the Azide Monomer



There was a problem with the azide monomer polymerising spontaneously during storage so inhibitors, 4-methoxyphenol and 4-tert-butylcatechol, were used to overcome this problem. Inhibitors have the ability to absorb free radicals and therefore stop or slow down the polymerisation process. The inhibitor molecule reacts with a free radical forming a stable free radical species that does not react further. Typical inhibitors include quinone, hydroquinone and substituted phenols. Quinones are generally added to monomers that are available commercially, e.g. styrene and acrylates, to prevent polymerisation during storage. The inhibitors can be removed by low pressure distillation or washing with an aqueous weak base.

It is worth mentioning at this point the safety aspect of handling and reacting compounds containing the azide group. All azides, organic and inorganic have the potential to be dangerously explosive. They can explode under the stimulus of heat, impact, friction or apparently spontaneously. Therefore careful handling is required at all times; ground glass joints were avoided and non-metallic vessels and equipment were used as metal azides are the most unstable of the azide compounds (only sodium azide is relatively safe). The aryl azides used in this work are relatively stable.

Other polymers incorporating the azide group have been made by adding the azide group onto PVA, PVC, cellulose, gelatin and copolymers of maleic anhydride. Azido methacrylates and azidostyrene have also been made<sup>5</sup>. These polymers have mainly been used as photoresists and not as the alignment layer of liquid crystal devices.

## 3.2 Experimental

### 3.2.1 Purification of Starting Materials

#### 1. AIBN

The purification method used for AIBN can be found in chapter 2 (p35).

#### 2. 4-Aminobenzoic acid

4-Aminobenzoic acid as supplied was dissolved in 4-5% HCl(aq.) at 50-60C, mixed with decolourising carbon (2% by mass) and stirred for 30 minutes, after filtration the colourless solution was carefully treated with 30% sodium carbonate solution to adjust the pH to 3.5-4. The 4-aminobenzoic acid which precipitated was recovered by filtration and recrystallised from ethanol.

#### 3. 2-Butanone

2-Butanone was dried over potassium carbonate (anhydrous) then purified by fractional distillation using standard distillation equipment.

#### 4. HEMA

The purification method used for HEMA can be found in chapter two (p33).

#### 5. Thionyl Chloride

The purification method used for thionyl chloride can be found in chapter two (p32).

### 3.2.2 Synthesis of Azido Homopolymer

#### *Synthesis of 4-Azidobenzoic acid*

4-Aminobenzoic acid (2g, 0.0145 moles) was placed in a two-neck, 250ml round bottom flask with distilled water (50ml). A dropping funnel and

condenser were attached to the flask and the apparatus was flushed with nitrogen gas. Aqueous hydrochloric acid (3.5ml, 1.18M) was added to the flask with stirring and then the mixture was cooled to 0-5C in an ice bath. Sodium nitrite (1g, 0.0145 moles) in water (15ml) was slowly added and the solution was left to stir at 0-5C for two hours. This solution was filtered and placed in a 500ml two-neck round bottom flask, sodium azide (0.95g, 0.0146 moles) in water (20ml) was added slowly to the cool solution and this was left to stir until no more gas was produced by the reaction. The reaction mixture was left to stand overnight. The next day the mixture was filtered to recover the product which was recrystallised from methanol to give pure, yellow 4-azidobenzoic acid (2.29g, 96% yield), characterisation data are presented and discussed in the Results and Discussion section.

#### *Synthesis of 4-Azidobenzoyl chloride*

4-Azidobenzoic acid (2.29g, 0.014 moles) was heated with redistilled thionyl chloride (30ml, 0.3 moles) at 50-60C for two hours. The thionyl chloride was removed by vacuum distillation (20mm Hg, 40C) and the product placed under vacuum ( $10^{-3}$  mm Hg) to dry overnight. The 4-azidobenzoyl chloride was yellow/orange in colour (2.16g, 97% yield).

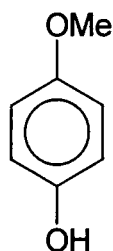
#### *Synthesis of Azido monomer*

Two different methods of reacting HEMA with 4-azidobenzoyl chloride to form the monomer were examined. The first method involved the reaction of the acid chloride with HEMA at room temperature in chloroform and triethylamine. 4-Azidobenzoyl chloride (4.94g, 0.0272 moles) was dissolved in

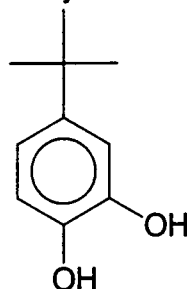
chloroform (80ml) in a two-neck round bottom flask with a condenser and a dropping funnel attached. Triethylamine (4ml, 0.0287 moles) was added to the stirring solution, the apparatus was flushed with nitrogen and left for 10 minutes. HEMA (4ml, 0.033 moles) dissolved in chloroform (15ml) was placed in the dropping funnel then added slowly to the stirring mixture. The solution was left to stir for 2 hours. Then the solution was washed three times with equal volumes of distilled water to remove the triethylamine and any excess HEMA. The product was difficult to characterise as it tended to spontaneously polymerise unless stored in solution, wrapped in aluminium foil and stored in the refrigerator at -5C. Free radical inhibitors (4-methoxyphenol and tert-butylcatechol) were added to the reagent mixture during monomer synthesis in all of several attempts to achieve this synthesis but polymerisation occurred every time.

Figure 3.11 Polymerisation Inhibitors

4-methoxyphenol



4-tert-butylcatechol



It was also found that not all the HEMA was being removed from the azido monomer during washing so when it was polymerised a copolymer with HEMA was formed.

The second method of synthesising the azido monomer investigated was to use the Schotten-Baumen reaction. 4-Azidobenzoyl chloride (5.84g, 0.0322 moles) dissolved in a 3:1 mixture of acetone (15g) and benzene (5g) was slowly

added to a mixture of NaOH solution (15% weight for weight in water, 48g) and HEMA (4.52g, 0.0373 moles) dissolved in a 3:1 acetone-benzene mixture (28g) with vigorous shaking. This mixture was stirred vigorously for 90 minutes. The product was extracted with diethyl ether, the combined organic extract was washed three times with equal volumes of water, once with dilute acid and a further three times with equal volumes of water. The solvents were removed by rotary evaporation and the product dried under vacuum at room temperature to give 4-azidobenzoate-2-ethyl methacrylate, 7.62g 86% yield. Characterisation data are presented and discussed later.

### *Homopolymer Synthesis*

The azido homopolymer was prepared by free radical polymerisation, using 2-butanone as the solvent and AIBN as the free radical initiator. The azido monomer (5.1g, 0.0185 moles) in 2-butanone (90ml) was placed in a 250ml flange flask with a condenser, overhead electrical stirrer, nitrogen inlet and outlet, a thermometer and a septum seal. The apparatus was flushed with nitrogen gas and the condenser was cooled with tap water throughout the experiment. The monomer solution was heated to 65C then AIBN (0.031g,  $1.8 \times 10^{-4}$  moles) in 2-butanone (10ml) was added using a syringe via the septum seal. The reaction mixture was left to stir for 3 hours. The polymer was precipitated by pouring the reaction mixture into hexane(800ml) then collected by filtration and dried in a vacuum oven at room temperature ( $10^{-3}$ mm Hg). The polymer, poly(para-azidobenzoate-2-ethyl methacrylate) was purified by reprecipitation from chloroform into hexane and dried in a vacuum oven, this

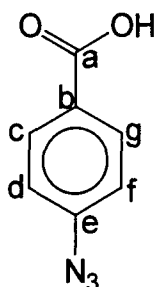
was performed three times. The polymer, poly(para-azidobenzoate-2-ethyl methacrylate) was pale yellow/beige (yield = 70%). Characterisation is discussed in the next section.

### 3.3 Results and Discussion

#### *4-Azidobenzoic acid*

4-Azidobenzoic acid was a pale yellow solid. A melting point was attempted on standard melting point apparatus but the compound decomposed, turning dark brown. Confirmation of decomposition was obtained by use of thermogravimetric analysis which showed decomposition starting at 114C, see appendix 3. Initially there was a rise in mass which was possibly due to oxidation of the sample by air. The curve showed a smooth decomposition of the sample in the temperature range 114C (onset) to 204C. There was not a step mass loss of 17.2% which would have been characteristic of a discrete nitrogen gas elimination. Electron impact mass spectroscopy gave the expected mass of  $m/e=163$  for 4-azidobenzoic acid and a fragmentation pattern consistent with the assigned structure, with peaks at  $m/e$  149 (M-14(N)), 135 (M-28(N<sub>2</sub>) base peak), 120 (M-43(N<sub>3</sub>H)).

Figure 3.12 4-Azidobenzoic Acid



Elemental analysis gave the following results which do not entirely agree with the theoretical values predicted. This is probably due to the product being slightly damp from residual solvent as it was not possible to dry the material any more effectively without decomposition.

Table 3.1 Elemental Analysis of 4-Azidobenzoic acid

	C	H	N
Theoretical	51.53	3.07	25.77
Experimental	50.23	2.95	25.19

In the  $^1\text{H}$  NMR spectrum (see appendix 3), there are two pseudo-doublets in the aromatic region (7.2 and 8.1 ppm), the system appears to be a simple AB coupling but multiplicities visible on expansion of the spectrum indicate the expected AA'BB' system.

Table 3.2 Assignment of  $^{13}\text{C}$  NMR Peaks for 4-Azidobenzoic acid

SHIFT/ppm	ASSIGNMENT
30.0	acetone
119.8	c and g
127.9	b
132.3	d and f
145.5	e
166.8	a

The  $^{13}\text{C}$  NMR spectrum (see appendix 3) contains all the carbon peaks expected.

Carbons c and g and also f and d are equivalent so only one peak is seen for each

pair. The  $^1\text{H}$  and  $^{13}\text{C}$  NMR spectra indicated that the product was pure and suitable for the next stage of the synthesis.

Table 3.3 Assignment of Peaks in the IR Spectrum of 4-Azidobenzoic acid

Peak ( $\text{cm}^{-1}$ )	Assignment
~3600	-OH
3040	C-H stretches
2140	$\text{N}_3$
1715	C=O

The main characterising peaks in the IR spectrum are recorded in the table above, the spectrum also showed peaks consistent with the presence of an aromatic ring, C-O bond and -OH in the fingerprint region. The azide peak is of most significance as IR spectroscopy was the main characterisation technique used to indicate the presence of the azide group.

#### *4-Azidobenzoyl chloride*

4-Azidobenzoyl chloride was pale orange, with a melting point of 57.1-58.2C which agrees with the literature value<sup>6</sup> (57-58C). Mass spectroscopy EI gave the expected mass  $m/e$  at 181 for the parent ion and the fragmentation pattern was consistent with the assigned structure, with peaks at  $m/e$  153 (M-28( $\text{N}_2$ )), 146 (M-35(Cl)), 118 (M-63( $\text{N}_2\text{Cl}$ )). The fragments of larger mass than 181 seen on some of the mass spectra for 4-azidobenzoyl chloride, were probably due to traces of coupling products, possibly azobenzene compounds, resulting from reactions of the 4-azidobenzoyl chloride or its decomposition products.

Elemental analysis produced the following data which are in reasonably good agreement with expected values.

Table 3.4 Elemental Analysis of 4-Azidobenzoyl chloride

	C	H	N
Theoretical	46.28	2.20	23.14
Experimental	45.86	2.15	23.15

Figure 3.13 4-Azidobenzoyl chloride

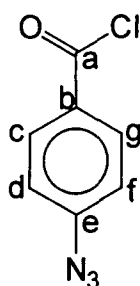


Table 3.5 Assignment of Peaks of  $^1\text{H}$  NMR Spectrum of 4-Azidobenzoyl chloride

SHIFT/ppm	INTEGRAL	ASSIGNMENT
2.06	--	acetone
7.3	2	c and g
8.16	2	d and f

As with the  $^1\text{H}$  NMR spectrum of 4-azidobenzoic acid, AA'BB' splitting can be seen in the two peaks in the aromatic region (see appendix 3). The peaks were slightly shifted compared to the 4-azidobenzoic acid  $^1\text{H}$  spectrum due to the effect of replacing the acid hydroxy group by a chlorine atom.

Table 3.6 Assignment of  $^{13}\text{C}$  NMR Spectrum of 4-Azidobenzoyl chloride

SHIFT/ppm	ASSIGNMENT
30.0	acetone
120.5	c and g
129.8	b
134.2	d and f
148.8	e
167.2	a

The  $^{13}\text{C}$  NMR spectrum (see appendix 3) was as expected with carbons c and g and also d and f equivalent so only one peak was seen for each pair. The  $^1\text{H}$  and  $^{13}\text{C}$  NMR spectra indicate that the product was pure.

Table 3.7 Assignment of Peaks of IR Spectrum of 4-Azidobenzoic acid

PEAK ( $\text{cm}^{-1}$ )	ASSIGNMENT
1715	C=O
2128	$\text{N}_3$
3003	C-H

IR spectroscopy showed all the main characterising peaks expected. The spectrum (see appendix 3) is virtually superimposable with that of the acid, apart from the large diminution in the intensity of the OH stretching at  $3400\text{cm}^{-1}$ , small variations in relative intensities and a few new bands in the fingerprint region.

The residual absorption at  $3400\text{cm}^{-1}$  could be due to the KBr disc being slightly damp or slight hydrolysis of the acid chloride.

### *Azido monomer*

The first method to synthesise the azido monomer did not work as expected. The reaction of HEMA and 4-azidobenzoyl chloride in the presence of triethylamine and chloroform did not go to completion so some HEMA remained with the azido monomer and hence a monomer mixture was formed. It was difficult to characterise this mixture as it tended to polymerise spontaneously. Characterisation had to be carried out immediately after synthesis and the monomer was kept at  $-5\text{C}$  during this time to slow down the polymerisation.

Figure 3.14 The Azide Monomer and HEMA in the Monomer Mixture

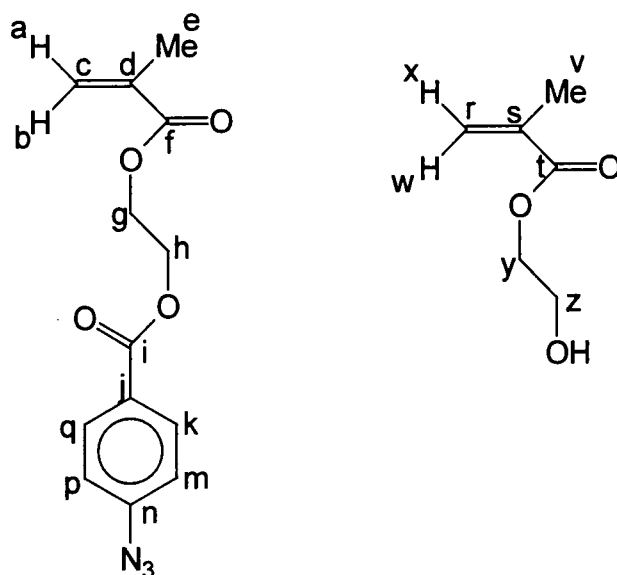


Table 3.8 Assignment of the IR Spectrum of the Monomer Mixture

PEAKS( $\text{cm}^{-1}$ )	ASSIGNMENT
3412	-OH
3003	C-H
2126	$\text{N}_3$
1715	C=O

IR spectroscopy showed all the main characterisation peaks for the monomer mixture, the -OH peak indicating the presence of HEMA. The fingerprint region contains peaks representing the aromatic ring, ester C-O and C=O.

Table 3.9 Assignment of the  $^1\text{H}$  NMR Spectrum of the Monomer Mixture

PEAK (ppm)	ASSIGNMENT
1.38	solvent
1.93	e, v
2.04	acetone
3.16	solvent
3.77	z
4.19	y
4.33	solvent
4.54	g, h
5.62	a, x
6.09	b, w
7.21	k, q
8.51	m, p

The  $^1\text{H}$  NMR spectrum (see appendix 3) showed peaks representing both monomers, there was also solvent and a small amount of other impurity present. This could not be removed as attempted purification of the monomer mixture resulted in it polymerising spontaneously. The  $^{13}\text{C}$  NMR spectrum (see appendix 3) was difficult to interpret due to the impurities in the sample but peaks could be seen representing the carbonyl carbons (166 and 167.5ppm), aromatic ring and C=C (120-140ppm).

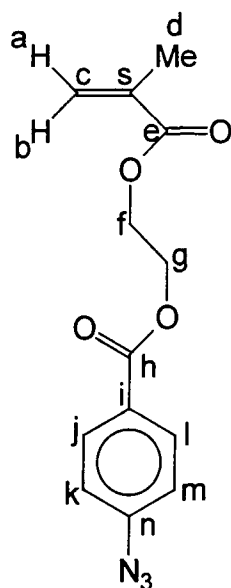
The second method of synthesising the azido monomer involved using the Schotten-Baumen reaction. 4-Azidobenzoyl chloride dissolved in benzene and acetone was added slowly with vigorous mixing to HEMA in benzene, acetone and 15% aqueous sodium hydroxide solution. This route gave a much cleaner product.

Table 3.10 Assignment of the IR Spectrum of 4-Azidobenzoate-2-ethyl methacrylate

PEAKS( $\text{cm}^{-1}$ )	ASSIGNMENT
3003	C-H
2107	$\text{N}_3$
1715	C=O

The IR spectrum (see appendix 3) showed the presence of the azide group and ester carbonyls and there was no remaining peak from the HEMA starting material.

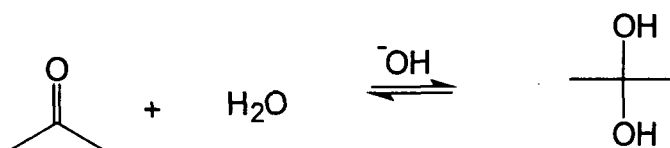
Figure 3.15 4-Azidobenzoate-2-ethyl methacrylate



This reaction works because the acid chloride is hydrolysed slowly compared to the rate of ester formation. A small amount of the 4-azidobenzoic acid was found in the reaction pot at the end of the synthesis and was successfully removed from the product by washing. The strong base, sodium hydroxide, prevents side reactions occurring with hydrogen chloride formed and no residual 2-hydroxyethyl methacrylate remained at the end of the reaction.

There was some concern initially about the use of acetone with sodium hydroxide as the production of a hydrate could result.

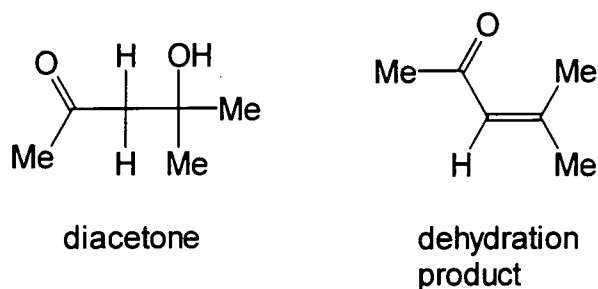
Figure 3.16 Reaction of Acetone with Sodium Hydroxide



Hydrates are usually stable only in water, otherwise the equilibrium shifts towards the carbonyl compound. The equilibrium in the acetone system is towards the carbonyl compound and the concentration of hydrate present is

negligible. No evidence of any interference from this reaction was found in the results. Another possibility with acetone in the presence of base is the formation of diacetone alcohol and its dehydration product.

Figure 3.17 Products of the Reaction of Acetone in the presence of NaOH



No evidence for interference from this reaction was found either in the products of the Schotten-Baumen reaction.

Table 3.11 Assignment of  $^1\text{H}$  NMR Spectrum of Azidobenzoate-2-ethyl methacrylate

SHIFT(ppm)	ASSIGNMENT
1.91	d
2.06	acetone
3.87	solvent
4.56	g, f
5.63	a
6.09	b
7.20	j, l
8.05	k, m

In the  $^1\text{H}$  NMR spectrum (see appendix 3) the hydrogens of the methylene carbons g and f are not resolved and display a complicated splitting pattern and

must be taken as one group of peaks representing four hydrogens. The integration is not perfect for these peaks due to overlaps. The monomer, an orange liquid, is not easy to handle or purify as it tends to polymerise unless kept in a refrigerator at -5 to 0C, exposure to heat and/or light have to be avoided because of the potential for azide decomposition and these restrictions rule out most purification procedures.

Table 3.12 Assignment of  $^{13}\text{C}$  NMR Spectrum of 4-Azidobenzoate-2-ethyl methacrylate

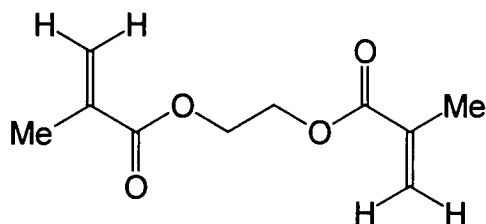
SHIFT/ppm	ASSIGNMENT
18	d
30	acetone
63	f, g
120-146	c, s, j, k, m, n, l, i
166 and 167	h, e

The  $^{13}\text{C}$  NMR spectrum (see appendix 3) indicated the pure monomer structure as assigned in the table above.

A sample of the monomer was analysed by GC mass spectroscopy. The GC trace showed the presence of two solvent peaks at lower retention volumes and then a large peak corresponding to the azido monomer. A mass spectrum was obtained for the azido monomer which showed peaks at  $m/e$  113,  $\text{M-C}_7\text{H}_4\text{O}_2\text{N}_3$  and  $m/e$  69,  $\text{M-C}_9\text{H}_8\text{O}_3\text{N}_3$ . No molecular ion was detected. On making a library database search comparing the mass spectrum obtained from the

azido monomer with the library of structures, 2-methyl-1,2-ethanediyl ester gave the nearest match (see appendix 3).

Figure 3.18 2-Methyl-1,2-ethanediyl ester



This is consistent with the presence of the double bond, short carbon chain and two ester groups in our product. Elemental analysis produced the following results.

Table 3.13 Elemental Analysis of 4-Azidobenzoate-2-ethyl methacrylate

	C	H	N
Theoretical	56.73	4.73	15.27
Experimental	57.55	4.96	15.17

The elemental analysis was not in good agreement with the theoretical values predicted. This was probably because the monomer contained some solvent but was difficult to purify due to its tendency to polymerise spontaneously. The amount of solvent present was negligible though so the monomer was used unpurified.

### *Azido Polymers*

The azido polymers were prepared by free radical initiated polymerisation, using 2-butanone as the solvent and azobisisobutyronitrile as the

initiator at 50-65C. The product was precipitated in hexane as a pale orange/brown solid by pouring the reaction mixture into excess hexane.

### *Azido Copolymer*

On polymerising the monomer mixture a copolymer was formed of 4-azidobenzoate-2-ethyl methacrylate with hydroxyethyl methacrylate, see figure 3.19.

Figure 3.19 Azide and HEMA Copolymer

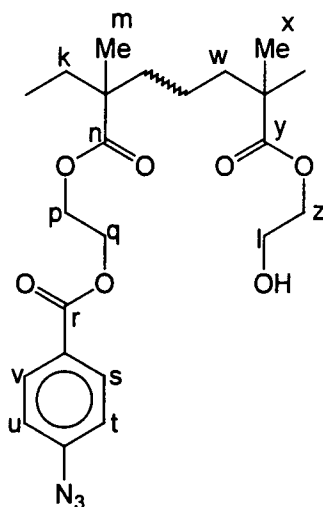


Table 3.14 Assignment of IR Spectrum of Monomer Spectrum

PEAK( $\text{cm}^{-1}$ )	ASSIGNMENT
3606	-OH
3002	C-H
2126	$\text{N}_3$
1713	C=O

The IR spectrum showed the presence of both monomers by the azide peak and the hydroxy peak. Peaks characteristic of the aromatic ring, ester C-O and C=O bonds could be seen in the fingerprint region.

Table 3.15 GPC Data for Azide Copolymers

$M_n$	$M_w$	PDI
4800	10200	2.1
8600	10500	1.2
12900	20100	1.6

There was a low molecular mass material present before purification which contained residual monomer and low molecular mass oligomers. It is also possible that a 1,3 dipolar cyclisation reaction could occur during polymerisation between the azide group and the C=C, this reaction would result in a five-membered triazoline ring (see Figure 3.20) and a depletion of monomer and the production of defects.

Figure 3.20 Triazole product

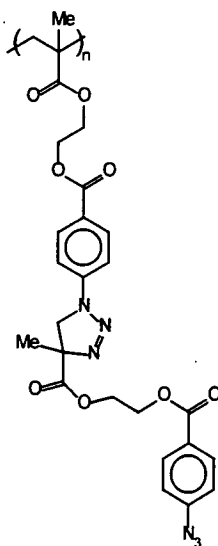


Table 3.16 Assignment of <sup>1</sup>H NMR Spectrum of Copolymer

SHIFT/ppm	ASSIGNMENT
0.90-1.40	m, x and solvent
2.00	k
2.05	acetone
2.88	w
3.18	solvent
3.77	z
4.04	l
4.32	p
4.53	q
7.16	v, s
8.05	u, t

In the <sup>1</sup>H NMR spectrum (see appendix 3), many of the peaks overlap in the aliphatic region of the spectrum, therefore it is difficult to calculate accurate integration values. Using peaks of the <sup>1</sup>H NMR spectrum that were not overlapping, it was calculated that the monomer incorporation ratio was 2:1 (azido monomer:HEMA).

It was difficult to obtain a good <sup>13</sup>C NMR spectrum (see appendix 3) as a concentrated solution could not be made due to low polymer solubility. A peak representing a carbonyl carbon can be seen at 166ppm and peaks in the aromatic/unsaturated region (120-145ppm) represent the benzene ring and C=C.

### *Azido homopolymer*

The azido homopolymer was prepared by free radical initiated polymerisation, using 2-butanone as the solvent and AIBN as initiator at 60-65C. When the polymerisation was performed at this temperature a soluble polymer was obtained. However, this polymer became insoluble if left to stand at room temperature, even when it was wrapped in aluminium foil. Therefore it can be concluded that a thermal process was occurring, probably involving the cross-linking of the azide groups forming an insoluble network. If the polymer is stored under nitrogen gas, wrapped in tin foil, in the freezer at -21C it remains soluble so the low temperature must stop or at least slow down the cross-linking process.

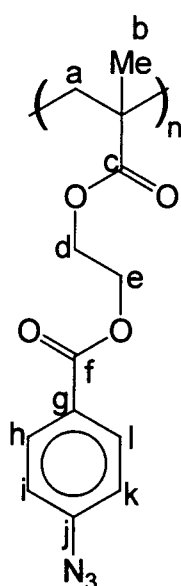
Table 3.17 Assignment of <sup>1</sup>H NMR Spectrum of Poly(4-azidobenzoate-2-ethyl methacrylate)

SHIFT (ppm)	ASSIGNMENT
0.90 - 2.20	a and b
4.25 and 4.42	d, e
6.99	h, l
7.26	chloroform
7.92	i, k

The <sup>1</sup>H NMR spectrum (see appendix 3) showed peaks which were consistent with the formation of the expected azide homopolymer. Broad peaks and the absence of the peaks representing the hydrogens of the monomer double bond

indicate that polymer has been formed. The resonances associated with the backbone methyl and methylenes, 0.8 to 2.2ppm, appeared as a set of broad overlapping peaks and were much less resolved than the analogous resonances in the anthracenoate polymers (Chapter 2) leading to the conclusion that these polymers are probably largely atactic and may have a significant frequency of structure defects.

Figure 3.21 Poly(4-azidobenzoate-2-ethyl methacrylate)



GPC chromatograms for three samples from separate experiments showed that high molecular masses were being achieved. The polydispersities are quite broad but this is often seen in free radical polymerisations of methacrylates.

Table 3.18 GPC Data for Azide Homopolymer

$M_n$	$M_w$	PDI
32300	129000	4.0
19800	63600	3.2
43800	154500	3.5

The IR spectrum (see appendix 3) showed all the functional groups expected were present in the homopolymer, see Table 3.19.

Table 3.19 Assignment of IR Spectrum of Poly(para-azidobenzoate-2-ethyl methacrylate)

PEAK (cm <sup>-1</sup> )	ASSIGNMENT
3003	C-H
2125	N <sub>3</sub>
1715	C=O

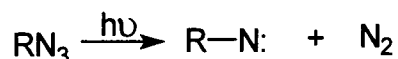
The <sup>13</sup>C NMR spectrum (see appendix 3) for the homopolymer shown in this report was recorded before purification as the purified polymer was not soluble enough to enable a carbon-13 NMR spectrum to be run. Peaks representing a carbonyl carbon, aromatic carbons, side chain methylene groups and methyl group can be clearly seen. Poly(azidostyrene) has been made and the group reported that it was 'difficult to evaluate sensitometrically due to its rather limited solubility'.<sup>8</sup>

Azide decomposition during polymerisation can be reduced by lowering the polymerisation temperature and increasing the amount of solvent used in the reaction.<sup>7</sup> Although as the polymer becomes insoluble at room temperature and it was assumed that a thermal reaction was taking place, it can be presumed that some reaction of the azide groups will occur during polymerisation due to the elevated temperature.

### 3.4 Film Forming and Cross-linking

It was thought that cross-linking of poly(4-azidobenzoate-2-ethyl methacrylate) would be accomplished by nitrogen elimination<sup>10</sup> from the aryl azide followed by dimerisation to form azobenzene links.

Photolysis

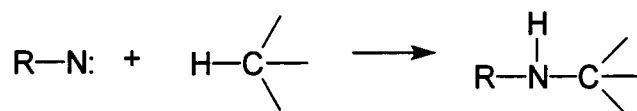


Dimerisation

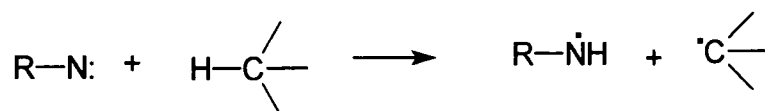


Azido photopolymers can also cross-link by methods<sup>11</sup> other than nitrene coupling to form an azobenzene link. Insertion into C-H bonds and reaction with double bonds forming rings can also occur. It was pointed out by Merrill and Unruh<sup>5,6</sup> that reactions of the nitrene depend upon the environment.

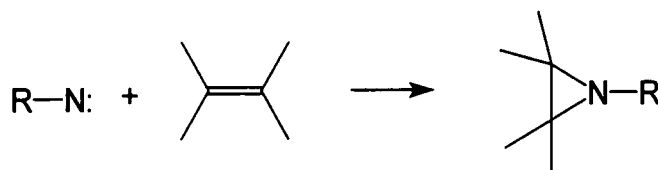
Direct Insertion



Hydrogen Abstraction



Cycloaddition



It was reported by the Defence Research Agency that the azide homopolymer was not forming cross-links by dimerisation as no evidence could be found in the spectra of irradiated films for azobenzene groups. Further investigation into the photochemistry occurring in this system needs to be undertaken, see chapter 5.

Film forming and cross-linking were investigated by the same methods described in chapter 2 (p54). Namely, spinning films from chloroform under a partial vacuum from a water pump and exposing a film of the polymer on a quartz slide to ultra-violet light from a deuterium lamp. The azide polymer formed films from chloroform under vacuum and became insoluble when irradiated by the deuterium lamp (30W). It was assumed that cross-linking had occurred, rendering the polymer insoluble.

### **3.5 Conclusions**

The synthesis of 4-azidobenzoyl chloride was very straight forward and produced pure product in high yields. The first method to produce the azido monomer, using triethylamine in chloroform did not work as expected. From the spectra of the product polymer it can be seen that a copolymer was the final product rather than the desired homopolymer. This was probably due to the incomplete reaction of HEMA with 4-azidobenzoyl chloride and incomplete removal of residual HEMA. Hence, when the monomer mixture was polymerised a copolymer of HEMA and the azido monomer was produced. The copolymers obtained had incorporation ratios calculated from  $^1\text{H}$  NMR spectral data of approximately 80:20 and 60:40 (azido monomer:HEMA) depending on

the amount of HEMA added to the acid chloride (1:1 and 1:1.3 mole ratio respectively).

The Schotten-Baumen reaction was used in an attempt to produce the monomer. It was hoped that this reaction would circumvent previous problems since it had been used before for a similar type of synthesis<sup>7</sup>. The reaction worked, producing the azido monomer and a side product (4-azidobenzoic acid) which can be returned to the synthetic pathway so limiting wastage. When polymerising the pure azido monomer, concentrated solutions produced an intractable cross-linked polymer as did polymerising temperatures of >70C so dilute solutions of the monomer were used at 60-65C. It was assumed that a thermal cross-linking reaction of the azide groups occurred at >70C producing an insoluble polymer network. As the cross-linking is a thermal process some cross-links probably form during polymerisation at 60-65C. However, the polymer produced is soluble when recovered so this must not be occurring to a large extent.

The azido polymer was found to form films and photochemically cross-link. This is necessary for its intended use as an alignment layer for liquid crystal devices. However, the azide polymer was difficult to produce, purify and store as it was thermally and photolytically unstable. Other research groups have noticed the tendency of azide containing polymers to cross-link at room temperature<sup>8</sup>. This problem can be circumvented by careful production, storing products wrapped in aluminium foil in the freezer (-21C) and using intermediate products immediately after production in the next stage of synthesis.

## References

1. Lee K.W., Paek S.H., Lien A., Durning C. and Fukuro H., Microscopic molecular reorientation of alignment layer polymer surfaces induced by rubbing and its effects on LC pretilt angles, Macromolecules (29), N° 27, 1996, pages 8894-99.
2. Nishikawa M., Kimiyasu S., Tsuyoshi M., Yokoyama Y., Bessho N., Seo D., Iimura Y. and Kobayashi S., Pretilt Angles of Liquid Crystal on Organic-Solvent-Soluble Polyimide Alignment Films, Jpn. J. Appl. Phys. (33), 1994, pages 4152-53.
3. Wilkins C.W., Feit E.D. and Wurtz M.E., Preliminary Investigations of azide containing negative resists: Poly(benzyl azide), Proc. Electrochem. Soc. (78-5), 1978, pages 341-52.
4. Vogel, Textbook of Practical Organic Chemistry, 5<sup>th</sup> edition, Longman Scientific and Technical, 1989.
5. Merrill S.H. and Unruh C.C., Improved light sensitive polymers for photomechanical printing processes, UK Patent 843541, 1956.
6. Merrill S.H. and Unruh C.C., Photosensitive Azide Polymers, J. Appl. Poly. Sci. (7), 1963, pages 273-9.
7. Nagamatsu G., Asano T. and Takahashi H., Synthesis and properties of the new azidopolymer, Graphic Arts Jpn. (4), 1972-3, pages 54-61.
8. Cohen H.L., The preparation and reactions of polymeric azides II. The preparation and reactions of various polymeric azides, J. Poly. Sci. Part A (19), 1981, pages 3269-84.

9. Williams J.L.R., Photopolymerisation and photocrosslinking of polymers, Fortsch Chem., Fortsch 13, 1969, pages 227-50.
10. Gilbert A., Photoelimination reactions, Photochemistry (3), 1972, pages 745-803.
11. L'Abbe G., Decomposition and addition reactions of organic azides, Chem. Revs. (69), 1969, pages 345-63.

## Chapter Four

### Synthesis and Investigation of Copolymers of the Anthracene and Azide Monomers with Methyl Methacrylate

#### 4.1 Introduction

When two or more monomers are polymerised together a copolymer is formed. The copolymerisation reaction is similar to homopolymerisation but there are more reactions occurring during the propagation step<sup>1</sup>, see later. The product copolymer contains a mixture of the monomers and often exhibits the better qualities of both parent homopolymers. There are several ways that two different monomers can form a copolymer.

1. Statistical copolymers - the two monomers join onto the growing chain statistically.



2. Alternating copolymers - monomers add to the propagating chain in a regular alternating order.



3. Block copolymers - a long sequence of one monomer is formed then a sequence of another monomer is added onto it.



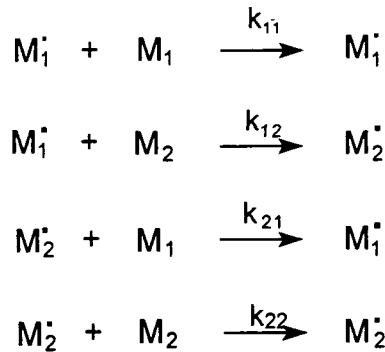
4. Graft copolymers - one monomer type forms a backbone polymer chain with side groups of the other monomer appended to it.

A-A-A-A-A-A-A-A-A-A-A-A-A-A-A-A  
 B      B      B      B  
 B      B      B      B  
 B      B      B      B  
 B      B      B      B  
 B      B      B      B  
 B      B      B      B

Copolymers of 9'-anthracenoate-2-ethyl methacrylate with methyl methacrylate(MMA) and para-azidobenzoate-2-ethyl methacrylate with MMA were made by a variety of methods. Free radical initiated solution polymerisation was used to find the reactivity ratios of the monomers with respect to one another.

Reactivity ratios are useful because in the polymerisation of a mixture of two or more monomers, the rate at which different monomers add to the growing chain determines the composition and hence the properties of the resulting copolymer. Therefore if we know the reactivity ratios we can predict the probable copolymer composition. The sequence distribution of the monomers in the copolymer as well as the ratio of amounts is determined by the reactivity ratios.

The copolymer equation<sup>1,2</sup> is used to determine the reactivity ratios of monomers and is an instantaneous expression relating the monomer feed and copolymer compositions at any given time. If we take  $M_1$  as monomer 1 and  $M_2$  as monomer 2, the four reactions occurring during propagation can be represented as follows.



$k_{11}$  and  $k_{22}$  are rate constants for self-propagating reactions

$k_{12}$  and  $k_{21}$  are corresponding cross-propagation rate constants

With the definition of the reactivity ratios as

$$r_1 = k_{11}/k_{12} \qquad r_2 = k_{22}/k_{21}$$

and assuming radical reactivity is independent of chain length and the steady-state principle applies (the steady state approximation assumes that during the major part of the reaction, the concentrations and the rates of change of all reaction intermediates are constant and small), the copolymer equation can be derived. The copolymer equation relates the instantaneous composition of a copolymer with the reactivity of the monomers involved.

$$\frac{d[M_1]}{d[M_2]} = \frac{[M_1](r_1[M_1] + [M_2])}{[M_2]([M_1] + r_2[M_2])}$$

An approximation is then used assuming that at low conversion  $[M_1]/[M_2]$  is essentially constant.

$$H = [M_1]/[M_2]$$

$$h = d[M_1]/d[M_2]$$

$$r_2 = r_1 H^2/h + H(1-h)/h$$

$r$  = reactivity ratios, defined more generally as the ratio of the reactivity of the propagating species with its own monomer to the reactivity of the propagating

species with the other monomer. This last equation is known as the copolymer equation.

Most procedures for evaluating the reactivity ratios involve experimental determination of the copolymer compositions for several different monomer feed mixtures. Many different methods can be used for copolymer analysis such as elemental analysis, radioisotope tagging and spectroscopy (IR, UV or NMR). <sup>1</sup>H NMR spectroscopy was used to calculate the incorporation of the monomers in the product copolymer in this work. The accuracy of the reactivity ratios depends on using feed ratios for which the copolymer compositions are most sensitive to variations in the reactivity ratios.

The copolymerisations were carried out to as low degree of conversion as possible (~5%) to minimise errors in the use of the differential form of the copolymerisation equation. It has been found that at these low degrees of conversion composition drift does not interfere with copolymer composition and hence the reactivity ratios.

Composition drift can also be determined with the aid of reactivity ratios, extending the reaction times of the copolymerisations and analysing the monomer content of the two monomers in the product copolymers. Staudinger<sup>3</sup> first noticed the phenomenon of composition drift in the 1930's and it is quite a straightforward concept. If the two monomers being reacted together have different reactivity ratios it means they will enter the copolymer at different rates. This in turn will affect the monomer feed composition as one monomer will be depleted faster than the other. If the feed is constantly changing the incorporation of the monomers will be affected and so the polymer composition

will alter hence the term composition drift. This is why the copolymer equation is only an instantaneous expression of the copolymer composition, as due to composition drift the equation is constantly changing.

## **4.2 Experimental**

### **4.2.1 Purification of Starting Materials**

The purification of most of the starting materials can be found in chapter 2 (page 32) and chapter 3 (page 68).

#### **1. Methyl methacrylate**

Methyl methacrylate polymerises on heating so low-pressure distillation (20mm Hg, 46C) was performed. Standard distillation equipment was used. The colourless methyl methacrylate was collected and stored under nitrogen over activated 4Å molecular sieves in a sealed flask, wrapped in aluminium foil at -21C prior to use.

### **4.2.2 Copolymer Synthesis**

#### *Synthesis of Anthracene Monomer/MMA Copolymers*

2-Butanone (70ml) was poured into a 250ml flange flask with condenser, overhead electrical stirrer, nitrogen inlet and outlet and a dropping funnel attached. The apparatus was flushed with nitrogen gas and the condenser was cooled with tap water throughout the entire experiment. A mixture of the anthracenyl monomer, MMA, 2-butanone (20ml) and AIBN (0.035g) was placed in the dropping funnel. The 2-butanone in the flange was heated to 65-70C then the monomer mixture was quickly added to the stirring solvent. The

polymerisation continued for 15 minutes, after this time the reaction was quenched by precipitation of the polymers; the contents of the flask were poured into a beaker of stirring hexane (750ml). The copolymer precipitated then was collected and dried in a vacuum oven ( $10^{-3}$ mm Hg/40C).

Table 4.1 Mass of the two Monomers used in each Copolymer Reaction

Mass of MMA in monomer feed	Mass of anthracenyl monomer in feed
1.8g (0.018 moles)	0.67g (0.002 moles)
1.6g (0.016 moles)	1.34g (0.004 moles)
1.4g (0.014 moles)	2.00g (0.006 moles)
1.2g (0.012 moles)	2.67g (0.008 moles)
1.0g (0.01 moles)	3.34g (0.01 moles)
0.8g (0.008 moles)	4.01g (0.012 moles)
0.6g (0.006 moles)	4.68g (0.014 moles)
0.5g (0.005 moles)	5.02g (0.015 moles)
0.4g (0.004 moles)	5.35g (0.016 moles)
0.3g (0.003 moles)	5.68g (0.017 moles)
0.2g (0.002 moles)	6.02g (0.018 moles)

Also, copolymers of 9'-anthracene-2-ethyl methacrylate and MMA (see Table 4.2) were made by solution polymerisation allowing the reaction to continue for the longer time of four hours. These polymers were precipitated in hexane (400ml) and dried in a vacuum oven ( $10^{-3}$ mm Hg, 50C). Characterisation data can be found in the Results and Discussion section of this chapter.

Table 4.2 Amount of the two Monomers in the Feed

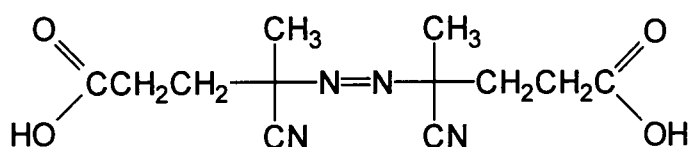
Experiment Code	9'-Anthracenoate-2-ethyl methacrylate	Methyl methacrylate
KEF47	15.63g (0.0467 moles)	5ml (0.0467 moles)
KEF49	12.5g (0.0374 moles)	8ml (0.0748 moles)
KEF50	7.82g (0.0234 moles)	10ml (0.0935 moles)
KEF51	6.26g (0.0187 moles)	12ml (0.112 moles)
KEF52	5.87g (0.0176 moles)	15ml (0.14 moles)
KEF53	4.69g (0.014 moles)	15ml (0.14 moles)
KEF54	3.52g (0.0105 moles)	18ml (0.168 moles)

Bulk copolymerisation<sup>4</sup> using 1,1'-azobis-(cyclohexanecarbonitrile) as the free radical initiator was attempted. 9'-Anthracenoate-2-ethyl methacrylate (1.56g, 0.0467 moles) and methyl methacrylate (8ml, 0.0748 moles) were placed in the reaction vessel (see chapter 2 page 41). The vessel was flushed with nitrogen gas before and during the experiment. The anthracene monomer dissolved in the MMA was heated to 65C with stirring then the initiator 1,1'-azobis-(cyclohexanecarbonitrile) (0.06g,  $2.46 \times 10^{-4}$  moles) was added to the mixture and the temperature was elevated to 85C. The reaction mixture was heated and stirred until the mixture became solid then the product was cooled, dissolved in chloroform and precipitated in ethanol. The copolymer was dried in a vacuum oven ( $10^{-3}$  mm Hg, 40C). The copolymers were characterised and this data can be found in the Results and Discussion section.



Finally dispersion polymerisation<sup>4</sup> was attempted to synthesise the copolymer. Anthracenyl monomer (3.01g, 0.009 moles) was dissolved in MMA (10ml, 0.935 moles). Distilled water (300ml) was placed in a reaction flask and heated to 70C whilst being stirred with an overhead electrical Ultra-Turrax stirrer. The initiator, 4,4'-azobis-(4-cyanopentanoic acid) (0.17g, 6.63x10<sup>-4</sup> moles) was added to the hot, stirring water then the monomer mixture was added dropwise to the water.

Figure 4.1 4,4'-Azobis-(4-cyanopentanoic acid)



When all the monomer had been added the reaction was left to stir for three hours. Then the remaining mixture was left to cool, the water removed on a rotary evaporator and the product dissolved in chloroform then precipitated in ethanol. The product was dried in a vacuum oven (20C, 10<sup>-3</sup>mm Hg). A second reaction was attempted using 4,4'-azobis-(4-cyanopentanoic acid) (0.29g, 1.13x10<sup>-3</sup> moles) and leaving the reaction to stir for 5 hours. A final attempt using AIBN as the initiator was tried but produced the same results as the reaction with 4,4'-azobis-(4-cyanopentanoic acid). Characterisation data can be found in the Results and Discussion section.

#### *Synthesis of the Azide/MMA Copolymers*

The copolymers of the azide monomer with MMA were synthesised using solution free radical initiated polymerisation. 2-Butanone (90ml) and AIBN (0.035g, 2.13x10<sup>-4</sup> moles) were used and the reaction was stopped after 20

minutes. The copolymers were precipitated in stirring methanol then re-precipitated from chloroform and dried in a vacuum oven ( $10^{-3}$  mm Hg/room temperature) for two hours.

Table 4.3 Mass of the two Monomers used in the Copolymer Feed

Mass of MMA in Monomer Feed	Mass of Azido Monomer in Feed
1.8g (0.018 moles)	0.55g (0.002 moles)
1.6g (0.016 moles)	1.10g (0.004 moles)
1.4g (0.014 moles)	1.65g (0.006 moles)
1.2g (0.012 moles)	2.20g (0.008 moles)
1.0g (0.01 moles)	2.75g (0.01 moles)
0.6g (0.006 moles)	2.48g (0.009 moles)
0.53g (0.0053 moles)	2.68g (0.00974 moles)
0.45g (0.0045 moles)	2.89g (0.01 moles)
0.38g (0.0038 moles)	3.10g (0.011 moles)
0.3g (0.003 moles)	3.30g (0.012 moles)
0.23g (0.0023 moles)	3.51g (0.013 moles)
0.15g (0.0015 moles)	3.72g (0.0135 moles)

The copolymers were characterised by IR,  $^1\text{H}$  NMR and  $^{13}\text{C}$  NMR spectroscopy which is described in the Results and Discussion section.

### 4.3 Results and Discussion

#### 4.3.1 Results of Synthesis

##### *Bulk Polymerisation*

The bulk polymerisation was successful in producing a copolymer of high molecular mass, see Table 4.4, but the polymer was only slightly soluble. This was probably due to branching and possibly very light cross-linking occurring during polymerisation which is a common occurrence during bulk polymerisation of methacrylates and is probably due to a chain transfer mechanism involving hydrogen abstraction from the backbone chain. The copolymer obtained in a yield of 91% was a pale yellow solid.

Table 4.4 GPC Data for Bulk Polymerisation of Anthracenoate Copolymer

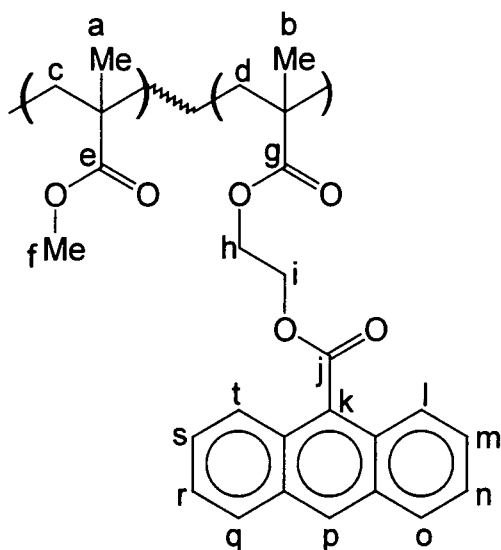
$M_n$	$M_w$	PDI
93000	371300	4.0

The IR spectrum (see appendix 4) showed the main peaks for the carbonyl group and C-H bonds but there was also an OH peak, probably due to damp KBr or residual ethanol from precipitation of the copolymer.

Table 4.5 Assignment of Peaks of IR Spectrum for Anthracenoate Copolymer

PEAK ( $\text{cm}^{-1}$ )	ASSIGNMENT
3440	-OH
2950	C-H
1730	C=O
1625	benzene ring

Figure 4.2 Poly(9'-anthracenoate-2-ethyl methacrylate-co-methyl methacrylate)



The  $^1\text{H}$  NMR spectrum (see appendix 4) was clean, indicating that the copolymer formed was pure and contained no residual monomer. From the integration of the resonances associated with the anthracenoate monomer residue (aromatic hydrogen peaks at 7.5 to 8.6ppm) and methyl methacrylate ( $-\text{OCH}_3$  peak at 3.5ppm) of this spectrum the incorporation of 9'-anthracenoate-2-ethyl methacrylate:MMA was measured as 1:15.

Table 4.6 Assignment of  $^1\text{H}$  NMR Spectrum of Anthracenoate Copolymer

SHIFT (ppm)	ASSIGNMENT
0.85	b
1.02	a
1.25	ethanol
1.62	d
1.90	c
3.60	f
3.72	ethanol
4.44	h
4.82	i
7.26	chloroform
7.55	m, n, s, r
8.07	t, l, o, q
8.60	p

The  $^{13}\text{C}$  NMR spectrum (see appendix 4) displayed poor signal to noise and the copolymer was only slightly soluble so the solution was too dilute to obtain a good  $^{13}\text{C}$  NMR spectrum.

Table 4.7 Assignment of  $^{13}\text{C}$  NMR Spectrum of Anthracenoate Copolymer

SHIFT (ppm)	ASSIGNMENT
16.48	a
18.44	b
44.73	f
51.83	c
54.4	d
58.5	solvent
125.0-130.9	anthracene aromatic ring carbons
177.0	e
177.8	g
178.1	j

As a consequence, not all the expected carbon resonances can be seen in the spectra. Most of the main shifts expected were present, consistent with the expected structure of the copolymer.

#### *Dispersion Polymerisation*

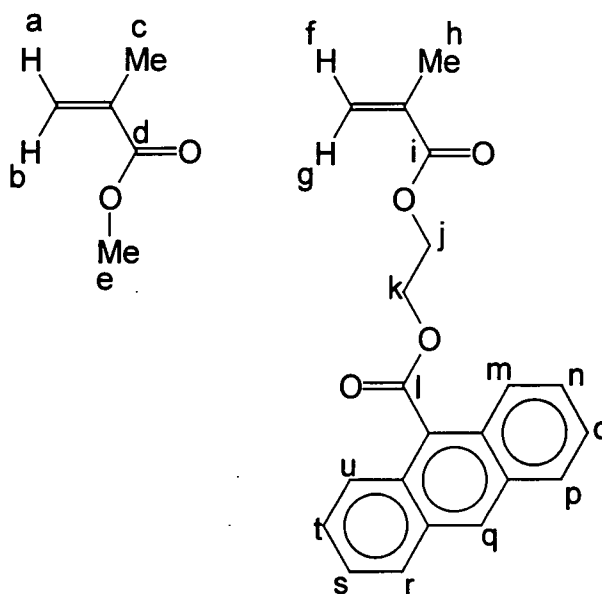
The attempted dispersion polymerisation was unsuccessful, no polymer was formed. It was found that the monomer still remained after the polymerisation attempt.

Table 4.8 Assignment of IR Spectrum for Dispersion Copolymerisation

PEAK (cm <sup>-1</sup> )	ASSIGNMENT
3430	-OH
3000	C-H
1725	C=O

The OH peak in the IR spectrum was probably due to residual solvent (water) or damp KBr.

Figure 4.3 Methyl methacrylate and 9'-Anthracenoate-2-ethyl methacrylate



The <sup>1</sup>H NMR spectrum (see appendix 4) indicated no polymer had been formed as the peaks were sharp (whereas polymer resonances tend to be broad) and the shifts from the hydrogens of the carbon double bond of the monomer were still clearly present.

Table 4.9 Assignment of <sup>1</sup>H NMR Spectrum for Dispersion Copolymerisation

SHIFT (ppm)	ASSIGNMENT
1.25	solvent
1.66	h
2.08	c
2.95	e
4.61	j
4.88	k
5.64	f, a
6.23	g, b
7.26	chloroform
7.50	t, s, n, o
8.06	u, m, p, r
8.54	q

There was a lot more 9'-anthracenoate-2-ethyl methacrylate recovered from the reaction flask than methyl methacrylate which was due to MMA being lost during the product recovery. This was because methyl methacrylate had a greater solubility than 9'-anthracenoate-2-ethyl methacrylate and was a volatile liquid so was more difficult to recover.

Table 4.10 Assignment of  $^{13}\text{C}$  NMR Spectrum for Dispersion Copolymerisation

SHIFT (ppm)	ASSIGNMENT
18.5	h
21.7	c
35.2	solvent
38.0	e
62.5	j
63.4	k
77.0	chloroform
125-136	C=C and aromatic carbons
167.2	i, d
169.4	l

The  $^{13}\text{C}$  NMR spectrum (see appendix 4) was in agreement with the presence of the monomers and no polymer being formed. This reaction may have worked if emulsifiers had been added to the reaction such as salts with lecithin or poly(vinyl alcohol). Emulsifiers aid in efficient mixing of the monomers, initiator and solvents by forming an emulsion of very small droplets of monomer suspended in the aqueous phase. However, for this study emulsifiers were not added because no ionic impurities could be tolerated in the product polymer and it would have been difficult if not impossible to remove all ions or separate other emulsifying polymers from the product. A method of improved mixing may also improve the chances of success of the reaction as the smaller the monomer

droplets are, the greater the surface area and this increases the likelihood of initiation by a free radical species.

### *Solution Polymerisation*

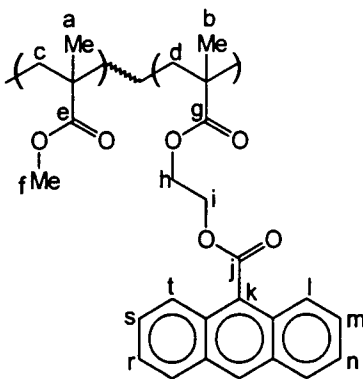
The solution polymerisations were successful and produced copolymers in fairly good yields(65-76% for reactions of 4 hours). The reactions that were stopped after 15 minutes had yields <5% to comply with using the differential form of the copolymer equation..

Table 4.11 GPC Data for Anthracenoate Copolymers (4 hour reaction time)

Experiment code	$M_n$	$M_w$	PDI
KEF47	14800	30200	2.04
KEF49	14200	29200	2.05
KEF50	16600	31800	1.92
KEF51	16700	30000	1.80
KEF52	14500	27700	1.92
KEF53	16500	30400	1.84
KEF54	18000	29900	1.66

The polydispersity was around 2 which indicates a classical free radical polymerisation mainly terminated by disproportionation.

Figure 4.4 Poly(9'-anthracenoate-2-ethyl methacrylate-co-methyl methacrylate)



The  $^1\text{H}$  NMR spectrum (see appendix 4) showed a pure product and the ratios of 9'-anthracenoate-2-ethyl methacrylate to methyl methacrylate could be calculated from the integration of the appropriate resonances in the spectra, see earlier.

Table 4.12 Assignment of  $^1\text{H}$  NMR Spectrum of Solution Copolymers

SHIFT (ppm)	ASSIGNMENT
0.79	b
1.02	a
1.26	ethanol
1.45	c
1.82	d
3.51	f
3.60	ethanol
4.44	h
4.81	i
7.27	chloroform
7.53	m, n, r, s
8.06	l, o, q, t
8.57	p

The  $^1\text{H}$  and  $^{13}\text{C}$  NMR spectra (see appendix 4) showed all the peaks expected for the copolymer and agree with the spectra found for the bulk copolymerisation.

The spectra indicated a pure product containing no residual monomers.

Table 4.13 Assignment of  $^{13}\text{C}$  NMR Spectrum of Solution Copolymers

SHIFT (ppm)	ASSIGNMENT
16.42	b
18.67	a
44.73	f
51.78	c
54.14	d
62.49	h
62.87	i
77.00	chloroform
125-131	aromatic ring carbons
169.2	e
175.8	g
177.77	j

Table 4.14 Assignment of Peaks of IR Spectrum of Solution Copolymers

PEAK (cm <sup>-1</sup> )	ASSIGNMENT
3440	-OH
2950	C-H
1730	C=O

All the main peaks for the functional groups present could be seen in the IR spectrum (see appendix 4). Peaks representing the benzene rings and C-O bonds could be found in the fingerprint region.

#### *Azide Copolymer*

The azido copolymer was only made in very small amounts in order to calculate the reactivity ratios of the two monomers involved. As the copolymer was only produced in small amounts and cross-linked at room temperature or in light, purification was difficult and characterisation was carried out as quickly as possible. Residual monomers were removed from the copolymers but solvent remained.

Figure 4.5 Poly(para-azidobenzoate-2-ethyl methacrylate-co-methyl methacrylate)

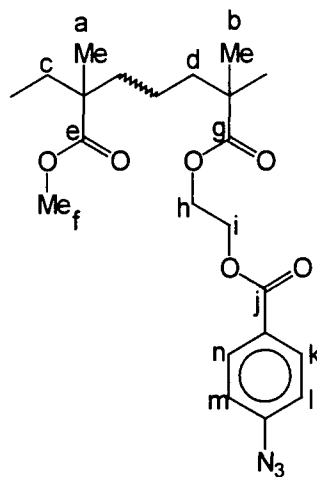


Table 4.15 Assignment of  $^1\text{H}$  NMR Spectrum of Azidobenzoate Copolymer

SHIFT (ppm)	ASSIGNMENT
0.88	b
1.03	a
1.27	c
1.90	d
2.45	solvent
3.49	f
3.60	solvent
4.30	h
4.52	i
7.13	n, k
8.06	m, l

The  $^1\text{H}$  NMR spectrum (see appendix 4) was in agreement with the copolymer structure and incorporation of the two monomers could be calculated from the integration of the resonances associated with the azidobenzoate monomer residue (aromatic hydrogen peaks at 7.13 and 8.06ppm) and methyl methacrylate ( $-\text{OCH}_3$  peak at 3.6ppm) spectra. The IR spectrum (see appendix 4) showed the presence of the azide group at  $2125\text{cm}^{-1}$  and other main peaks, see Table 4.16.

Table 4.16 Assignment of IR Spectrum of Azidobenzoate Copolymer

PEAK $\text{cm}^{-1}$	ASSIGNMENT
2960	C-H
2125	$\text{N}_3$
1715	C=O

The  $^{13}\text{C}$  NMR spectrum (see appendix 4) had a low signal to noise ratio as there was not enough copolymer sample in solution to obtain a good spectrum. Some of the main characterising peaks can be seen, C=O at 177ppm, the benzene ring at 120-130ppm,  $\text{CH}_2\text{-CH}_2$  of the azide monomer at 62ppm and methyl groups at 14-22ppm. The copolymers had yields <5% to comply with the conditions for using the differential form of the copolymer equation.

#### 4.3.2 Reactivity Ratios

The copolymerisations produced samples of the anthracene/MMA copolymer and the azide/MMA copolymer that contained no residual monomer after purification. Copolymers used for reactivity ratio calculations had been produced in yields of <5% to comply with the restrictions for proper use of the

differential form of the copolymer equation. At these low conversions it is assumed that the monomer feed ratio  $[M_1] / [M_2]$  is essentially constant and there is minimal composition drift.  $^1\text{H}$  NMR spectroscopy was used to determine the amount of each monomer present in the product copolymer.<sup>5</sup>

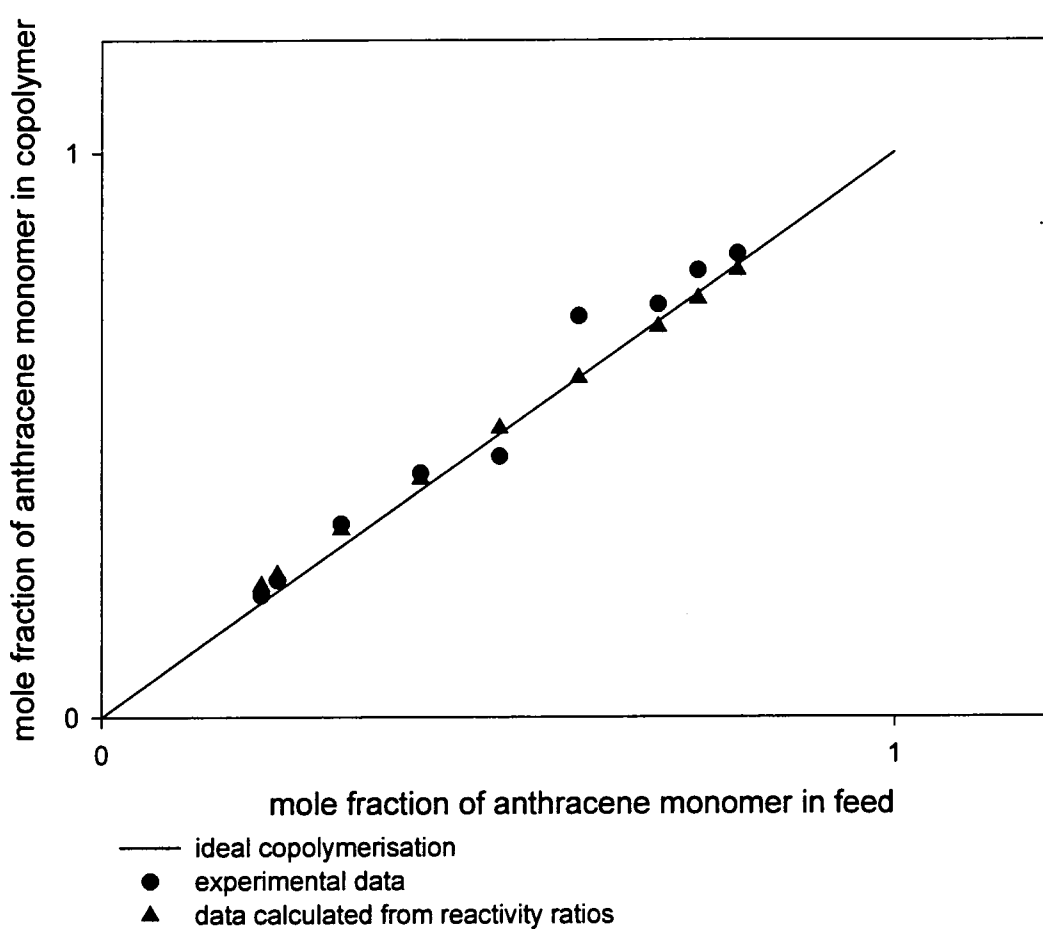
Table 4.17 Mole Fractions of Monomers in the Feed and in the Product Copolymer (calculated from  $^1\text{H}$  NMR data)

Anthracenoate Copolymer		Azidobenzoate Copolymer	
Mole fraction of Anthracenoate monomer in the Feed	Mole fraction of Anthracenoate monomer in Copolymer	Mole fraction of Azidobenzoate monomer in the Feed	Mole fraction of Azidobenzoate monomer in Copolymer
0.2	0.21	0.1	0.07
0.22	0.24	0.2	0.15
0.3	0.34	0.3	0.51
0.4	0.43	0.4	0.59
0.5	0.46	0.55	0.66
0.6	0.71	0.7	0.72
0.7	0.73	0.85	0.77
0.75	0.76		
0.8	0.82		

Table 4.17 contains the mole fractions of the monomers calculated from the  $^1\text{H}$  NMR data. These values were then plotted in graphs of mole fraction of monomer 1 in the copolymer v. mole fraction of monomer 1 in the feed (graphs 4.1 and 4.2).

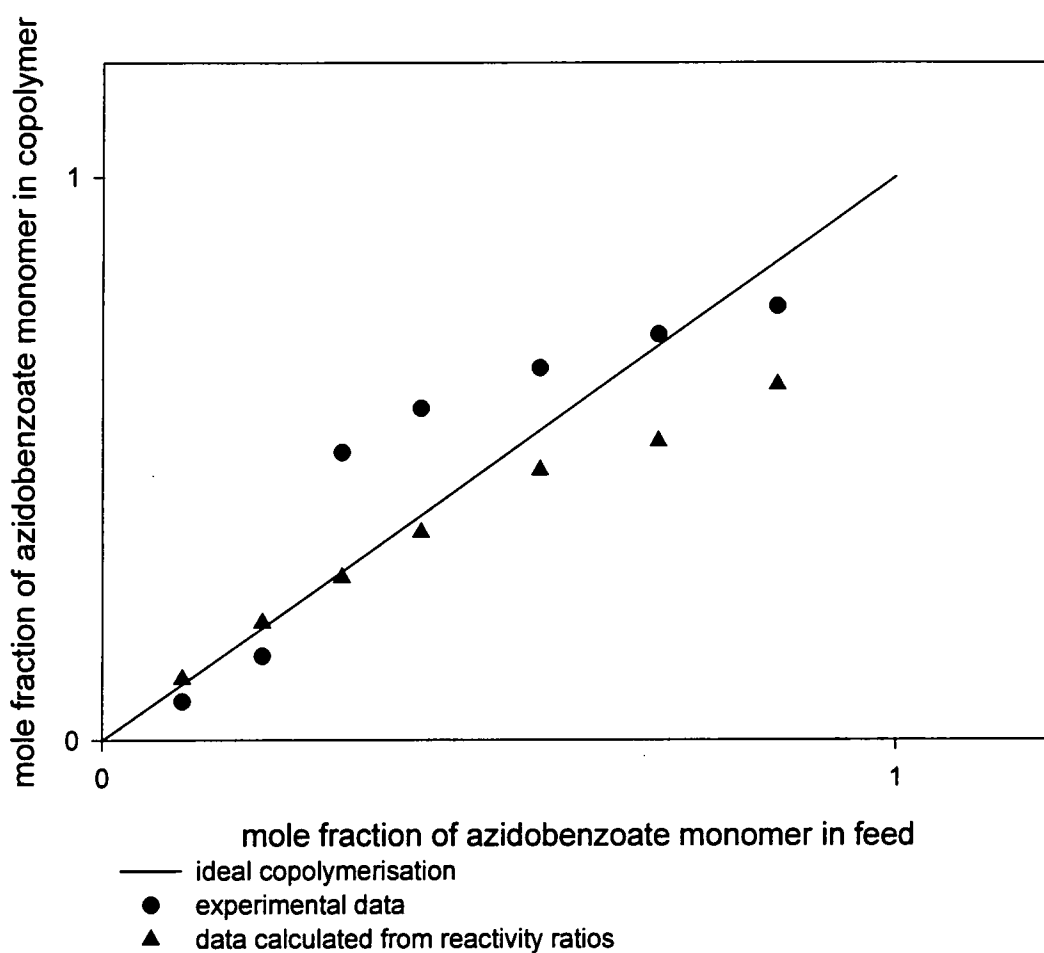
Graph 4.1

Graph of mole fractions of the Anthracenoate monomer in the copolymer v. feed



Graph 4.2

Graph of Mole fraction of monomer units in azidobenzoate copolymer v. Mole fraction in feed



Graphs 4.1 and 4.2 each show three plots; the straight lines represent the results for an ideal copolymerisation where  $r_1 \approx r_2 \approx 1$ , the circles are points determined from experimental data ( $^1\text{H}$  NMR spectra of the copolymers and the feed mole fractions) and the triangles are the results of applying the values for the reactivity ratios obtained later in this section to the following equation.

$$F_1 = \frac{r_1 f_1^2 + f_1 f_2}{r_1 f_1^2 + 2f_1 f_2 + r_2 f_2^2}$$

where  $r_1$  and  $r_2$  are the reactivity ratios and  $f_1$  and  $f_2$  are the mole fractions of the feed compositions.

From the graphs it can be seen that the data for the copolymer systems investigated in this work lies close to the plot for an ideal copolymerisation but as the plot values lie between  $0 < r < 1$ , composition drift will occur. However, where the curves cross the ideal copolymerisation line there is a point which represents a feed consistency where no composition drift will occur, this is known as the azeotropic copolymer composition (see the later section on composition drift).

To find the reactivity ratios of the two monomers the following equation was applied. The procedure used here to estimate the values of the reactivity ratios was established by Fineman and Ross<sup>6</sup>.

$$r_2 = r_1 H^2/h + H(1-h)/h$$

$r_2$  and  $r_1$  are the reactivity ratios

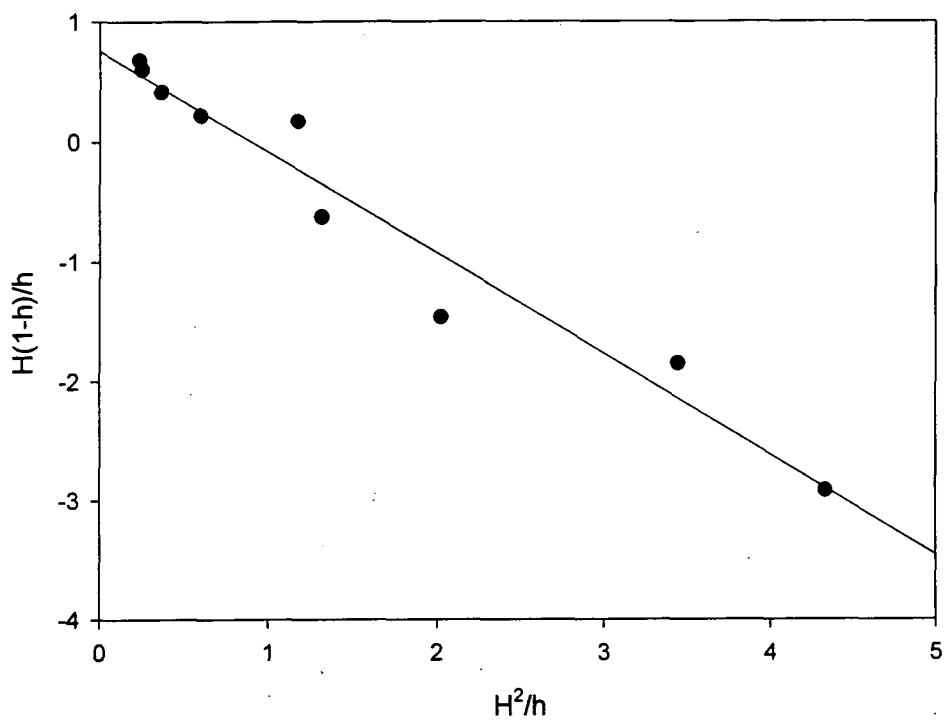
$H$  = mole ratio in the monomer feed of monomer 1 to monomer 2

$h$  = mole ratio in the product copolymer of monomer 1 to monomer 2

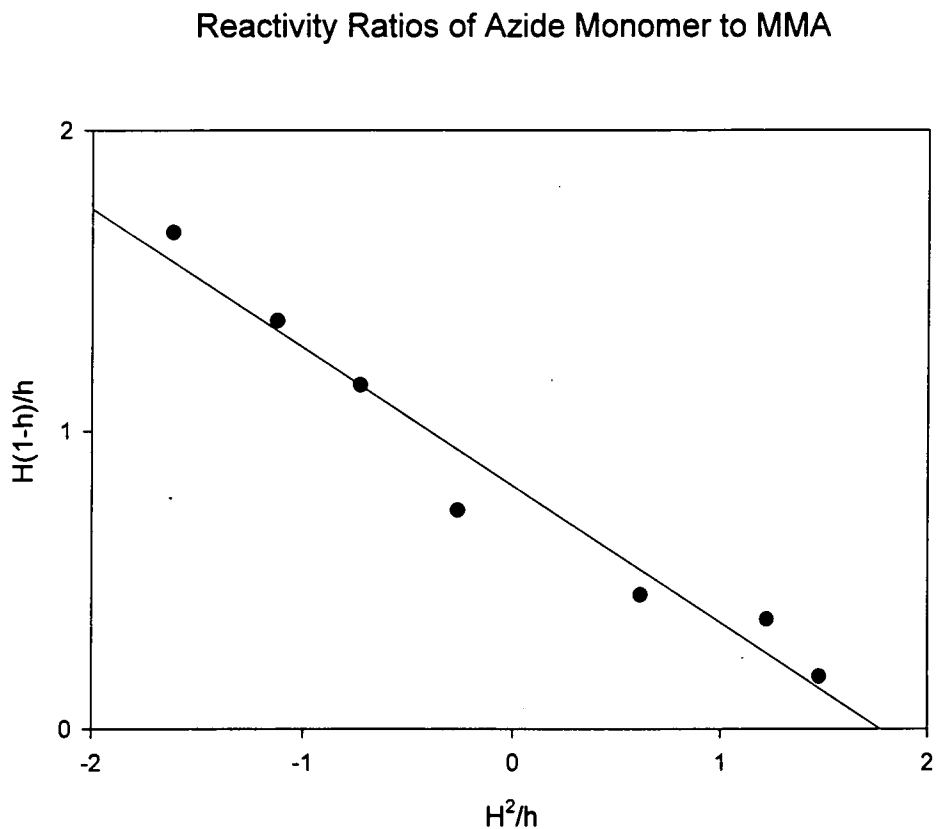
Values for  $H$  and  $h$  were calculated for each polymerisation and graphs (graphs 4.3 and 4.4) of  $H^2/h$  v.  $H(1-h)/h$  were plotted for each copolymer system.<sup>4</sup>

Graph 4.3  $H^2/h$  v.  $H(1-h)/h$  for Anthracenoate Copolymers

Reactivity Ratios of Anthracene Monomer and MMA



Graph 4.4  $H^2/h$  v.  $H(1-h)/h$  for Azidobenzoate Copolymers



From the graphs the values of  $r_1$  and  $r_2$  can be found from the slope and the intercept.

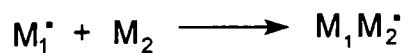
Slope =  $r_1$  = reactivity ratio of functionalised methacrylate monomer

Intercept =  $r_2$  = reactivity ratio of methyl methacrylate

Table 4.18 Reactivity Ratios of Monomers in the two Copolymer Systems

	$r_1$	$r_2$	$r_1 r_2$
Anth./MMA	0.84	0.76	0.64
Azide/MMA	0.46	0.82	0.38

In the two copolymer systems investigated in this work, the reactivity ratios are less than unity. When both reactivity ratios are less than one, cross-propagation is favoured by both monomers, i.e.,



are the favoured reactions. Therefore there is a tendency towards alternation in the polymer chain. The closer the value of  $r_1 r_2$  is to unity, the greater is the extent of alternation in the copolymer chains.

Structural effects influence the monomer reactivity ratios and hence the copolymer composition.<sup>2</sup> The main effects to consider in the case of the systems investigated here are resonance and polar effects. In the monomers used in these experiments there was little difference in their steric and polar effects due to their similar structures, all the monomers being methacrylates.

The errors of the values of the reactivity ratios have not been discussed yet. It should be kept in mind that reactivity ratio errors are fairly large and are often underestimated. However, uncertainty in reactivity ratio values is not as important as would be expected. Large errors are usually due to the insensitivity of the copolymer composition to the actual values of  $r_1$  and  $r_2$  used. In some instances variations of up to 30% in the values of  $r_1$  and  $r_2$  only cause a very small change in the copolymer composition curve.

## *Errors Applied to Reactivity Ratios*

Errors are difficult to calculate for the reactivity ratio determination experiments due to the method by which the copolymers are analysed. The data obtained to use in the copolymer equation is acquired from weighing the feed monomers on an electronic balance and calculating the ratio of monomers in the copolymer using  $^1\text{H}$  NMR spectroscopy.

Two initial measurements are made, the mass of the two monomers being put in the reaction pot and the ratio of the two monomers calculated from the integration of peaks in the  $^1\text{H}$  NMR spectra. So initially we must consider mass and NMR integration.

### 1. Mass

Errors made on a digital display balance are usually ignored as they are assumed to be negligible. As the same balance was used in every measurement, only systematic errors would affect the actual mass of monomer going into the pot. To actually calculate the error in the mass, the sample of monomer should be weighed approximately ten times and an average value found and the deviation from this average is the error. In this work the errors arising from mass measurements were considered to be negligible compared to errors originating from the  $^1\text{H}$  NMR integration. Therefore the errors from mass have been assumed to be minimal and have been disregarded.

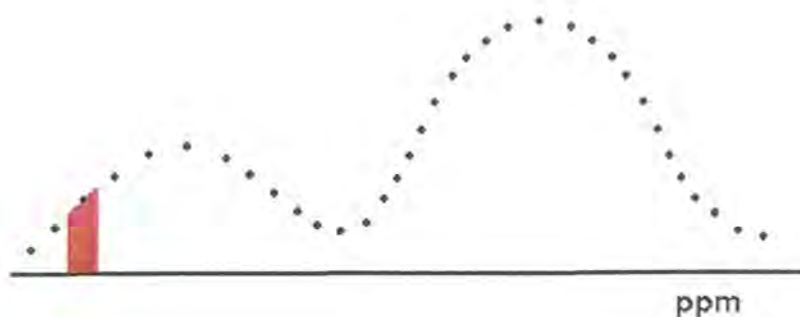
### 2. $^1\text{H}$ NMR Integration

Errors originating from the  $^1\text{H}$  NMR spectra of the copolymers are innumerable and cannot be easily estimated. The first source of errors arises

from baseline variations in the spectra which cause the results from the integration of the peaks to be inaccurate. Broad peaks are difficult to integrate precisely as there is a lack of obvious cut-off points for the peaks. This can be seen in diagram 4.6 where the two peaks merge into one another and it cannot be determined exactly where one peak ends and the next peaks starts. The cut-off points have to be estimated by eye and this leads to further error in the fact that cut-off points will not be placed at exactly the same point every time. This is not a reproducible variable and the errors from it are difficult to determine.

The integration algorithm is also a source of error. A  $^1\text{H}$  NMR spectrum is recorded as a series of points that when joined together form the peaks. The integration algorithm takes each point separately and integrates the area under that point (see diagram 4.6). The integration values from each point are then added together producing the final result. Therefore this method does not take into account overlapping peaks.

Figure 4.6 Representation of Integration Calculation for  $^1\text{H}$  NMR



Errors for the integration of  $^1\text{H}$  NMR spectra are usually estimated at ~5%, an estimate is all that can be used due to the number of variables that have to be

considered. For broad peaks, as in the case of the spectra for poly(para-azidobenzoate-2-ethyl methacrylate-co-methyl methacrylate), the error is underestimated and the error would be at least 5% and probably much more.

Estimating the error involved is therefore extremely difficult but has been attempted to try to give some indication of the accuracy of the reactivity ratio values. The  $^1\text{H}$  NMR spectrum of one sample was run several times on a 400MHz spectrometer. The following data were obtained.

Table 4.19 Integration Values of Peaks from  $^1\text{H}$  NMR Spectra

RUN	PEAK 1 (2 hydrogens)	PEAK 2 (2 hydrogens)	PEAK 3 (5 hydrogens)
1	75.14	66.93	190.36
2	137.59	124.92	336.10
3	56.83	51.47	129.38
4	92.12	82.16	210.57
5	129.23	132.50	316.05
6	81.03	81.87	211.85
7	135.18	127.50	340.30
8	107.30	113.07	250.38

The integration values for each individual hydrogen were then calculated.

Table 4.20 Integration Values for single Hydrogens from <sup>1</sup>H NMR Spectra

RUN	PEAK 1	PEAK 2	PEAK 3
1	37.57	33.47	38.07
2	68.80	62.46	67.22
3	28.42	25.74	25.88
4	46.06	41.08	42.11
5	64.62	66.25	63.21
6	40.52	40.94	42.37
7	67.59	63.75	68.06
8	53.65	56.54	50.08

Finally the average values and standard deviation from these average values were calculated.

Table 4.21 Average Values and Standard Deviations for Integration Values

	PEAK 1	PEAK 2	PEAK 3
Average	50.90	48.78	49.63
Standard deviation	14.18	14.42	14.32

However, it is not the error in the integrations that should be considered but the difference in the ratios of integration between peaks of the same spectrum.

This information was then applied to the reactivity calculations for the anthracene and azide systems and the results are shown below.

Errors:-

Anthracene system  $r \pm 0.75$

Azide system  $r \pm 0.96$

These are large errors so the reactivity ratio values should be taken as a semi-quantitative estimate which, never-the-less, gives an indication of the relative ease of incorporation of the monomers. Despite these reservations the lines of best fit of the graphs representing  $H^2/h$  v.  $H(1-h)/h$  are straight and appear to be a good fit with confidence limits of  $r^2 = 0.95$ , the results should not be wildly inaccurate. However, the method to determination the errors of the reactivity ratio values used here is not statistically sound. Reactivity ratios are not independent variables, i.e., the values of one reactivity ratio directly effect the other so therefore errors are usually predicted by a joint confidence limit which can be represented by a two-dimensional area on the monomer mole fraction graphs.

#### **4.3.3 Composition Drift of the Anthracene Monomer/MMA System**

The phenomenon of the alteration of the feed composition during polymerisation was first realised by Staudinger<sup>3</sup> and is known as composition drift. Composition drift can occur in systems where  $r_1$  and  $r_2$  are both less than unity. The magnitude and direction of the drift depend upon the feed composition in the copolymerisation vessel. Copolymer composition plots for systems with  $r_1$  and  $r_2$  less than one are sigmoidal and cross the line for an ideal copolymerisation ( $r_1 \approx r_2 \approx 1$ ) at a point indicating the azeotropic copolymer

composition. This point represents a feed composition that will form a copolymer without composition drift. This is known as azeotropic copolymerisation. Above the azeotrope, the drift will occur in favour of one monomer, and below it, in favour of the other.

The composition of the azeotrope can be calculated using the copolymer composition equation. At the azeotropic feed,

$$\frac{d[M_1]}{d[M_2]} = \frac{[M_1]}{[M_2]}$$

$$\text{thus, } r_1[M_1] + [M_2] = [M_1] + r_2[M_2]$$

$$\text{i.e. } \frac{r_1[M_1]}{[M_2]} + 1 = \frac{[M_1]}{[M_2]} + r_2$$

$$\text{or } \frac{[M_1]}{[M_2]}(r_1 - 1) = r_2 - 1$$

$$\text{Therefore, } \frac{[M_1]}{[M_2]} = \frac{r_2 - 1}{r_1 - 1}$$

Therefore, the exact position of the azeotropic point depends on the relative sizes of  $r_1$  and  $r_2$ .

The reactivity ratios for the two copolymer systems and the graphs of monomer fraction in the copolymer v. monomer fraction in the feed (see graphs 4.1 and 4.2) give the best indication of composition drift.

Table 4.22 Reactivity Ratios of Monomers in the two Copolymer Systems

	$r_1$	$r_2$
Anth./MMA	0.84	0.76
Azide/MMA	0.46	0.82

From graphs 4.1 and 4.2 it can be seen that composition drift can occur in either direction depending on the feed composition, apart from at the azeotropic point. Using the reactivity ratios and the following equation

$$f_{ap} = (1-r_2)/\{2-(r_1 + r_2)\}$$

the point of the azeotrope can be calculated. For the anthracene system  $f_{ap}=0.6$  and the azide system  $f_{ap}=0.25$ .

For further evidence of composition drift in the MMA-anthracenoate-2-ethyl methacrylate copolymerisations several copolymers were made from different feed ratios of the two monomers. These copolymerisations were allowed to continue for 4 hours. The table below shows the monomer ratios used in the feed compared to the ratios found in the copolymers.

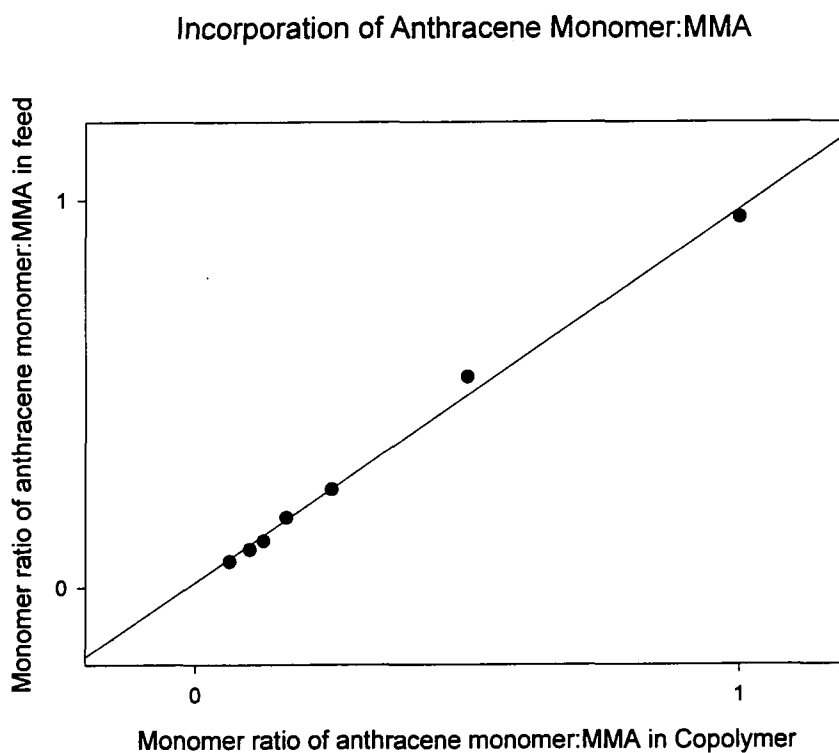
Table 4.23 Ratios of MMA:Anthracenoate Monomer in Feed and Copolymers

Experiment Code	Ratio MMA:Anthracenyl monomer in feed	Ratio MMA: Anthracenyl monomer in product
KEF47	1:1	1.047:1
KEF49	2:1	1.842:1
KEF50	4:1	3.953:1
KEF51	6:1	5.56:1
KEF52	8:1	8.33:1
KEF53	10:1	10.20:1
KEF54	16:1	14.93:1

This information can be represented in a graph and appears to follow a straight line (see graph 4.5), although it should be emphasised that as

composition drift is occurring the feed ratios are no longer correct values. Therefore these results have been used to exhibit the change found as the copolymerisation progresses.

Graph 4.5 Anthracenoate Monomer:MMA in Feed v. Anthracenoate Monomer:MMA in Copolymers

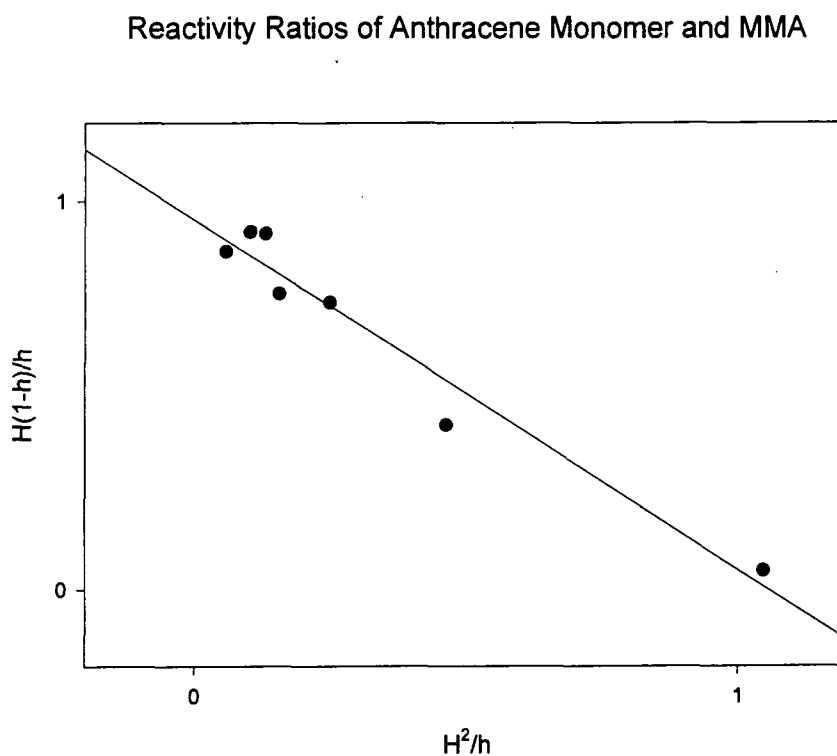


The copolymer equation was then applied to these results.

$$r_2 = r_1 H^2/h + H(1-h)/h$$

Then the following graph of  $H^2/h$  v.  $H(1-h)/h$  was plotted.

Graph 4.6  $H^2/h$  v.  $H(1-h)/h$  for Anthracenoate Copolymers



The reactivity ratios were calculated from this graph (slope =  $r_1$  and intercept =  $r_2$ ). Values for the reactivity ratios at 4 hours (yield 65-76%) could then be compared with the values found after 15 minutes (yield <5%).

Table 4.24 Reactivity Ratios of MMA and Anthracenoate Monomer from Copolymers made after 15 minutes and after 4 hours

	$r_1$	$r_2$
Copolymer at 15 minutes	0.84	0.76
Copolymer at 4 hours	0.90	0.95

It was discovered that after 15 minutes reaction time  $r_1 > r_2$  but after 4 hours reaction time  $r_2 > r_1$ , this is a result of composition drift. However, as  $r_1$  and  $r_2$  are both less than one, the direction and degree of composition drift will depend on the feed composition.

#### 4.4 Conclusions

Bulk polymerisation worked well, producing copolymer in large yields with a high molecular mass. However, this large molecular mass together with the low solubility of the polymer led to the conclusion that cross-linking had occurred during polymerisation. This is a common effect during free radical bulk polymerisations of methacrylates probably caused by a chain transfer mechanism involving hydrogen abstraction from the polymer chain.

The attempted dispersion polymerisation did not produce any polymer at all, only monomer was left at the end of the reaction. Emulsifiers were not used in the reaction as it was hoped that the vigorous stirring would be sufficient to form small droplets of the monomers. Conceivably this may have been the fault with the reaction and adding an emulsifier may have made the reaction produce copolymer. Emulsifiers were not added to the reaction because there had to be no ions present in the product polymer and adding emulsifiers would have made purification of the copolymers difficult if not impossible.

Solution polymerisation was found to be the best method for producing the copolymers using 2-butanone as the solvent. Copolymerisations were achieved using different ratios of the two monomers involved in order to calculate reactivity ratios and estimate composition drift.

The reactivity ratios of the anthracenyl monomer and MMA are similar but the anthracenyl monomer has a slightly larger reactivity ratio. The opposite result was found for the azide system with the MMA with a larger reactivity ratio than the azide monomer. Statistical copolymers will be formed from both systems but with a greater degree of alternation in the copolymer as  $r_1 r_2$  approaches zero. As the monomers are used in making the copolymers, the feed stock composition will alter and hence the copolymer composition will differ as composition drift occurs, although this depends on the feed composition. Composition drift was noticed in the anthracenoate copolymer system but the effect was relatively small. Drift could occur in either direction depending on the feed stock consistency unless the feed for an azeotropic copolymerisation is used, then no composition drift will occur.

## References

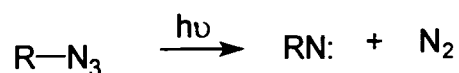
1. Alfrey Jr. T. and Goldfinger G., J. Chem. Phys (12), 1944, page 205.
2. Mayo F.R. and Lewis F.M., J. Am. Chem. Soc. (66), 1944, page 1594.
3. Alfrey T., Bohrer J.J. and Mark H., High Polymers vol. 8  
Copolymerisation, Interscience Publishers 1952, chapter 1.
4. Collins E.A., Bares J. and Billmeyer F.W., Experiments in Polymer Science, John Wiley and Sons, 1973, pages 20-21 and 342-45.
5. Krufft M.B. and Koole L.H., A Convenient Method to Measure Monomer Reactivity Ratios. Application to Synthesis of Polymeric Biomaterials Featuring Intrinsic Radiopacity, Macromolecules (29), N° 17, 1996, pages 5513-19.
6. Fineman F.R. and Ross S.D., J. Poly. Sci. (5), 1944, page 269.

## Chapter Five

### Suggestions for Future Work on the Synthesis of Alignment Layers for Liquid Crystal Devices

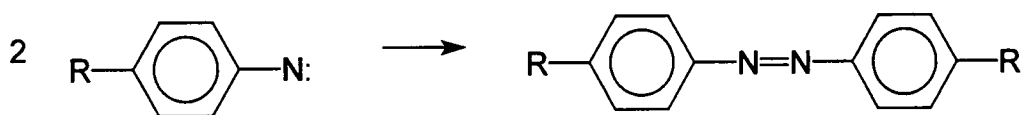
#### 5.1 Photochemistry of Poly(para-azidobenzoate-2-ethyl methacrylate)

Azides exhibit photoelimination<sup>1,2</sup> of a molecule of nitrogen on irradiation with ultra-violet light and a nitrene results.



Also, nitrene intermediates are formed by thermal decomposition of azide compounds but only the photoreaction is of concern in this section. Due to the elimination of nitrogen the photoelimination reaction is irreversible. The nitrene species is extremely reactive and has a short lifetime (several microseconds). On irradiation of poly(para-azidobenzoate-2-ethyl methacrylate) it was hoped that the nitrene species formed would dimerise to yield azobenzene cross-links, see Figure 5.1.

Figure 5.1 Azobenzene Formation



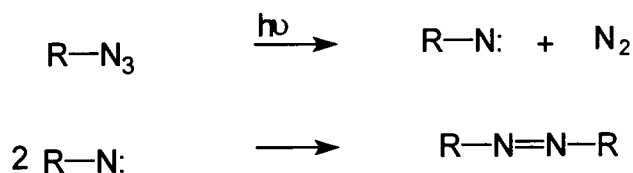
Scientists at the Defence Research Agency reported that azobenzene links were not formed on ultra-violet irradiation of the polymer which we provided, so further investigation into the process occurring is necessary.

Azido photocross-linkable polymers have been described as, "A class of useful photopolymers that cross-link by non-dimerisable groups."<sup>3</sup> From this statement it appears that it should not be expected that ultra-violet irradiation of

an azido polymer will result in azobenzene cross-links and maybe our initial objectives were a little naive. As nitrenes are so reactive there are many possibilities as to what could be happening.<sup>4,5</sup>

### 1. Recombination

It was hoped that recombination would occur to cross-link the azide polymer system.



Two of the nitrene species react together to form an azobenzene cross-link.

However, in continuous photolysis of azides there exists only a low concentration of nitrene present at any time, so azobenzene formation is unlikely.

Recombination requires little activation energy so is more often witnessed at low temperatures when no other reactions are occurring in competition. If flash photolysis is used a high concentration of nitrenes will be formed in the same instant so there would be a greater chance of azobenzene formation.<sup>4</sup>

### 2. Electrophilic attack on bond pairs

#### a. Insertion into C-H bonds

Figure 5.2 Insertion into C-H bonds



Insertion into C-H bonds yields secondary amines. The selectivity of this reaction is that aromatic nitrenes insert into C-H bonds in the order primary < secondary < tertiary.

b. Insertion into O-H bonds

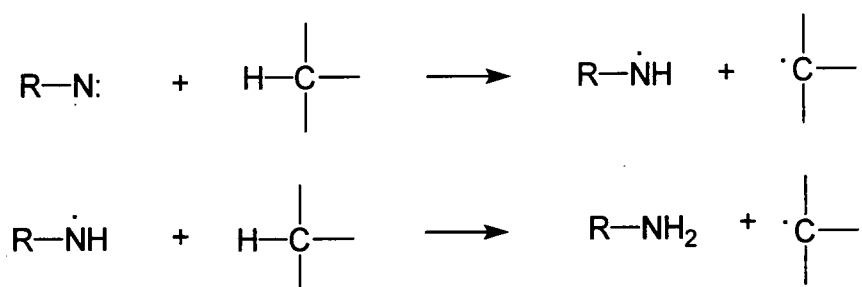
Insertion of a nitrene into an O-H bond yields a hydroxylamine. This reaction could not occur in the poly(para-azidobenzoate-2-ethyl methacrylate) system as there are no O-H bonds present.

c. Insertion into N-H bonds

This reaction could occur only if a C-H bond insertion reaction had yielded a secondary amine. However, N-H bond insertion reactions tend to favour primary amines so this reaction is very unlikely in the poly(para-azidobenzoate-2-ethyl methacrylate) system.

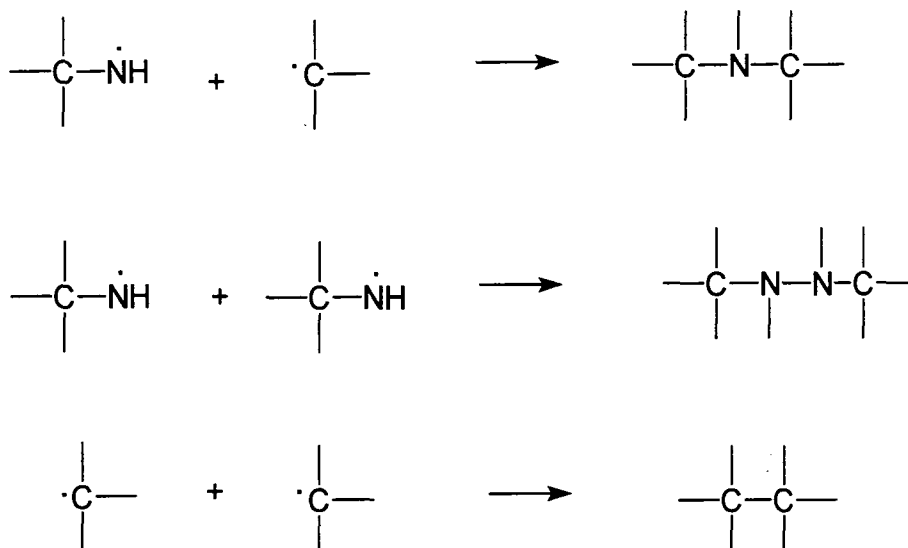
d. Hydrogen abstraction

Figure 5.3 Hydrogen Abstraction



Hydrogen abstraction involves a two-step process to form an amine as shown in Figure 5.3. However, as the products are radicals and radicals are highly reactive species, other reactions can be expected as well, see Figure 5.4.

Figure 5.4 Radical side reactions occurring with hydrogen abstraction

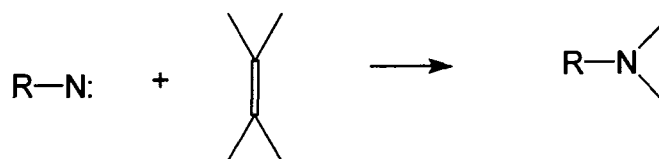


3. Addition to multiple bonds

a. Addition to C=C

The nitrene inserts into the double bond forming a heterocyclic ring, there are no C=C bonds present in poly(para-azidobenzoate-2-ethyl methacrylate) so this process could not occur.

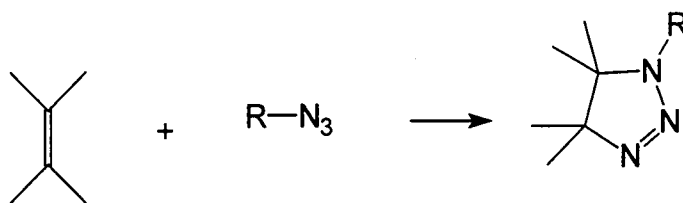
Figure 5.5 Addition to C=C



b. 1,3 Dipolar cycloadditions

This process involves the reaction of the double bond with the azide group, see Figure 5.6.

Figure 5.6 1,3 dipolar cycloaddition reaction



As there are no C=C bonds present in the azide polymer system under investigation, this process could not be happening. Although, addition to C=C may be a complicating factor during polymer formation leading to structural defects (see Chapter 3).

Azobenzene linkages were not formed on the irradiation of poly(para-azidobenzoate-2-ethyl methacrylate) with UV light so the most probable reactions occurring are hydrogen abstraction or C-H bond insertion of the nitrene.

According to Merrill and Unruh<sup>6</sup> the photocross-linking reaction is subject to variations depending on organic structure, i.e. the fate of the nitrene is a function of its environment. This is illustrated by the example that when 4-azidobenzoic acid is irradiated with ultra-violet light, 4,4'-dicarboxyazobenzene is formed. However, when phenyl azide is irradiated, an amorphous solid with the empirical formula C<sub>6</sub>H<sub>6</sub>ON is formed containing no azobenzene groups. They also claim that the photo and thermal decomposition reactions are comparable. Therefore the same process was probably occurring when poly(para-azidobenzoate-2-ethyl methacrylate) became insoluble at room temperature as when the polymer was irradiated with ultra-violet light.

Preliminary investigations into the photochemistry occurring showed that when films of poly(4-azidobenzoate-2-ethyl methacrylate) were exposed to UV

light, the polymer film turned from pale yellow to orange. Orange colouration is often a characteristic of azo compounds but there only needs be a very small amount present to cause a strong colour. The small amount of azobenzene cross-links formed may remain undetected on analysis of the photo-product due to the low concentration.

Further research into the products of this photo-reaction is required to determine the mechanism of the process occurring and the structures of the photo-products obtained. 4-Azidobenzoic acid does cross-link forming azobenzene links on irradiation.<sup>6</sup> Therefore, it seems likely that azobenzene groups can be formed on irradiation of the phenyl azide esters used in this work but in the polymer, poly(para-azidobenzoate-2-ethyl methacrylate), the environment of the azide provides many other sites where insertion or abstraction reactions could occur.

Organic aromatic azides are characterised by an absorbance in the UV spectrum centred at 285nm. Therefore, to observe the photochemistry of the azide homopolymer, the polymer should be exposed to an UV source at  $\lambda \cong 285\text{nm}$ , although there may be some overlap with the weak absorption associated with the ester carbonyl. It would be beneficial to observe the photochemical behaviour of fragments of the polymer, e.g. 4-azidobenzoic acid, 4-azidobenzoate-2-ethyl methacrylate and 4-azidobenzoic acid with poly(methyl methacrylate) as models for the reaction. The homopolymer photochemistry may be complicated with several processes occurring, yielding a variety of photo-products. Therefore, if fragments of the homopolymer are irradiated with UV light and the photo-products analysed, it may be easier to ascertain what products

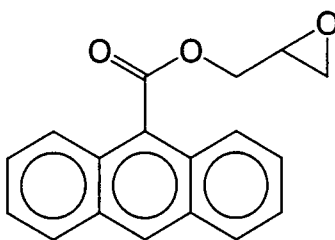
are formed and hence what reactions have occurred. These results could be compared with the photo-products of the homopolymer and deductions made as to the mechanisms occurring during the photoreaction.

## 5.2 Future Work

There is still a lot of work to be done in the area of photocross-linking polymers for use as alignment layers for liquid crystal displays. The new polymers described in this thesis, although they do give the desired effect, do not function at the standard necessary for use in commercial liquid crystal display cells. The poly(9'-anthracenoate-2-ethyl methacrylate) does not introduce pre-tilt in the liquid crystal molecules and the cross-linking mechanism of poly(para-azidobenzoate-2-ethyl methacrylate) is unclear so does not allow sufficient control over the alignment process. Investigation into the photochemistry of the azide system is necessary to discover if hydrogen abstraction or C-H bond insertion is occurring and what product is formed after irradiation with UV light.

Altering the spacer chain length between the chromophore and the polymer may affect the alignment properties. The spacer chain length affects the mobility of the chromophore, longer side chains provide greater mobility and vice versa. There may be an optimum side chain length that provides the chromophores with enough mobility to easily encounter one another and cross-link but prevents side chain entanglement which would alter the polymer conformation and therefore the alignment properties. A variation of the anthracenoate polymer could involve the polymerisation of the glycidyl ester<sup>7</sup> of anthracene, see figure 5.7.

Figure 5.7 Glycidyl ester of anthracene

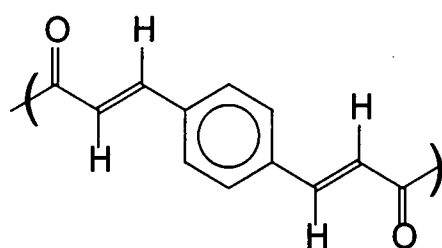


This polymer would have a shorter spacer unit which may alter the alignment properties, the bulk of the anthracene units may cause steric hindrance with the main chain and might inhibit polymerisation. Longer chain lengths may prove to be more beneficial as the anthracene units in the derived polymers would possess a greater mobility so would be more likely to come into contact with one another and dimerise. A proper understanding of the factors influencing the process of photodimerisation requires a range of structures to be investigated.

New polymers must be designed that function in an ideal way for a liquid crystal alignment layer. They must introduce unidirectional anisotropic alignment and pre-tilt to the liquid crystal molecules which allows efficient and fast functioning of the liquid crystal cell. The cross-linking mechanism must be fully understood to allow control of the alignment and all the other criteria introduced in chapter one must be included, see page 18. Photocross-linkable polymers can include the chromophore unit in the main chain or appended to the main chain. In this thesis only polymers with appended chromophores have been investigated but a main chain chromophore polymer may function well as an alignment layer for liquid crystal display cells.

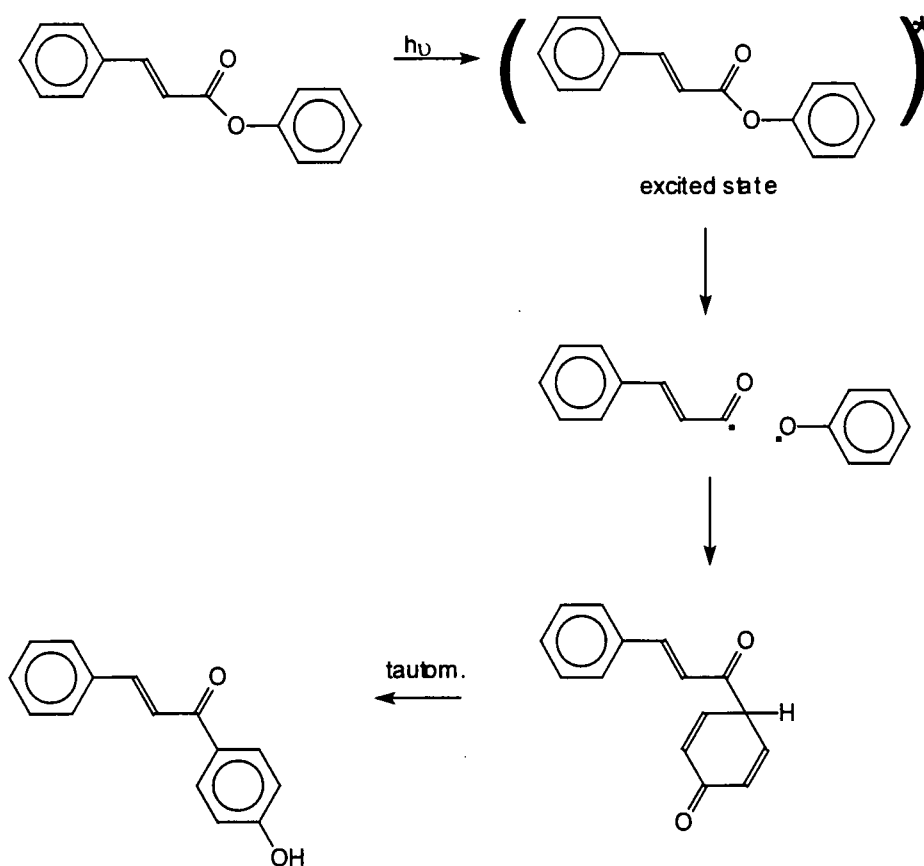
As poly(vinyl cinnamate) behaved quite well as an alignment layer, a main chain cinnamate polymer may prove to be worth investigation. Main chain cinnamates have already been synthesised but not for use as alignment layers for liquid crystal.<sup>8,9</sup>

Figure 5.8 Main chain cinnamate polymers<sup>10</sup>



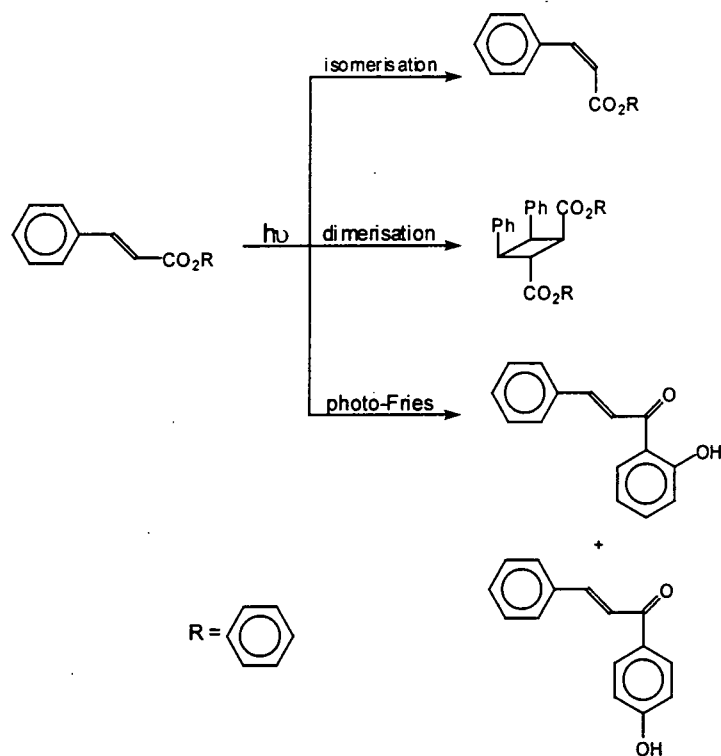
When irradiated with ultra-violet light these polymers cross-link forming a thermally stable, insoluble polymer network. The C=C bond undergoes 2+2 photocycloaddition but other reactions have been found to occur as well, such as photo-Fries rearrangement<sup>11</sup>, see Figure 5.10. Photo-Fries rearrangement produces a 2-hydroxychalcone derivative. This reaction is an intramolecular free radical process<sup>12</sup> as shown in figure 5.9.

Figure 5.9 Photo-Fries Rearrangement Mechanism



According to Creed et al.<sup>12</sup> it is unlikely that the photo-Fries reaction will occur between polymer chains so cross-linking by this mechanism is unlikely but not impossible. The photo-Fries rearrangement product causes the polymer film to turn yellow which is not ideal for a liquid crystal alignment layer as the film is to be part of the transparent window of the liquid crystal display cell. To eliminate the likelihood of photo-Fries rearrangements the spacer group between the cinnamate moieties should be fairly rigid to prevent the units coming in contact with one another and hence prevent their reaction.

Figure 5.10 Reactions of Cinnamate after UV irradiation<sup>13</sup>



The isomerisation, see Figure 5.10, has not been studied extensively yet but is thought to only occur in polymers where the chains are very mobile so again, rigid chains are preferable to flexible spacer chains.

Some main chain cinnamate polymers have been found to possess a nematic liquid crystalline phase<sup>10</sup> at relatively low temperatures but this depends on the structure of the polymer. This would be undesirable as the alignment layer could then interfere with the functioning of the liquid crystal cell. The nematic liquid crystal properties of the main chain cinnamate are structure dependent so a polymer must be designed that does not possess a nematic phase by incorporating flexible spacer groups between the chromophore units but this may allow the

other photochemical processes of isomerisation and photo-Fries rearrangement to occur.

As the cinnamate chromophore can be introduced into the main chain of a polymer it may also be possible for other chromophores such as anthracene or other groups containing the chromophoric  $-C=C-CO-$  unit to be incorporated into the chain.

Other ways of producing a material for use as an alignment layer might be to synthesise a polymer that cross-linked when exposed to ultra-violet light at a high temperature and then use the material at a lower temperature so no further reaction could occur. This is to prevent the problem of further reaction after irradiation with UV light, as it was established that not all the chromophores would react on UV exposure and also some relaxation probably would occur. If some of the chromophores remain unreacted they could photocross-link in daylight and the alignment of the polymer film would be changed. Therefore it is necessary to ensure no further reaction occurs after the UV irradiation that initially align the polymer film. Another method of circumventing this problem would be to 'neutralise' the chromophore as part of the post-exposure processing. That is, to find a way to 'wash' the mixture to remove the unreacted chromophore units or react the cross-linked polymer film with a reagent to remove unreacted chromophores or irradiate at a different wavelength to destroy one component selectively.

Photocross-linkable polymers are a growing area of polymer science as there is a great need to find a clean, simple and efficient replacement for the rubbed polyimide films that are currently used as alignment layers in liquid

crystal device technology. This thesis has described an increase in knowledge in this area but there is clearly much more to do.

## References

1. Gilbert A., Photoelimination reactions, Photochemistry (3), 1972, pages 745-803.
2. Reid S.T., Photoelimination, Photochemistry (19), 1986-7, pages 421-56.
3. Labana S.S. (editor), Ultraviolet light induced reactions in polymers, Am. Chem. Soc., 1976.
4. Patai S. (editor), The chemistry of the azido group, Interscience Publishers, 1971.
5. L'Abbe G., Decomposition and addition reactions of organic azides, Chem. Revs. (69), 1969, pages 345-63.
6. Merrill S.H. and Unruh C.C., Photosensitive Azide Polymers, J. Appl. Poly. Sci. (7), 1963, pages 273-9.
7. Brochu S. and Ampleman G., Synthesis and Characterisation of Glycidyl Azide Polymers Using Isotactic and Chiral Poly(epichlorohydrin)s, Macromolecules (29), 1996, pages 5539-45.
8. Jin X., Carfagna C., Nicolais L. And Lanzetta R., Synthesis, Characterisation and in Vitro Degradation of a Novel Thermotropic Ternary Copolyester Based on p-Hydroxybenzoic Acid, Glycolic Acid and p-Hydroxycinnamic acid, Macromolecules (28) N° 14, 1995, pages 4785-94.
9. Haddleton D.M., Creed D., Griffin A.C., Hoyle C.E. and Venkataram K., Photochemical crosslinking of main-chain liquid-crystalline polymers containing cinnamoyl groups, Makromol. Chem. Rapid Commun. (10), 1989, pages 391-96.

10. Li C., Cheng H., Chang T. and Chu T., Studies on the Thermotropic Liquid-Crystalline Polymer IX. Synthesis and Properties of Crosslinkable Copoly(amide-ester)s Containing Conjugated Double Bonds, J. Poly. Sci. Part-A (31), 1993, pages 1125-33.
11. Subramanian P., Creed D., Griffin A.C., Hoyle C.E. and Venkataram K., The mechanism of photo-Freis fragmentation of aryl cinnamates in polymer films and in solution, J. Photochem. Photobiol. A:Chem (61), 1991, pages 317-27.
12. March J., Advanced Organic Chemistry Reactions, Mechanisms and Structure, 4<sup>th</sup> edition, John Wiley & Sons Inc., 1992.
13. Creed D., Griffin A.C., Gross J.R.D., Hoyle C.E. and Venkataram K., Photochemical Crosslinking of Novel Polycinnamate Main Chain Mesogens, Mol. Cryst. Liq. Cryst. (155), 1988, pages 57-71.

# APPENDICES

## Appendix One - Instrumentation

$^1\text{H}$  and  $^{13}\text{C}$  NMR Spectra were recorded using a Varian VXR 400 NMR spectrometer at 399.952 MHz ( $^1\text{H}$ ) and 100.577 MHz ( $^{13}\text{C}$ ) and a Varian Gemini 200 NMR spectrometer at 199.532 MHz ( $^1\text{H}$ ) and 50.289 MHz ( $^{13}\text{C}$ ).

Mass spectra were recorded using a VG Analytical Model 7070E Mass Spectrometer.

Infra-red Spectra were recorded using a Perkin Elmer 1600 series FTIR.

Gel Permeation Chromatography was carried out using a Waters Model 590 Chromatogram with a refractometer detector, PL gel 5 $\mu\text{m}$  mixed styrene-divinylbenzene beads, solvent - chloroform and calibrated with polystyrene standards.

Thermogravimetric Analysis was performed using a Stanton Redcroft TG760 thermobalance.

UV/vis. spectra were recorded using a Unicam UV/vis. spectrometer UV2 using Vision 2.0 software.

Elemental analysis was performed on a CE-440 Elemental Analyzer from EAI Exeter Analytical Inc.

## Appendix Two - Analytical Data for Chapter Two

### *<sup>1</sup>H NMR Spectra*

1. Anthracene carboxylic acid
2. Anthracene carboxylic acid chloride
3. 9'-Anthracenoate-2-ethyl methacrylate
4. Poly(9'-anthracenoate-2-ethyl methacrylate) (solution polymerisation)
5. Poly(vinyl alcohol) + Anthracene carboxylic acid chloride in triethylamine
6. Poly(vinyl alcohol) + Anthracene carboxylic acid chloride in pyridine

### *<sup>13</sup>C NMR Spectra*

1. Anthracene carboxylic acid
2. Anthracene carboxylic acid chloride
3. 9'-Anthracenoate-2-ethyl methacrylate
4. Poly(9'-anthracenoate-2-ethyl methacrylate) (solution polymerisation)
5. Poly(vinyl alcohol) + Anthracene carboxylic acid chloride in triethylamine

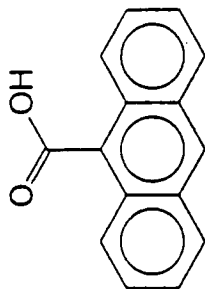
### *IR Spectra*

1. Anthracene carboxylic acid
2. Anthracene carboxylic acid chloride
3. 9'-Anthracenoate-2-ethyl methacrylate
4. Poly(9'-anthracenoate-2-ethyl methacrylate) (solution polymerisation)
5. Poly(9'-anthracenoate-2-ethyl methacrylate) (bulk polymerisation)
6. Poly(vinyl alcohol) + Anthracene carboxylic acid chloride in triethylamine

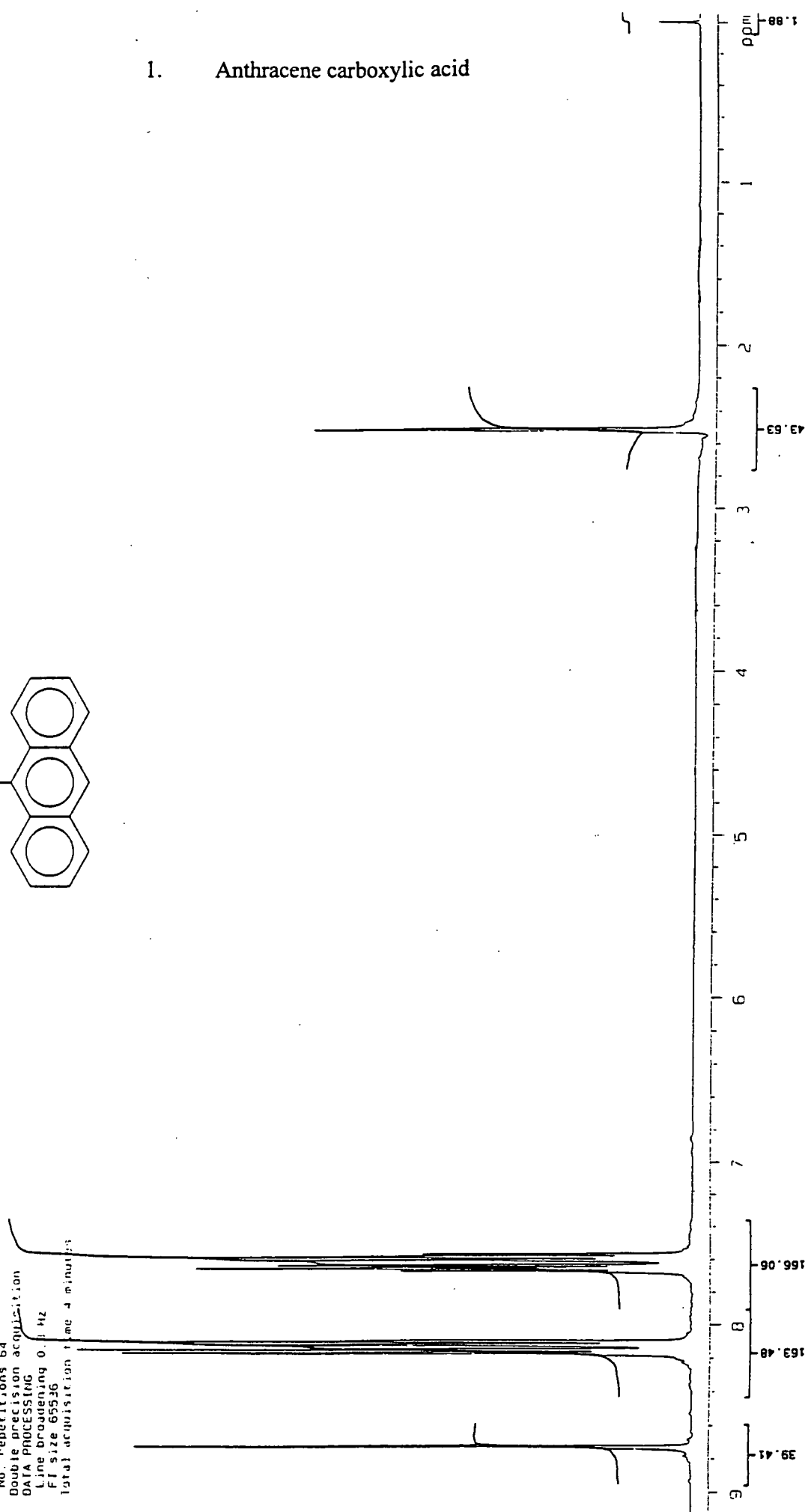
7. Poly(vinyl alcohol) + Anthracene carboxylic acid chloride in pyridine

SOLVENT DMSO

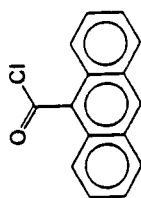
OBSERVE H1  
Frequency 399.906 MHz  
Spectral width 5000.0 Hz  
Acquisition time 3.744 Sec  
Relaxation delay 0.000 Sec  
Pulse width 5.0 usec  
Ambient temperature  
No. repetitions 64  
Double precision acquisition  
DATA PROCESSING  
Line broadening 0.1 Hz  
FI size 65536  
Total acquisition time 4 minutes



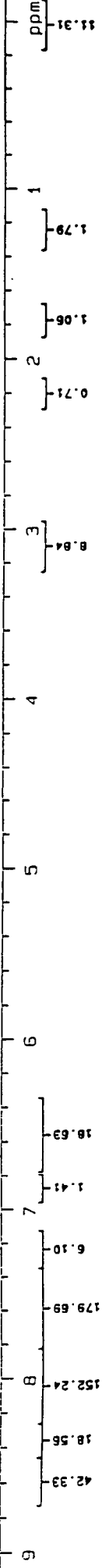
1. Anthracene carboxylic acid



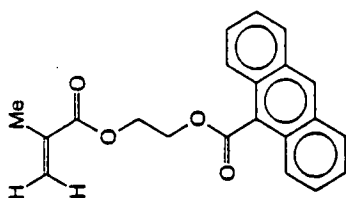
2. Anthracene carboxylic acid chloride



KCF 6  
FILE /data/curd/ksf231ana.fid  
RUN ON Jan 23 95  
SOLVENT CCl<sub>4</sub>  
OBSERVE f1  
Frequency 399.967 MHz  
Spectral width 5000.0 Hz  
Acquisition time 3.744 sec  
Relaxation delay 0.000 sec  
Pulse width 5.8 usec  
Ambient temperature  
No. repetitions 4  
Double precision acquisition  
DATA PROCESSING  
Line broadening 0.3 Hz  
FT size 65536  
Total acquisition time 4 minutes

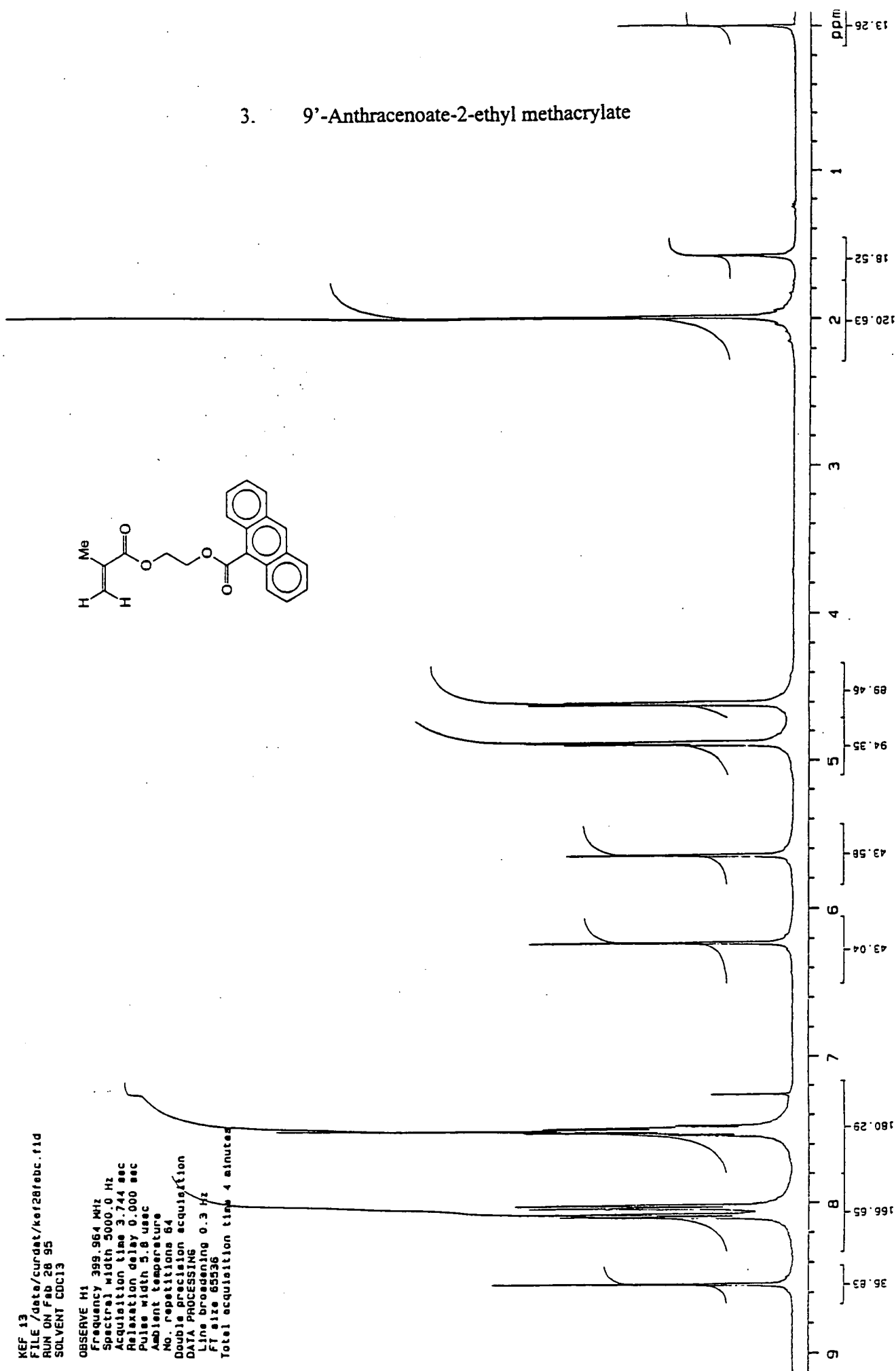


3. 9'-Anthracenoate-2-ethyl methacrylate



KEF 13  
 FILE /data/curdatt/kef28feb.c.fid  
 RUN ON Feb 28 95  
 SOLVENT CDCl3

OBSERVE H1  
 Frequency 399.964 MHz  
 Spectral width 5000.0 Hz  
 Acquisition time 3.744 sec  
 Relaxation delay 0.000 sec  
 Pulse width 5.8 usec  
 Ambient temperature  
 No. repetitions 64  
 Double precision acquisition  
 DATA PROCESSING  
 Line broadening 0.3 Hz  
 FI size 65536  
 Total acquisition time 4 minutes

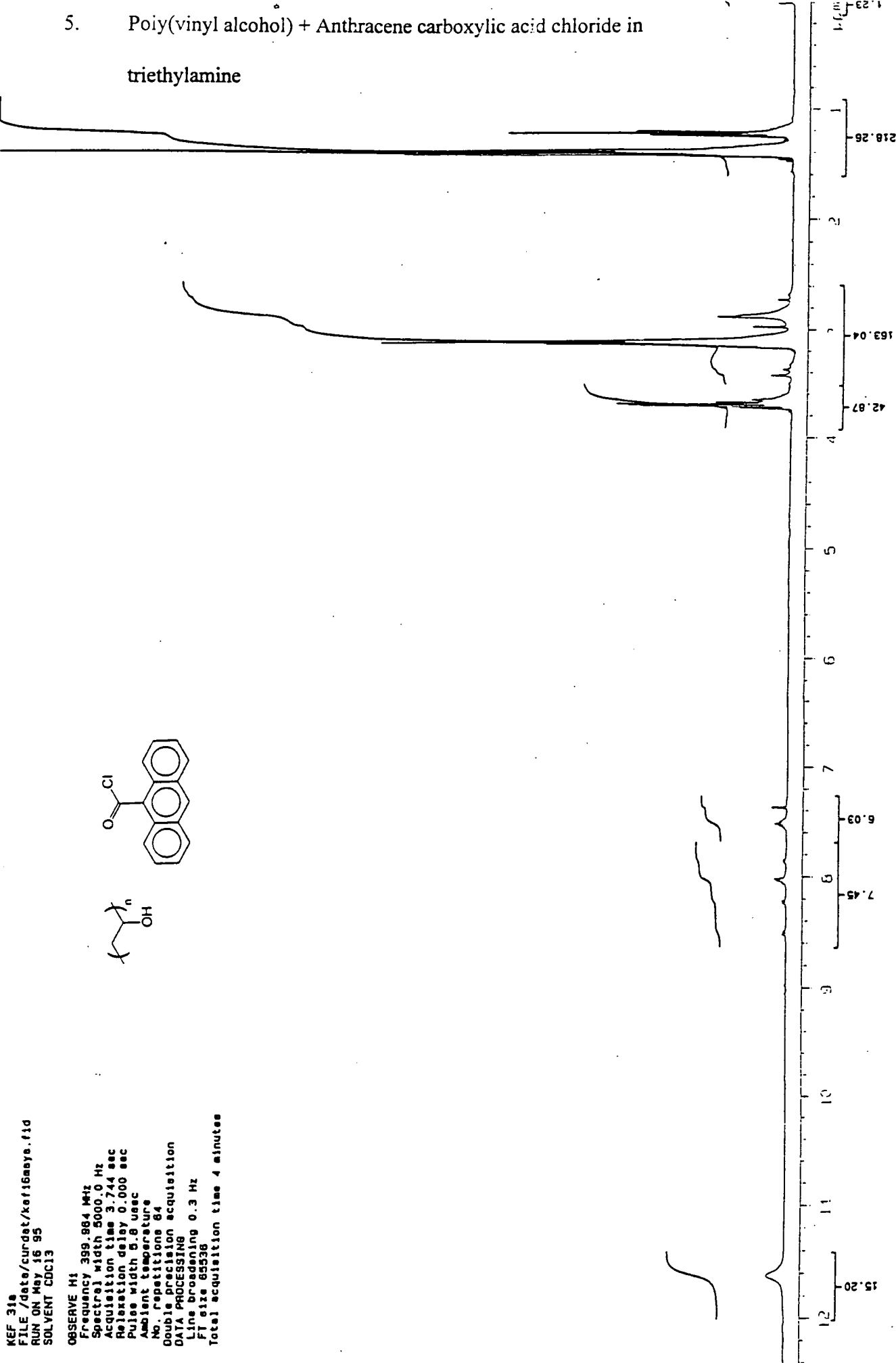
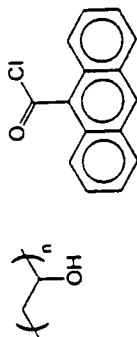




5. Poly(vinyl alcohol) + Anthracene carboxylic acid chloride in triethylamine

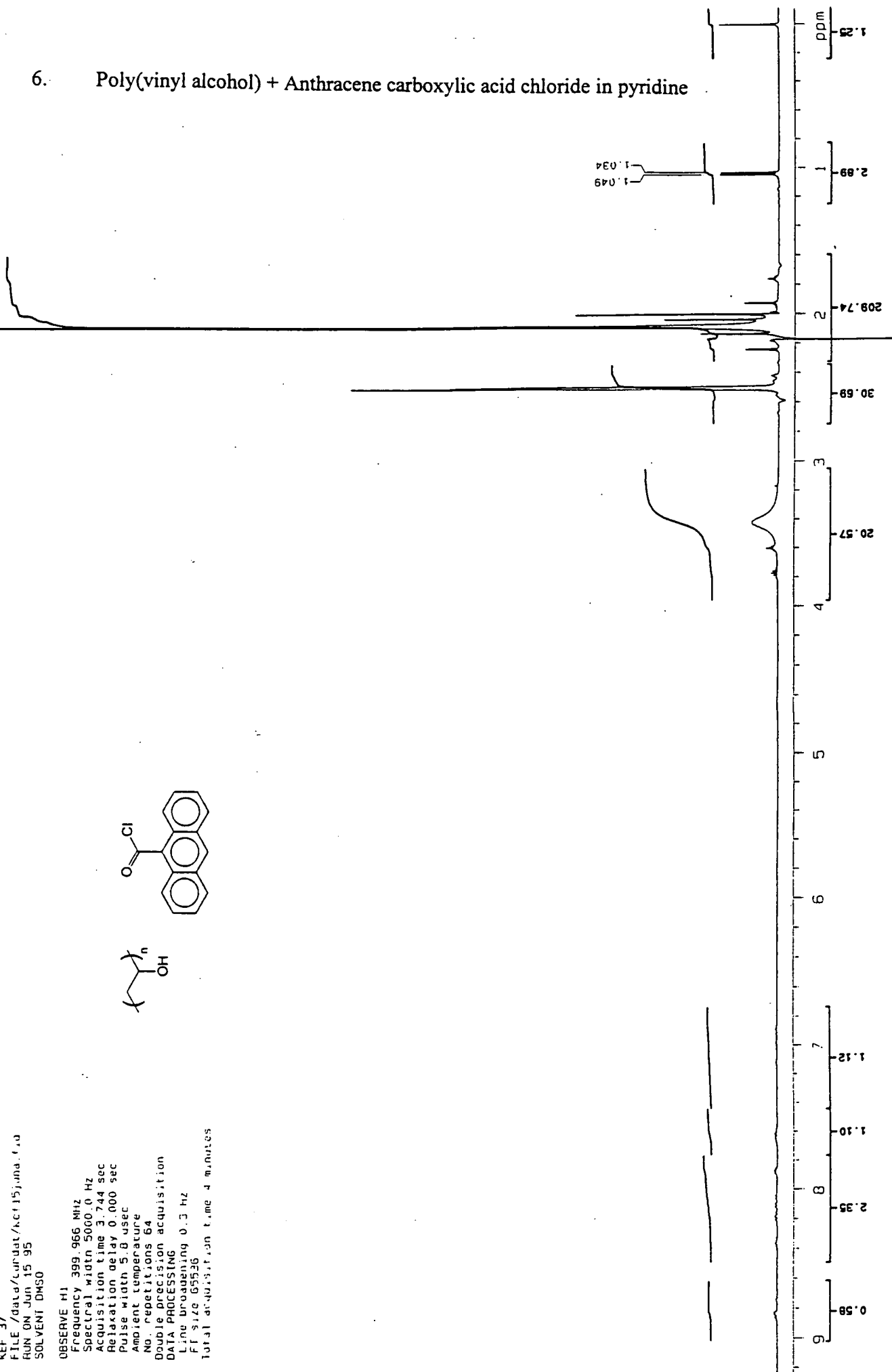
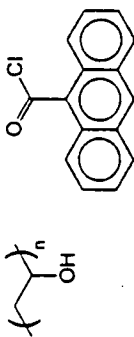
KEF 31a  
FILE /date/curdet/kef16mays.fid  
RUN ON May 16 95  
SOLVENT CDCl3

OBSERVE H1  
Frequency 399.984 MHz  
Spectral width 5000.0 Hz  
Acquisition time 3.744 sec  
Relaxation delay 0.000 sec  
Pulse width 8.8 usec  
Ambient temperature  
No. Repetitions 64  
Double precision acquisition  
DATA PROCESSING  
Line broadening 0.3 Hz  
FI size 65536  
Total acquisition time 4 minutes



6. Poly(vinyl alcohol) + Anthracene carboxylic acid chloride in pyridine

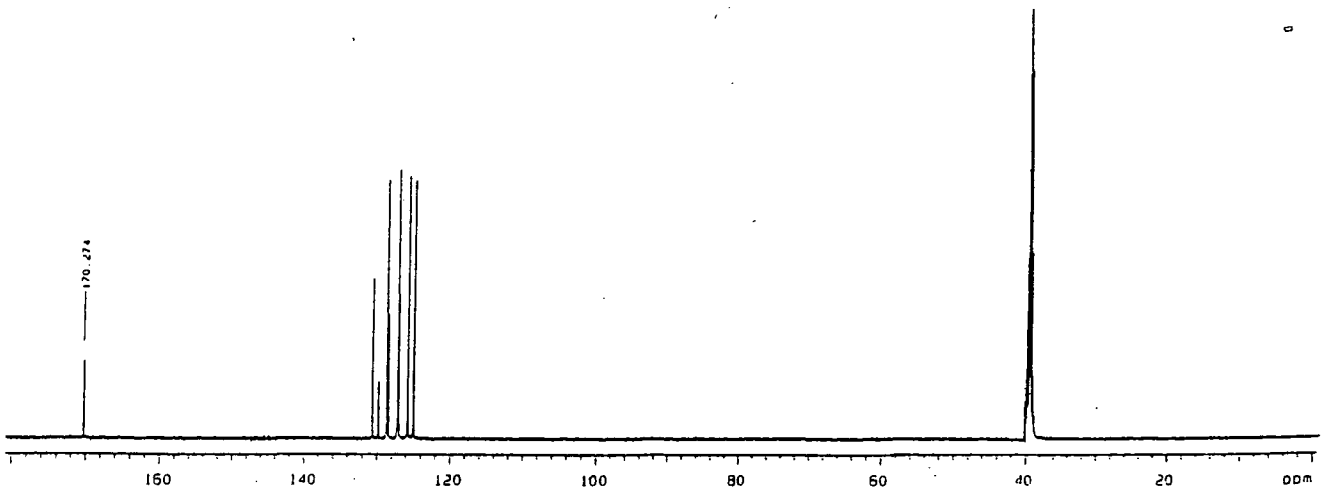
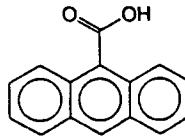
KEF 37  
 FILE /data/cupdat/kc115juna.f.d  
 RUN ON Jun 15 95  
 SOLVENT DMSO  
 OBSERVE H1  
 Frequency 399.966 MHz  
 Spectral width 5000.0 Hz  
 Acquisition time 3.744 sec  
 Relaxation delay 0.000 sec  
 Pulse width 5.8 usec  
 Ambient temperature  
 No. repetitions 64  
 Double precision acquisition  
 DATA PROCESSING  
 Line broadening 0.3 Hz  
 FI size 65536  
 Total acq. time 4 minutes



REF 35  
FILE /data/curdet/kef15junc.fid  
RUN ON Jun 15 95  
SOLVENT DMSO

OBSERVE C13  
Frequency 100.583 MHz  
Spectral width 25000.0 Hz  
Acquisition time 1.199 sec  
Relaxation delay 3.000 sec  
Pulse width 9.2 usec  
Ambient temperature  
No. repetitions 256  
DECOUPLE M1  
High power 40  
Decoupler continuously on  
Double precision acquisition  
DATA PROCESSING  
Line broadening 1.2 Hz  
Gain/amplification 0.800 sec  
FT size 131072  
Total acquisition time 17 minutes

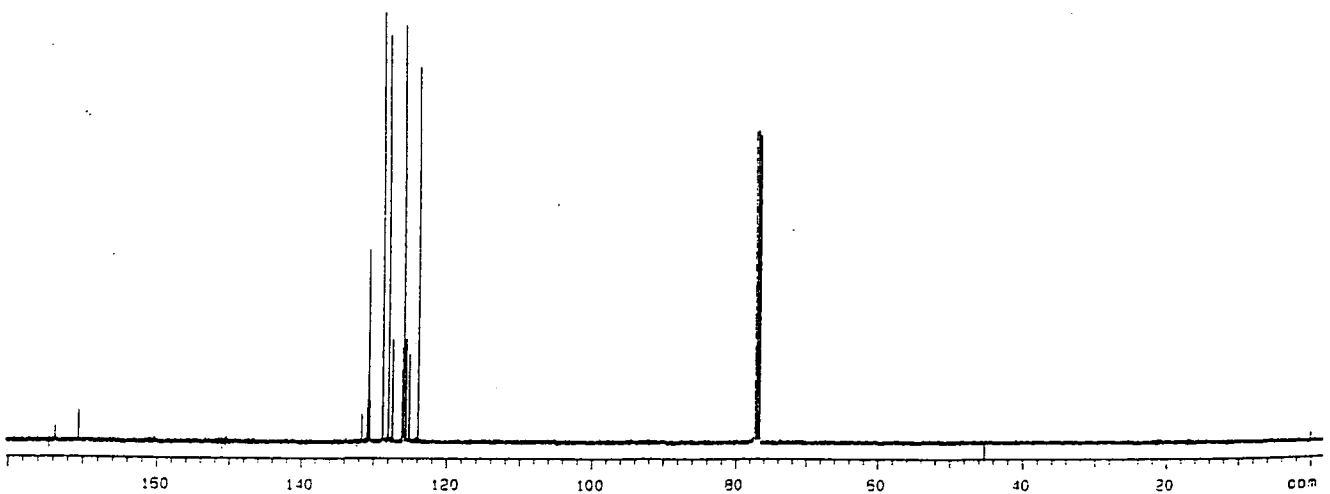
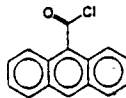
1. Anthracene carboxylic acid



REF 6  
FILE /data/curdet/kef23jano.fid  
RUN ON Jan 23 95  
SOLVENT CDCl3

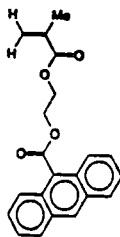
OBSERVE C13  
Frequency 100.582 MHz  
Spectral width 25000.0 Hz  
Acquisition time 1.189 sec  
Relaxation delay 3.000 sec  
Pulse width 9.2 usec  
Ambient temperature  
No. repetitions 1024  
DECOUPLE M1  
High power 40  
Decoupler continuously on  
Double precision acquisition  
DATA PROCESSING  
Line broadening 0.8 Hz  
FT size 131072  
Total acquisition time 71 minutes

2. Anthracene carboxylic acid chloride

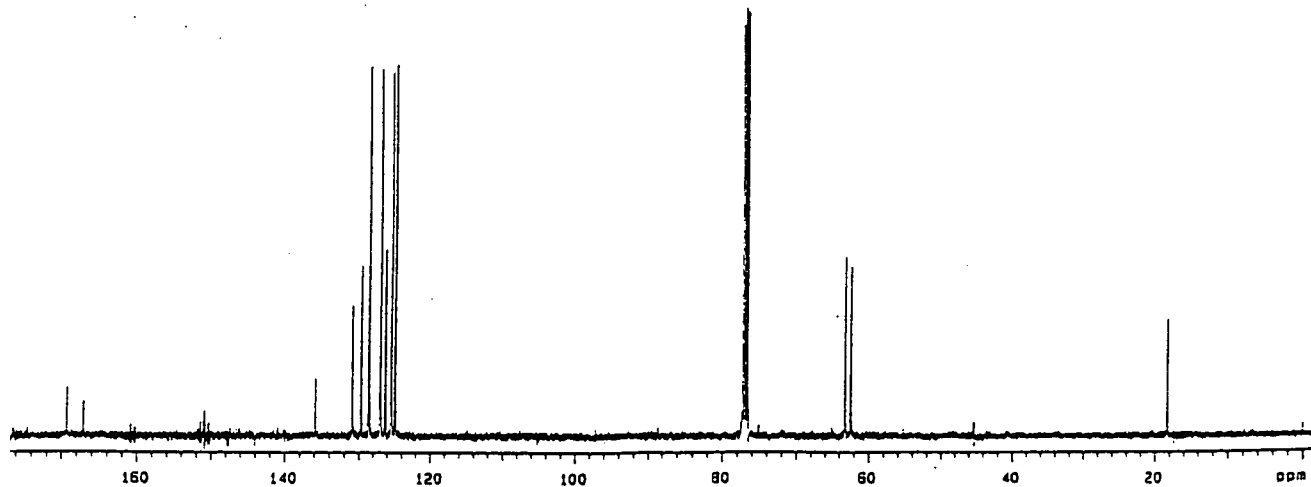


KEF 13  
FILE /data/curdet/ker20feb.f16  
RUN ON Feb 28 83  
SOLVENT CDCl3

OBSERVE C13  
Frequency 100.582 MHz  
Spectral width 25000.0 Hz  
Acquisition time 1.198 sec  
Relaxation delay 3.000 sec  
Pulse width 8.2 usec  
Ambient temperature  
No. repetitions 1024  
DECUPLE M1  
High power 40  
Decoupler continuously on  
Double precision acquisition  
DATA PROCESSING  
Line broadening 1.0 Hz  
Scausing modulation 1.000 sec  
FT size 131072  
Total acquisition time 71 minutes



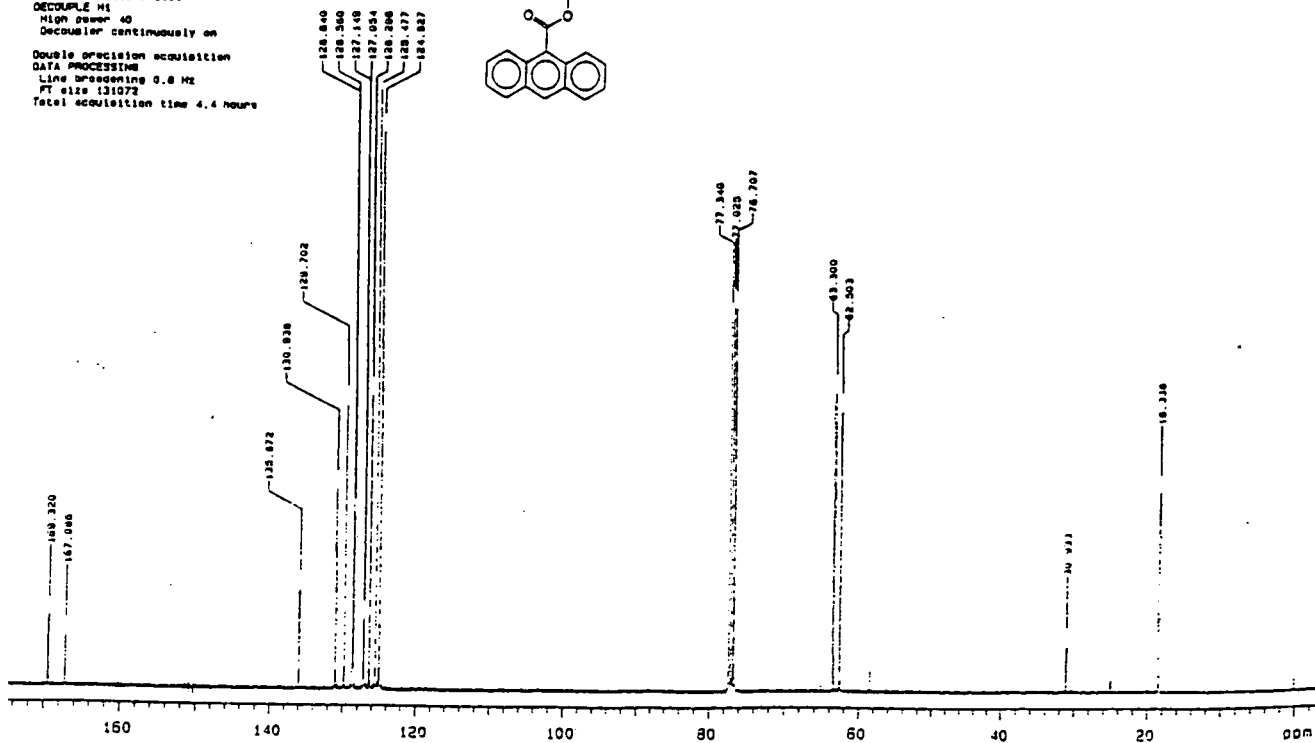
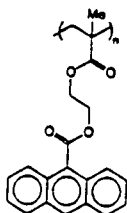
3. 9'-Anthracenoate-2-ethyl methacrylate



4. Poly(9'-anthracenoate-2-ethyl methacrylate) (solution polymerisation)

KEF 13b  
FILE /data/curdet/ker10feb.f16  
RUN ON Feb 19 83  
SOLVENT CDCl3

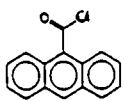
OBSERVE C13  
Frequency 100.582 MHz  
Spectral width 25000.0 Hz  
Acquisition time 1.198 sec  
Relaxation delay 2.000 sec  
Pulse width 8.2 usec  
Ambient temperature  
No. repetitions 5000  
DECUPLE M1  
High power 40  
Decoupler continuously on  
Double precision acquisition  
DATA PROCESSING  
Line broadening 0.8 Hz  
FT size 131072  
Total acquisition time 4.4 hours



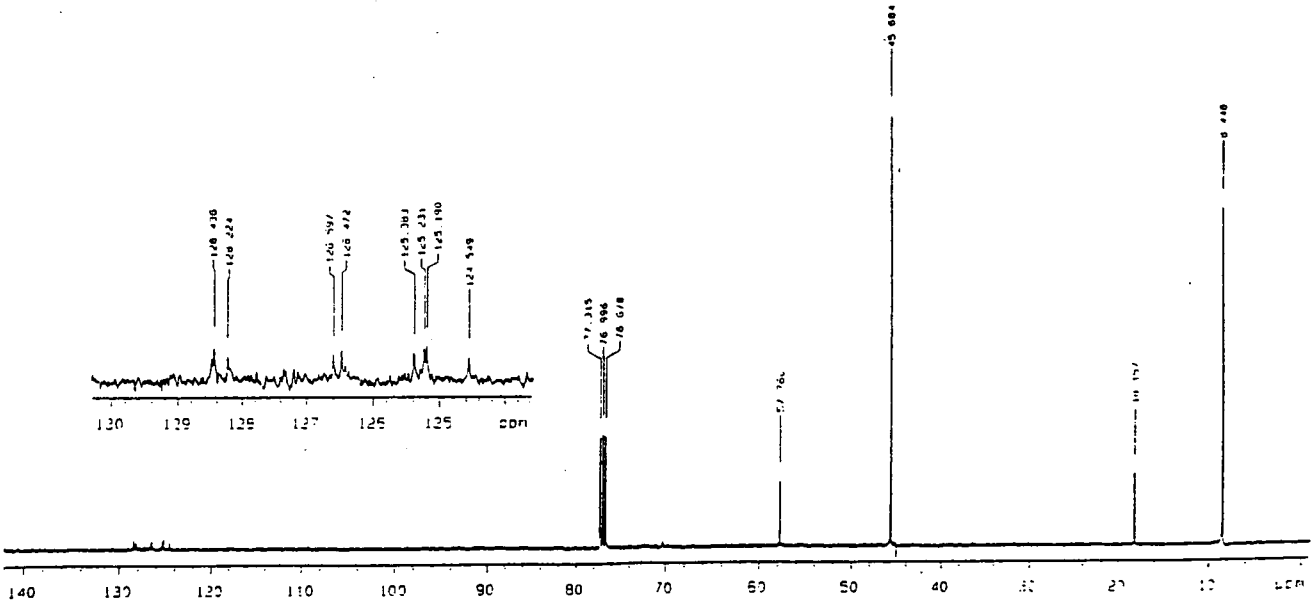
REF 316  
FILE /data/curdet/taf16mayb.116  
RUN ON May 18 85  
SOLVENT CDCl3

5. Poly(vinyl alcohol) + Anthracene carboxylic acid chloride in

triethylamine

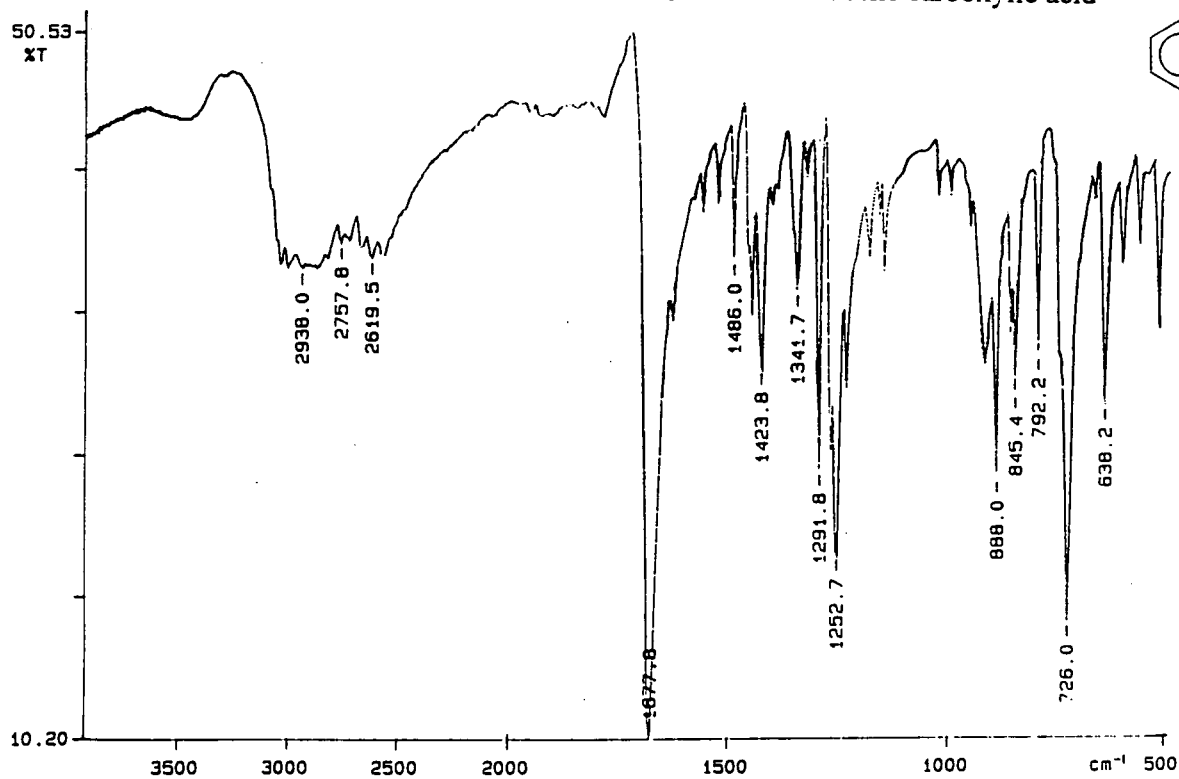
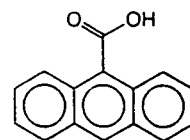


OBSERVE C13  
Frequency 100.622 MHz  
Spectral width 20000.0 Hz  
Acquisition time 1.188 sec  
Relaxation delay 3.000 sec  
Pulse width 8.2 usec  
Ambient temperature  
No. repetitions 1024  
DECUPLE M1  
High power 40  
Decoupler continuously on  
Double precision acquisition  
DATA PROCESSING  
Line broadening 1.1 Hz  
Gaussian apodization 0.800 sec  
FT size 131072  
Total acquisition time 71 minutes



PERKIN ELMER

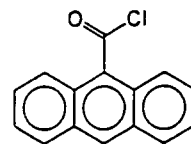
1. Anthracene carboxylic acid



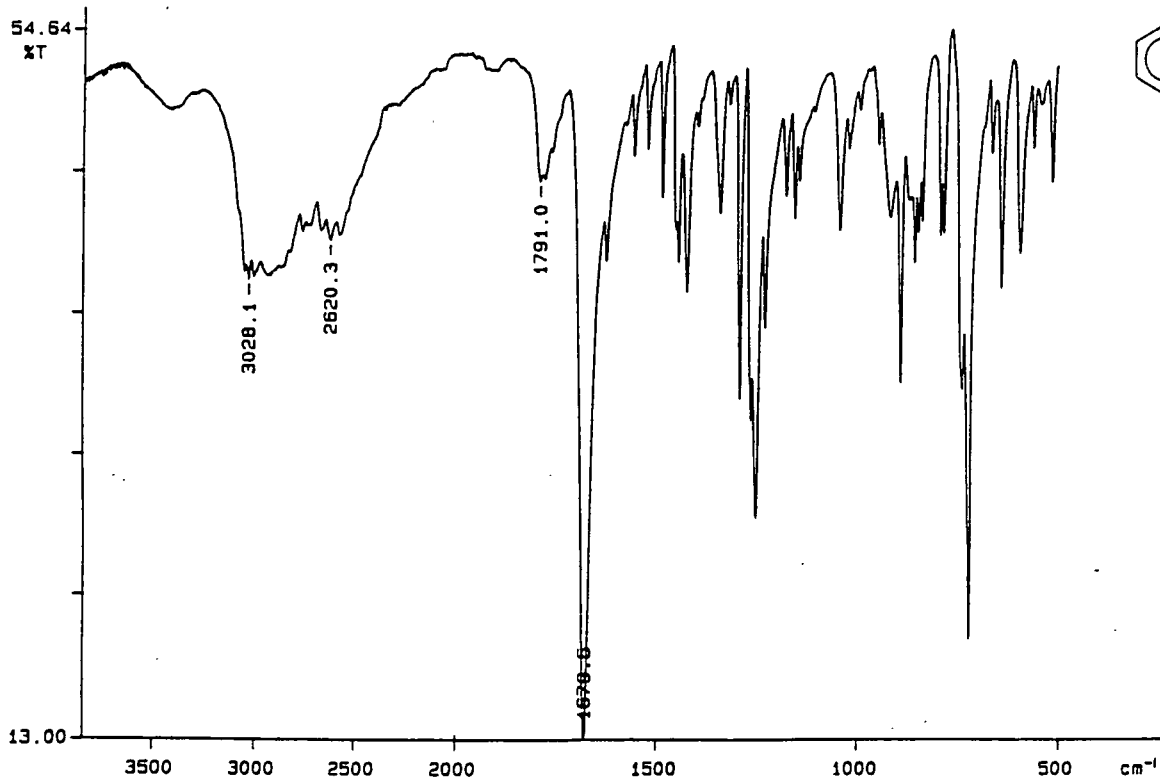
95/06/13 15:09

X: 16 scans, 4.0cm-1, flat

2. Anthracene carboxylic acid chloride



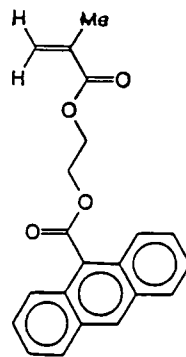
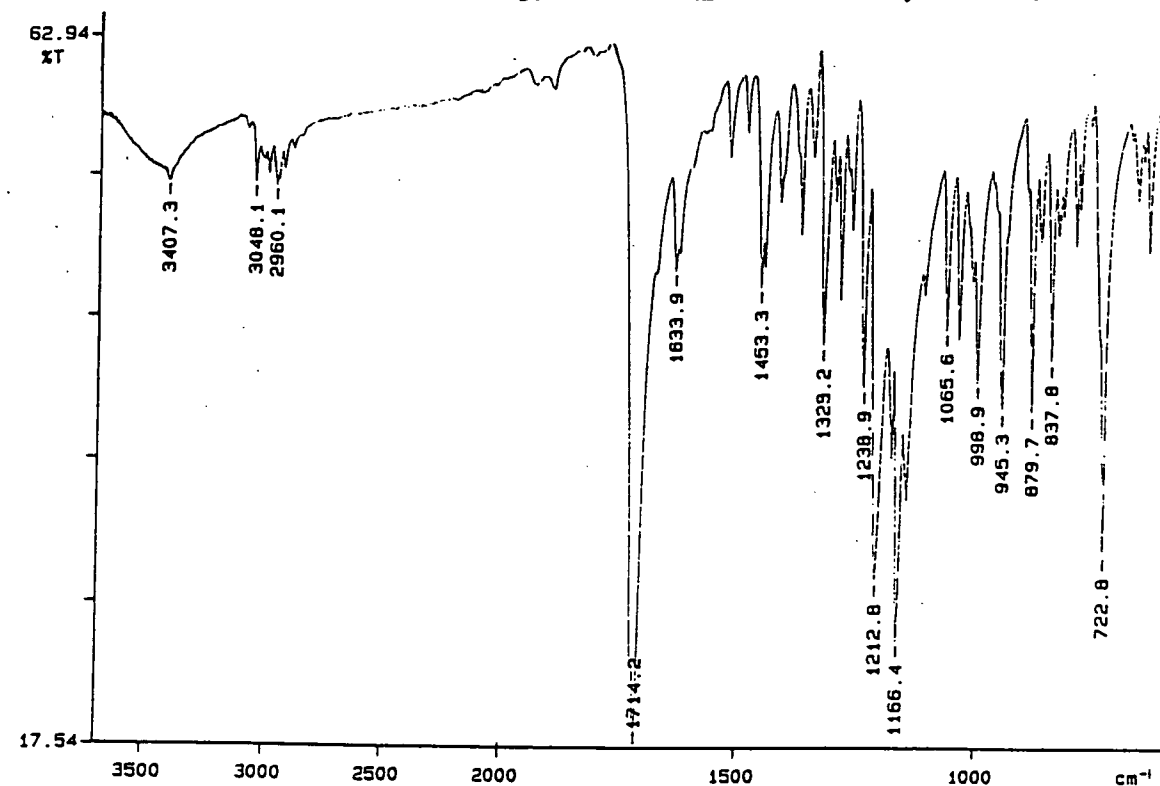
PERKIN ELMER



95/01/24 10:25 s-373

X: 16 scans, 4.0cm-1, flat

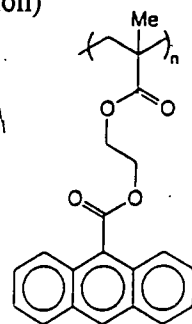
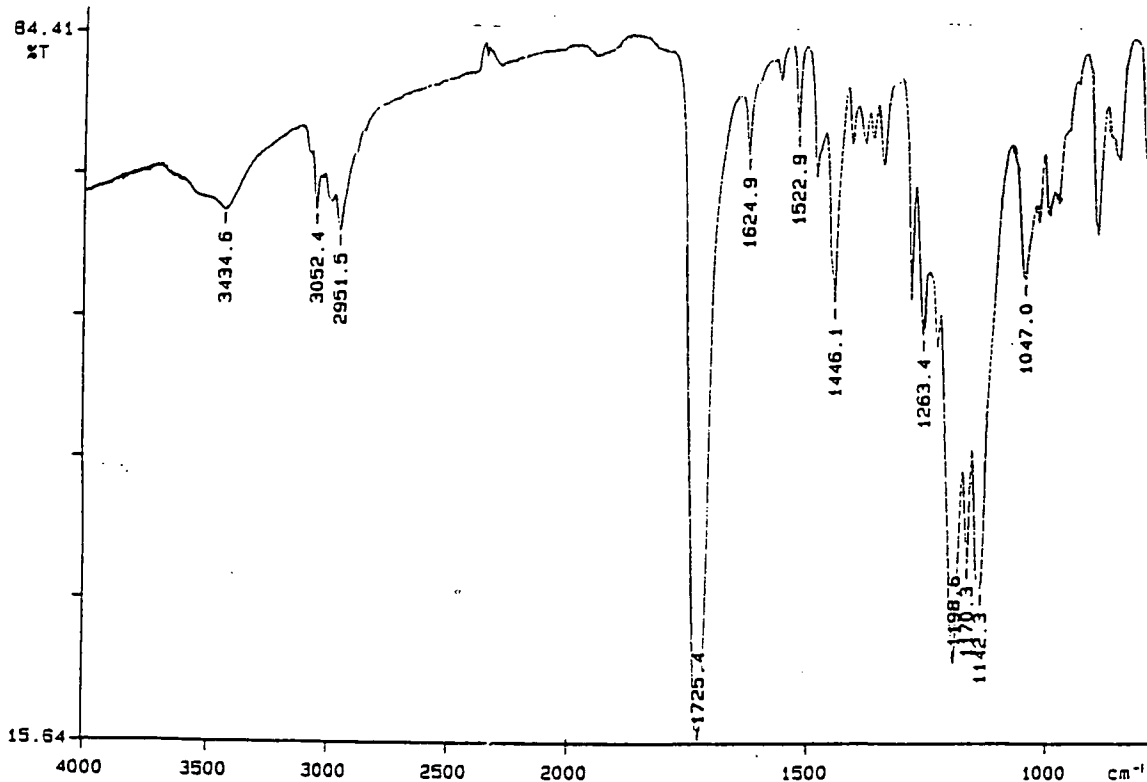
3. 9'-Anthracenoate-2-ethyl methacrylate



95/05/23 12: 24

X: 16 scans, 4.0cm-1, flat

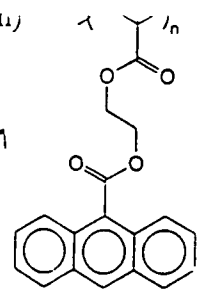
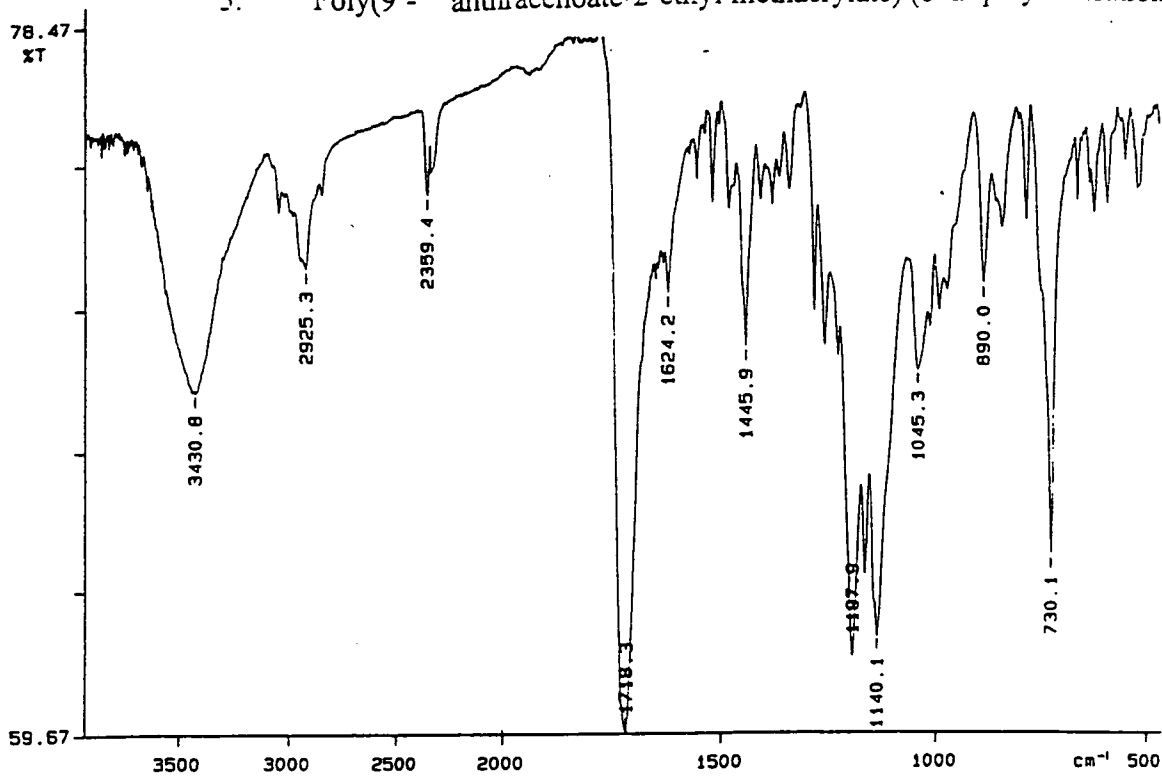
4. Poly(9'-anthracenoate-2-ethyl methacrylate) (solution polymerisation)



95/05/23 11: 50

X: 16 scans, 4.0cm-1

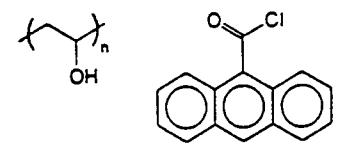
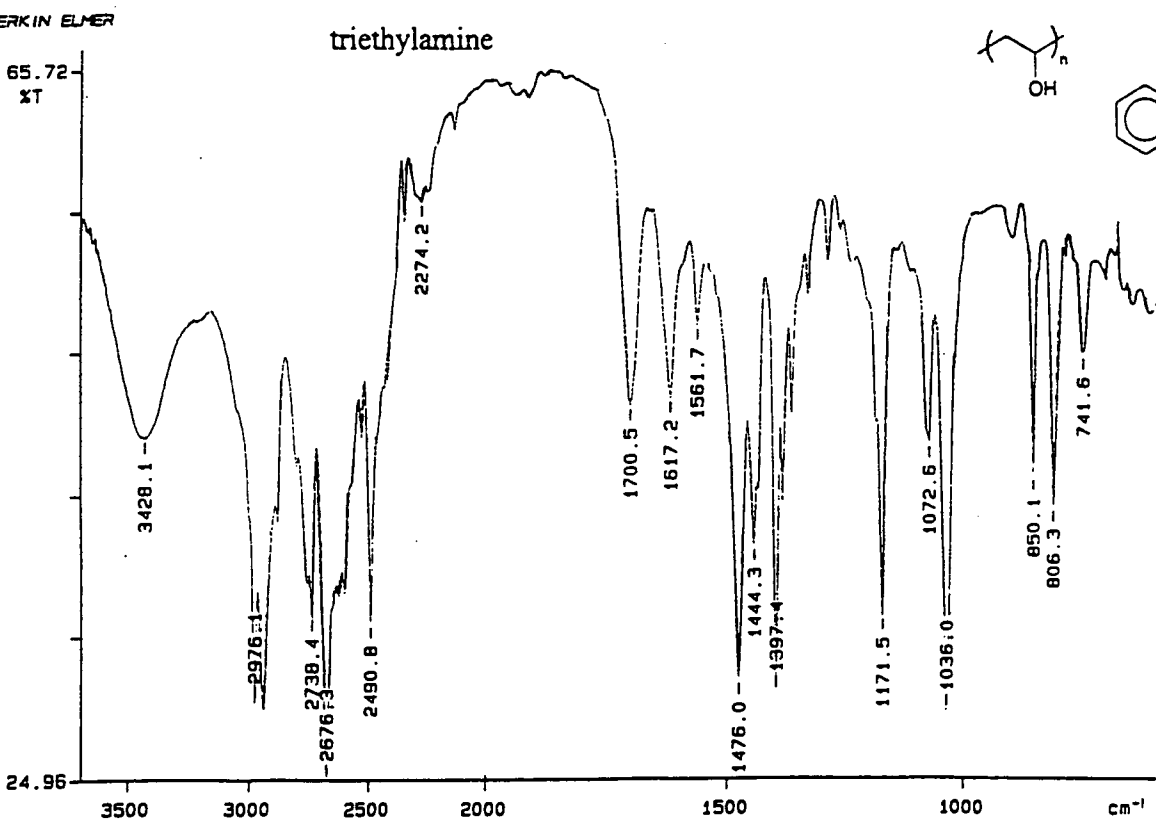
5. Poly(9'- anthracenoate-2-ethyl methacrylate) (bulk polymerisation)



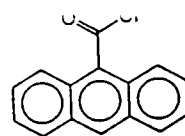
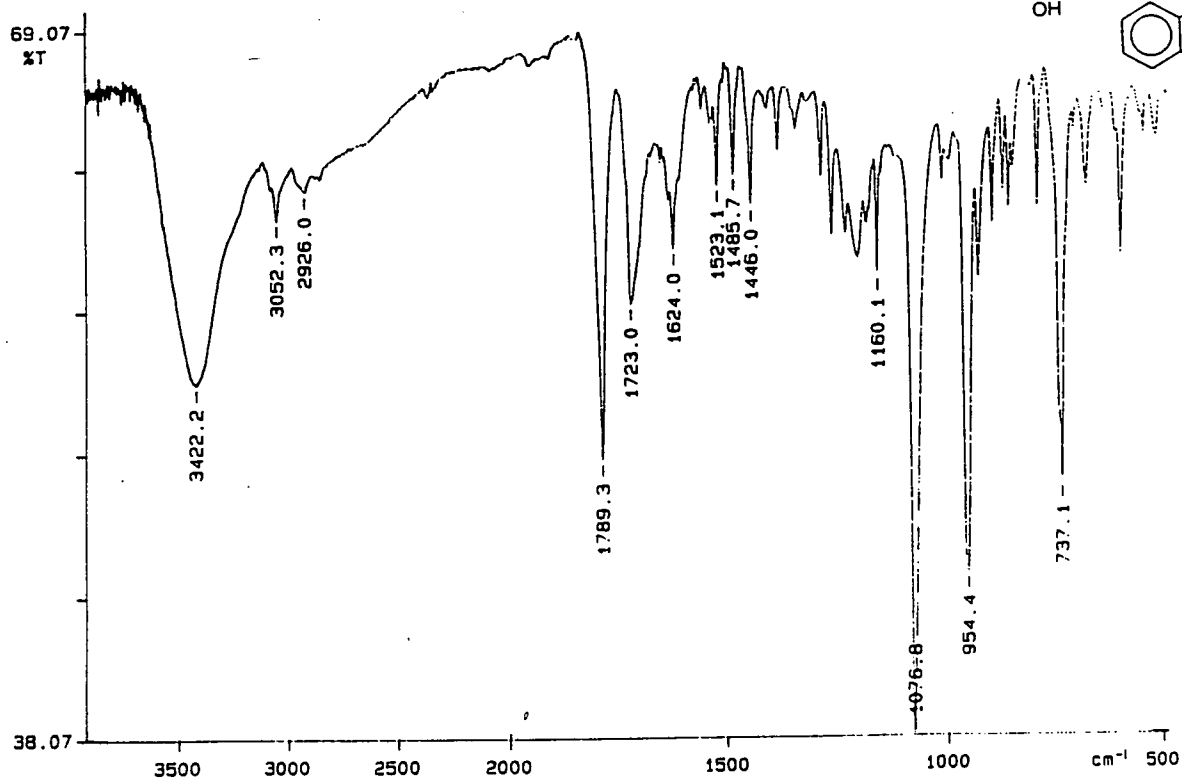
95/06/28 11:11  
X: 16 scans, 4.0cm-1, flat

6. Poly(vinyl alcohol) + Anthracene carboxylic acid chloride in

triethylamine



95/05/23 12:56  
X: 16 scans, 4.0cm-1, flat



95/06/13 16:18

X: 16 scans, 4.0 $\text{cm}^{-1}$ , flat

## 7. Poly(vinyl alcohol) + Anthracene carboxylic acid chloride in pyridine

## Appendix Three - Analytical Data for Chapter Three

### *<sup>1</sup>H NMR Spectra*

1. 4-Azidobenzoic acid
2. 4-Azidobenzoyl chloride
3. 4-Azidobenzoate-2-ethyl methacrylate
4. 4-Azidobenzoate-2-ethyl methacrylate + hydroxyethyl methacrylate
5. Poly(azidobenzoate-2-ethyl methacrylate)
6. Poly(azidobenzoate-2-ethyl methacrylate-co-hydroxyethyl methacrylate)

### *<sup>13</sup>C NMR Spectra*

1. 4-Azidobenzoic acid
2. 4-Azidobenzoyl chloride
3. 4-Azidobenzoate-2-ethyl methacrylate
4. 4-Azidobenzoate-2-ethyl methacrylate + hydroxyethyl methacrylate
5. Poly(azidobenzoate-2-ethyl methacrylate)
6. Poly(azidobenzoate-2-ethyl methacrylate-co-hydroxyethyl methacrylate)

### *IR Spectra*

1. 4-Azidobenzoic acid
2. 4-Azidobenzoyl chloride
3. 4-Azidobenzoate-2-ethyl methacrylate
4. 4-Azidobenzoate-2-ethyl methacrylate + hydroxyethyl methacrylate
5. Poly(azidobenzoate-2-ethyl methacrylate)
6. Poly(azidobenzoate-2-ethyl methacrylate-co-hydroxyethyl methacrylate)

### *TGA Trace*

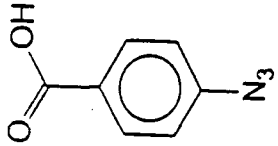
1. 4-Azidobenzoic acid

*Mass Spectrum*

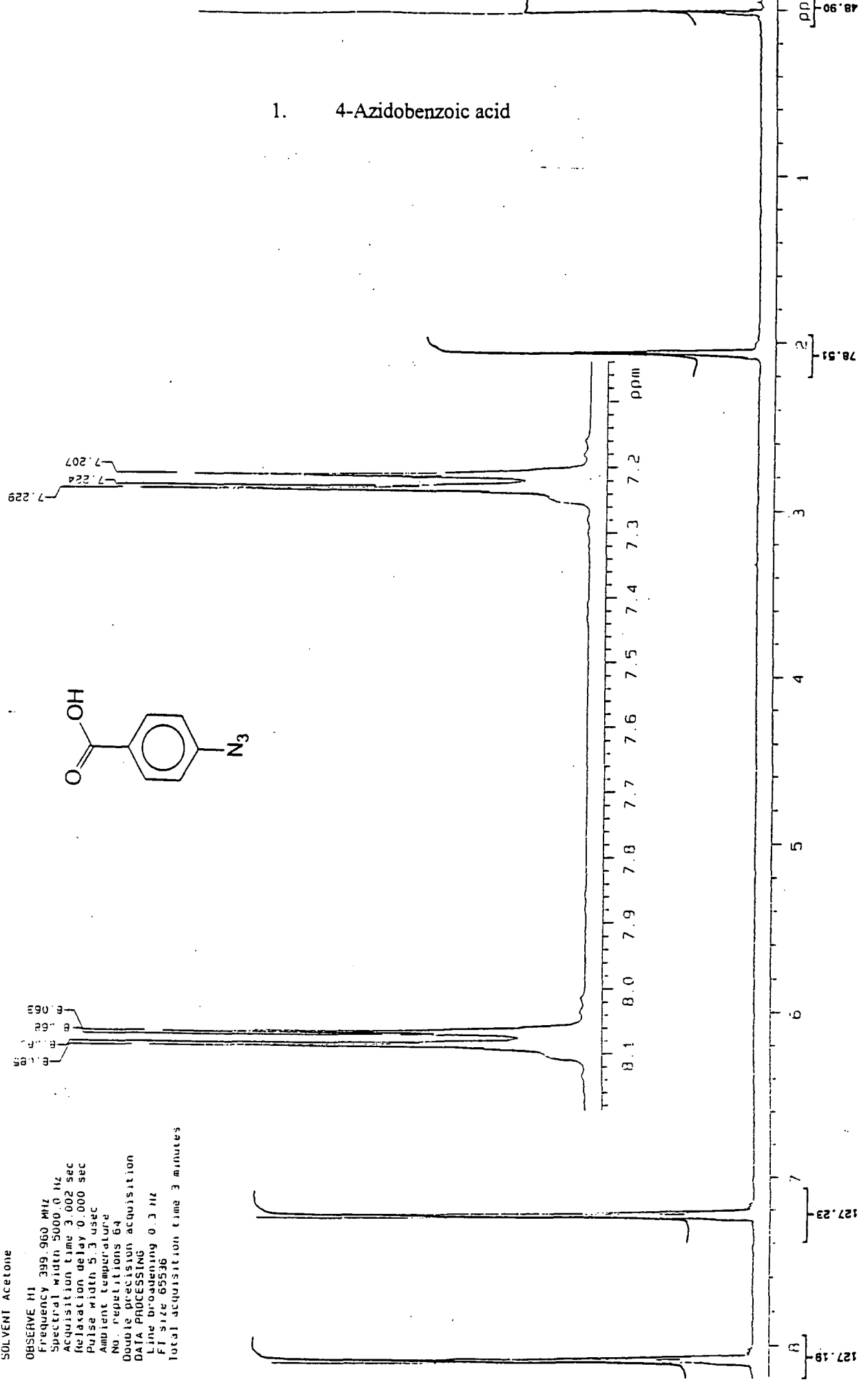
1. 4-Azidobenzoate-2-ethyl methacrylate

KEF 214  
FILE /data/curdat/kef19sept.a.fid  
RUN ON Sep 19 96  
SOLVENT Acetone

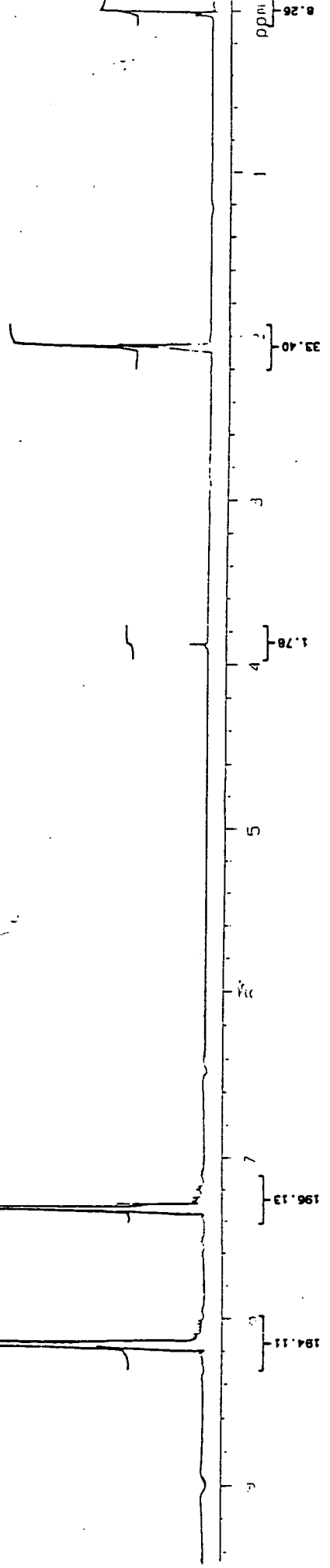
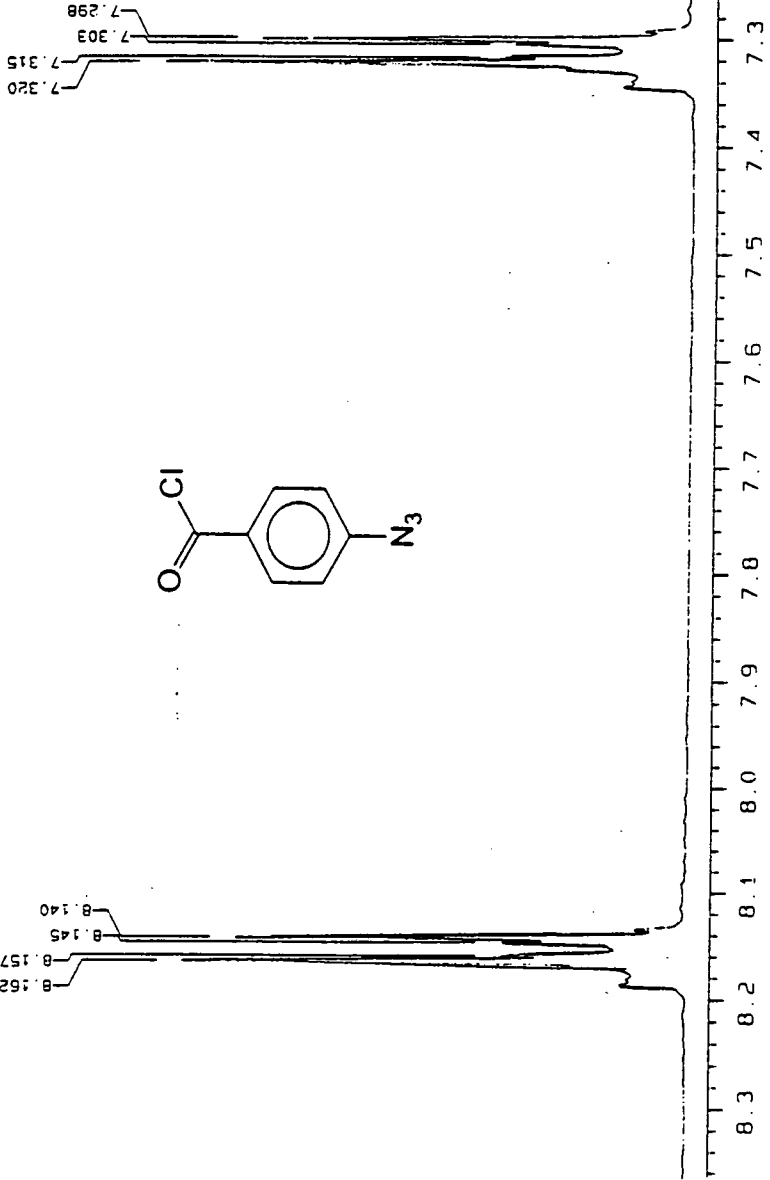
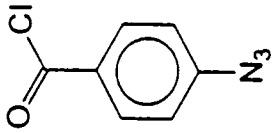
OBSERVE H1  
Frequency 399.960 MHz  
Spectral width 5000.0 Hz  
Acquisition time 3.002 sec  
Relaxation delay 0.000 sec  
Pulse width 5.3 usec  
Ambient temperature  
No. repetitions 64  
Double precision acquisition  
DATA PROCESSING  
Line broadening 0.3 Hz  
FI size 65536  
Total acquisition time 3 minutes



1. 4-Azidobenzoic acid



2. 4-Azidobenzoyl chloride

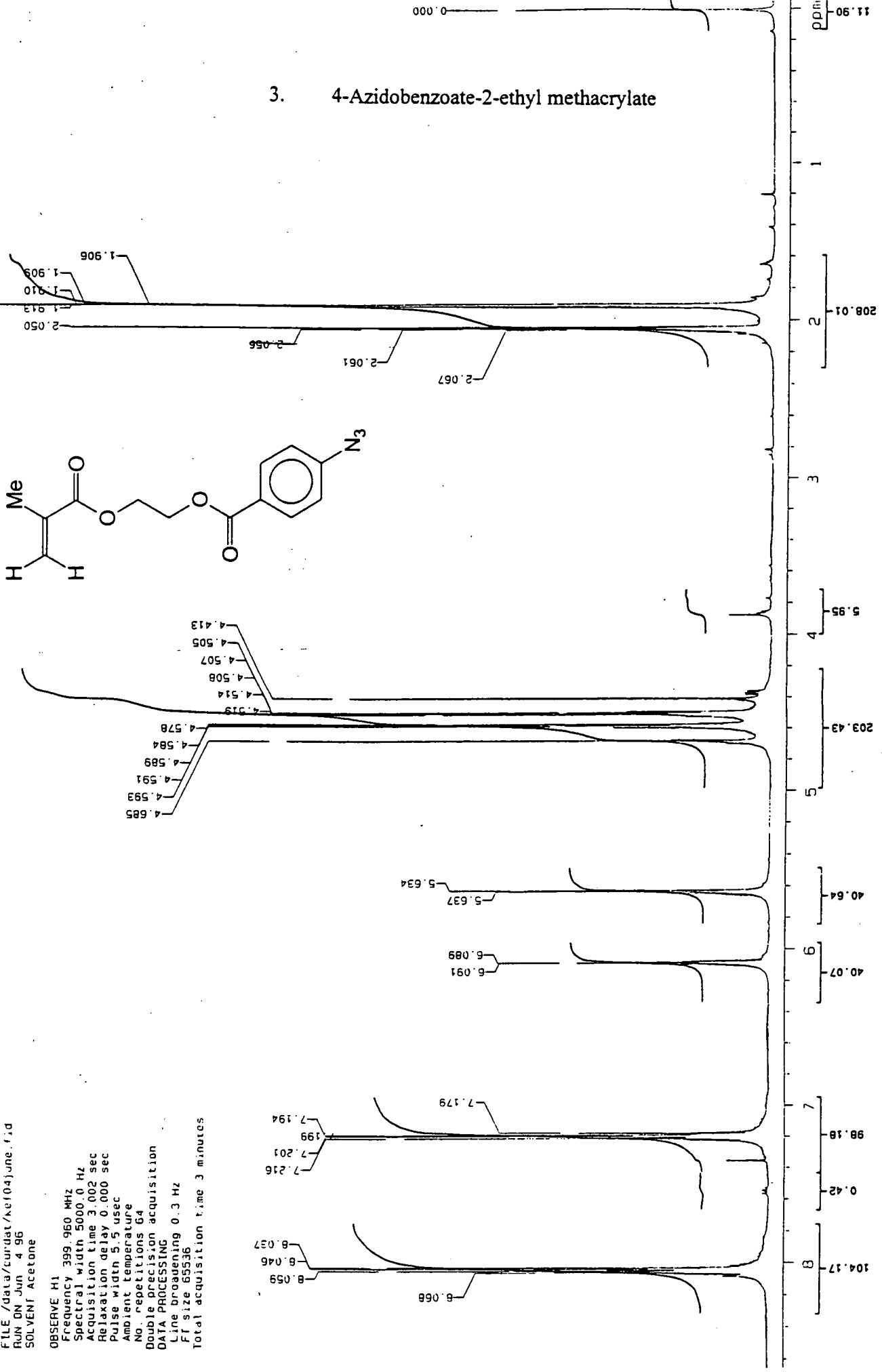
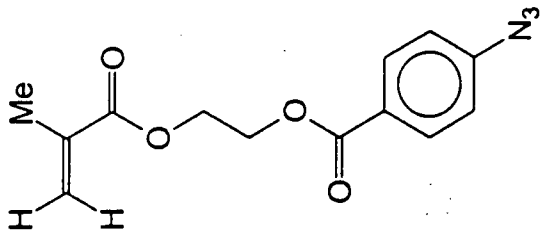


KEF 215  
 FILE /data/curdal/kef20sept.a.fid  
 RUN ON Sep 20 96  
 SOLVENT Acetone  
 OBSERVE H1  
 Frequency 399.960 MHz  
 Spectral width 5000.0 Hz  
 Acquisition time 3.002 Sec  
 Relaxation delay 0.000 Sec  
 Pulse width 5.3 usec  
 Ambient temperature  
 No. repetitions 64  
 Double precision acquisition  
 DATA PROCESSING  
 Line broadening 0.3 Hz  
 FT size 65536  
 Total acquisition time : minutes

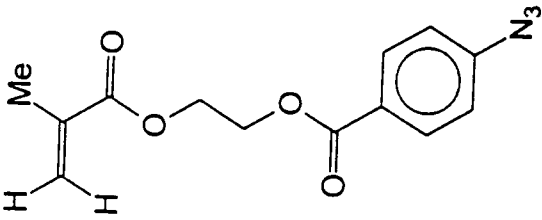
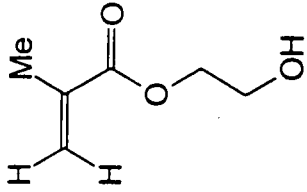
KEF 170  
 FILE /data/cuir/dat/kef(04)june.f;d  
 RUN ON Jun 4 96  
 SOLVENT Acetone

OBSERVE H1  
 Frequency 399.960 MHz  
 Spectral width 5000.0 Hz  
 Acquisition time 3.002 sec  
 Relaxation delay 0.000 sec  
 Pulse width 5.5 usec  
 Ambient temperature  
 No. repetitions 64  
 Double precision acquisition  
 DATA PROCESSING  
 Line broadening 0.3 Hz  
 Ff size 65536  
 Total acquisition time 3 minutes

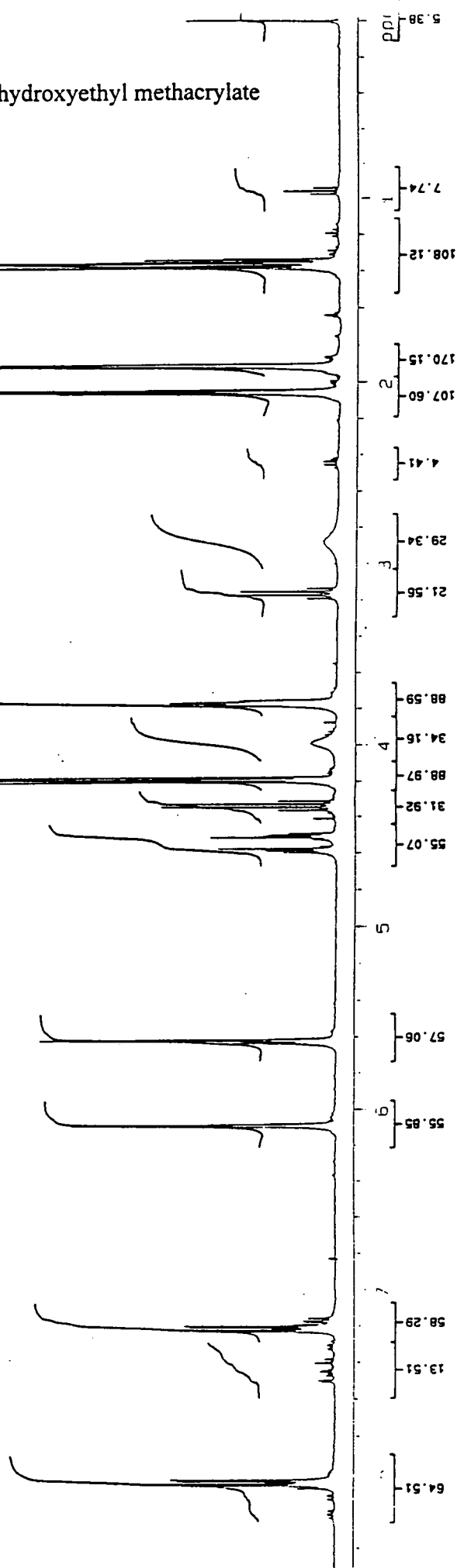
3. 4-Azidobenzoate-2-ethyl methacrylate



4. 4-Azidobenzoate-2-ethyl methacrylate + hydroxyethyl methacrylate



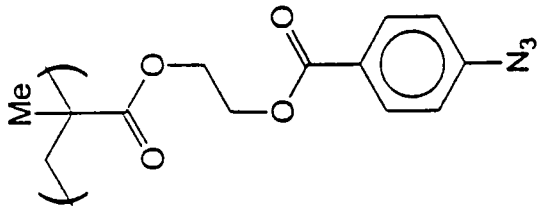
OPSER/E H1  
 Frequency 393.960 MHz  
 Spectral width 5000.0 Hz  
 Acquisition time 3.002 sec  
 Relaxation delay 0.000 sec  
 Pulse width 6.0 usec  
 Ambient temperature  
 No. repetitions 64  
 Double precision acquisition  
 DATA PROCESSING  
 FT size 05536  
 Total acquisition time 3 minutes



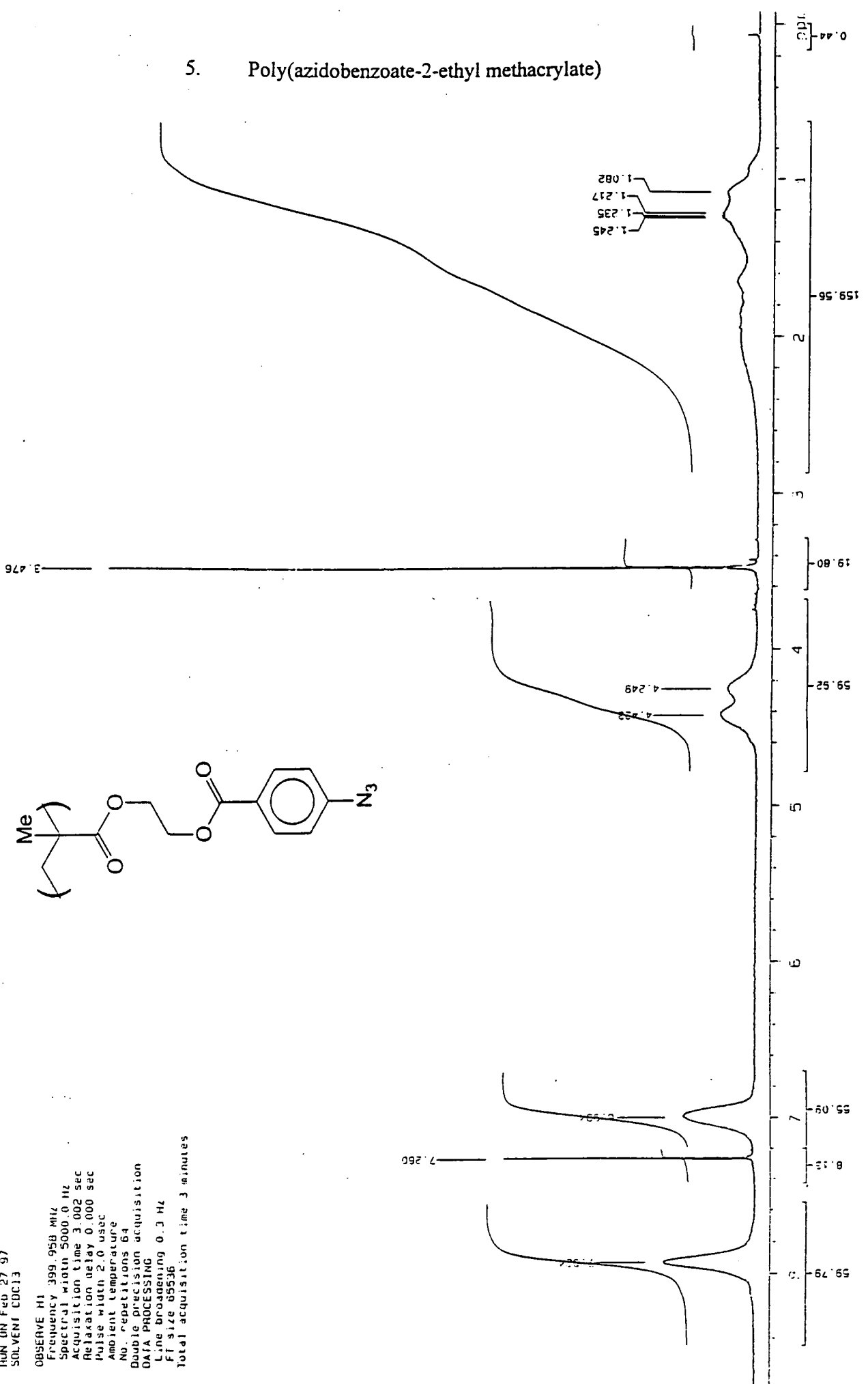
REF 105  
 FILE /data/urmet/kef12/eba.f13  
 RUN ON Feb 12 1986  
 SOLVENT Acetone

KEF300B  
FILE /data/curdal/kef27iebu.fid  
RUN ON Feb 27 97  
SOLVENT CDCl3

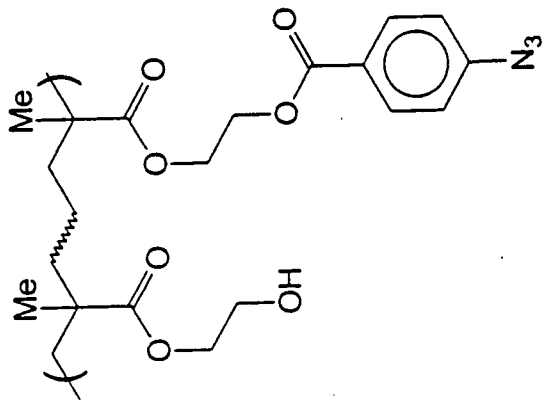
OBSERVE H1  
Frequency 399.958 MHz  
Spectral width 5000.0 Hz  
Acquisition time 3.002 sec  
Relaxation delay 0.000 sec  
Pulse width 2.0 usec  
Ambient temperature  
No. repetitions 64  
Double precision acquisition  
DATA PROCESSING  
Line broadening 0.3 Hz  
Ff size 65536  
Total acquisition time 3 minutes



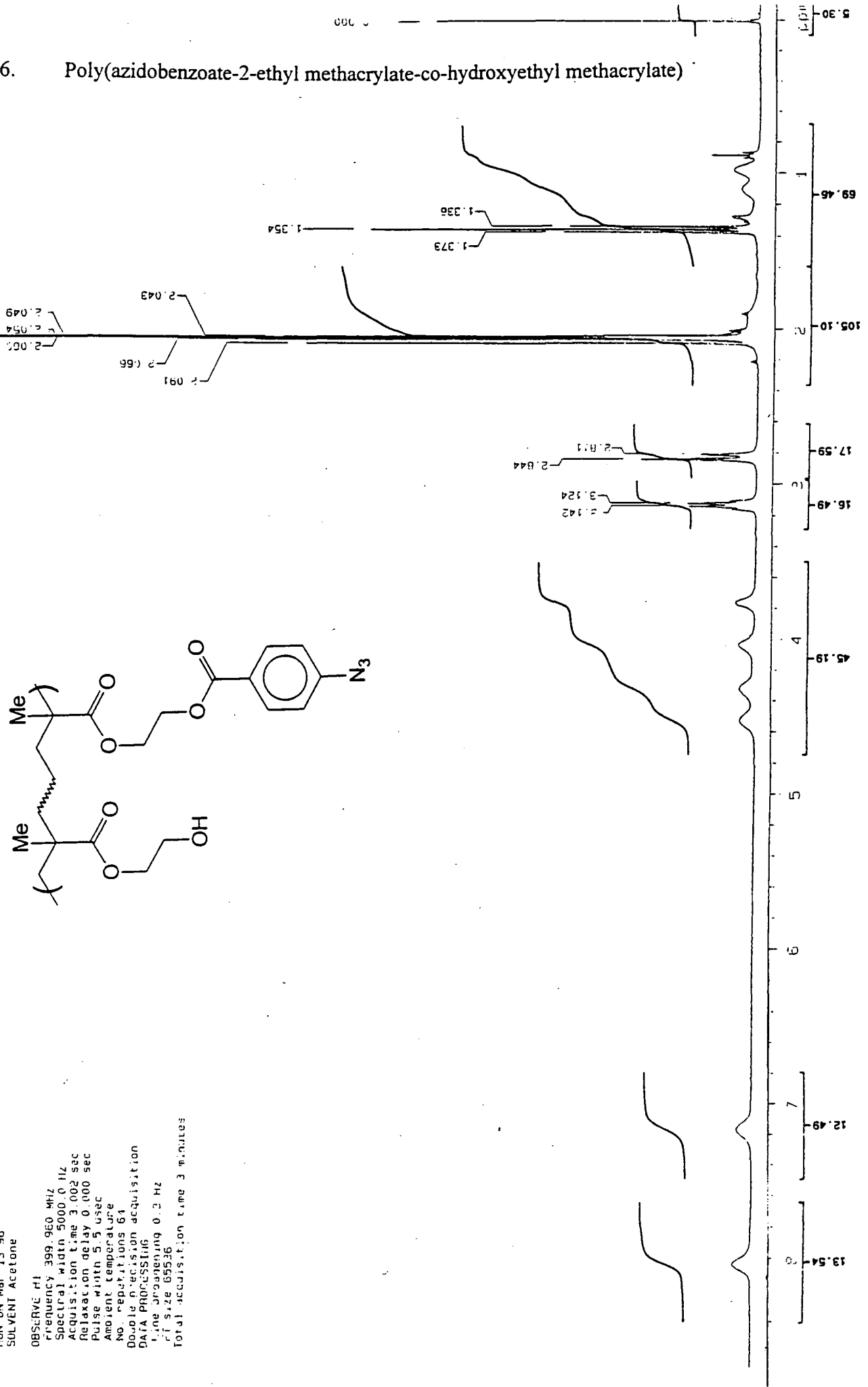
5. Poly(azidobenzoate-2-ethyl methacrylate)



6. Poly(azidobenzoate-2-ethyl methacrylate-co-hydroxyethyl methacrylate)

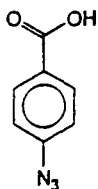


REF 1180  
 FILE //data/candata/xcfl2marc.f.d  
 RUN ON Mar 15 96  
 SOLVENT Acetone  
 OBSERVE H1  
 Frequency 399.960 MHz  
 Spectral width 5000.0 Hz  
 Acquisition time 3.002 sec  
 Relaxation delay 0.000 sec  
 Pulse width 5.5 usec  
 Ambient temperature  
 No. repetitions 64  
 Double precision acquisition  
 DATA PROCESSING  
 Line broadening 0.2 Hz  
 File size 65536  
 Total acquisition time 3 minutes

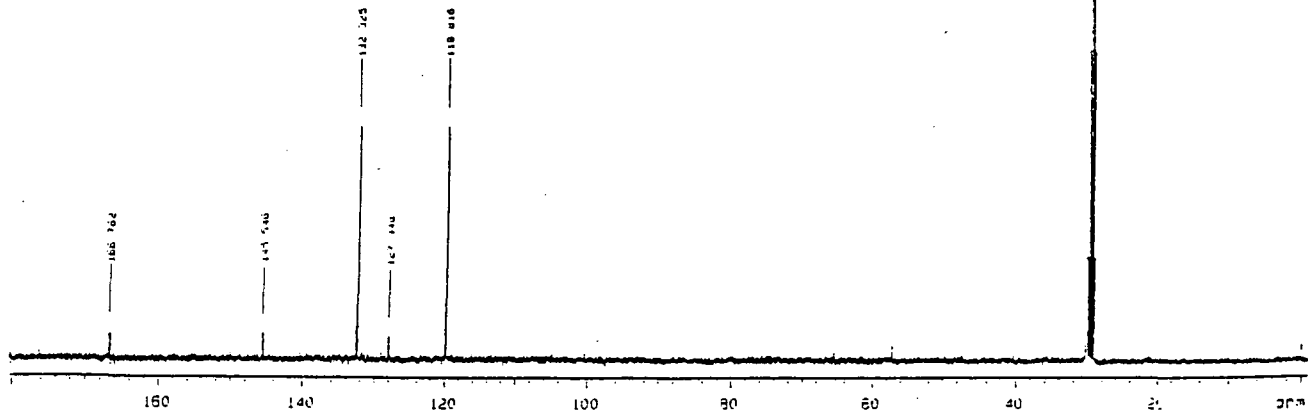


REF 210  
FILE /data/cumdat/kef19septb.fid  
RUN ON Sep 19 98  
SOLVENT Acetone

OBSERVE C13  
Frequency 100.581 MHz  
Spectral width 25000.0 Hz  
Acquisition time 1.199 sec  
Relaxation delay 3.000 sec  
Pulse width 9.1 usec  
Ambient temperature  
No. acquisitions 512  
DECOUPLE H1  
High power 40  
Decoupler continuously on  
Double precision acquisition  
DATA PROCESSING  
Line broadening 1.4 Hz  
Gaussian smoothing 0.700 sec  
FT size 131072  
Total acquisition time 33 minutes

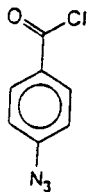


1. 4-Azidobenzoic acid

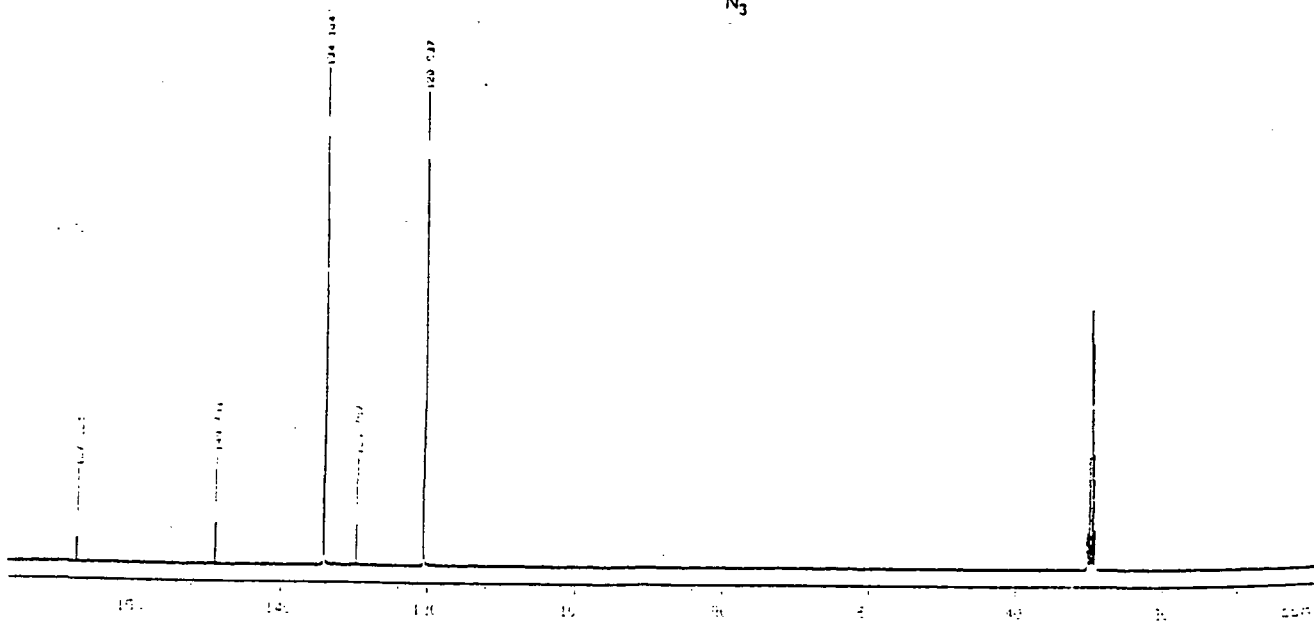


REF 213  
FILE /data/cumdat/kef20septb.fid  
RUN ON Sep 20 98  
SOLVENT Acetone

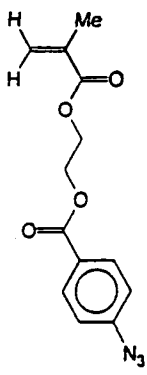
OBSERVE C13  
Frequency 100.581 MHz  
Spectral width 25000.0 Hz  
Acquisition time 1.199 sec  
Relaxation delay 3.000 sec  
Pulse width 9.1 usec  
Ambient temperature  
No. acquisitions 540  
DECOUPLE H1  
High power 40  
Decoupler continuously on  
Double precision acquisition  
DATA PROCESSING  
Line broadening 1.2 Hz  
Gaussian smoothing 0.300 sec  
FT size 131072  
Total acquisition time 44 minutes



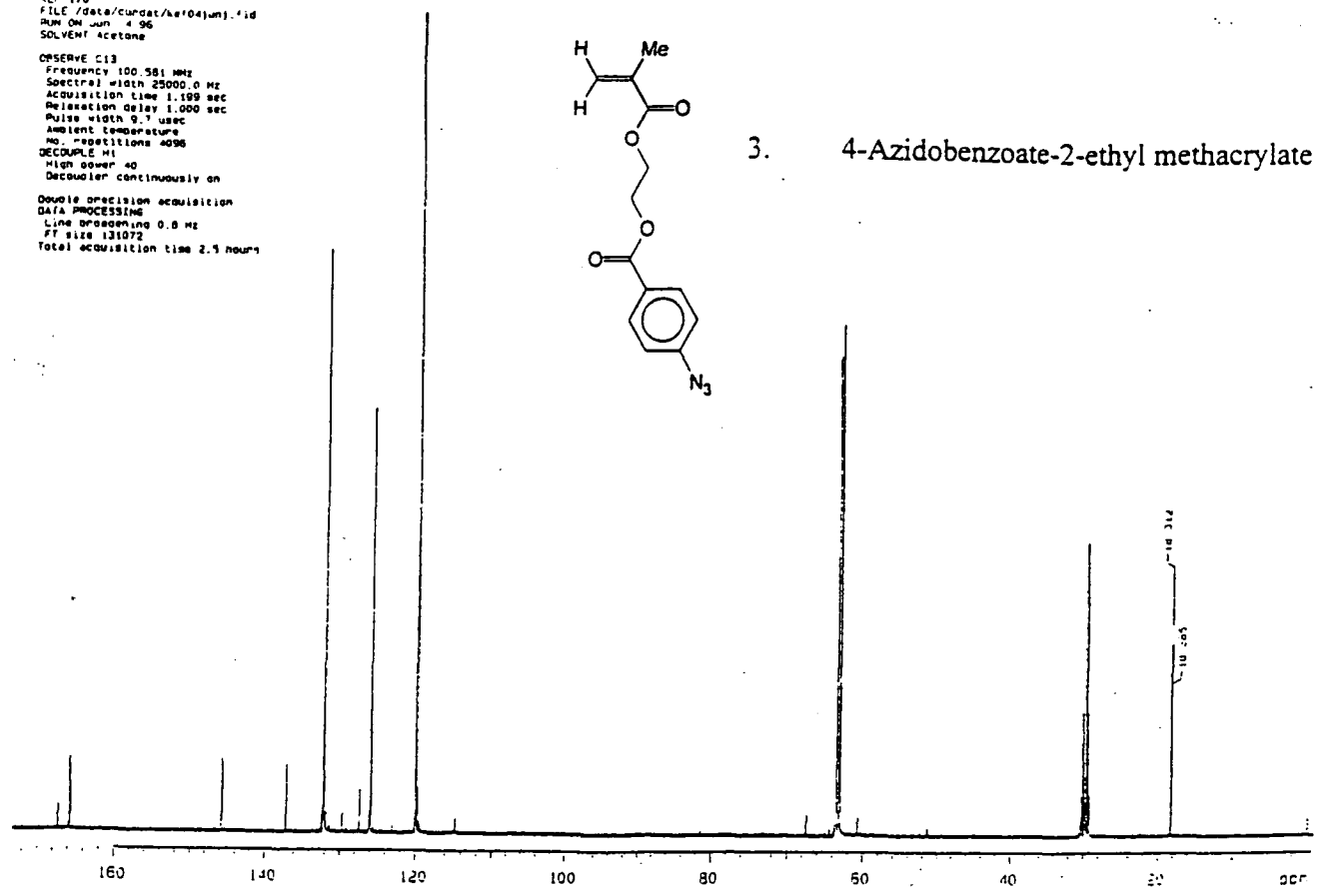
2. 4-Azidobenzoyl chloride



REF 170  
 FILE /data/curdac/ker04junj.fid  
 RUN ON Jun 4 96  
 SOLVENT Acetone  
 OBSERVE C13  
 Frequency 100.581 MHz  
 Spectral width 25000.0 Hz  
 Acquisition time 1.109 sec  
 Relaxation delay 1.000 sec  
 Pulse width 9.7 usec  
 Ambient temperature  
 No. repetitions 4096  
 DECOUPLE H1  
 High power 40  
 Decoupler continuously on  
 Double precision acquisition  
 DATA PROCESSING  
 Line broadening 0.0 Hz  
 FT size 131072  
 Total acquisition time 2.5 hours

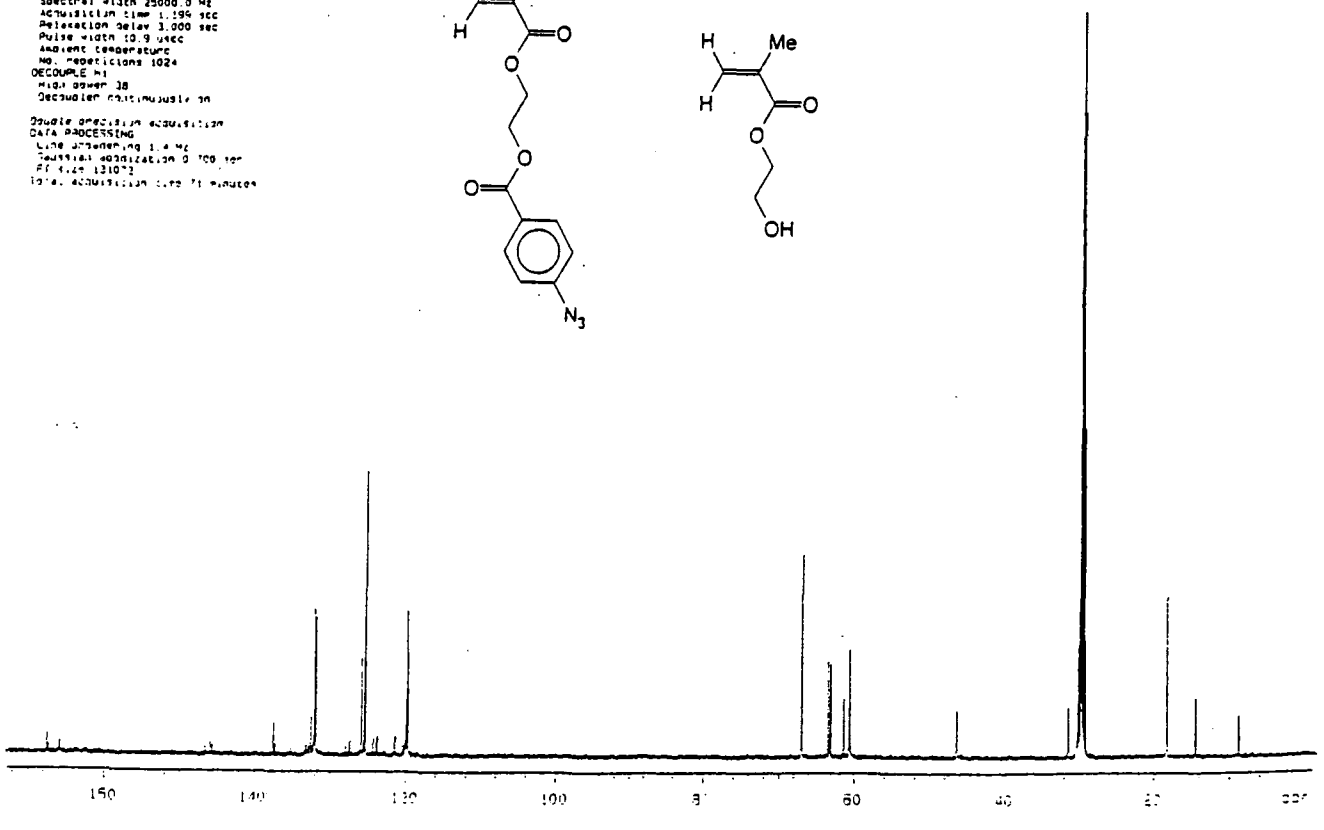
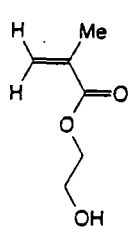
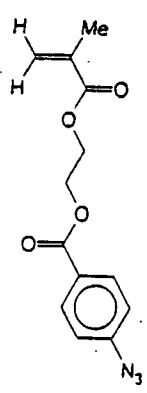


3. 4-Azidobenzoate-2-ethyl methacrylate

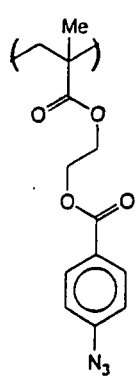


4. 4-Azidobenzoate-2-ethyl methacrylate + hydroxyethyl methacrylate

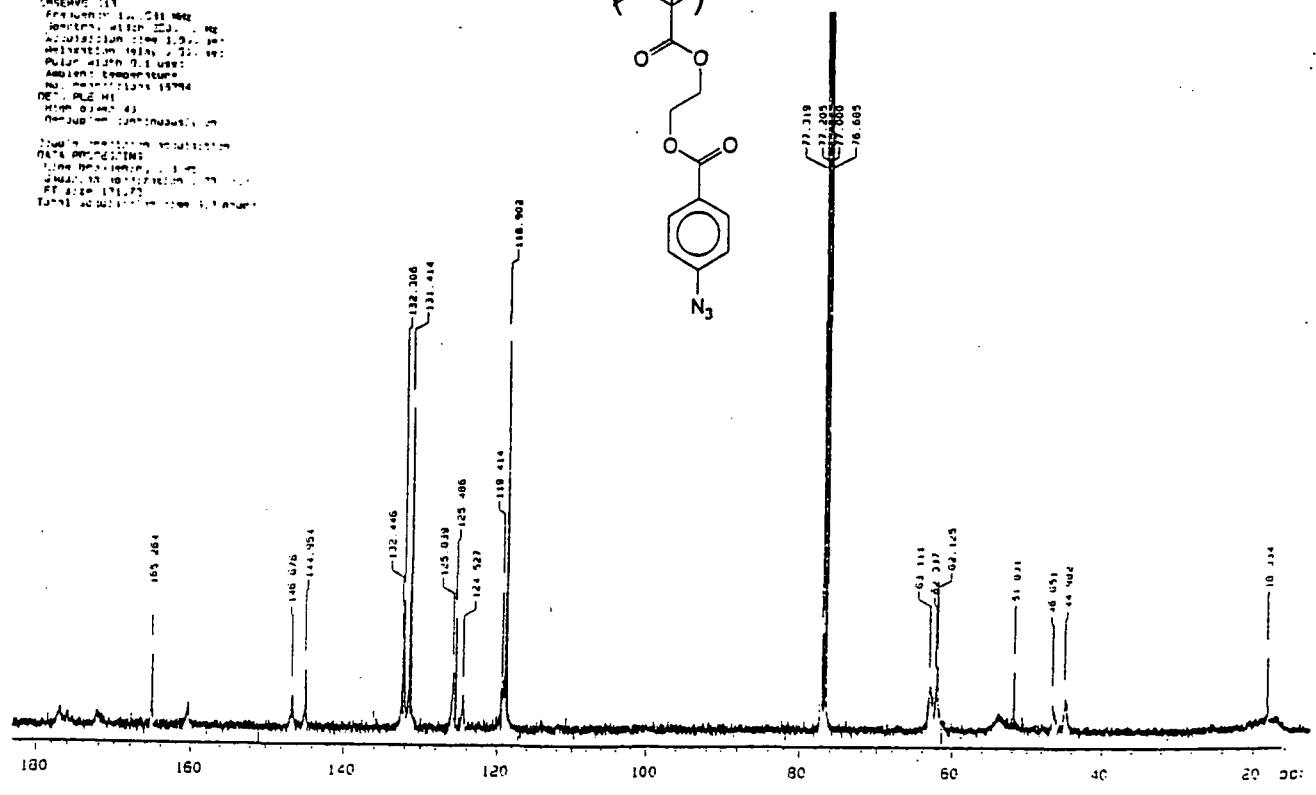
REF 105  
 FILE /data/curdac/ker12feb.fid  
 RUN ON Feb 12 96  
 SOLVENT Acetone  
 OBSERVE C13  
 Frequency 100.581 MHz  
 Spectral width 25000.0 Hz  
 Acquisition time 1.194 sec  
 Relaxation delay 1.000 sec  
 Pulse width 10.9 usec  
 Ambient temperature  
 No. repetitions 1024  
 DECOUPLE H1  
 High power 38  
 Decoupler continuously on  
 Double precision acquisition  
 DATA PROCESSING  
 Line broadening 0.0 Hz  
 FT size 131072  
 Total acquisition time 21 minutes



REF 200  
 FILE /data/cumdat/46707hans.fid  
 RUN ON Mar 2 85  
 SOLVENT CDCl3  
 OBSERVE C13  
 Frequency 101.251 MHz  
 Spectral width 25000.0 Hz  
 Acquisition time 1.199 sec  
 Relaxation delay 1.000 sec  
 Pulse width 9.7 usec  
 Ambient temperature  
 No. repetitions 4096  
 DECOUPLE H1  
 High power 40  
 Decoupler continuously on  
 Double precision acquisition  
 DATA PROCESSING  
 Line broadening 2.0 Hz  
 Gaussian smoothing 0.500 sec  
 FT size 131072  
 Total acquisition time 1.199 hours

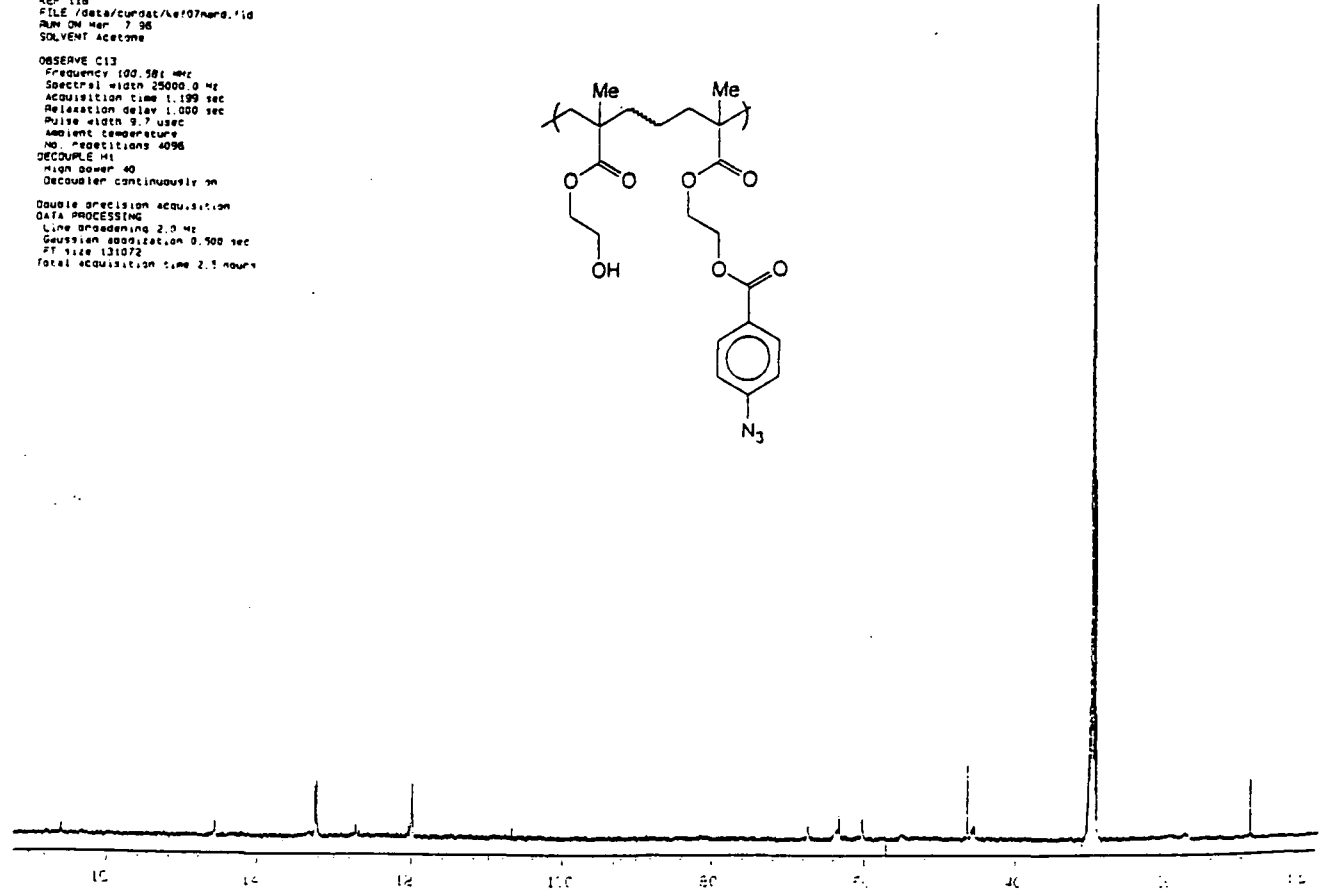
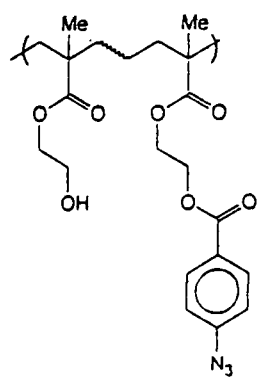


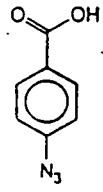
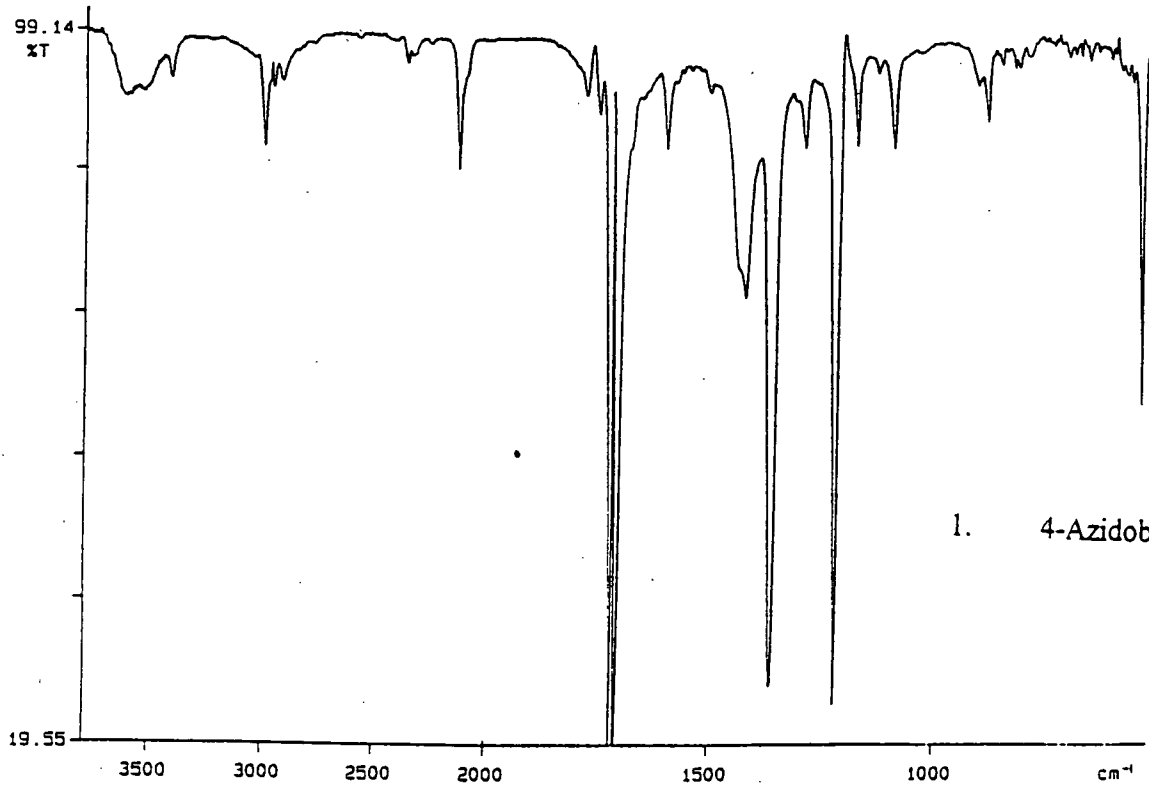
5. Poly(azidobenzoate-2-ethyl methacrylate)



6. Poly(azidobenzoate-2-ethyl methacrylate-co-hydroxyethyl methacrylate)

REF 118  
 FILE /data/cumdat/46707hans.fid  
 RUN ON Mar 2 85  
 SOLVENT Acetone  
 OBSERVE C13  
 Frequency 100.981 MHz  
 Spectral width 25000.0 Hz  
 Acquisition time 1.199 sec  
 Relaxation delay 1.000 sec  
 Pulse width 9.7 usec  
 Ambient temperature  
 No. repetitions 4096  
 DECOUPLE H1  
 High power 40  
 Decoupler continuously on  
 Double precision acquisition  
 DATA PROCESSING  
 Line broadening 2.0 Hz  
 Gaussian smoothing 0.500 sec  
 FT size 131072  
 Total acquisition time 2.5 hours

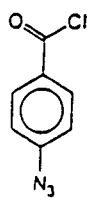
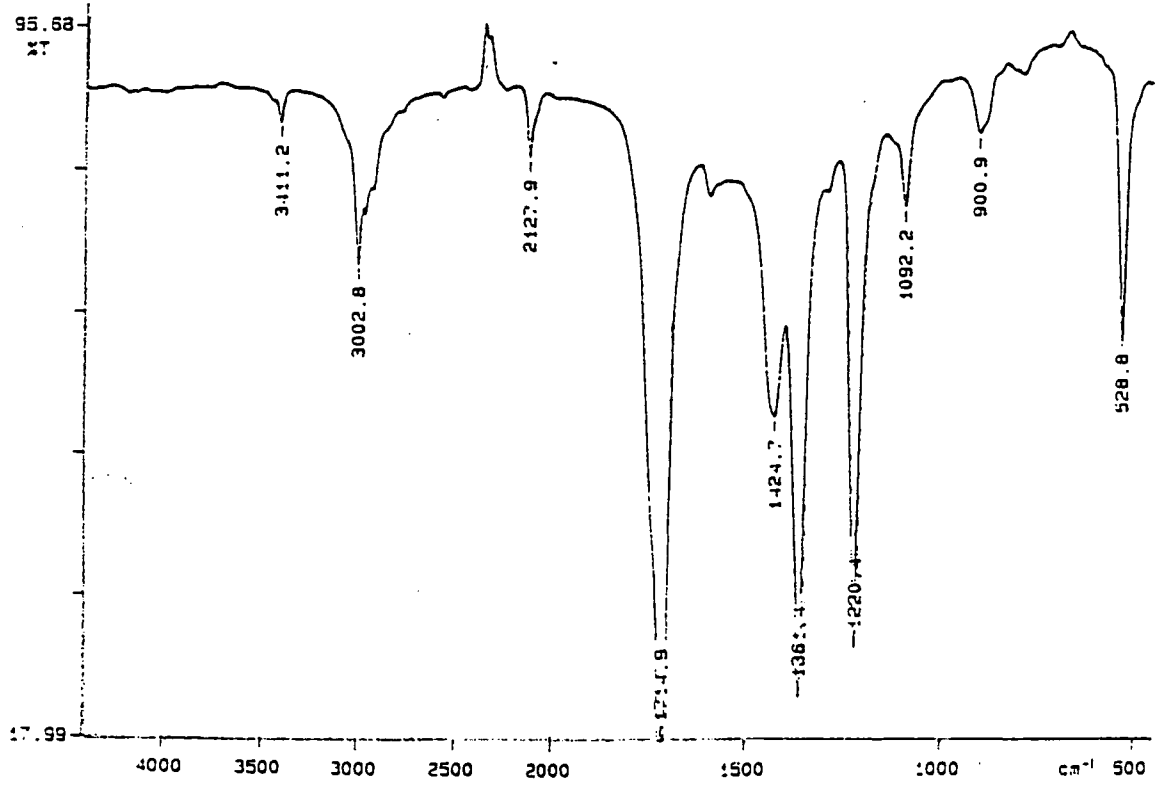




1. 4-Azidobenzoic acid

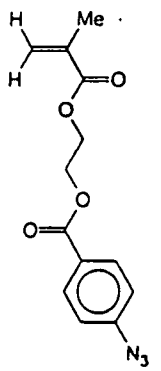
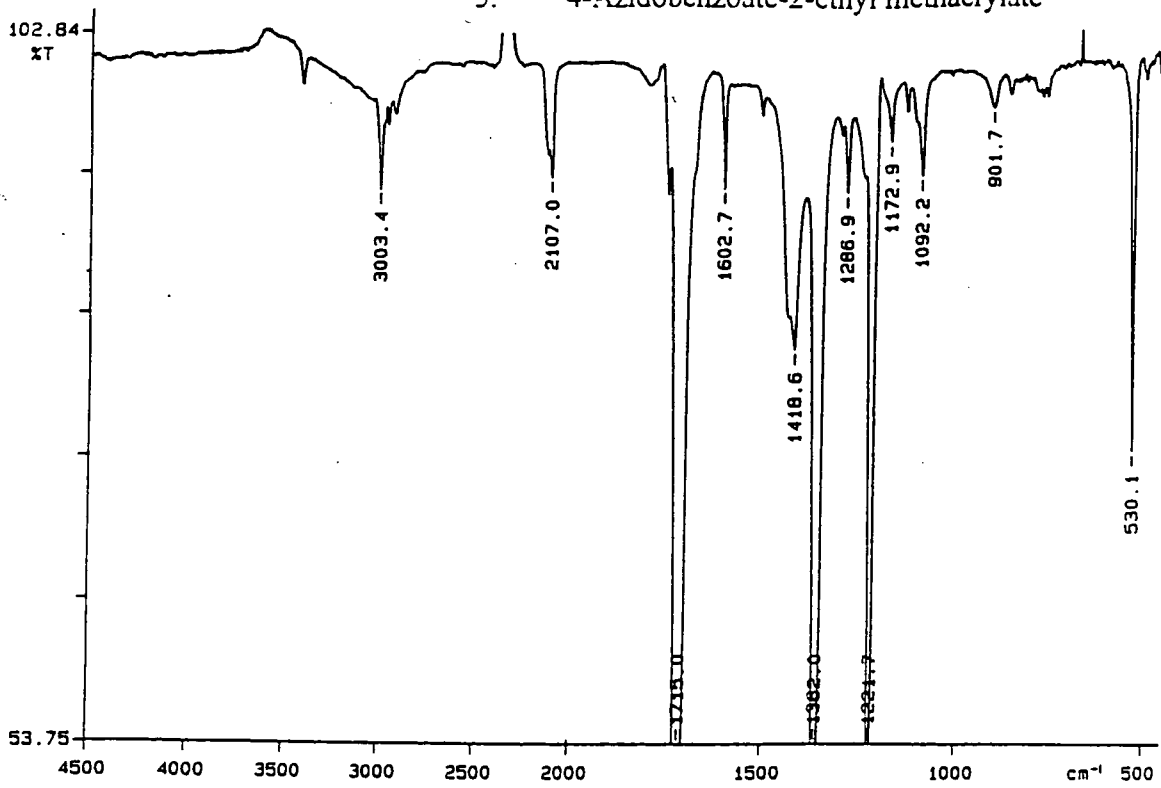
96/02/07 16:03 s-373  
 X: 1 scan, 4.0cm-1

2. 4-Azidobenzoyl chloride



96/09/19 13:49 s-373  
 X: 16 scans, 16.0cm-1, flat

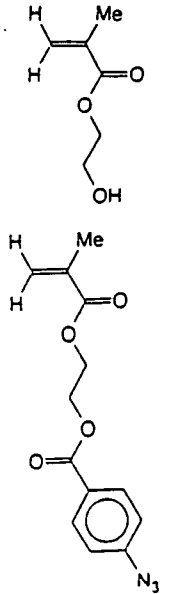
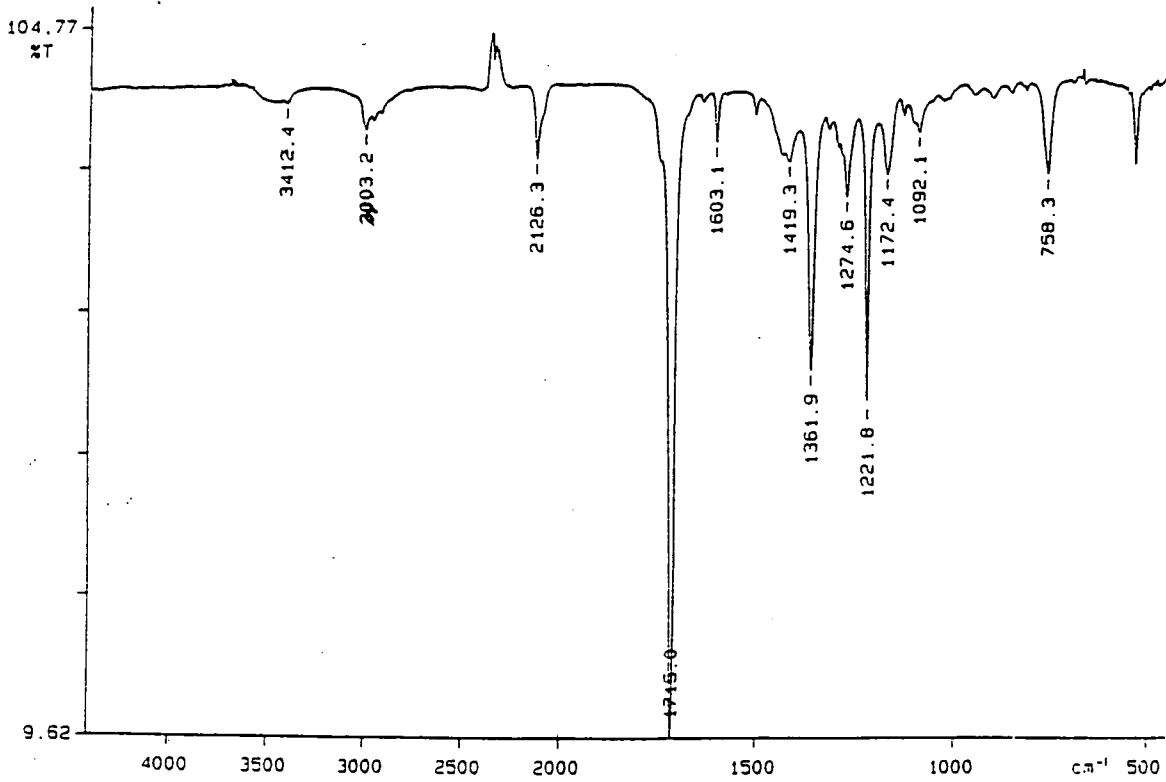
3. 4-Azidobenzoate-2-ethyl methacrylate



96/05/31 11:54 s-373  
X: 16 scans, 4.0cm-1, flat

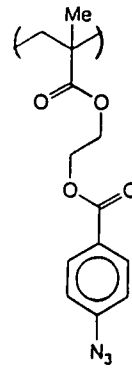
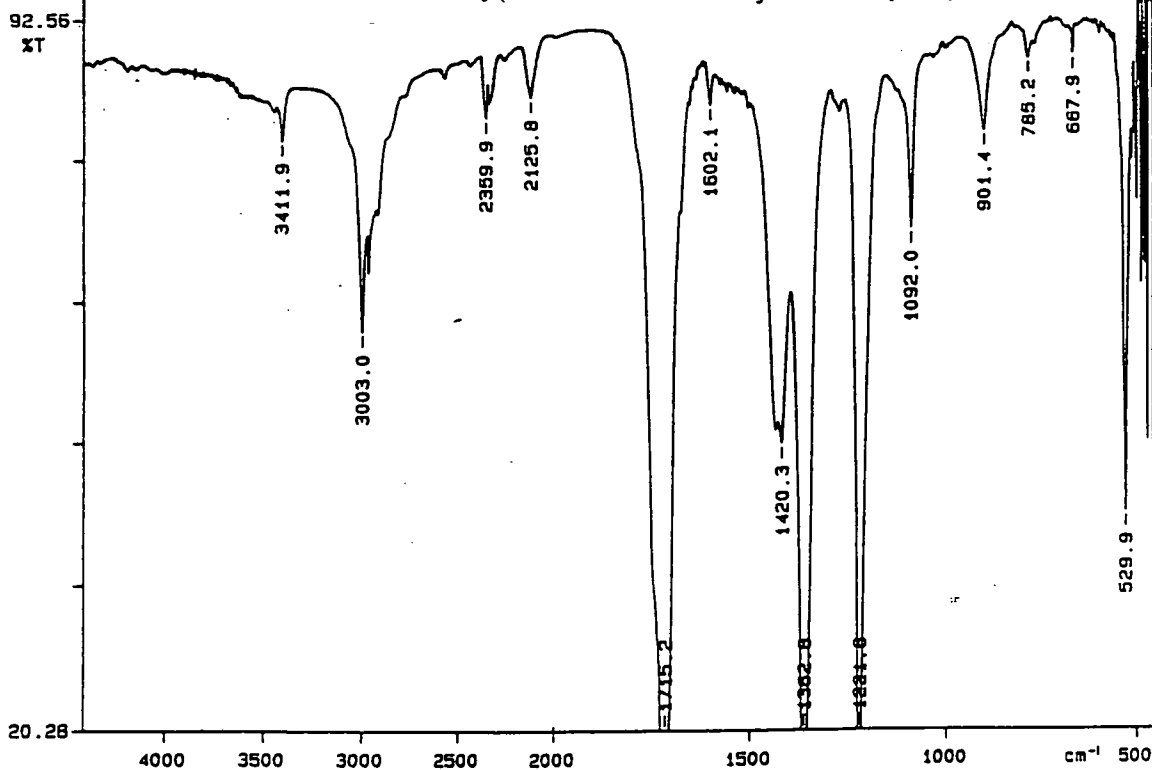
4. 4-Azidobenzoate-2-ethyl methacrylate + hydroxyethyl methacrylate

PERKIN ELMER



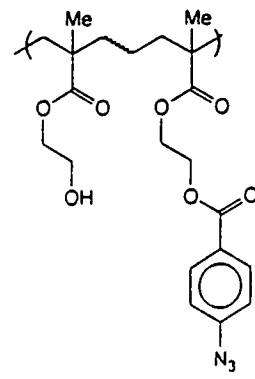
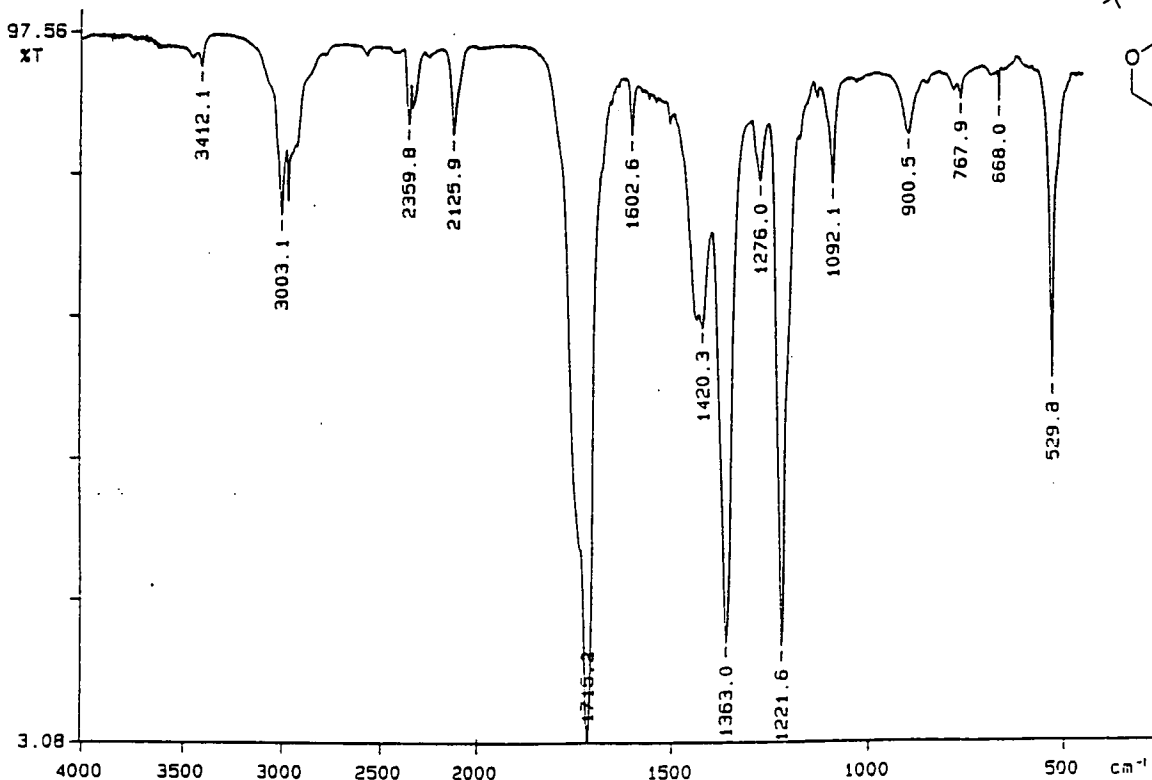
96/02/08 14:14  
X: 15 scans, 4.0cm-1

5. Poly(azidobenzoate-2-ethyl methacrylate)

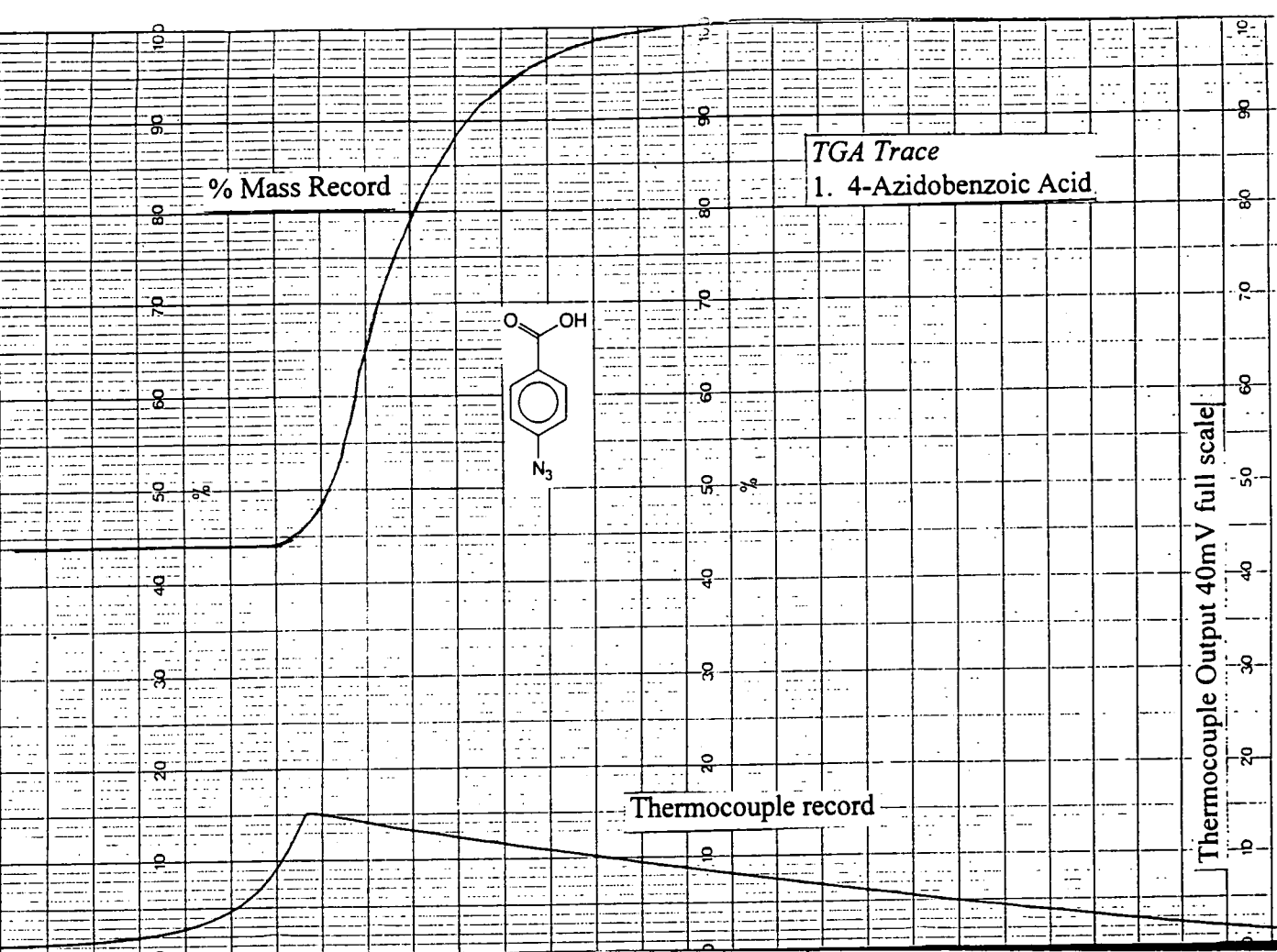


97/02/04 11:19 s-373  
X: 16 scans, 4.0cm-1, flat

6. Poly(azidobenzoate-2-ethyl methacrylate-co-hydroxyethyl methacrylate)



96/03/07 11:15 s-373  
X: 16 scans, 4.0cm-1



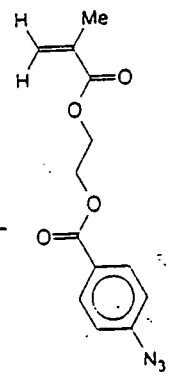
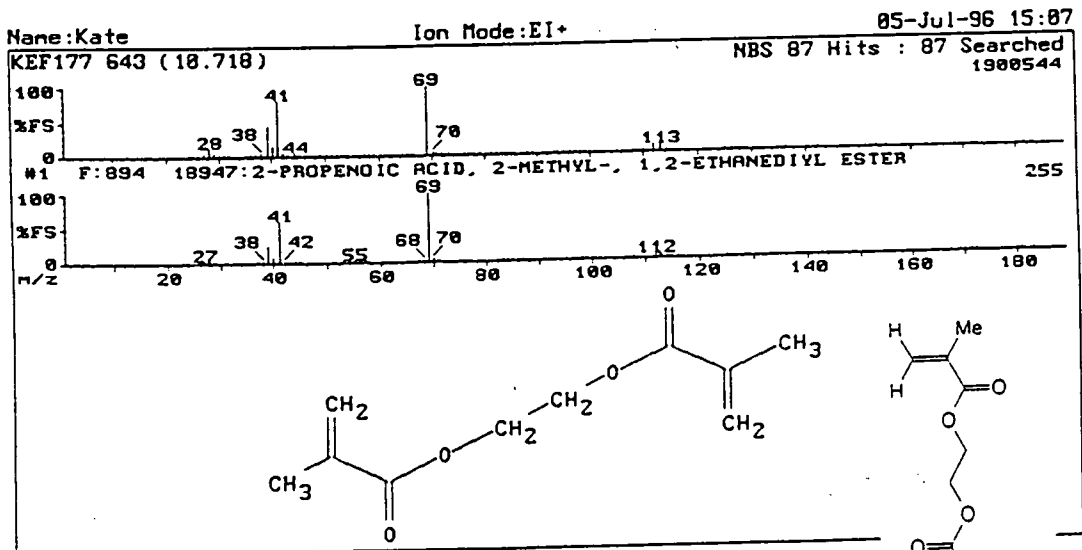
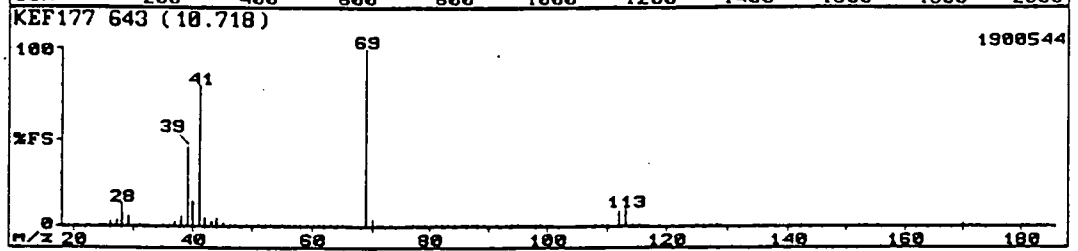
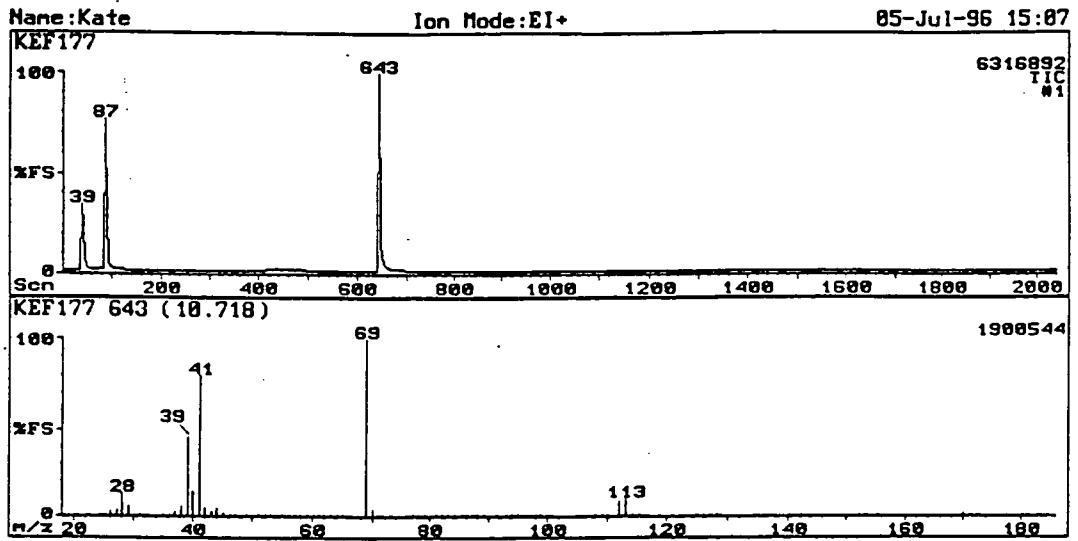
MILLIVOLTS TO DEGREE CELSIUS. (PT/PT:RH 13% THERMOCOUPLES)

Taken from (BS 4937:Pt 2:1973) REFERENCE JUNCTION AT 0°C (Correct to nearest whole number)

MILLI VOLTS	0,00	0,10	0,20	0,30	0,40	0,50	0,60	0,70	0,80	0,90	01	02	03	04	05	06	07	08	09
0,00	0	18	35	51	66	80	94	107	120	133	2	4	5	7	9	10	12	14	15
1,00	145	157	169	181	192	204	215	226	237	248	1	3	4	6	7	9	10	12	13
2,00	258	269	279	290	300	310	320	331	341	350	1	2	3	4	5	6	7	8	9
3,00	360	370	380	390	399	409	419	428	438	447	1	2	3	4	5	6	7	8	9
4,00	456	466	475	484	494	503	512	521	530	539	1	2	3	4	5	6	6	7	8
5,00	548	557	566	575	584	593	602	610	619	628	1	2	3	4	4	5	6	7	8
6,00	637	645	654	662	671	680	688	697	705	713	1	2	3	3	4	5	6	7	8
7,00	722	730	739	747	755	763	772	780	788	796	1	2	2	3	4	5	6	7	7
8,00	804	812	820	828	836	844	852	860	868	876		2	2	3	4	5	6	6	7
9,00	884	892	900	908	915	923	931	939	946	954	1	2	2	3	4	5	5	6	7
10,00	962	969	977	985	992	1000	1007	1015	1022	1030	1	2	2	3	4	5	5	6	7
11,00	1037	1045	1052	1060	1067	1075	1082	1089	1096	1104	1	1	2	3	4	4	5	6	7
12,00	1111	1119	1126	1133	1140	1148	1155	1162	1169	1177	1	1	2	3	4	4	5	6	7
13,00	1184	1191	1198	1206	1213	1220	1227	1234	1241	1248	1	1	2	3	4	4	5	6	6
14,00	1256	1263	1270	1277	1284	1291	1298	1305	1313	1320	1	1	2	3	4	4	5	6	6
15,00	1327	1334	1341	1348	1355	1362	1369	1376	1383	1391	1	1	2	3	4	4	5	6	6
16,00	1398	1405	1412	1419	1426	1433	1440	1447	1454	1461	1	1	2	3	4	4	5	6	6
17,00	1468	1476	1483	1490	1497	1504	1511	1518	1525	1532	1	1	2	3	4	4	5	6	6
18,00	1540	1547	1554	1561	1568	1575	1583	1590	1597	1604	1	1	2	3	4	4	5	6	6
19,00	1611	1619	1626	1633	1640	1648	1655	1662	1670	1677	1	1	2	3	4	4	5	6	7

Mass Spectrum

1. 4-Azidobenzoate-2-ethyl methacrylate



## Appendix Four - Analytical Data for Chapter Four

### *<sup>1</sup>H NMR Spectra*

1. Poly(9'-anthracenoate-2-ethyl methacrylate-co-methyl methacrylate)  
(solution polymerisation)
2. Poly(9'-anthracenoate-2-ethyl methacrylate-co-methyl methacrylate)  
(dispersion polymerisation)
3. Poly(9'-anthracenoate-2-ethyl methacrylate-co-methyl methacrylate)  
(bulk polymerisation)
4. Poly(azidobenzoate-2-ethyl methacrylate-co-methyl methacrylate)

### *<sup>13</sup>C NMR Spectra*

1. Poly(9'-anthracenoate-2-ethyl methacrylate-co-methyl methacrylate)  
(solution polymerisation)
2. Poly(9'-anthracenoate-2-ethyl methacrylate-co-methyl methacrylate)  
(dispersion polymerisation)
3. Poly(9'-anthracenoate-2-ethyl methacrylate-co-methyl methacrylate)  
(bulk polymerisation)
4. Poly(azidobenzoate-2-ethyl methacrylate-co-methyl methacrylate)

### *IR Spectra*

1. Poly(9'-anthracenoate-2-ethyl methacrylate-co-methyl methacrylate)  
(solution polymerisation)
2. Poly(9'-anthracenoate-2-ethyl methacrylate-co-methyl methacrylate)  
(dispersion polymerisation)
3. Poly(9'-anthracenoate-2-ethyl methacrylate-co-methyl methacrylate)  
(bulk polymerisation)

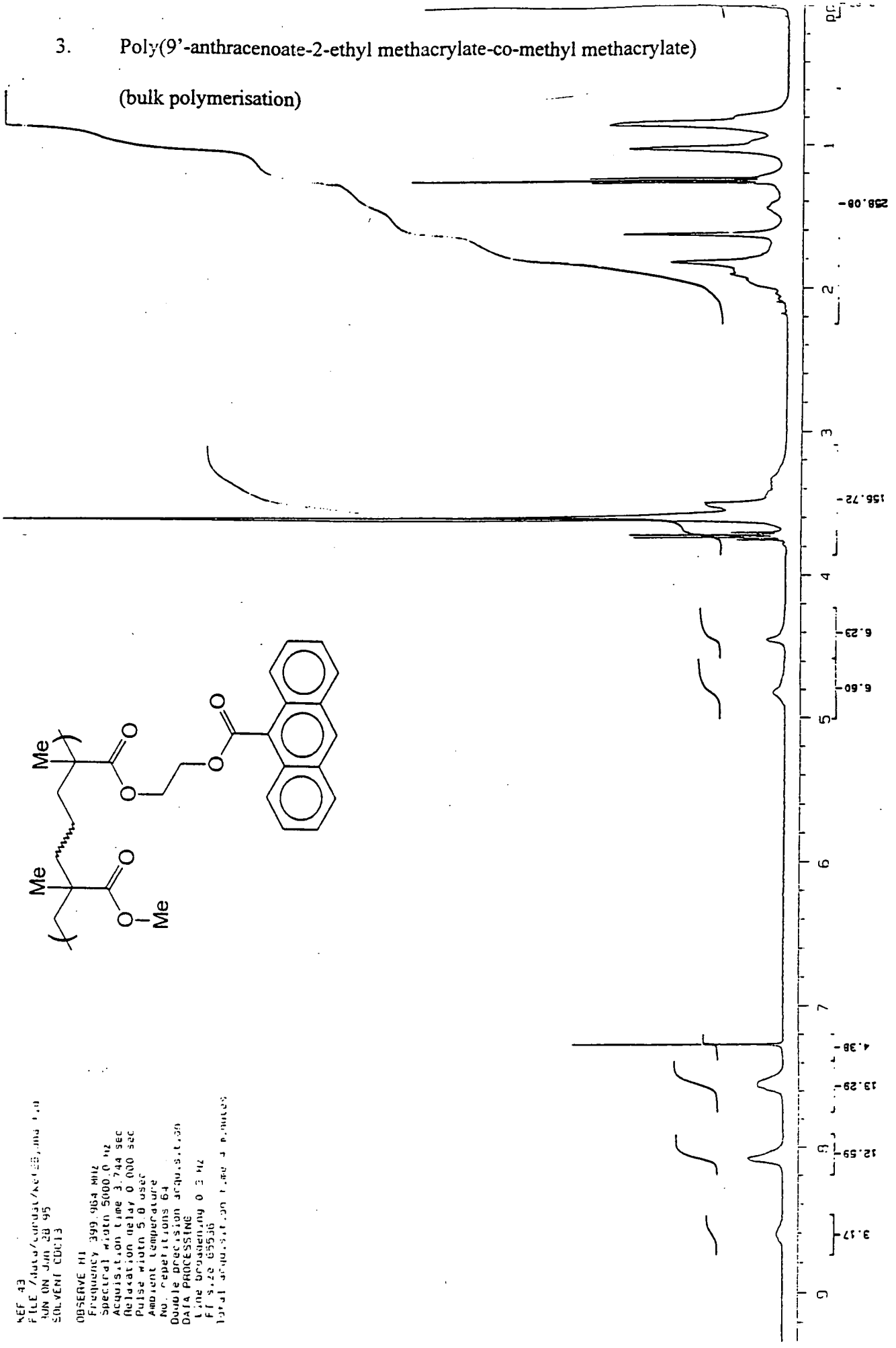
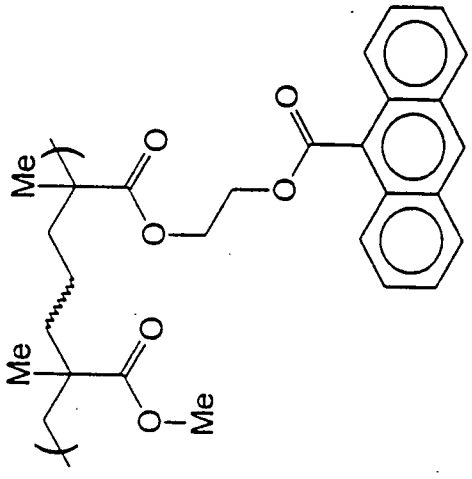
4. Poly(azidobenzoate-2-ethyl methacrylate-co-methyl methacrylate)





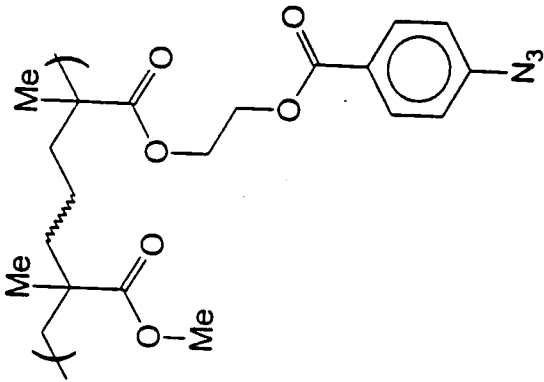
REF 43  
 FILE /data/cvdata/kec23.mh 1.0  
 RUN ON JUN 28 95  
 SOLVENT CDCl3  
 OBSERVE H1  
 Frequency 399.964 MHz  
 Spectral width 5000.0 Hz  
 Acquisition time 3.744 sec  
 Relaxation delay 0.000 sec  
 Pulse width 5.0 usec  
 Ambient temperature  
 No. repetitions 64  
 Double precision acqu.s.t. 30  
 DATA PROCESSING  
 Line broadening 0.3 Hz  
 Ff size 65536  
 Total acqu.s.t. time 3 minutes

3. Poly(9'-anthracenoate-2-ethyl methacrylate-co-methyl methacrylate)  
 (bulk polymerisation)

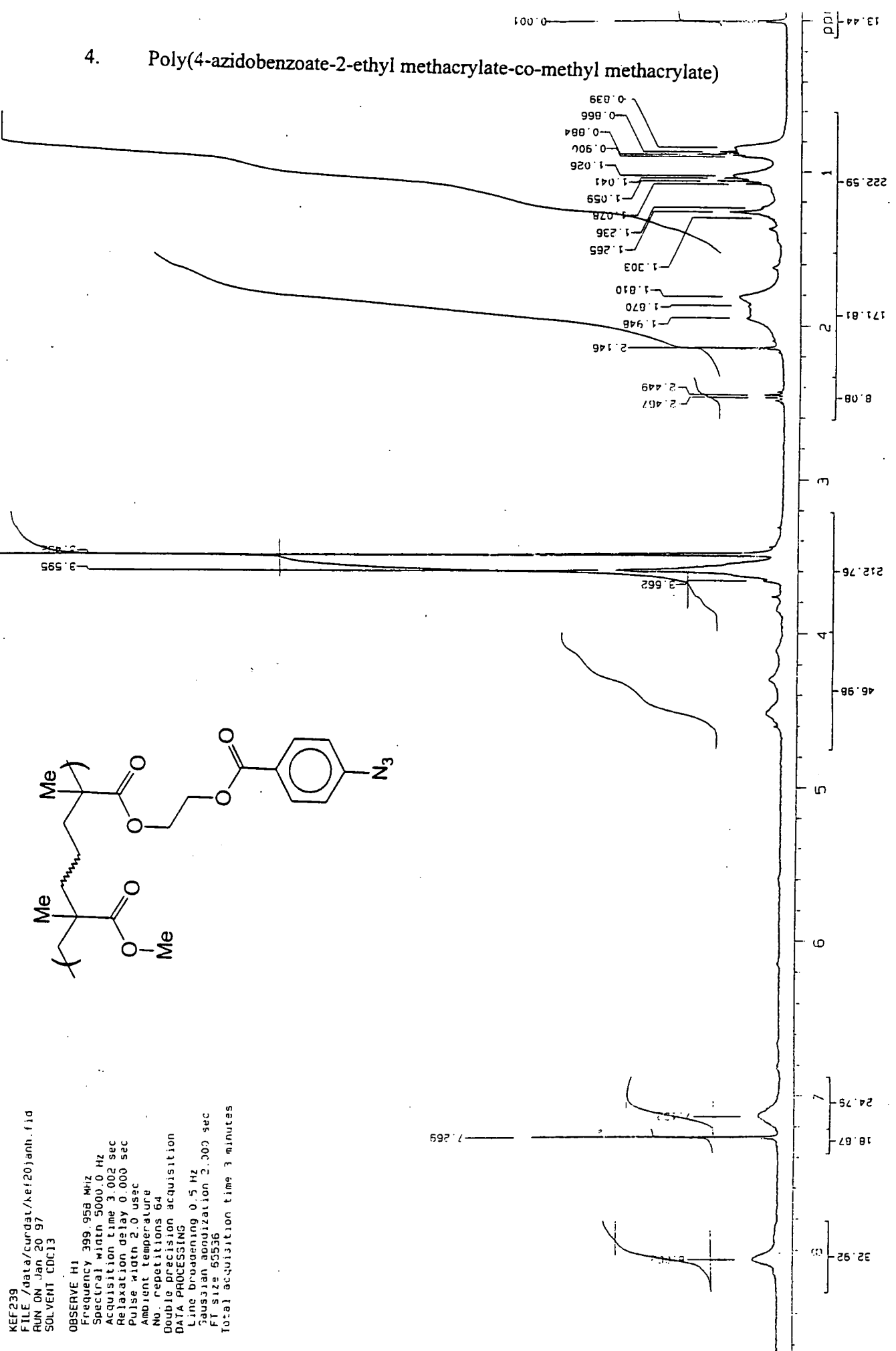


KEF239  
 FILE /data/curdai/kef20jnh.fid  
 RUN ON Jan 20 97  
 SOLVENT CDCl3

OBSERVE H1  
 Frequency 399.958 MHz  
 Spectral width 5000.0 Hz  
 Acquisition time 3.002 sec  
 Relaxation delay 0.000 sec  
 Pulse width 2.0 usac  
 Ambient temperature  
 No repetitions 64  
 Double precision acquisition  
 DATA PROCESSING  
 Line broadening 0.5 Hz  
 Gaussian smoothing 2.000 sec  
 FT size 65536  
 Total acquisition time 3 minutes

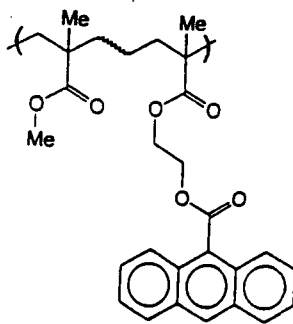


4. Poly(4-azidobenzoate-2-ethyl methacrylate-co-methyl methacrylate)

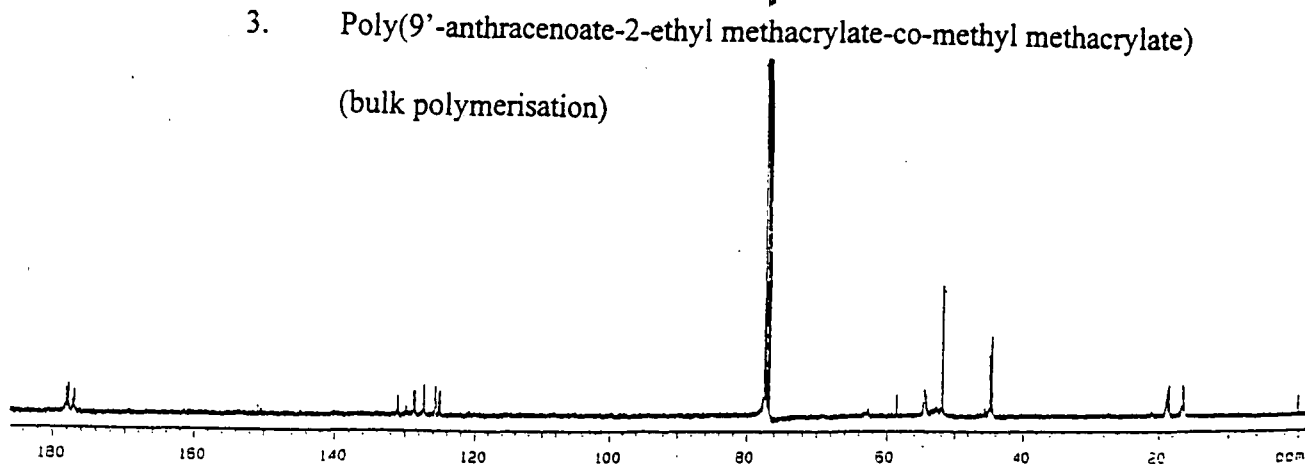




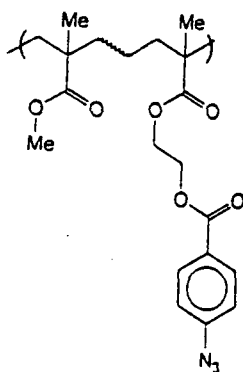
AEF 43  
 FILE /data/curdet/ae420)and.fid  
 RUN on Jun 28 95  
 SOLVENT CDCl3  
 OBSERVE C13  
 Frequency 100.622 MHz  
 Spectral width 25000.0 Hz  
 Acquisition time 1.000 sec  
 Relaxation delay 1.000 sec  
 Pulse width 9.2 usec  
 Ambient temperature  
 No. repetitions 15000  
 DECOUPLE W1  
 High power 40  
 Decoupler continuously on  
 Double precision acquisition  
 DATA PROCESSING  
 Line broadening 1.2 Hz  
 Gaussian optimization 0.000 sec  
 FT size 131072  
 Total acquisition time 9.0 hours



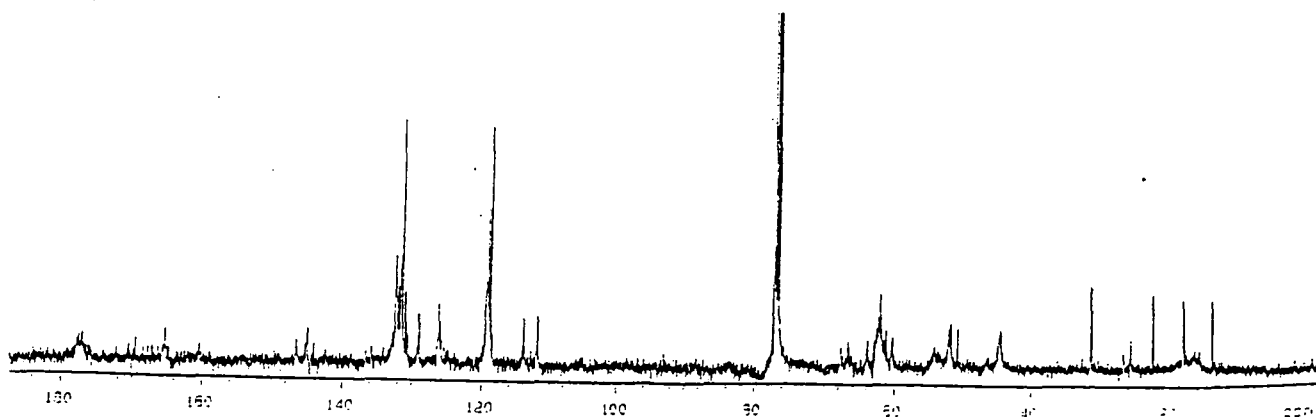
3. Poly(9'-anthracenoate-2-ethyl methacrylate-co-methyl methacrylate)  
 (bulk polymerisation)

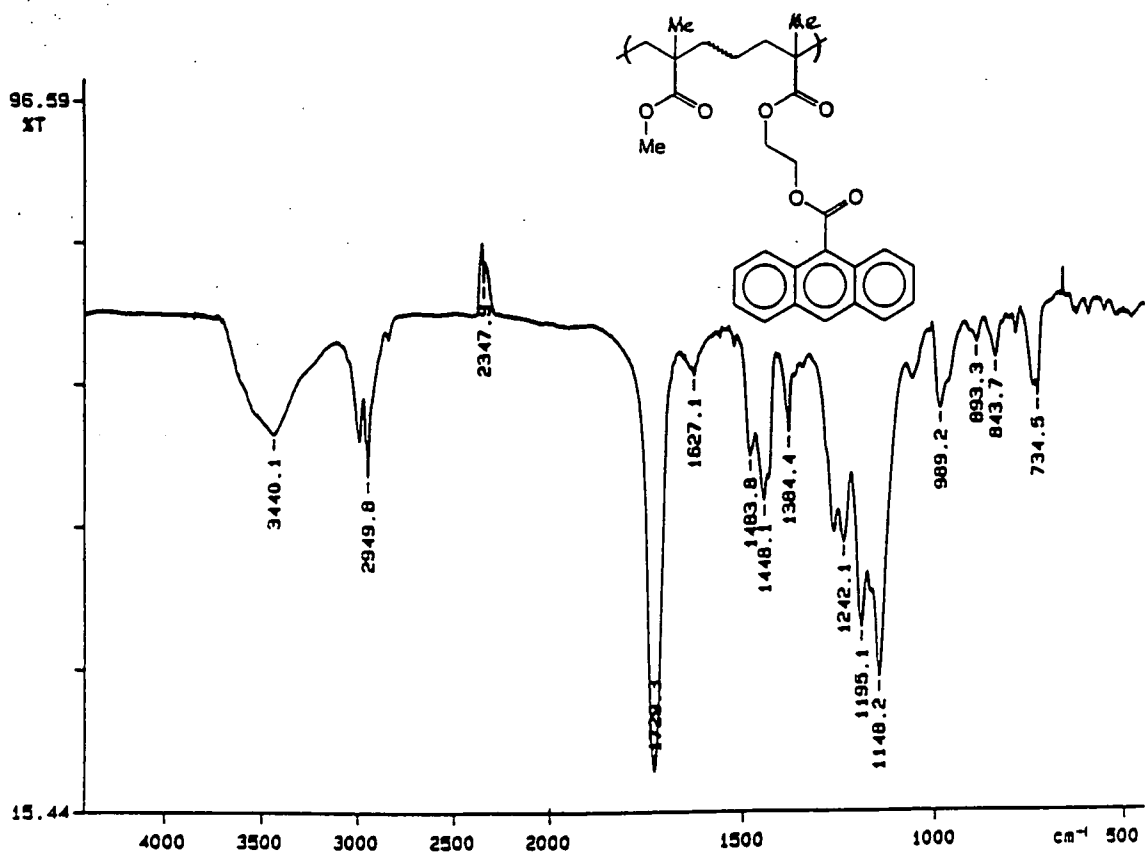


AEF298  
 FILE /data/curdet/ae420)and.fid  
 RUN on Jun 23 97  
 SOLVENT CDCl3  
 OBSERVE C13  
 Frequency 100.622 MHz  
 Spectral width 25000.0 Hz  
 Acquisition time 1.000 sec  
 Relaxation delay 1.000 sec  
 Pulse width 9.2 usec  
 Ambient temperature  
 No. repetitions 15000  
 DECOUPLE W1  
 High power 40  
 Decoupler continuously on  
 Double precision acquisition  
 DATA PROCESSING  
 Line broadening 1.2 Hz  
 Gaussian optimization 0.000 sec  
 FT size 131072  
 Total acquisition time 2.2 hours



4. Poly(4-azidobenzoate-2-ethyl methacrylate-co-methyl methacrylate)

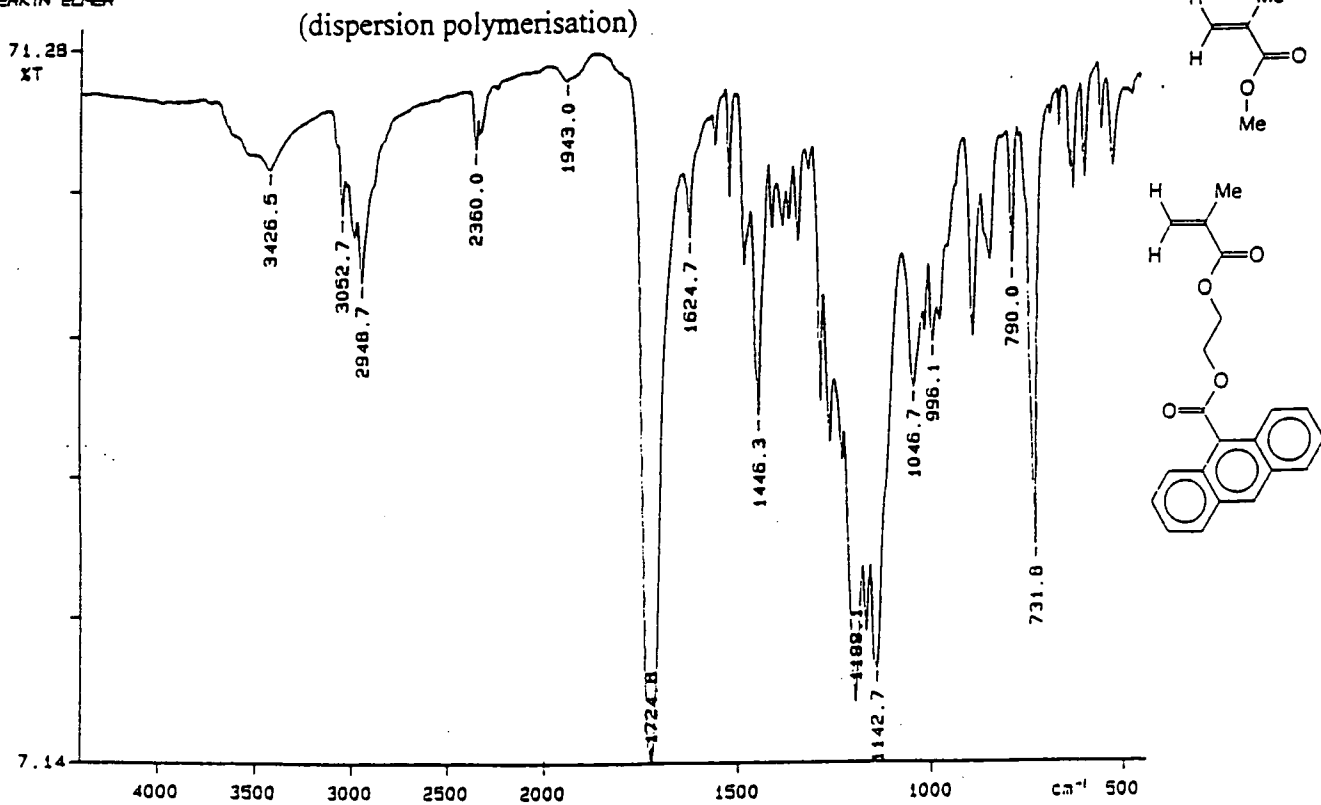




1. Poly(9'-anthracenoate-2-ethyl methacrylate-co-methyl methacrylate)  
(solution polymerisation)

2. Poly(9'-anthracenoate-2-ethyl methacrylate-co-methyl methacrylate)

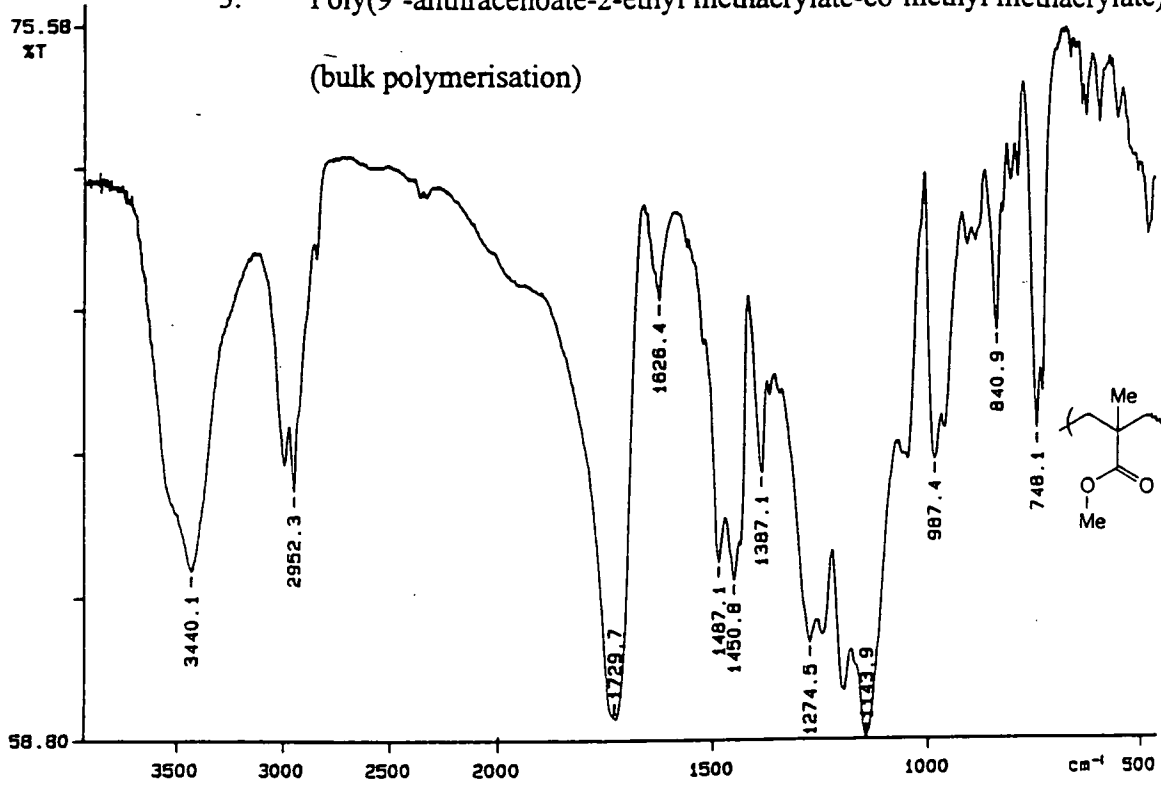
PERKIN ELMER



PERKIN ELMER

3. Poly(9'-anthracenoate-2-ethyl methacrylate-co-methyl methacrylate)

(bulk polymerisation)

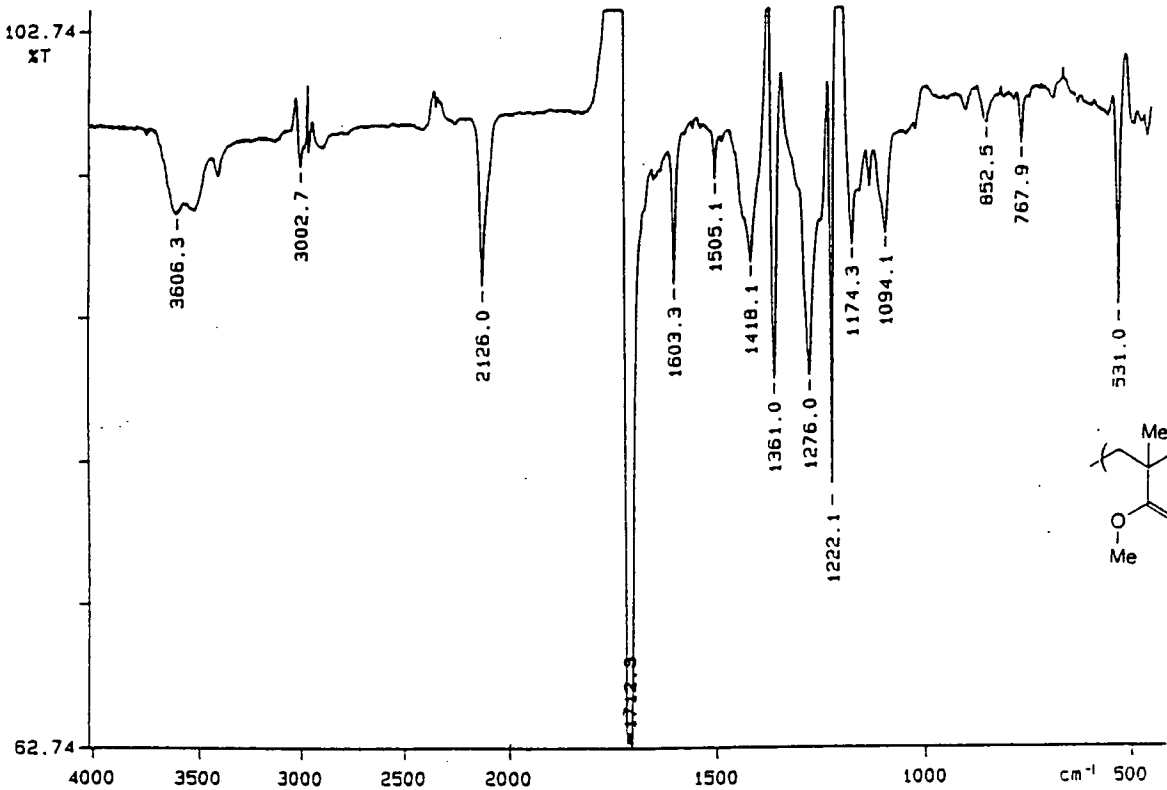


95/06/28 11: 20

X: 16 scans, 4.0cm<sup>-1</sup>. flat

4. Poly(4-azidobenzoate-2-ethyl methacrylate-co-methyl methacrylate)

PERKIN ELMER



96/05/02 15: 12 s-373

X: 16 scans, 4.0cm<sup>-1</sup>. flat

### Function Based on Organisation

November 6 Dr. Katharine Reid, Nottingham University,  
Probing Dynamic Processes with Photoelectrons

### 1997

January 16 Dr. Sally Brooker, Univ. Of Otago, NZ,  
Exciting yet Controlled Thiolate Coordination Chemistry

January 11 Dr. Sanders  
Enzyme Mimics

January 22 Dr. Neil Cooley, BP Chemicals Sunbury  
Synthesis and Properties of Polyketones

February 12 Dr. Geert-Jan Boons, Univ. of Birmingham,  
New Developments in Carbohydrate Chemistry

February 26 Dr. Tony Ryan, UMIST,  
Making Hairpins from Rings and Chains

March 12 Prof. David Cardin, Reading University

May 7 Prof. M.Harrington, Caltech Pasadena USA,  
Polymers both enable and limit the discovery of protein  
alterations in studies ranging from gene regulation to mad cow  
disease

### **Conferences Attended**

July 1995 ISOM 95, University of Durham

September 1995 IRC Club Meeting, University of Durham

29 July-2 August 1996 The Macrogrouop UK International Conference on  
'Recent Advances in Polymer Synthesis', University of  
York

January 1997 Tilden lecture and presentation, RSC London

2-4 March 1997 Macrogrouop UK Spring Meeting '97 for Younger  
Researchers, Queen's Hotel Leeds

## Bibliography

1. Aerle N.A.J.M., Barmentlo M. and Hollering R.W.J., Effect of Rubbing on the Molecular Orientation within polyimide orienting layers of liquid-crystal displays, J. Appl. Phys. (74) N° 5, 1993, pages 3111-20.
2. Alfrey T., Bohrer J.J. and Mark H., High Polymers vol. 8 Copolymerisation, Interscience Publishers, 1952.
3. Bauduin G., Boutevin B., Belbachir M. and Meghabar R., Determination of reactivity ratios in radical copolymerisation- A comparison of methods for a methacrylate N-vinylpyrrolidone system, Macromolecules (28) N° 6, 1995, pages 1750-53.
4. Bevington J.C., Radical Polymerisation, Academic Press Inc., 1961.
5. Blinov L.M., Electro-optical and magneto-optical properties of liquid crystals, John Wiley and Sons Ltd., 1983.
6. Boogers J.A.F., Klasse P.Th.A., de Vlieger J.J., Alkema D.P.W. and Tinnemans A.H.A., Cross-linked polymer materials for nonlinear optics 1. UV-cured acrylic monomers bearing azobenzene dyes, Macromolecules (27), 1994, pages 197-204.
7. Brochu S. and Ampleman G., Synthesis and Characterisation of Glycidyl Azide Polymers Using Isotactic and Chiral Poly(epichlorohydrin)s, Macromolecules (29), 1996, pages 5539-45.
8. Brown M.E., Introduction to thermal analysis techniques and applications, Chapman and Hall Ltd., 1988.
9. Chandrasekhar S., Liquid Crystals, Cambridge University Press, 1977.
10. Cohen H.L., The preparation and reactions of polymeric azides II. The

- preparation and reactions of various polymeric azides, J. Poly. Sci. Part A (19), 1981, pages 3269-84.
11. Collins E.A., Bares J. and Billmeyer F.W., Experiments in Polymer Science, John Wiley and Sons, 1973.
  12. Coursan M. and Desvergne J.P., Reversible photodimerisation of  $\omega$ -anthrylpolystyrenes, Macromol. Chem. Phys. (197), 1996, pages 1599-1608.
  13. Cowie J.M.G., Polymer: Chemistry and physics of modern materials, 2<sup>nd</sup> edition, Thomson Litho Ltd., 1991.
  14. Creed D., Griffin A.C., Gross J.R.D., Hoyle C.E. and Venkataram K., Photochemical crosslinking of novel polycinnamate main chain mesogens, Mol. Cryst. Liq. Cryst. (155), 1988, pages 57-71.
  15. Creed D., Griffin A.C., Hoyle C.E. and Venkataram K., Chromophore aggregation and concomitant wavelength dependent photochemistry of a main-chain liquid crystalline poly(aryl cinnamate), J. Am. Chem. Soc. (112), 1990, pages 4049-50.
  16. Delzenne G.A., Photoresists, Encyclo. Poly. Sci. and Tech., Part Title supplement 1, 1976, pages 401-43.
  17. Durr H. and Bouas-Laurent H.(editors), Photochromism Molecules and Systems, Elsevier Science Publishers B.V., 1990.
  18. Egerton P.L., Pitts E. and Reiser A., Photocycloaddition in solid poly(vinyl cinnamate). The photoreactive polymer matrix as an ensemble of chromophore sites, Am. Chem. Soc. (14) N<sup>o</sup> 1, 1981, pages 95-100.
  19. Fieser and Fieser, Reagents for Organic Synthesis, John Wiley and Sons,

- 1967.
20. Fischer P., Schmidt C. and Finkelmann H., Amphiphilic liquid-crystalline networks- phase behaviour and alignment by mechanical fields, Macromol. Rapid Commun. (16), 1995, pages 435-47.
  21. Fischer Th., Lasker L. and Stumpe J., Photoinduced optical anisotropy in films of photochromic liquid crystalline polymers, J. Photochem. Photobiol. A, 80(1-3), 1994, pages 453-59.
  22. Gibbons W.M., Shannon P.J. and Sun S., Alignment of Nematic Liquid Crystal with Laser, Preliminary Communications Taylor and Francis Ltd., 1992.
  23. Gilbert A., Photoelimination reactions, Photochemistry (3), 1972, pages 745-803.
  24. Gilbert A. and Baggett J., Essentials of Molecular Photochemistry, Blackwell Scientific Publications, 1991.
  25. Goeckner N.A. and Snyder H.R., The reaction of cyanide ion with carbonyl compounds in dipolar aprotic solvents, J. Org. Chem. (38) N° 3, 1973, pages 481-3.
  26. Green G.D., Weinschenk III J.I., Mulvaney J.E. and Hall H.K., Synthesis of polyesters containing a nonrandomly placed highly polar repeat unit, Macromolecules (20), 1987, pages 722-26.
  27. Greiss P., A New Class of Organic Acid, Zeitschrift fur Chemotherapie Un., 1867, pages 165-66.
  28. Haddleton D.M., Creed D., Griffin A.C., Hoyle C.E. and Venkataram K.,

- Photochemical cross-linking of main chain liquid-crystalline polymers containing cinnamoyl groups, Makromol. Chem. Rapid Commun. (10), 1989, pages 391-6.
29. Ham G.E. (editor), High Polymers vol. 18 Copolymerisation, Interscience Publishers, 1964.
  30. Hanemann T. and Haase W., Polyfunctional cinnamic acid derivatives as versatile photocrosslinkable material in thin polymer films for nonlinear optics, Abstracts of Papers of the Am. Chem. Soc. 208(2), 1994, pages 432-POLY.
  31. Hart, Craine and Hart, Organic Chemistry - a short course, 9<sup>th</sup> edition, Houghton Mifflin Company, 1995.
  32. Hercules Power Company, Improvements in or relating to cross-linking polymers, UK Patent 996350, 1965.
  33. Hu C.J., Oshima R. and Seno M., Synthesis and photogeneration properties of copolyacrylate having carbazole donor and trinitrofluorenone acceptor chromophores, J. Poly. Sci. Part A (26), 1988, pages 1239-48.
  34. Ibbett R.N. (editor), NMR Spectroscopy of Polymers, Blackie Academic and Professional, 1993.
  35. Ide N., Tsujii Y., Fukada T. and Miyamoto T., Gelation processes of polymer solutions I. Photodimerisation of free and polymer-bound anthryl groups, Macromolecules (29), 1996, pages 3851-56,
  36. Iglesias M.T., Guzman J. and Riande E., Copolymerisation and

- terpolymerisation of methacrylic ester monomers containing hydroxyl groups in their structure, Polymer (37) N° 8, 1996, pages 1443-52.
37. Ishihara S., Wakemoto H., Nakazima K. and Matsuo Y., The effect of rubbed polymer films on the liquid crystal alignment, Liquid Crystals (4) N° 6, 1989, pages 669-75.
38. Ito T., Nakanishi K., Nishikawa M., Yokogama Y. and Takeuchi Y., Regularity and Narrowness of the Intervals of the Microgrooves on the Rubbed Polymer Surfaces for Liquid Crystal Alignment, Polymer Journal (27) N° 3, 1995, pages 240-46.
39. Jain S.C. and Kitzerow H-S., Bulk-induced alignment of nematic liquid crystals by photopolymerisation, Appl. Phys. Letters (64) N° 22, 1994, pages 2946-48.
40. Jayakrishnan A., Sunny M.C. and Rajan M.N., Photocrosslinking of Azidated Poly(vinyl chloride) Coated onto plasticised PVC surface: Route to containing plasticiser migration, J. Appl. Poly. Sci. (56), 1995, 1187-95.
41. Jin X., Carfagna C., Nicolais L. and Lanzetta R., Synthesis, Characterisation and in Vitro Degradation of a Novel Thermotropic Ternary Copolyester Based on p-Hydroxybenzoic Acid, Glycolic Acid and p-Hydroxycinnamic Acid, Macromolecules (28), N° 14, 1995, pages 4785-94.
42. Katawatsuki N., Takatsuka H., Yamamoto T. and Sengen O., Synthesis and photo-crosslinking of orientated side-chain liquid crystalline polymers, Macromol. Rapid Commun. (17), 1996, pages 703-12.

43. Kawanishi Y., Tamaki T., Seki T., Sakurgi M., Suzuki Y. and Ichimura K., Multifarious Liquid Crystalline Textures Formed on a Photochromic Azobenzene Polymer Film, Langmuir (7), 1991, pages 1314-15.
44. Korner H., Shiota A., Bunning T.J. and Ober C.K., Orientation-on-demand thin films curing of liquid crystalline networks in ac electric fields, Science (272), 1996, pages 252-55.
45. Koseki K., Koshiha M., Nakamura A., Yamaoka T. and Tsunoda T., Effect of Molecular Structure on Photosensitivity of Azido Polymer, Kobunshi Ronbunshu (37) N° 4, 1980, pages 235-41.
46. Kruft M.B. and Koole L.H., A Convenient Method to Measure Monomer Reactivity Ratios. Application to Synthesis of Polymeric Biomaterials Featuring Intrinsic Radiopacity, Macromolecules (29) N° 17, 1996, pages 5513-19.
47. Kurihara S., Ohta H. and Nonaka T., Polymerisation of liquid crystalline monomers with diene groups and formation of a polymer network with uniaxial molecular alignment, J. Appl. Poly. Sci. (61) N° 2, 1996, pages 279-83.
48. Labana S.S. (editor), Ultraviolet light induced reactions in polymers, Am. Chem. Soc., 1976.
49. L'Abbe G., Decomposition and addition reactions of organic azides, Chem. Revs. (69), 1969, pages 345-63.
50. Lee K.W., Paek S.H., Lien A., Durning C. and Fukuro H., Microscopic molecular reorientation of alignment layer polymer surfaces induced by rubbing and its effects on LC pretilt angles, Macromolecules (29), N° 27,

- 1996, pages 8894-99.
51. Levin D. (Zeneca), Toxicological Concerns, Chem. and Ind. N° 1, 1997, page 2.
  52. Li C., Cheng H., Chang T. and Chu T., Studies on the thermotropic liquid-crystalline polymer IX. Synthesis and properties of crosslinkable copoly(amide-ester)s containing double bonds, J. Poly. Sci. Part A (31), 1993, pages 1125-33.
  53. Lwowski W. (editor), Nitrenes, Interscience Publishers, 1970.
  54. March J., Advanced Organic Chemistry Reactions, Mechanisms and Structure, 4<sup>th</sup> edition, John Wiley & Sons, 1992.
  55. Marusii T.Ya. and Reznikov Yu.A., Photosensitive orientants for liquid crystal alignment, Mol. Mat. (3), 1993, pages 161-8.
  56. McMurry J., Organic Chemistry, 2<sup>nd</sup> edition, Brooks/Cole Publishing Company, 1988.
  57. Meier G., Sackmann E. and Grabmaier J.G., Applications of Liquid Crystals, Springer Verlag, 1975.
  58. Merrill S.H. and Unruh C.C., Improved light sensitive polymers for photomechanical printing processes, UK Patent 843541, 1956.
  59. Merrill S.H. and Unruh C.C., Photosensitive Azide Polymers, J. Appl. Poly. Sci. (7), 1963, pages 273-9.
  60. Minsk L.M., Smith J.G., Van Deusen W.P. and Wright J.F., Photosensitive polymers I. Cinnamate esters of poly(vinyl alcohol) and cellulose, J. Appl. Poly. Sci. (2) N° 6, 1959, pages 302-7.
  61. Minsk L.M., Van Deusen W.P. and Robertson E.M., Photosensitisation of

- polymeric cinnamic acid esters, US Patent 2610120, 1952.
62. Nagamatsu G., Asano T. and Takahashi H., Synthesis and properties of the new azidopolymer, Graphic Arts Jpn. (4), 1972-3, pages 54-61.
  63. Nakayama Y. and Matsuda T., Preparation and characteristics of photocrosslinkable hydrophilic polymer having cinnamate moiety, J. Poly. Sci. Part A: Poly. Chem. (30), No 11, 1992, pages 2451-57.
  64. Negi Y.S., Yamamoto N., Suzuki Y., Kawamura I., Yamoda Y., Kakimoto M. and Imai Y., Alignment Layers for Ferro and Antiferroelectric Liquid Crystal Cells, Jpn. J. Appl. Phys. (31), 1992, pages 3934-39.
  65. Nishikawa M., Kimiyasu S., Tsuyoshi M., Yokoyama Y., Bessho N., Seo D., Iimura Y. and Kobayashi S., Pretilt Angles of Liquid Crystal on Organic-Solvent-Soluble Polyimide Alignment Films, Jpn. J. Appl. Phys. (33), 1994, pages 4152-53.
  66. Norman R.O.C., Principles of Organic Synthesis, Chapman and Hall, 1978.
  67. Odian G., Principles of Polymerisation, 2<sup>nd</sup> edition, John Wiley and Sons, 1981.
  68. Patai S. (editor), The chemistry of alkenes, Interscience Publishers, 1963.
  69. Patai S. (editor), The chemistry of the azido group, Interscience Publishers, 1971.
  70. Perrin D.D. and Armarego W.L.F., Purification of laboratory chemicals, 3<sup>rd</sup> edition, Butterworth-Heinemann Ltd., 1988.
  71. Rami Reddy A.V., Subramanian K., Krishnasamy V. and Ravichandran

- J., Synthesis, characterisation and properties of novel polymers containing pendant photocrosslinkable chalcone moieties, Eur. Poly. J. (32) N° 8, 1996, pages 919-26.
72. Reid S.T., Photoelimination, Photochemistry (19), 1986-7, pages 421-56.
73. Salari H., Yeung M., Douglas S. and Morozowich W., Detection of prostaglandins by high-performance liquid chromatography after conversion to para-(9-anthroyloxy) phenacyl esters, Analytical Biochemistry (165), 1987, page 222.
74. Sandner M.R. and Osborn C.L., Acetophenone-Type photosensitisers for Radiation Curable Coatings, US. Patent 3715293, 1973.
75. Sano R. and Hasegawa K., Optical properties of azide polymers of potential utility in a photographic system, Photographic science and Engineering (15) N° 4, 1971, 309-16.
76. Schadt M., Schmitt K., Kozinkov V. and Chigrinov V., Surface-induced parallel alignment of liquid crystals by linearly polymerised photopolymers, Jpn. J. Appl. Phys. (31), 1992, pages 2155-64.
77. Seki T., Fukuda R., Tamaki T. and Ichimura K., Alignment Photoregulation of Liquid Crystals on Precisely area controlled azobenzene Langmuir-Blodgett monolayers, Thin Solid Films (243), 1994, pages 675-78.
78. Sekkat Z., Buchel M., Orendi H., Knobloch H., Seki T., Ito S., Koberstein J. and Knoll W., Anisotropic Alignment of a Nematic Liquid Crystal, Optics Communications III, 1994, pages 324-30.
79. Seo D., Muroi K., Isogami T., Matsuda H. and Kobayashi S., Polar

- anchoring strength and the temperature dependence of nematic liquid crystal (5CB) aligned on rubbed polystyrene films, Jpn. J. Appl. Phys. (31), 1992, pages 2165-69.
80. Silverstein R.M., Clayton G., Bassler and Morrill T.C., Spectrometric identification of organic compounds, 5<sup>th</sup> edition, John Wiley and Sons Inc., 1991.
81. Smets G., Photochemical cross-linking of polymer materials, Inf. Chemie, 1978 pages 197-203.
82. Stenger-Smith J.D., Fischer J.W., Henry R.A., Hoover J.M., Nadler M.P., Nissan R.A. and Lindsay G.A., Poly(4-N-ethylene-N-ethylamino)-cyanocinnamate: A nonlinear optical polymer with a chromophoric mainchain 1. Synthesis and spectral characterisation, J. Poly. Sci. Part A (29), 1991, pages 1623-31.
83. Subramanian P., Creed D., Griffin A.C., Hoyle C.E. and Venkataram K., The mechanism of photo-Freis fragmentation of aryl cinnamates in polymer films and in solution, J. Photochem. Photobiol. A:Chem. (61), 1991, pages 317-27.
84. Suling C., Von Bonin W., Logemann H. and Holtschmidt H., Polymers crosslinkable with UV-light, Brit. Patent 1138929, 1967.
85. Sun S., Gibbons W.M. and Shannon P.J., Alignment of guest-host liquid crystals with polarised laser light, Preliminary Communications Taylor and Francis Ltd., 1992.
86. Tonelli A.E., NMR Spectroscopy and polymer microstructure. The conformational connection, VCH Publishers, 1989.

87. Trost B.M. and Fleming I. (editors), Comprehensive Organic Synthesis vol. 8 Reduction, Pergamon Press 1991, pages 383-6.
88. Turro N.J., Modern Molecular Photochemistry, The Benjamin/Cummings Publishing Company Inc., 1978.
89. Vogel A., Textbook of Practical Organic Chemistry, 5<sup>th</sup> edition, Longman Scientific and Technical, 1989.
90. Weissberger A. (editor), Techniques of organic chemistry vol. III Part 1 Separation and Purification, 2<sup>nd</sup> edition, Interscience Publishers, 1956.
91. Whitcombe M.J., Gilbert A. and Mitchell R., Synthesis and photochemistry of side-chain liquid crystal polymers based on cinnamate esters, J. Poly. Sci. Part A (30), 1992, pages 1681-91.
92. Wilkins C.W., Feit E.D. and Wurtz M.E., Preliminary Investigations of azide containing negative resists: Poly(benzyl azide), Proc. Electrochem. Soc. (78-5), 1978, pages 341-52.
93. Williams D.H., Fleming I., Spectroscopic methods in organic chemistry, 4<sup>th</sup> edition, McGraw-Hill Book Company (UK) Ltd., 1989.
94. Williams J.L.R., Photopolymerisation and photocrosslinking of polymers, Fortsch Chem., Fortsch 13, 1969, pages 227-50.
95. Yamashita K., Kyo S., Miyagawa T., Nango M. and Tsuda K., Synthesis and characterisation of liquid crystal photoresist, J. Appl. Poly. Sci. (52), 1994, pages 577-81.
96. Zhao Y. and Lei H., A Polarised infra-red spectroscopic study of mechanically induced orientation in side-chain liquid crystalline polymers, Polymer (35) N° 7, 1994, pages 1419-24

